UNIVERSITY OF STRATHCLYDE

Modelling Offshore Wind Farm Operation and Maintenance with View to Estimating the Benefits of Condition Monitoring

XI YU

A thesis presented in fulfilment of the requirements
for the degree of Doctor of Philosophy

Centre for Doctoral Training in Wind Energy Systems
Department of Electronic and Electrical Engineering
University of Strathclyde
Glasgow, UK

2016

Acknowledgements

I would like to express my very great appreciation to the Centre for Doctoral Training for Wind Energy, University of Strathclyde, which provides me the great opportunity to explore the field of wind energy by providing a thorough training process covering all relevant knowledge, studying on the specific PhD topics, and outreach activities. I would like to thank my academic supervisors, Professor David Infield, and Professor William E. Leithead, for their valuable and constructive suggestions. I would like to acknowledge my sponsor company, EDF, and my industrial supervisors, Mr Sami Barbouchi and Mr Redouane Seraoui, who have provided industrial advice and brought my analysis results and suggestions to the entire company and its wind farms. I would like to thank Dr Julian B. Feuchtwang for sharing his knowledge on the cost model development. I would also like to extend my thanks to Vattenfall Research & Development and Dr Eoghan Maguire, for their generous data support and technical advice. I would like to thank all the people whom I have worked with and who have provided valuable advice, data and administrative support.

Abstract

Offshore wind energy is progressing rapidly and playing an increasingly important role in electricity generation. Since the Kyoto Protocol in February 2005, Europe has been substantially increasing its installed wind capacity. Compared to onshore wind, offshore wind allows the installation of larger turbines, more extensive sites, and encounters higher wind speed with lower turbulence. On the other hand, harsh marine conditions and the limited access to the turbines are expected to increase the cost of operation and maintenance (O&M costs presently make up approximately 20-25% of the levelised total lifetime cost of a wind turbine). Efficient condition monitoring has the potential to reduce O&M costs. In the analysis of the cost effectiveness of condition monitoring, cost and operational data are crucial. Regrettably, wind farm operational data are generally kept confidential by manufacturers and wind farm operators, especially for the offshore ones.

To facilitate progress, this thesis has investigated accessible SCADA and failure data from a large onshore wind farm and created a series of indirect analysis methods to overcome the data shortage including an onshore/offshore failure rate translator and a series of methods to distinguish yawing errors from wind turbine nacelle direction sensor errors. Wind turbine component reliability has been investigated by using this innovative component failure rate translation from onshore to offshore, and applies the translation technique to Failure Mode and Effect Analysis for offshore wind. An existing O&M cost model has been further developed and then compared to other available cost models. It is demonstrated that the improvements made to the model (including the data translation approach) have improved the applicability and reliability of the model. The extended cost model (called StraPCost+) has been used to establish a relationship between the effectiveness of reactive and condition-based maintenance strategies. The benchmarked cost model has then been applied to assess the O&M cost effectiveness for three offshore wind farms at different operational phases.

Apart from the innovative methodologies developed, this thesis also provides detailed background and understanding of the state of the art for offshore wind technology, condition monitoring technology. The methodology of cost model developed in this thesis is presented in detail and compared with other cost models in both commercial and research domains.

CONTENTS

Chapter 1 Introduction and Motivation for the Research

It has been generally accepted that renewable energy has been taking an increasingly important role in energy generation worldwide, especially since the entry into force of the Kyoto Protocol in February 2005, when the adoption of renewable energy formally became governmental action. Wind energy, as an important form of renewable energy generation, has been taken increasingly attention all over the world, within which offshore wind energy is now progressing rapidly. Europe has been substantially increasing its installed offshore wind capacity in recent years. The offshore market in the UK has been enlarged rapidly during this period with large political and economic supported projects.

Compared to onshore wind, offshore wind farm allows the installation of turbines of both larger structural size and rated capacity. It can access more extensive sites with higher wind speed with lower turbulence. These obvious advantages have brought a large amount of commercial attention. On the other hand, harsh marine conditions and limited access to the turbines are expected to increase the cost of operation and maintenance (O&M). O&M costs make up 20-25% of the total lifetime cost of an onshore wind turbine [1], and a typical 500MW offshore wind farm normally spends the order of £25-40 million on O&M annually [2]. Maintenance consists of preventative and corrective maintenance, and accounts for the main proportion of the entire O&M cost. It is therefore important to find a way to reduce O&M costs, especially the maintenance component.

For reducing the cost for maintenance, one train of thought is to improve the maintenance strategy. One way is to apply condition-based maintenance as a planned preventative method and reduce the dependence on reactive maintenance as a corrective method since this usually costs more. Efficient condition monitoring has the potential to reduce O&M costs, but it is important to make sure the investment in condition monitoring system is worthwhile. The indicative cost for a condition monitoring including Supervisory Control and Data Acquisition **(**SCADA) system is in the order of £0.4-0.8 million for a typical 500MW wind farm per year [3]. It is relatively cheap if compared with the overall O&M costs but still considerable for the entire turbine life time. A promising approach is to use information from the SCADA system as much as possible so as to reduce the costs of any additional condition monitoring hardware.

For studying the cost effectiveness of condition monitoring, cost and operational data are important. However, being a new technology in energy generation, wind farm operational data are generally kept confidential by manufacturers and wind farm operators, especially for offshore ones. The lack of historical cost and operational data (especially the failure rate) from offshore wind farms makes it difficult to investigate the reliability and undertake the desired cost effectiveness analysis.

This chapter covers the novelty of the research in Section 1.1, overview of the thesis in Section 1.2 with a process diagram highlighting the main research points, and publications in Section 1.3.

1.1 Novelty of the research

In this situation, this thesis has investigated accessible SCADA and failure data from a large onshore wind farm and SCADA data from selected offshore wind farms, and innovatively created a series of indirect analysis methods to overcome the data shortage including an onshore/offshore failure rate translator and a series of methods to distinguish yawing errors from turbine nacelle direction sensor errors. Another novelty of his thesis is that it has creatively applied this failure rate translator to a Failure Modes Effect Analysis (FMEA) for ranking component risks for offshore wind turbines to fill this gap in research domain. This data translation approach has been used to improve and further develop an existing O&M cost model. The extended cost model (called StraPCost+) has been used to establish a relationship between the effectiveness of reactive and condition-based maintenance strategies. The cost model has also been benchmarked against a number of cost models already in the commercial or academic use and this has demonstrated it to be reliable and practical. The cost model has then been applied to assess the O&M cost effectiveness for three offshore wind farms at different operational phases including planning phase.

This thesis provides detailed background to the subject including a comprehensive literature review. It develops and applies innovative methods to modelling O&M and the impact of condition monitoring. Particular highlighted topics include current condition of offshore wind energy, the state of art condition monitoring techniques and costs, a detailed introduction of the cost model developed in this thesis, and the methodology of other cost models in both commercial and research domains with detailed comparisons of model results.

1.2 Overview of thesis

Chapter 2 begins this thesis with a thorough review of the relevant literature including a comparison of onshore and offshore wind farms and their O&M requirements. It then presents a technical introduction to condition monitoring (CM) including the benefits, performance and costs. It lists the different condition monitoring techniques in use. Finally, this chapter reviews the current situation as regards turbine and component failure rate and provides the motivation of the failure rate analysis developed in this thesis.

Chapter 3 begins with a technical introduction to the actual wind farms used in this thesis. It then provides a detailed environmental and generational analysis of an offshore wind farm that is investigated in detail in this thesis. This chapter principally presents a series of yaw error and turbine nacelle direction sensor error identification methods developed in order to improve the interpretation of operational data. This technique filters the data with misleading failure information and improves the data reliability for the further failure rate analysis and cost effectiveness analysis in the next chapters.

Chapter 4 investigates wind turbine component reliability. It presents a method of failure rate translation from onshore to offshore data that is developed and used in this thesis, and discusses its wider potential for application, in particular, the translation of an FMEA component risk ranking from onshore to offshore. It quantifies for the first time the risks associated with key component ranks in an offshore operational context.

Chapter 5 comprehensively introduces the cost model developed and improved for offshore wind farm performance and O&M cost estimation. This chapter begins with

a detailed technical introduction to the existing cost model. A number of other cost models in the research and commercial domain are reviewed, and compared with this existing model. The next section presents the improvement of the original cost model, called StraPCost+, including the application of the onshore/offshore failure rate translator developed in Chapter 4. This chapter then compares the StraPCost+ with other accessible cost models by an offshore wind farm case study, and discusses the results. As an innovative function among all cost models, StraPCost+ provides estimation of condition-based maintenance. This chapter then presents a series detailed condition monitoring system detection effectiveness analyses from StraPCost+. The last section in this chapter presents a series of sensitivity analyses to examine the impact of changing key factors: the wind and wave parameters, the weather window threshold, overall turbine annual failure rate, condition monitoring detection statuses and distance to shore.

Chapter 6 presents two real site case studies using StraPCost+, with comparison of other cost models. It firstly provides the analyses on an existing offshore wind farm and demonstrates the reliable applicability of StraPCost+. After that, it presents a case study aiming to provide estimates on a planned offshore wind farm, which shows the potential practical use of StraPCost+ in term of assisting decision making for vessel planning.

Chapter 7 concludes this thesis and proposes areas of the potentially useful future work.

Chapter 8 lists the references used in this thesis.

A series of Appendices are presented at the end of the thesis. Appendix-A presents the wind farm statistics. Appendix-B presents results for the cost model analysis. In the

thesis content, the citation from appendix is given an indication after the table number of “a” for Appendix-A, and “b” for Appendix-B.

A progress diagram for the main points in this thesis is presented in the next page for better understanding of the coherence of each research point.

Figure 1. Process diagram for the research points in each chapter in this thesis

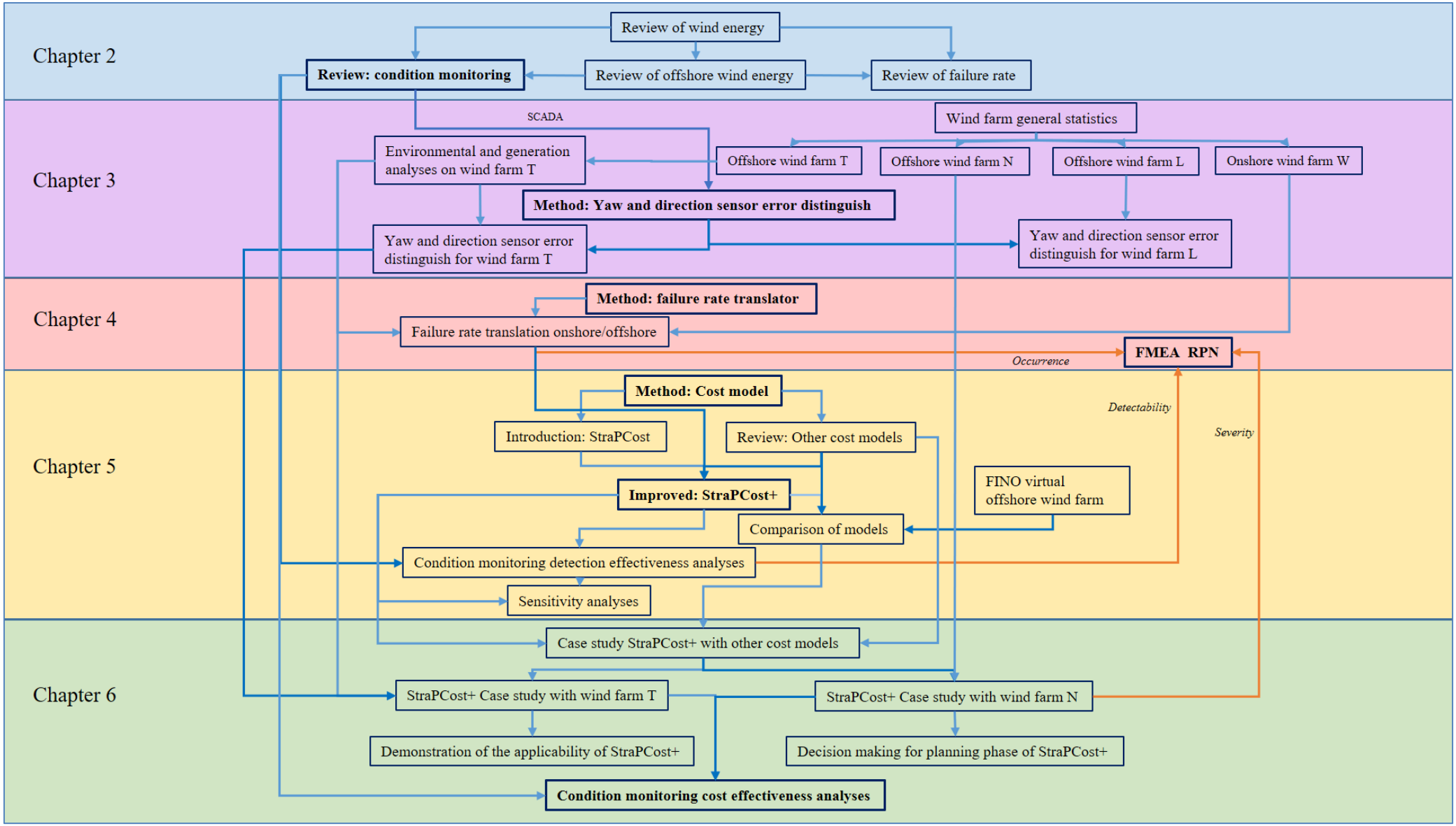

1.3 Publications

[1] Yu X., Martin R., Infield D., Barbouchi S. and Seraoui R., Determining the Applicability of Onshore Wind FMECAs to Offshore Wind Applications, ***EWEA*** *Offshore*, 20th Nov 2013

[2] Yu X., Infield D., Barbouchi S. and Seraoui R., Numerical Methods for Applying Onshore Failure Rate to Offshore Operational Conditions and Assessing the Benefits of Condition Monitoring, ***AWEA*** *2015*, 18th May 2015

[3] Yu X., Infield D., Barbouchi S. and Seraoui R., Adjusting Onshore Failure Rate Data for Cost Effectiveness Analysis of Wind Turbine Condition Monitoring Offshore, *ACSEE2015*, 11th June 2015 (with Oral Presentation)

[4] Yu X., Infield D., Barbouchi S. and Seraoui R., A numerical method to transfer an onshore wind turbine FMEA to offshore operational conditions, *RENEW2014*, 24th Nov 2014 (with Oral Presentation)

[5] Yu X., Infield D. and Maguire E., Wind direction error in the Lillgrund offshore wind farm in *Renewable Power Generation Conference (RPG 2013), 2nd IET*, 9-11 Sept. 2013 (Oral Presentation)

[6] Yu X., Yue H. and Leithead W. E., Feed-forward pitch control of HAWT using LIDAR, *EAWE 2012*, 12-13 Sept. 2012

Chapter 2 Literature review

In order to have a general understanding of the motivation and the issues investigated in the later contents; this chapter provides a thorough literature review with topics of wind energy, offshore wind, condition monitoring and failure rate.

In Section 2.1, the review of offshore wind, it lists the top ten largest operating offshore wind farms in the world, compares the environmental and technical difference between the onshore and offshore wind farm.

In Section 2.2 of condition monitoring, it introduces the main categories of maintenance strategies in use, introduces the benefit of condition monitoring, and lists the different condition monitoring data acquisition and processing techniques in use.

The last section in this chapter, Section 2.3, reviews the current situation of component failure rate which motivates the failure rate analysis undertaken in the next chapters.

2.1. Review of Offshore Wind

This section presents a general review of onshore and offshore wind farm, introduction of wind turbines, comparison between onshore and offshore wind energy, and the current situation of offshore wind energy development in the world and in Europe.

2.1.1 Wind farm

A wind farm is a site that consists of a number of wind turbines, installed onshore or offshore. Both onshore and offshore wind farms have been rapidly increasing their generating capacity in the past decade. Wind energy delivered in total 3.4% of the world's electricity in the year 2014 [4]. The world's largest onshore wind farm can have as many as multi-thousand turbines. For example, Gansu wind farm, China, has installed more than 3,500 turbines with a current capacity of over 6GW [5][6]. Offshore wind farms, on the other hand, seek enhancing the total capacity by not only increasing the total number of turbines but also having higher individual capacity of each turbine, e.g. 25 MHI Vestas 8MW turbine has been installed in the Burbo Bank offshore wind farm (DONG Energy), Liverpool Bay, UK [7].

With the large number of turbines, an onshore wind farm can have the total capacity of over several thousand Mega Watts. Onshore wind farms can be built in a wide range of different terrains such as mountainous areas, plains, coastal areas, desserts and even in Polar Regions. As stated above, many of the world's largest onshore wind farms are located in China and India. Led by Gansu Wind Farm, Muppandal wind farm in India that has 3000 turbines making up 1.5GW of installed capacity [8].

Offshore wind farms, on the other hand, are constructed in bodies of water, where the wind resource quality is better in terms of higher wind speed and lower wind turbulence. Dong Energy, Vattenfall and E.ON are leading operators in the offshore wind industry [4]. The leading countries for offshore wind farms are UK, Germany and Denmark [9]. By 2015, the London Array in UK, inaugurated on 4th July 2013, remains the world's largest operating offshore wind farm, with 175 Siemens SWT-3.6-120 wind turbines and 630MW total capacity [10]. This position is followed with 9 other top 10 operating offshore wind farms.

Table 1 lists the top 10 largest operating offshore wind farm in the world. It provides a series of technical details such as distance to shore, maximum water depth, wind farm area, number of turbines, turbine type, installed capacity and commission year. The location country clearly shows that all of these largest offshore wind farms are located in Europe. 7 out of 10 are within the UK. In the next section, it continues discussing this table in the perspective of wind turbine types.

Table 1. List of top 10 largest operating offshore wind farms in the world by 2015

No.	Wind farm	Location country	Distance to shore	(Max.) Water depth	Area	No. turbine	Turbine type	Installed capacity	Commission year	reference
1	London Array	UK	27.6km	0-25m	100km^2	175	Siemens SWT-3.6-120	630MW	4th July 2013	[10]
2	Gwynt y Môr	UK	18km	12-28m	86km^2	160	Siemens SWT-3.6-107	576MW	2015	[11]
3	Greater Gabbard	UK	32.5km	20-32m	146km^2	140	Siemens SWT-3.6-120	504MW	2012	[12]
4	BARD Offshore 1	North Sea, Germany	90-101km	40m	59km^2	80	BARD 5.0	400MW	2013	[12]
5	Anholt	Denmark	22.6km	15-19m	116km^2	111	Siemens SWT-3.6-120	400MW	2013	[13]
6	West of Duddon Sands	UK	20.1km	17-24m	67km^2	108	Siemens SWT-3.6-120	389MW	2014	[14]
7	Walney	Cumbria, UK	19.3km	19-28m	28km2	102	Siemens SWT-3.6-107	367.2MW	phase 1: 2011	[15]
			22km	25-30m	45km^2				phase 2: 2012	
8	Thorntonbank	North Sea, Belgium	27.9km	18-28m	1 km2	6	Senvion 5MW	325MW	phase 1: 2009	[16][17]
			28.2km	12-24m	12km^2	48	Senvion 6.15MW		phase 2: 2012	
			28.1km	12-26m	7km^2				phase 3: 2013	
9	Sheringham Shoal	Greater Wash, UK	21.4km	15-22m	35km^2	88	Siemens SWT-3.6-107	315MW	2012	[18]
10	Thanet	Kent, UK	17.7km	20-25m	35km^2	100	Vestas V90-3MW	300MW	2010	[19]

2.1.2 Wind turbine

A wind turbine is the device that extracts energy from the wind and converts it into mechanical energy, and then electrical energy. Wind turbine can rotate both horizontally and vertically, known as horizontal-axis wind turbines (HAWT) and vertical-axis wind turbines (VAWT), respectively. The power from an onshore wind turbine is usually less than offshore ones mainly because of the quality of wind, and it usually encounters more noise and visual issues. Offshore wind turbines can be over 6MW. Vestas and Siemens are the two largest wind turbine suppliers worldwide, followed by GE Energy, Goldwind and Enercon [4]. From the 10 largest offshore wind farms, as shown in Table 1, 7 out of 10 are using Siemens wind turbines. This indicates that Siemens wind technology is presently favoured by European large offshore wind farm developers. In this thesis, the main wind farms with accessible data are using Siemens 2.3 MW rated wind turbines, for both onshore and offshore. This coincidence has proved that this type of turbine is widely utilized in Europe. The consistency of the turbine type for onshore and offshore has provided the possibility and eased the development of onshore/offshore failure rate translation introduced in Chapter 4.

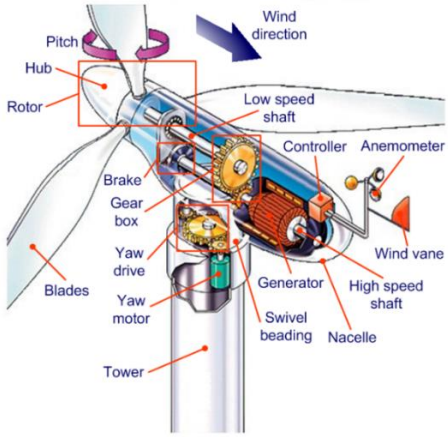

Figure 2. Typical wind turbine structure with detailed drive train system in the nacelle [20]

One example is the drive train system. The complexity of the drive train system increases the frequency and cost of maintenance. A conventional wind turbine drive train mainly consists of a low-speed shaft, gearbox, brake, high-speed shaft and generator, as shown in Figure 2. Alternatives to a traditional gearbox arrangement are direct drive and hybrid drives in which a low ratio gearbox is combined with a multi-pole generator. One major branch in direct drive is permanent magnet generators (PMGs).

Direct drive system removes the intermediate link, the gearbox, to improve the turbine availability, and hence to reduce the total maintenance cost. Figure 3 shows a low speed direct drive from an Enercon turbine, whose rotor hub is mounted on the fixed axle [21]. To avoid the complexity and thus the high failure rate of the gearbox, wind turbine manufacturers such as Siemens and GE have been devoting themselves into the development of direct drive turbines. The share of direct drive turbines has increased from around 16% in 2006 to 26% in 2013 [22]. However, since direct drive is still a new concept to wind turbine generation, some research shows that the economic benefits for direct drive turbines are unclear or even lower than the gearbox-driven ones [23].

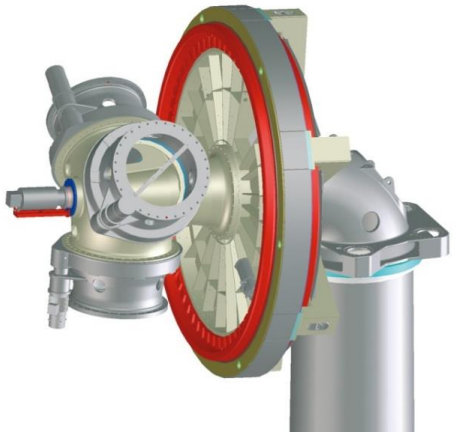

Figure 3. Image of a direct drive of E-48 from Enercon [21]

The hybrid drive system is in the middle route between the conventional gearbox drive train and a direct drive system. It uses a gearbox with a reduced number of stages which improves efficiency and reliability and uses intermediate, not high speed generators. Companies such as Gamesa use multiple permanent magnet induction generators, as shown in Figure 4 [24].

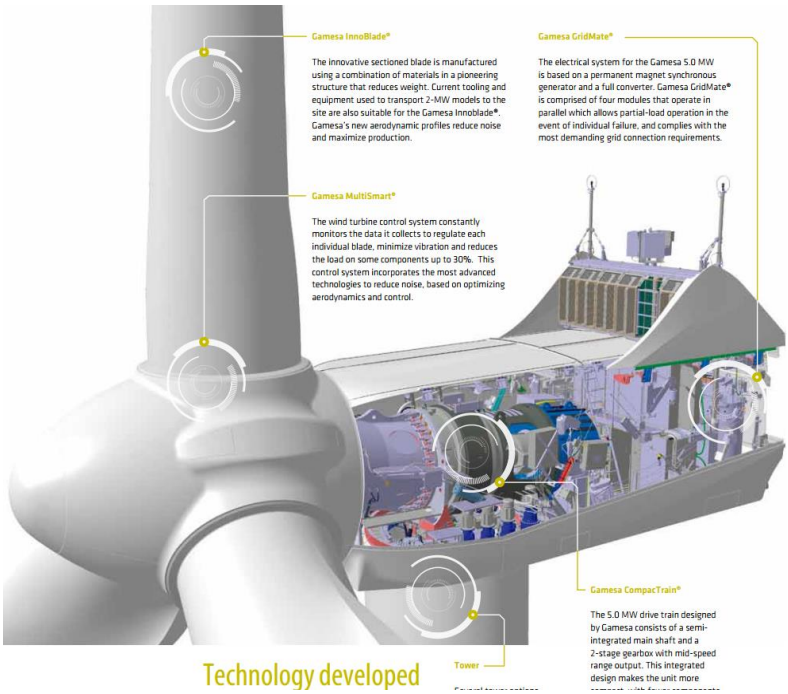

Figure 4. Hybrid drive system with multiple PMGs turbine from Gamesa [24]

The different designs of drive train outlined above provides an example of wind turbine component design improvement aiming to reduce the failure rate cost and enhance the reliability. From the trends outlined, direct drive arrangement with a large multi-pole (usually PMG) is steadily developing and taking over from conventional geared turbines for large offshore wind turbines. EDF, for example, has selected the Haliade® (GE-Alstom) direct drive 6MW turbine for their French offshore sites [25].

2.1.3 Offshore vs. onshore

No matter from technical or cost perspective, there are significant difference between onshore and offshore wind farms. Over the years, the debate of installing the cheaper easy-maintenance onshore wind farm or the less-visual-pollution higher-output offshore wind farm has never stopped. Compared to onshore wind, the offshore wind has rather different characteristics. For example, the total electricity production is generally higher since wind speeds are higher, and they are also more persistent which adds value to the electricity generated. From the environmental perspective, offshore wind farms are more exposed in extreme weather conditions, waves and corrosion due to salt water. In addition, the marine environment makes maintenance much more difficult than onshore, which leads to longer down time and lower availability. In addition, offshore maintenance and repair is more expensive due to the cost to go offshore.

Table 2, as first presented in [26], lists the benefits and disadvantages of both onshore and offshore wind farms, and some of the disadvantages address the issues that the O&M might encounter. O&M costs for offshore wind could be higher for more challenging offshore sites further from shore. Preventive condition based maintenance can help to reduce this cost by doing inspection and maintenance before the catastrophic failure occurs.

Table 2. Comparison of characteristics offshore vs. onshore [26]

	Offshore	Onshore
Site related and technological characteristics		
Specific electricity production	High (due to high average wind speeds)	Generally lower than offshore
General restrictions	Water depth, nautical routes, nature reserves, distance from the coast	Wind exposure, residential areas, nature reserves
Environmental conditions	Rather strong and steady wind speeds, salt water and salt spray, waves, extreme weather conditions	Lower, less steady and more turbulent winds than offshore due to surface roughness
Access conditions	Erection only during calm wind and sea conditions, restricted access (e.g. for trouble shooting, maintenance), potentially long distances	Erection at calm wind conditions, road access required, transport of rotor blades more challenging than offshore, but maintenance easier
Environmental impacts	Visual impact & noise of little relevance, potential impacts on sea birds and migrating birds, impacts due to foundation and grid connection	Visual impact and noise often highly relevant
Grid connection	Long distances to coupling points, condition monitoring necessary, separate licence procedure(s), weak costal grids	Low to medium distances, grid integration less problematic because wind farm size smaller
Economic characteristics		
Major cost drivers	Turbines, foundations, grid connection and transformer station	Foundations and grid connection less costly
Capital need	High	Low compared to offshore
Risks	High, lack of insurance	Low compared to offshore
Income	Governmental support schemes, partly with extra incentives for offshore wind	Limited governmental support schemes
Organizational aspects		
Planning and licensing procedures	Huge national differences, often complex and time consuming	Different procedures but can also be time consuming
Grid connection	Close coordination with grid operator essential (especially when grid expansion required)	Coordination also important but less critical
Project size	Large	Generally smaller than offshore
Number of different parties/subcontractors	Large, more complex project management	Smaller, less complex
Further particularities	Field work/schedules highly dependent on weather and sea conditions, availability of e.g. vessels may cause bottlenecks	Lower dependencies compared to offshore

2.1.4 Offshore Wind Energy Development in Europe

Europe, led by Asia, holds the second position in terms of installed onshore and offshore wind capacity, with 35.8% of the world's wind power capacity and 23.7% of the 2014 global installations [4]. The trend of European wind energy installation is moving from onshore to offshore. By the end of 2015, a total capacity of around 11,027MW has been installed with 3,230 offshore wind turbines in 84 offshore wind farms across 11 European countries. 754 new offshore wind turbines with total capacity of 3,019 MW in 15 wind farms were fully grid connected and 14 projects were completed in 2015. In addition, there were 6 projects under construction with an expected capacity of 1.9 GW. This will bring the cumulative capacity in Europe to over 12.9 GW [28][9][27]. Figure 5 shows the cumulative and annual installed offshore wind capacity in Europe from 1993 to 2015 [9].

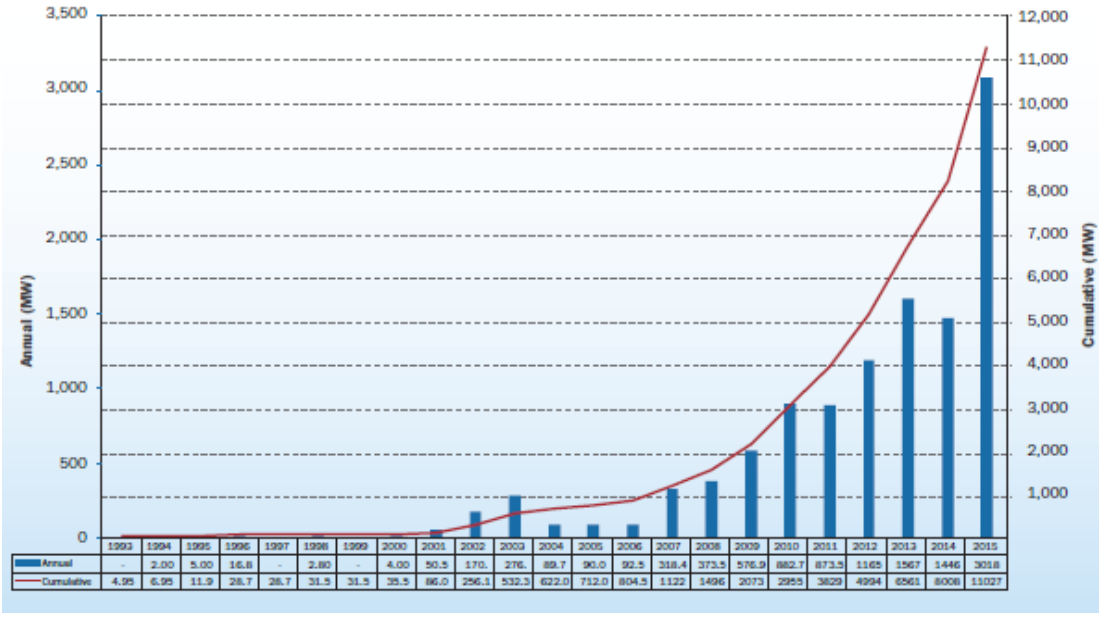

Figure 5. Cumulative and annual offshore wind installation in Europe to 2015 [9]

The size of turbines has been increased rapidly over the last 15 years. With a slight drop in 2014, this figure soars to double the previous year in 2015. By the end of 2015, the average offshore wind turbine size became 4.2 MW, the average offshore wind farm size was 337.9 MW with large offshore wind farms such as Gwynt y Môr and Gemini of 576 to 600 MW [9]. The average water depth was 27.2 m, and the average distance to shore was 43.3 km [9][28].

The UK presently has the highest installed offshore capacity with 5,060.5 MW, accounting for 45.9% of total offshore capacity in Europe, as shown in Figure 6. The offshore market in the UK has been enlarged rapidly during this period due to political and economic support.

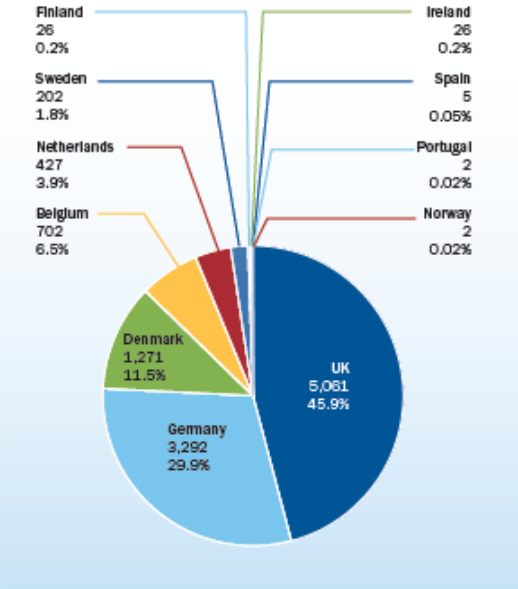

Figure 6. Installed capacity-cumulative share by European country 2015 [9]

The offshore wind industry has received dramatically increasing investment since 2010, as shown in Figure 7 [29]. Total investments in offshore wind in 2015 were more than €18 billion, of which the industry raised €5 billion of non-recourse debt *, equivalent to 1.3 GW of gross capacity [9].

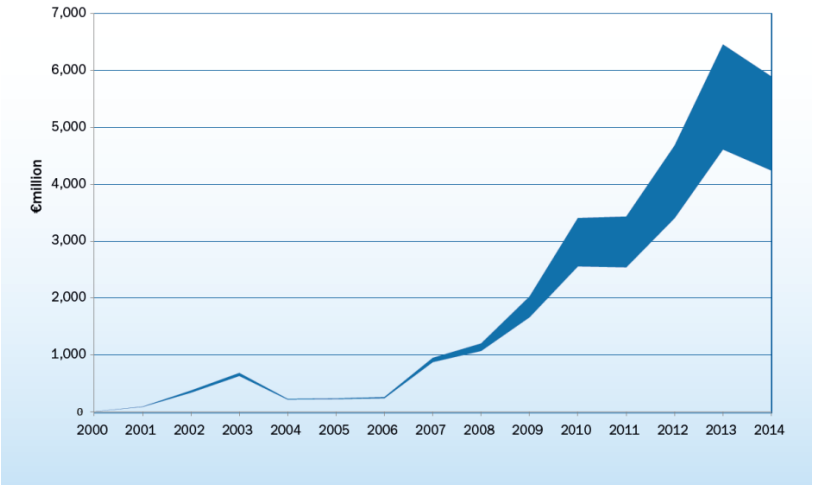

Figure 7. Estimated range of annual investments in offshore wind farms [29]

* Non-Recourse Debt: A type of loan that is secured by collateral, which is usually property. If the borrower defaults, the issuer can seize the collateral, but cannot seek out the borrower for any further compensation; even the collateral does not cover the full value of the defaulted amount.

2.2. Condition monitoring

With the current development of offshore wind farms, especially when the distance to shore is getting larger, maintenance is becoming one of the key issues for offshore wind energy. Condition based maintenance, with its technical and economic benefits, has attracted an increasing number of researches in both commercial and academic field.

In this section, a brief introduction of basic categories of maintenance strategies currently used in wind energy is presented. Condition based maintenance, as one of the rising maintenance strategies, is introduced here with a list of state-of-the-art data acquisition techniques for both SCADA based and additional sensors based techniques. Corresponding data processing methods for these two main acquisition types are then introduced.

2.2.1 Maintenance strategy

The aim of maintenance work is to achieve high turbine availability while at the same time keeping operating costs as low as possible. Unplanned outages should be avoided where possible. Maintenance strategies can be basically categorized into reactive and preventive strategy from a high level perspective.

Figure 8 is a plot of remaining component life time against operating time showing different maintenance interventions. For simplicity, the life time is divided by mean time between failures (MTBF) of the component [30]. Here lists the definition of the maintenance strategies.

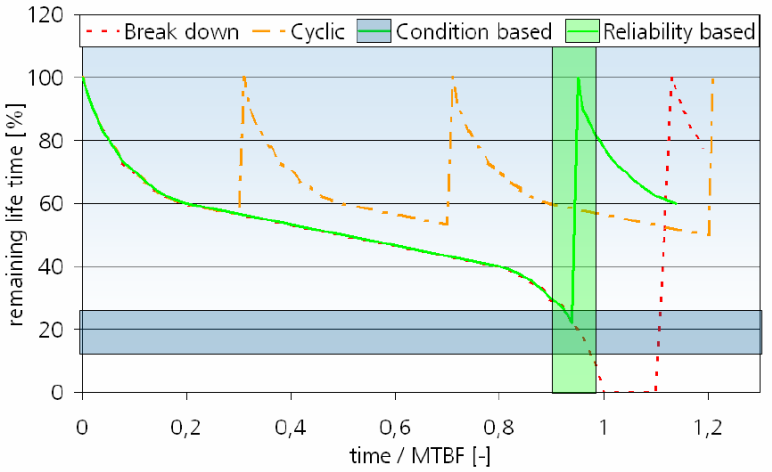

Figure 8. Comparison of different maintenance strategies with remaining life time against mean time between failures (MTBF) [30]

Break down maintenance, also recognised as reactive or corrective maintenance, is the simplest case where the system is kept operating until a major failure of a component occurs that results in the turbine being shut down. Once the component is repaired or replaced, the remaining life time is assumed in theory to return to 100% for the replaced component. Even though in reality, the life time of the component can hardly reach 100%.

Cyclic or periodic maintenance is a planned preventive maintenance strategy in which components get maintained after a fixed period of time irrespective of their actual condition.

Reliability based maintenance aims to find the “right” time for maintenance by assessing the state of health of the turbine drawing on judgement based on past experience of reliability functions. Shown with vertical shading (green) in Figure 8, reliability based maintenance traces the MTBF and connects it with probability of failure occurrence.

Condition based maintenance aims to identify the best time point for repair by monitoring the real time condition of key components. Shown by horizontal shading (grey) in Figure 8, condition based maintenance identifies the point when the remaining life time of the component drops below a specified level.

Both reliability based and condition based maintenance aim to find the optimum maintenance point, and have some overlap in terms of the approach taken to identify this. For example, in condition based maintenance analysis, reliability data is also an important input and reference. As shown in by Figure 9, reliability based maintenance is more efficient when components have frequent failures with short downtimes; whereas condition based maintenance is more efficient when applied to components that seldom fail, but which result in large downtimes. Some components with low failure rate and short downtimes which have little impact on the entire system can be ignored in the maintenance strategy making stage [30], as shown in the middle part of the figure.

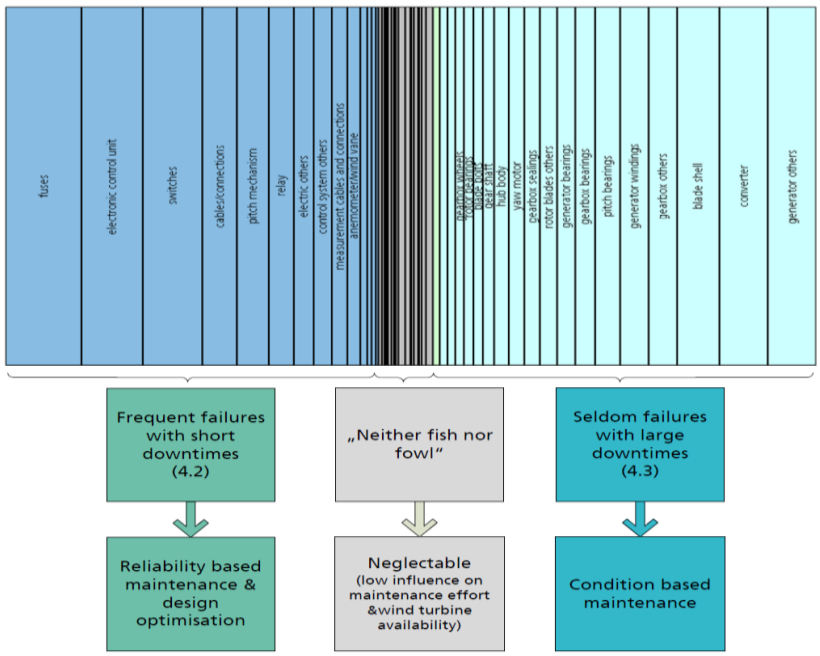

Figure 9. Wind turbine subsystem reliability share on annual downtime [30]

Since the reactive maintenance requires the failure occurs to shut the turbine down, the maintenance required is usually heavy repair or replacement. For an offshore wind farm, the heavy maintenance related failure not only causes high repair or replacement costs, but also increases the transportation cost dramatically for unscheduled vessel usage. In addition, because of the safety regulation, the vessel has to wait for a restricted weather condition which leads to longer waiting time and thus longer down time and higher loss of production. From the personnel point of view, because the reactive maintenance is unscheduled, the wind farm needs to have the number of technicians required stand by for heavy maintenance during normal operational days in case of the urgent heavy maintenance, which causes considerably more personnel costs. In addition, because the reactive maintenance is unscheduled, the maintenance action may be incomplete within one visit. This increases both the vessel cost and the waiting time for the next suitable weather condition.

Preventive maintenance, on the other hand, gives the wind farm opportunity to hire the vessel with a much lower rate and schedule the maintenance with acceptable weather in advance. This largely reduces the waiting time and increases the chance to complete maintenance in one visit. It doesn't need a large number of technicians always waiting at site, and reduces the cost for technicians. Because preventive maintenance undertakes the maintenance action before the failure becomes severe, the maintenance level can be lower than the reactive one, which largely reduces the maintenance costs.

Periodic maintenance, undertaking maintenance no matter there is a failure or not, may incur cost on unnecessary inspection or maintenance in terms of vessel hire and personnel. Condition based maintenance, on the other hand, can avoid the cost due to

the unnecessary planned visit by monitoring the turbine condition and only scheduling the maintenance when there is a need. However, most of the condition based maintenance requires additional sensing devices which increases the capital expenditures (CAPEX) and service cost. False positive is another drawback of condition based monitoring which causes unnecessary vessel and personnel costs. Therefore, the accuracy of the condition monitoring system is significant, and the cost effectiveness of condition monitoring requires investigation. Later chapters, especially Chapter 5 and Chapter 6, investigate these issues.

2.2.2 Condition monitoring—benefit, performance and cost

This subsection introduces the basics of condition monitoring, and lists the data acquisition and processing techniques for condition monitoring use.

2.2.2.1 Condition monitoring basics

Condition monitoring is defined as the process of detecting the condition of a machine or component by a number of separate or combined techniques and the resulting knowledge used for planning machine operation and maintenance in order to improve both safety and economy [31]. It is a major branch of predictive condition-based maintenance, which aims for maintenance to be undertaken shortly before actual failure occurs. More specifically, the condition monitoring system sends prompt feedbacks or alarms when a component is in danger of having a failure so the maintenance team can start to schedule the maintenance before it actually becomes severe. A lower-level maintenance decision can therefore be made. Compared to corrective maintenance and planned maintenance, condition monitoring can in principal prevent both the significant consequences of a major failure and also

unnecessary maintenance upon a component. Usually one or more indicators are used to show the condition of the certain component. Condition monitoring is widely used in conventional power generation and many other industrial processes with complex machinery are used. In wind energy, condition monitoring is believed to be beneficial from safety, economy and efficiency aspects.

The potential benefits of condition monitoring are to reduce the number of catastrophic failures, prevent the number of secondary damage, and the turbine downtime. Therefore:

- *the turbine and turbine components' life can be extended;*
- *productivity of the turbine can be improved;*
- *overhaul routines can be reduced and better scheduled;*
- *maintenance time can be better scheduled;*
- *secondary damage can be minimized;*
- *maintenance cost and therefore productive cost can be lowered;*
- *and operation safety can be enhanced. [32]-[35]*

2.2.2.2 Condition monitoring performance and cost

Condition monitoring has great potential to detect incipient failures which incur long downtimes and high costs in advance. Table 3 shows the estimates of failure rates and corresponding availabilities for subsystems of a generic onshore 1.5-2-MW 80-metre-rotor-diameter wind turbine [36]. This table shows that auxiliary equipment has the highest failure rate compared to other subsystems, whereas the rotor module has the lowest availability followed by the power module, the structural module, auxiliary

equipment and the drive train module. The condition monitoring system itself is not 100% reliable and has also been included as a component in the table.

Table 3. Failure rates and availabilities of sub-systems [36]

Wind turbine Subsystems	Mean Time to Repair of Total (%)	Normalised Failure Rate (%)	Normalised Availability (%)
Wind Turbine Generator （Total）	14.83	100.0	-
Auxiliary Equipment	1.72	35.4	99.73
Rotor Module	42.83	26.5	95.30
Power Module	10.83	15.2	99.29
Nacelle Module	1.91	9.2	99.92
Control and communication system	3.26	4.4	99.94
Structural Module	16.80	3.9	99.72
Drive Train module	6.89	3.4	99.90
Wind farm System	0.49	1.7	99.99
Condition monitoring system	0.43	0.2	99.99

Because of the harsh environmental conditions experienced by offshore wind farms and high cost of the offshore O&M, as indicated in previous sections, condition monitoring can be specifically beneficial to offshore wind farm operators.

Actual data describing the performance of CM systems in identifying wind turbine faults is difficult to find before 2013. A presentation at EWEA 2013 from GL [37] listed has provided some important results.

Table 4, taken from this work, shows the results of a validation study covering different wind turbines. This table lists predicted failures and the CM system detection performance for wind farms in different countries. It indicates that the turbines located in A have the highest CM true alarm rate whereas Irish based case C have the lowest true alarm rate. The UK based installation E has the highest false alarm rate while those located in Italy, Ireland (case C) and UK (case D) have 0 false alarm rates during the period assessed.

Table 4. Results of validation study on condition monitoring [37]

Site	Location	Operational data set years	Predicted failures	Actual failure	True detections	False detections	Score True/False
A	Italy	4.8	7	8	7	0	88%/0%
B	Ireland	6.0	7	8	6	1	75%/13%
C	Ireland	6.5	1	4	1	0	25%/0%
D	UK	7.0	5	6	5	0	83%/0%
E	UK	2.5	7	10	5	2	50%/20%

As introduced in Chapter 1, the indicative cost for condition monitoring and SCADA system is in the order of £400,000 to 800,000 for a typical 500MW wind farm per year (1% to 3% of the typical total annual O&M cost) [3]. That is to say, a wind farm with from 63 to 217 turbines (with turbine capacity of from 2.3MW to 8MW to share the 500MW) spends in the order of £8 to 16 million for CM and SCADA system for 20 years running time, and this cost is from £1,800 to 4,000 (with 2.3MW turbines) to £6,300 to 12,700 (with 8MW turbines) per turbine per year.

The cost of CM systems is confidential and varies from different CM companies. The main commercial CM system suppliers are SKF, GE, Mita-Teknic, Brüel and Kjær Vibro, Gram and Juhl, and Romax. An incomplete and confidential investigation, as presented in Table 5.

Table 5. Incomplete and confidential investigation on CM costs from different companies

CM brand	CM hardware cost	CM service cost	Service duration	Number of turbines
Brüel and Kjær Vibro	$1,650,000		5	100
Gram and Juhl	$14,000	$37,000	20	1
Romax (before 2012)	£25,000	-	1	1
Romax (after 2012)	£5,000	-	1	1

This table shows that Brüel and Kjær Vibro charges roughly $1,650,000 for the CM hardware service for 100 turbines for 5 years; Gram and Juhl provides CM hardware for about $14,000 with a service fee of the order of $37,000 for 1 turbine over 20 years.

A noticeable progress in the CM market is that Romax has claimed that it has dramatically reduced the CM hardware price from £25,000 to £5,000 since 2012. This 5-times reduction in price implies a significant CM technique update. Attention needs to be made that these CM systems are focus the technology on the drive train.

2.2.2.3 Condition monitoring techniques

From the perspective of condition monitoring, data acquisition (hardware) and data processing (software) are equally important. This subsection lists state-of-the-art techniques for these two aspects, in Section 2.2.2.3.1 and 2.2.2.3.2, respectively. Even though this thesis places the emphasis on wind turbine reliability and CM cost effectiveness analysis mainly based on SCADA data, it is important to have a general view and understanding of the main techniques used in CM, which broadens the horizon when improving the wind turbine reliability and cost modelling methodology by considering more means of CM systems as inputs in future work.

The basic means of data acquisition in a wind turbine system is the Supervisory Control and Data Acquisition (SCADA) system. The complexity and data collection rate vary depending on the actual hardware and operational settings, where 10 minutes is the most common data record interval. Standards are starting to evolve covering SCADA system practicability, functionality, and also interoperability.

Commercial wind turbine condition monitoring also relies on additional sensors, such as vibration, lubrication oil quality, acoustic emission, shock pulse recording, thermography, ultrasonic testing, strain measurement and radiographic inspection [38]-[40]. There are a large range of data analysis and processing algorithms developed, in particular for vibration data analysis.

Data analysis and processing is the other main topic in condition monitoring, once the data have been acquired by the sensing systems outlined above. Data processing works in both slow- and fast-sampling-rate domains. SCADA systems usually have a slow-sampling rate (e.g. 10-minute interval), and additional sensors such as vibration, fast power measurement, and power system harmonics, etc. usually have a fast-sampling rate (typically taking data at kilo-hertz). Fast data analysis techniques include Fourier analysis [41][42], its extensions [43], and wavelet analysis [44]-[46].

Because of the indispensable and relatively high accessibility of SCADA data, there is an increasing interest in further exploiting this resource for condition monitoring purposes. A number of data processing and machine health assessment techniques depending only on SCADA data have been published in recent years [47]-[58]. Recent research methodologies include Monte Carlo methods, Hidden Markov models, K-means, NSET (Smart Signal), Kriging, Artificial neural networks, Support Vector Machine and Gaussian Process theory [37][59].

The detailed introduction is presented below.

2.2.2.3.1 Data acquisition

This subsection lists the main data acquisition methods (hardware) of the condition monitoring system, in categories of SCADA system and additional sensors.

2.2.2.3.1.1 SCADA system

SCADA, fully named as Supervisory Control and Data Acquisition, is a type of industrial control system which can be applied in multiple sites and large distances. It consists of a series of sensors. In wind energy, SCADA system mainly acquires data

of wind direction, yaw direction, temperatures (including oil and key bearing temperatures etc), and power production. Techniques such as NSET, Neural Network, Support Vector Machine, Monte Carlo method, K-means, and hidden Markov etc., are well-developed mathematical data analysis methods in signal processing and machine learning area. They have been applied to the analysis of wind turbine SCADA data [37][59]. Techniques will be presented in the Section 2.2.2.3.2 in details.

2.2.2.3.1.2 Additional sensor systems

Different from SCADA system, additional sensor systems normally require additional hardware installed for specific wind turbine components, and require specific data processing for the corresponding hardware.

Vibration sensing system

The technique of vibration sensing in conventional rotating mechanical system has already been well developed and widely used. In wind energy, vibration sensors have also been introduced and employed for condition monitoring since the early days.

The main application of vibration sensors is in the gearbox and bearings (including bearings for the generator and the main bearing) [38][59][60]. Other devices, such as rotor [60][61], tower [62] and blades [63]-[65] have also been reported to be applied with vibration sensors.

Vibration sensing signals are mainly used in the frequency domain. For different frequency ranges there are different types of sensors [40]:

- *Position transducers are working in the low-frequency range, few Hz*
- *Velocity sensors are in the middle-frequency range, order of 0.1kHz*
- *Accelerometers are in the high-frequency range, ≥kHz*
- *and Spectral Emitted Energy (SEE) sensors are for the very high frequencies, which are normally considered as acoustic vibrations.*

Acoustic emission

Acoustic emission (AE) is the wave produced when an external stress applies on a material. AE sensors track the elastic waves which are transferred and analysed for early faults detection [66]. AE sensors are widely used for turbine blades [38][63][67], bearings [68][69], and gearbox [68][69]. The processing methods for AE is similar to the very high frequency vibration monitoring. Both of the systems can be solidly attached to the object to be monitored and settled with flexible glue [38][59]. Acoustic emission is specifically suitable for low-speed operation [68], therefore suitable for direct drive and hybrid drive systems.

Oil analysis

In both lubrication and hydraulic oil system, the chemical and physical conditions, which mainly are the wear particles, moisture, viscosity, oxidation level, acidity and temperature of the oil, are essential of the health of wind turbine components [39]. Oil analysis is suitable for the oil system in the gearbox, generator and bearing system [70]. The oil analysis can not only monitor the quality of the oil itself, but also monitor the health state of the turbine components that it contacts, by analysing the wear particles in the oil [40]. Oil analysis is mainly applied offline, where samples and lab equipment are required. However, online and inline oil systems are increasingly developed [70].

Both online and inline systems are continuous monitoring systems. The difference is the volume of the oil sample. Online system extracts a small amount of the circulated oil, whereas inline system samples the entire amount [71][72].

For the oil quality itself, the techniques are mainly applied offline, such as Karl Fischer water test [73], Capillary tube viscometer [74], rotary viscometer [75], and fluorescence spectroscopy [76] etc.. However, there is still potential for online application for some methods, such as Calcium hydride water test [77], photoacoustic spectroscopy (PAS) [78][79], and solid state viscometer [80].

For particulate analysis, on the other hand, it is more likely to be applied as online sensing methods, among which some have already been used as online sensors. The sensing parameters are source and composition, type of wear, and number of particles [70]. Inductively coupled plasma optical emission spectroscopy (OES) has been declared being used as an online system with detection limits of 10 μm [81]. Electromagnetic detection (EMD) is an in-use online/inline lubrication condition monitoring in conventional industries [70]. There are a number of techniques that have high potential to be used online: ferrography [82][83], fluorescence spectroscopy [84], particle counters [85], and radioactive tagging [86] etc.. However, the main in-use particulate analyses are still offline, such as scanning electron microscope (SEM) [87], atomic spectroscopy (AS) [70], inductively coupled plasma mass spectroscopy (ICPMS) [88][89], flame atomic absorption spectroscopy (FAAS) [90], and laser-induced breakdown spectroscopy (LIBS) [91] etc.. Microfluidics Lab-on-a-chip technique also has a potential use in oil particulate analysis.

Shock pulse method

Shock pulse method (SPM) as a condition monitoring method for rolling bearings has existed since 1966. The principal of shock pulse method is that when a roller in a bearing contacts a damaged area or debris, mechanical shocks are then generated [92]. The SPM takes the normalized maximum shock value as the only simple measurement. This eliminates the data interpretation required in many other methods [93]. These shocks have a frequency in range of 35-40 kHz, which avoids the machine component resonances [92]. This technique is implemented on a periodic basis.

Thermography

Thermography is often used for electronic and electrical condition monitoring; while one particular branch, the infrared camera, is also frequently used for blade crack visualization. Traditional thermography operates offline, but the recent imaging technique allows the system operating online. The thermography is categorized as passive and active methods. The passive thermography compares the temperature of the investigated object and the ambient; whereas the active method applies external stimulus to receive the thermal reflection [38][40][94][95].

Ultrasonic testing

Ultrasonic testing (UT) are based on Doppler Effect, where an ultrasonic wave is emitted to the investigated object, shifted and reflected by the defect. The transmit time and the amplitude of the ultrasound is measured. The former is used to determine the distance between the defect and the transducer, while the latter determines the severity of the defect. The ultrasonic testing is usually applied to the wind turbine blades and

tower for surface and subsurface structural defects [59][96][98], while some research also shows a use of ultrasonic for electronic convertors [97] and rotors [39].

Strain measurement

Strain gauges are suitable for wind turbine components under high stress level, such as blades and rotors [40]. The techniques in use are Fibre-optic Bragg Grating (FBG); however optical fibre sensors are still very expensive. The drawback of the strain measurement is that the strain gauges are not robust, therefore it is usually used for assessing wind turbine lifetime prediction and blades stress level [40][99].

Radiographic inspection

Radiography is a non-destructive method usually by using Gamma radiation. There are also reports indicating using neutron radiography for defect analysis. Both methods can be used in 2D mode or 3D mode. Radiographic inspections are undertaken offline by a portable unit. The device measures the defect by the different levels of absorption of the X-ray photons applied on the surface of the material. Radiography is used for blades in wind turbine technology, however is not often used [100][101].

2.2.2.3.2 Data analysis and processing algorithm

Once the data have been acquired by sensing system indicated above, analyses and processing algorithms are applied to these data. Data processing covers both slow and fast sampling rate. Slow sampling rate is usually for SCADA (e.g. 10-minute interval), and fast sampling rate which refers to sensors such as vibration in kilo-hertz is usually used for fast power measurement, power system harmonics etc.. In this subsection, fast sampling processing is presented first, followed by SCADA analysis.

2.2.2.3.2.1 Fast data analysis

Standard Fourier analysis and extensions

Standard Fourier analysis and its extensions have played an important role in frequency domain analysis. The benefit of using Fourier analysis is that the certain frequencies of interest can easily be identified and have their amplitude tracked. The fast-Fourier transform (FFT), for example, has been applied in gearbox and bearing monitoring [99][102], and to constant speed wind turbines where turbine vibrational modes are easier to identify [40].

There are mathematical extensions of the Fourier transform known as higher order spectra that can be applied. For example, the bispectrum is a statistic tool for measuring nonlinear phases coupled interactions [103], and it is promising in wind data processing.

Enveloping spectra are also frequently used in addition of Fourier analysis. In enveloping spectra signal processing, harmonics and fundamental frequency are added up inside a given filter range and enhance the information in the selected FFT range. This is the method to make the signals which are buried in noises shown. Enveloping is often used in bearing analysis [104]-[106]. The drawback of the enveloping spectrum method is the shape of the window will lead to Gibbs Phenomenon, where oscillations are generated when the log amplitude spectrum changes rapidly [107].

Wavelet analysis

Wavelet analysis provides an alternative to Fourier analysis. It is a time-frequency technique suitable to non-stationary signals. Wavelet analysis can be seen very close

to short time Fourier transform (STFT), but can provide more localized temporal, spatial and frequency information [108]. Wavelet analysis is widely used in diagnosis in wind turbine gears, bearings, and rotors [45][102]. This data processing method has been successfully applied to vibration and acoustic signals [46], and also power signals [102].

2.2.2.3.2.2 SCADA data analysis

Monte Carlo method

The Monte Carlo method is a probabilistically computational algorithm that relies on random sampling to obtain numerical solutions for complicated systems [109]. This method is usually used to investigate what the condition monitoring system fitted to a turbine might do in practice [54]. It is also used in analysis of wind hazard assessment, as in [110], for example. Monte Carlo method, as a mainstream of method used for wind farm cost estimation, is introduced in detail in Chapter 5 Section 2.

Hidden Markov models

Hidden Markov models (HMM) are statistical Markov models which are applied to a Markov process with unobserved states. It is a branch of dynamic Bayesian network. HMM has been applied for the wind dynamics prediction, bearing fault detection [56], power prediction [57], and wind farm residual variability [58]. Similar to Monte Carlo method, Hidden Markov model is also a mainstream method of wind farm cost estimation, and detailed introduction can be found in Chapter 5 Section 2. The two methods sometimes are combined for wind farm cost estimation [111].

Gaussian Process theory

The Gaussian process is a stochastic process in probability theory. It is an infinite-dimensional generalization of the multivariate normal (Gaussian) distribution [112]. The Gaussian process is widely used in conventionally industrial signal processing. It has been used as wind power forecasting method [113].

NSET (Smart Signal®--General Electric)

Nonlinear state estimation technique (NSET)—as Smart Signal in commercial application—is used to construct the normal operating model of the wind turbine generator bearing temperature. An estimate temperature at each time step is generated, and compared with the real measured temperature. When the residual between the estimate and the real data is different (usually larger) from the normal operating state, the assumption of a generator fault can be made. The non-linear operator used in modelling the data set can be as simple as the Euclidean distance between the temperature vectors [47][48].

Kriging

Kriging is an optimal two-dimensional interpolation based on regression of a random field. The Kriging method gives estimation error as Kriging variance. It has been applied to estimate power production [49]. Estimating power production of a turbine from surrounding turbines in this manner can give a reference against which performance should be assessed.

Artificial Neural Network

Artificial Neural Network (ANN) is —often called neural network for short—the data processing method which imitates biological nervous systems such as human brain. It requires a large data set for training process. The neural network connects artificial neurons by connectionist approach to computation. In wind energy, the ANN is usually applied in wind speed forecasting [114][115], and wind power prediction [116][117]. Estimating power production of a turbine in this manner can give a reference against which performance should be assessed.

Support Vector Machine

A support vector machine (SVM) is a supervised learning model which often used for classification and regression analysis. It is a useful model for wind speed [118]-[120] and wind power [53] forecasting sometimes combined with other algorithm such as Markov model [121]. These forecasts can be compared with actual operation to assess turbine health.

K-means

K-means clustering is a data mining method which partitions observations into the nearest mean (clusters). This clustering approach is applied for short-term wind power prediction [55].

2.2.2.3.2.3 Analysis of combination of SCADA and fast data

To obtain both the advantages of SCADA and fast data analysis, a new data processing technique combines these two data acquisitions. This combination can compensate the

shortage of data from the limited individual frequency range. For example, the investigated offshore wind farm T in this thesis is constructing Siemens SCADA systems combining with Gram and Juhl vibration sensors. General Electric (GE) has also developed a SCADA system with vibration data. The Flow project also has a research orientation of the combination of SCADA and vibration [122].

2.2.2.3.3 Conclusion

This subsection has reviewed the main techniques used in the area of condition monitoring in categories of data acquisition which requires the hardware and data processing which reflects the software. It shows that various additional sensing systems can provide more specific and more precise measurements for specific wind turbine components, but the additional hardware increases the cost of the turbine. Therefore, more recent research show interests in exploring additional information from SCADA data for CM use. Among the SCADA data processing methods, the time-based simulation Monte Carlo method and Hidden Markov models are most researched. These two methods are further introduced in Chapter 5 Section 2 for a better understanding in terms of the main-stream wind farm cost modelling in comparison of the analytical cost modelling used and improved in this thesis. To have both the benefit from the precise measurement of the additional sensing system and the wide accessibility of SCADA system, more recent work has paid attention on the analysis of a combination of the two systems.

2.3 Failure Rates

Component failure rate is highly relevant to any analysis of condition monitoring systems, and in particular for an assessment of the cost effectiveness of such systems; it is therefore a key research focuses of this thesis. There is regrettably limited access in the public domain to failure rate data for wind turbines, especially for those operating offshore. Even though such data is important for improving wind turbine technology, actual failure rate for offshore wind is almost completely unavailable to researchers.

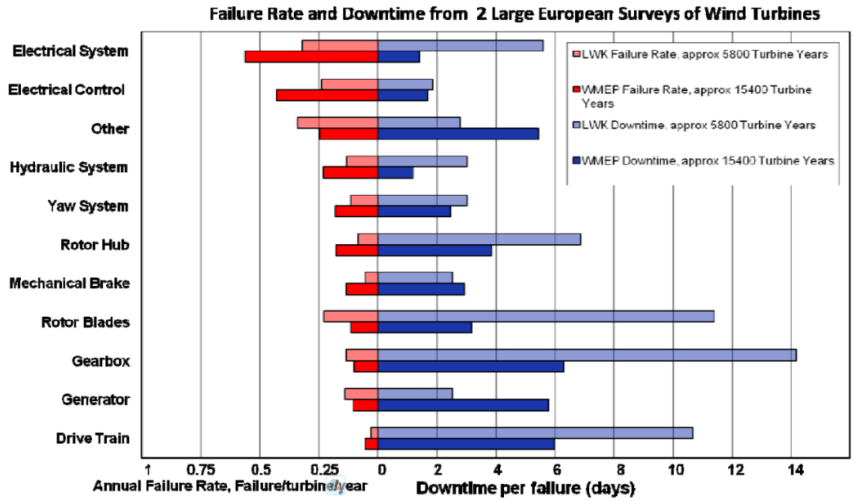

Figure 10. Failure rate and downtime of onshore wind turbines [123]

In this situation, a possible solution is to use the onshore information as a reference for the offshore wind turbine operation with an empirically based statistical analysis to compensate for the difference between onshore and offshore operational conditions. Some onshore wind turbine subsystem/component breakdown failure rate is available. Figure 10 shows the quantified failure rate and downtime of wind turbines from European onshore wind farms, taken from the European ReliaWind project [123]. From this result, the electrical system seems to have the highest failure rate over the

year, while the gearbox failure seems to cause the longest downtime. For offshore wind turbines, this downtime will be extended because of the marine conditions and the time taken for transportation of the maintenance crews.

Failure rate is not the only significant factor when considering condition monitoring. Electronic power converters have a high failure rate, for example, but they have a relatively low impact on turbine downtime thanks to straightforward repair and replacement, requiring no heavy lifting. In fact, at this time, there is no commercial condition monitoring systems for electronic components in wind turbines, due to the rapidity with which faults develop and the difficulty of failure prediction.

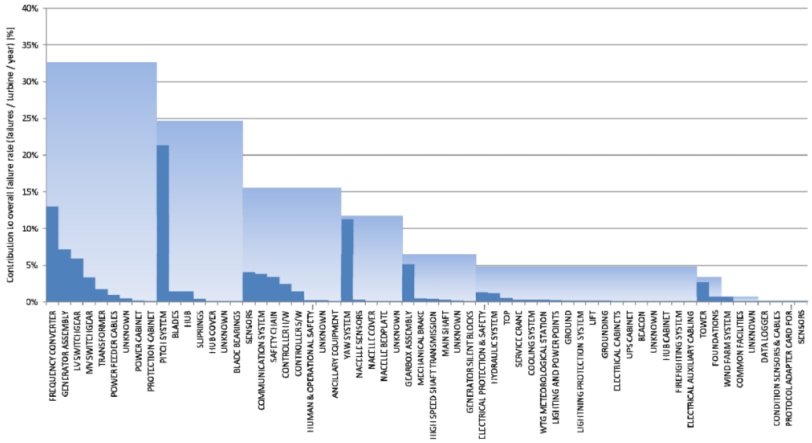

Figure 11. Normalised failure rate of sub-systems and assemblies for onshore turbines [123]

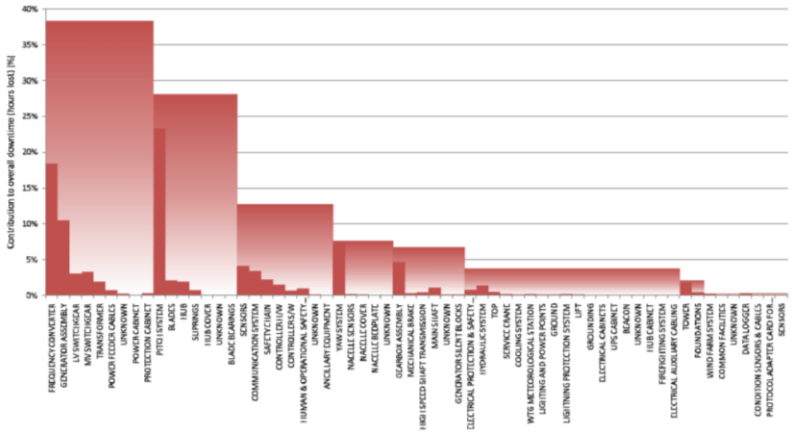

Figure 12. Normalised downtime of sub-system and assemblies for onshore turbines [123]

A further detailed contribution to total failure rate and downtime for a list of onshore wind turbine subsystems and assemblies is shown in Figure 11 and Figure 12 [123]. From these figures, the pitch system, frequency converter, yaw system, gearbox assembly and sensors are the components that fail the most, and they are more or less the same components which result in the longest downtime.

Unlike onshore wind farms, the offshore wind farm has higher installation costs and higher O&M costs due to the marine environment. Condition monitoring system hence should play a more important role in the offshore wind industry. As failure rate is an important input element for offshore wind cost analysis, considerable effort has been taken to understand the failure process for this thesis.

The high preliminary cost input of the condition monitoring system, together with recurrent costs for support of such systems, underpins the need for research to assess the cost effectiveness of the whole system that is the main research focus of this thesis. A statistical cost model is used and improved in this research [124]. The detailed introduction can be found in Chapter 5. As mentioned, O&M cost data are still protected by the wind industry, especially for the offshore. Failure rate is the key for modelling wind turbine conditions and costs, although limited failure rate data is available in the public domain. With indirect cooperation from the operators of the largest onshore wind farm in the UK, a three-year-period operational data record is accessible for this research, and translated for the offshore condition. Wind and wave parameters are calculated from the accessible offshore data and set as inputs of the cost model, the cost model compares the O&M cost of reactive maintenance and condition based maintenance. The original cost model available in [124] uses empirical failure rates based on onshore data and so cannot fully represent the offshore situation as

failure rates are expected to be affected by offshore operational conditions. To overcome this limitation, a mathematical translation of failure rate from onshore to offshore is applied to the operational data. The way this translation is calculated is sensitive to the way the relevant probability distributions are represented, and improved curve fitting approaches have been explored.

2.4 Conclusion

This chapter has reviewed in detail the current status of wind energy, the comparison of the advantages and disadvantages of onshore and offshore, and the condition monitoring system in terms of data acquisition and data processing techniques. It has addressed the operational challenges of offshore wind and listed the various approaches available for condition monitoring. It has highlighted the lack of data in quantifying the benefit of condition based maintenance for offshore wind, which calls for the development of the onshore/offshore failure rate translation method in Chapter 4.

The next Chapter investigates the wind farms with accessible data, and a data purifying process developed in this thesis will be introduced.

Chapter 3 Investigation of selected existing and planned wind farms

Before carrying out the analysis on no matter wind turbine reliability or cost effectiveness, it is important to have a close insight on the wind farms being investigated and to make sure the failure data used as inputs reflect real failures that cause production loss.

Power production loss, which is directly linked to revenue loss, is therefore one of the research concerns and can be used as a measure of system effectiveness. A detailed wind farm statistically based investigation for the main offshore wind farms analysed all through this thesis is presented. In SCADA, the "yaw direction" data are often recorded by a nacelle angle sensor which is not involved in the actual yaw control. The turbine nacelle direction sensor error therefore is shown to be often misleading and incurring the overestimation of the yaw error and even false positive of the yaw system which might cause unnecessary and expensive maintenance activities.

A methodology is introduced here to identify the turbine nacelle direction sensor error from actual yaw error in order to make sure the failure data fed to further analyses are the ones that actually caused production loss. This methodology is applied to wind farm T and wind farm L, in Section 3.2 and Section 3.3, respectively.

Section 3.1 introduces the technical data of all wind farms investigated in this thesis and presents a closer statistical analysis for wind farm T.

3.1. Wind farms in research

In this section, one onshore and three offshore wind farms have been investigated in some detail to provide an understanding of operational issues.

3.1.1 Wind farm general statistics

The onshore wind farm W, commissioned in 2009, is the largest onshore wind farm in the UK. It is located 15 km outside Glasgow and has a site area of 55 km^2. The wind farm has a total installed capacity of 539 MW and comprises 215 Siemens SWT-2.3-93 wind turbines.

The offshore wind farm T, commissioned in 2013, is located 1.5 km north off the coast in the north-east of England with site area of 10 km^2. The maximum water depth is up to 16 m. The wind farm has 27 Siemens SWT-2.3-93 in 3 rows with total installed capacity of 62MW.

The offshore wind farm L, commissioned in 2008, is the largest Swedish offshore wind farm and is located 10 km off the coast of southern Sweden. The maximum water depth is 4-8 m and the average annual wind speed is in the range 8-10 m/s. The wind farm has 48 Siemens SWT-2.3-93 wind turbines in 8 rows with a total installed capacity of 110 MW.

The large offshore wind farm N was in its planning process to be located 14.3 km from shore in the south of England. The maximum water depth was 32-53 m. The planned site area was 155 km^2. The project was awarded by the Crown Estate in 2010. The preferred wind turbine was the V164-8MW from Vestas. However, by the date this

thesis was editing, it was announced that the planning had been refused. Detailed analyses and estimation of this planned wind farm are in Chapter 6 Section 2.

3.1.2 Statistics of wind farm T

In this section, wind turbine environmental and wind farm operational statistics of wind farm T are presented. It can be seen as a typical procedure of the wind farm environmental investigation.

3.1.2.1 Wind Rose

The wind rose is a statistical tool to show the distribution of the wind incoming direction and wind speed at the wind farm location for a selected period of time. Because of the lack of met mast data, wind roses for individual turbines have been calculated using nacelle directions, and compared to present a general view of the wind quality over the wind farm. Figure 13 shows one typical wind rose of each row in wind farm T. The results are from a full 6-month SCADA data set dating from 1st October 2013 to 1st June 2014. Southwest is the clear prevailing wind direction as would be expected at this UK location, with the range of 185-260 degrees accounting for most of the data.

The first/front row of this wind farm is the nearest row to the shore, and comprises turbines WTG19 to WTG27. From the wind rose, the first row shows a stronger wind cluster coming around 185 degrees, and less strong but more distributed wind cluster coming from 210-240 degrees.

The second row has stronger wind coming from the direction sector 210-240 degrees. It still has the strongest wind cluster from around 185 degree, but it has less strength than in the first row.

The third row changes the highest wind strength to 240 degrees and has generally stronger wind than the first and second row. It is hard to perceive any significant wake effect in these results and the differences are most likely related to distance from the shore.

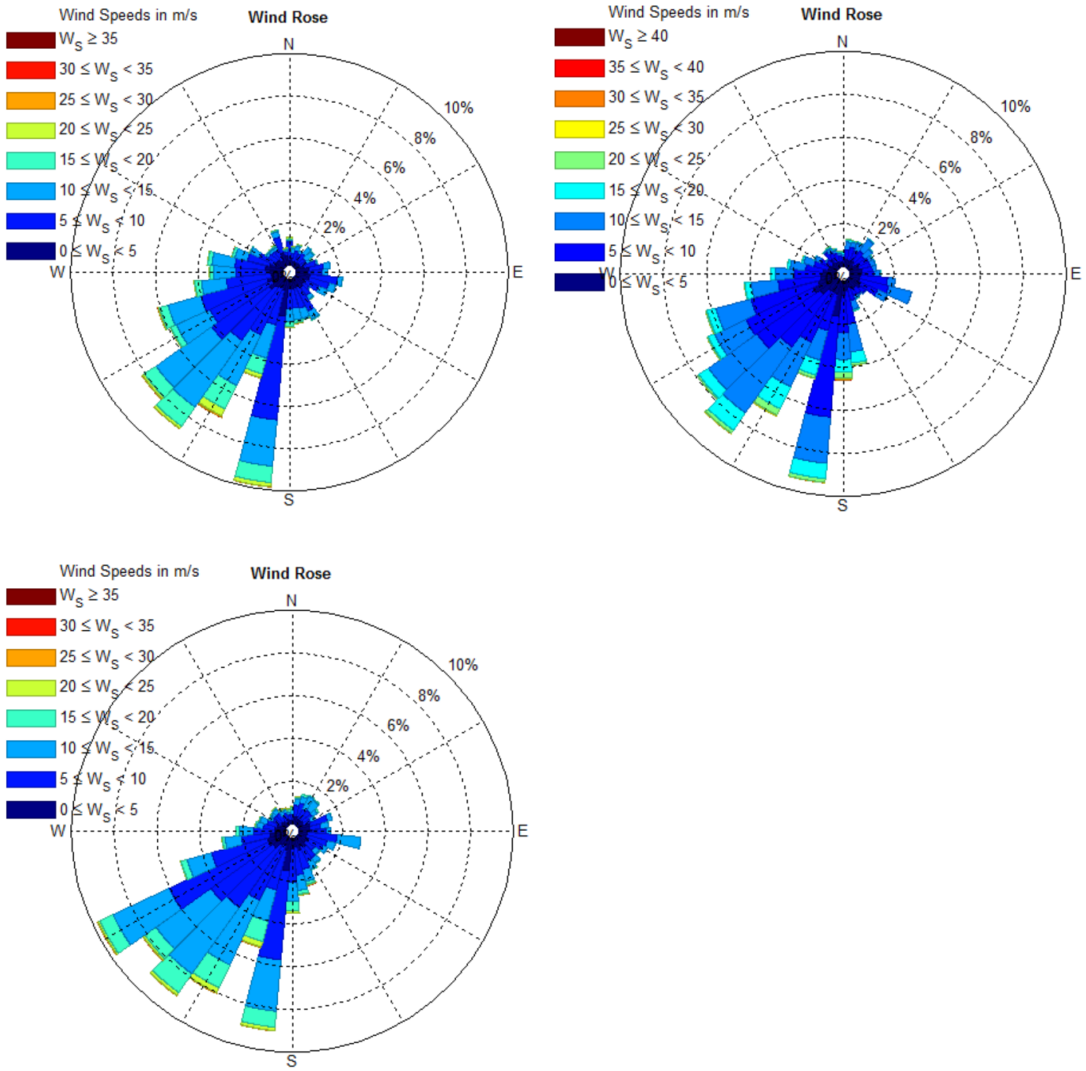

Figure 13.Typical wind rose from first row (upper left: WTG 26), second row (upper right: WTG16) and third row (lower: WTG9) of wind farm T

3.1.2.2 Wind speed distribution

Wind speed distribution is based on the wind speed data of the selected period taken from the nacelle anemometers. It summarises the wind exposure of the wind farm. Figure 14 shows the frequency distribution and the Weibull distribution fitted to the wind speed data taken from a typical wind turbine in the front row (WTG26). The fitted Weibull scale parameter, *C*, is 10.13, and the shape parameter, *k*, is 2.34. It shows the highest probability of wind speed occurs at around 8-9m/s, with a probability of approximately 1.8%. The wind speed concentrates mainly in the range of 5-12m/s. The detailed wind parameters at different location in this wind farm can be found in Chapter 6 Section 1.

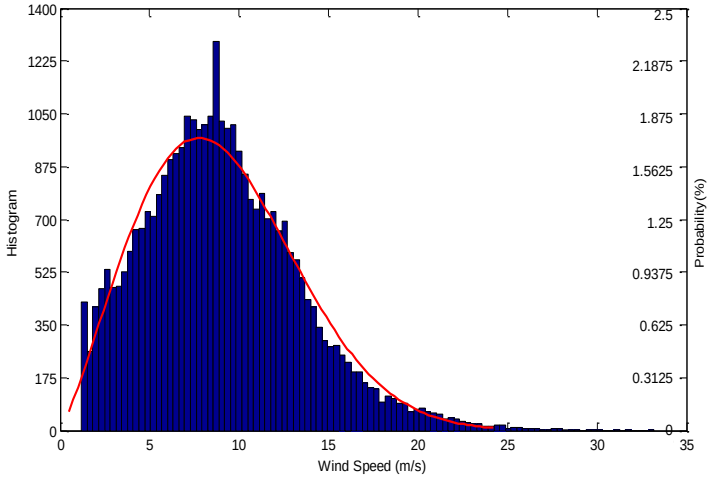

Figure 14. Histogram and Weibull distribution of wind speed from a typical wind turbine (WTG26) of wind farm T

3.1.2.3 Turbine availability

Turbine availability is an important parameter indicating the turbine operational condition. It is here calculated on the basis of the proportion of "Faultless" entries in "WpsStatus" record in the selected SCADA data. As indicated by the turbine status

flag instruction, "Faultless" condition is assumed to be the normal operational condition. As shown in Table 6, WTG3 has the highest availability, with 85.9%. WTG18 and the potential problematic WTG8 have the lowest availabilities, with 8.4% and 10.1%, respectively.

Table 6. Wind turbine availability calculated by the "Faultless" in "WpsStatus" for wind farm T

Ranking	Turbine	Availability
1	3	85.9%
2	16	83.2%
3	12	73.8%
4	13	73.5%
5	26	69.8%
6	21	68.2%
7	7	65.5%
8	5	64.1%
9	23	63.4%
10	2	62.2%
11	25	60.7%
12	15	54.2%
13	9	52.5%
14	24	50.1%
15	6	49.5%
16	20	48.3%
17	11	39.2%
18	22	38.9%
19	17	37.8%
20	4	37.6%
21	19	36.5%
22	27	27.6%
23	10	25.4%
24	14	25.1%
25	1	15.4%
26	8	10.1%
27	18	8.4%

3.1.2.4 Turbine Capacity Factor

The capacity factor is a further indication of turbine availability and operational performance. It is defined in Equation 1 below.

$$Capacity\ Factor = \frac{\sum Energy\ Yield}{\sum Time \cdot Rated\ Power} \quad (1)$$

In contrast to the "WpsStatus" calculation for turbine availability, the capacity factor integrates the actual power generated by the individual wind turbine. It divides the results by the rated power output (2300 kW, and multiplies the time, as shown in Equation 1. Since under certain circumstances, turbine active power can be negative (i.e. it is drawing power from the grid), $\sum Energy\ Yield$ calculates the total amount of positive power generated during the selected period of time. Invalid values are all removed.

The total number of the entire SCADA time stamps indicating the total generation time is used in this calculation. This sets every turbine on the same basis.

Table 7.Wind Turbine capacity factors and ranking for wind farm T

Rank	Turbine	Capacity factor
1	3	43.6%
2	16	41.4%
3	26	39.0%
4	25	36.7%
5	9	36.7%
6	11	36.5%
7	21	34.7%
8	23	34.7%
9	13	33.7%
10	7	33.3%
11	5	30.2%
12	2	30.1%
13	15	29.6%
14	24	28.5%
15	6	25.9%
16	12	24.5%
17	17	24.1%
18	22	24.0%
19	19	22.5%
20	4	21.1%
21	20	20.5%
22	10	18.3%
23	14	17.5%
24	18	16.5%
25	27	14.8%
26	1	14.0%
27	8	6.3%

From Table 7, it can be seen that WTG3 has the highest capacity factor, with 43.6%, whereas the majority of the turbines in this wind farm have a capacity factor of around 30%. The problematic turbine WTG8 has only 6.3% during the selected period of time. WTG18 which has the lowest availability also has a low capacity, with 16.5%.

This result shows that less than half of the turbines in wind farm T are within the range of annual capacity factors expected for large European offshore wind farms such as Horns Rev 2 and wind farm L which comprise the same turbine type (Siemens-2.3-93), with capacity factors of 46.7% and 35.1%, respectively, [125]-[127]. Apart from the fact that it is the first year of operation which normally have a much lower availability than the average; it can also be accounted for by the fact that wind farm T is very close to the shoreline.

3.1.2.5 Array efficiency

Array efficiency, as a preparatory indicator for wake effect analysis, is a further step of the wind farm investigation. According to the wind rose, the major effective wind direction is in a range of 185-260 degrees. The front row in this case is the row of WTG19-27. The array efficiency is calculated within this direction range. Because of its poor behaviour, WTG8 is not considered in the calculation. The period selected is when all turbines are in full operation, which means this is when they are not being curtailed, shut-down or having invalid values in the SCADA set.

The calculation is shown in Equation 2 [128].

$$Array\ Efficiency = \frac{mean\ power\ generated\ by\ the\ selected\ row(s) in\ selected\ period}{mean\ power\ generated\ by\ the\ front\ row\ in\ selected\ period} = \frac{mean\ capacity\ factor\ of\ the\ selected\ row(s)\ \ in\ selected\ period}{mean\ capacity\ factor\ of\ the\ front\ row\ in\ selected\ period} \quad (2)$$

Table 8 shows the array efficiency of each row compared with the front row. The array efficiency of the second and third rows (*Rest Total*) relative to the front row is 86.62%. This result is between the reference wind farms Horns Rev (87.6%) and wind farm L (77 %) [125][129][130]. A simple estimation of the overall array efficiency can be made since the named first row is almost always the first to see the wind with the directions indicated by the wind rose. In this case the overall efficiency can be estimated from (100%+91.12%+81.56%)/3 = 90.9%.

Table 8. Array efficiency when compared with selected row groups for wind farm T

Compared row	Array efficiency
Second row	91.12%
Third row	81.56%
Rest Total	86.62%

3.2 Yawing error and turbine nacelle direction sensor error identification for offshore wind farm T

Operation of the wind turbine yaw system can directly affect power generation. Moreover, persistent operation with a large yaw error increases the fatigue loads and can lead to premature failure of the turbine. However, the existence of measurement error by the turbine nacelle direction sensor (which turns out to be quite common) can create the illusion that the turbine yaw system is not operating properly. SCADA data often does not include the yaw error signal generated by the wind vane located on the turbine nacelle that is used for yaw control, so it is not easy to check for correct yaw operation. Often, a turbine with turbine nacelle direction sensor error shows misalignment of the yaw system with the wind incoming direction, but in fact the yaw system is functioning well. This generates potential problems of not only false alarm signals but also can result in inappropriate maintenance. Therefore, to distinguish turbine nacelle direction sensor error from actual yaw problem is an initial step for the research in this thesis.

Wind farm T, with the most accessible data and thus as the main wind farm under analysis, is investigated thoroughly in this section. The SCADA data used was recorded every three seconds and averaged over ten minutes for the 6-month period introduced in the previous section. This section provided the first methodology innovatively developed in this thesis which filters the failure data fed to the wind turbine reliability analysis in Chapter 4 and cost effectiveness analysis in Chapter 5 and 6.

3.2.1 Methodology

In order to investigate and distinguish the turbine with a yaw problem and/or with a turbine nacelle direction sensor error, a multi-tier analysis approach is created comprising four main methods: animation, time series analyses, power curve and overall diagnosis.

A visual tool has been created that presents the SCADA apparent yaw direction from each turbine and shows them continuously in an animated wind farm map [131]. This helps not only engineers but also non-technical employees to easily read and initially identify the potentially problematic turbines by comparing their directions with the alignment of nearby turbines. Therefore, attention can be concentrated on specific turbines for further analyses. This technique has practical value, especially for wind farm with large number of wind turbines.

After the general view of the wind farm has been gained, time series of local wind speed, yaw angle and active power are generated and compared with emphasis on the identified time period with potentially problematic turbines.

A power curve is generated for each wind turbine using the selected SCADA data for comparison with the nominal power curve from the manufacturer.

The overall diagnosis compares and considers all the results comprehensively and presents the conclusion of the investigation. This result is relatively reliable and can be used as basis for planning wind turbine inspection by the wind farm operator.

3.2.2 Animation

The animation is a visualization tool designed to check the wind turbine apparent yaw directions and their evolution in time. In this animation method, each frame indicates the apparent yaw direction of each turbine at the given time stamp. The time stamp number is shown at the top of the frame. Each turbine is represented by a black dot placed at the turbine location in the wind farm map. Blue arrows indicate the real-time apparent yaw direction of each turbine with written angle in degrees shown above each black dot. Figure 15 shows example snapshots of the animation interface. To assist interpretation of the animation statistical tables, bar charts and graphs are also presented.

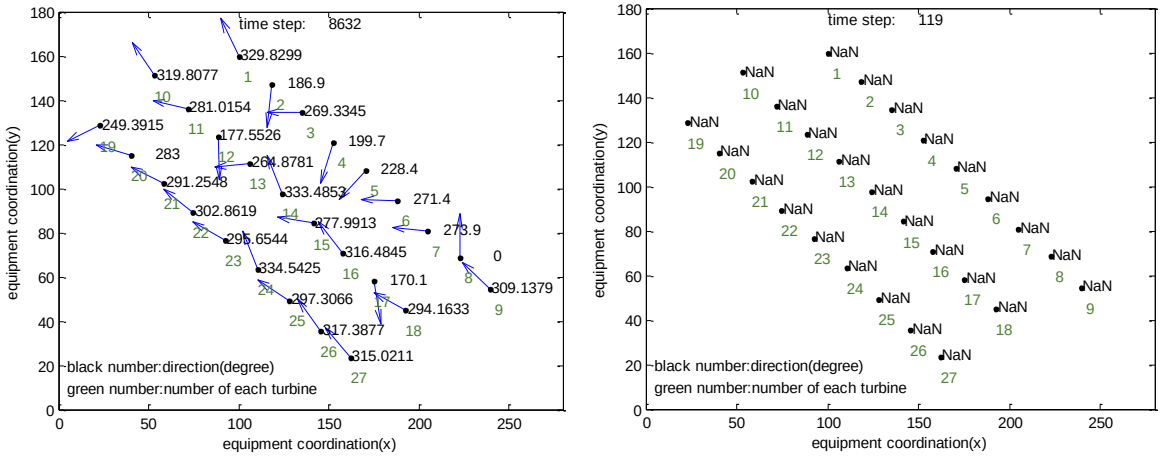

Figure 15. Snapshots of yaw angle animation with regular running mode (left), and with invalid value mode (right) of wind farm T

In theory, because of the small size of the wind farm and the fact that turbines are located relatively close to each other, the yaw directions at any time should be similar for the normal operational wind speed. The yaw effect should only cause slight differences between rows, depending on changes in wind direction and the dynamics of the yaw controllers.

For this particular wind farm, met mast data are not available from the operator. However, met mast data can be important as it provides a relatively reliable reference for wind speed and direction that can be used to characterise the performance of the wind farm.

Invalid values shown as “Intf shut” and “I/O Timeout” appear in the SCADA data for every turbine with different frequencies and at different times. They provide important information and can make the identification of problematic turbines difficult. Their statistics are calculated, listed and compared in this section. It is observed that for certain period of time, some turbines have no yaw angle value displayed, and for other periods of time, some turbines show a persistent value of “0”. From this initial observation, the shown value”0” is suspected to be another form of SCADA error such as “Intf shut” or “I/O Timeout”. More investigations have been undertaken later.

The selected SCADA data provides a useful picture of the wind farm operational condition. The total numbers of 34993 data records contain around 3% invalid values (“Intf shut” or “I/O Timeout”). These “Intf shut” or “I/O Timeout” can be simply planned outage or loss of communication, and have been removed for later analyses. In the initial investigation, for better understanding of the wind farm operation, they were kept for the animation. Figure 15 (left) shows a snapshot of the animation with normal data values, compared with a snapshot of invalid values (denoted in the figure as NaN) on the right.

Statistics show that every turbine has a total invalid value period of approximately 1076 time stamps. Combined with the animation, it shows that the majority of the invalid numbers begins at the earliest 100 time stamps. All turbines show high

synchronization indicating a SCADA system-wide problem. Figure 16 (upper) provides a bar chart showing the number of invalid values of each turbine.

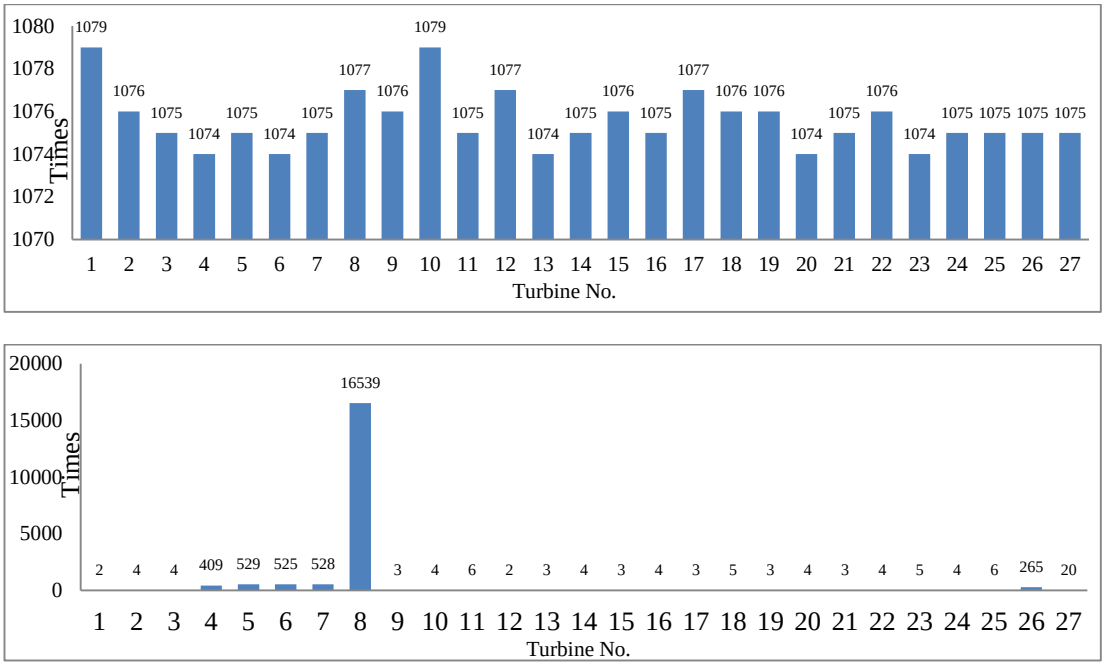

Figure 16. Bar charts of invalid value (upper) and "0" value (lower) of each turbine yaw direction with selected 6-month SCADA from wind farm T

Consistent with the animation, apart from the invalid values, some of the turbines also show a high frequency of "0" values. As shown in Table 9, WTG 4, 5, 6, 7, 8 and 26 have "0" values at more than 100 time stamps, among which turbine WTG 8 shows 16539 time-stamp "0"s. This accounts for over 48% of the total operation time of WTG 8. Figure 16 (lower) provides a bar chart showing how much "0" entries make up of each turbine's operational time.

Table 9. Number of "0" degree of each turbine yaw direction with selected 6-month SCADA from wind farm T

No. Turbine	1	2	3	4	5	6	7	8	9	10	11	12	13	14
No. 0	2	4	4	409	529	525	528	16539	3	4	6	2	3	4
No. Turbine	15	16	17	18	19	20	21	22	23	24	25	26	27	
No. 0	3	4	3	5	3	4	3	4	5	4	6	265	20	

Instead of being the actual geographic direction, the "0" value is suggested to be a form of wind turbine stoppage or yaw system fault signal (similar to "Intf shut" and "I/O Timeout"). The SCADA report shows that when the "0" value occurs at "YawDirection", it also occurs for other variables including the "ActivePower".

Table 10. Longest stoppage yaw direction angle (°) and percentage of time of each turbine with selected 6-month SCADA from wind farm T

Turbine No.	Direction (°)	Stoppage (stamps)	Percentage (%)
1	213.3	9473	27.93
2	103.9	3030	8.93
3	146.7	1887	5.56
4	199.7	2875	8.48
5	228.4	3530	10.41
6	271.4	3530	10.41
7	273.9	3530	10.41
8	0	16539	48.76
9	187.5	1331	3.92
10	230.1	3463	10.21
11	224.9	4606	13.58
12	23.7	3403	10.03
13	167.7	854	2.52
14	199.1	2728	8.04
15	156	1512	4.46
16	190.2	1742	5.14
17	222.8	6968	20.54
18	180.5	6454	19.03
19	190	7899	23.29
20	319.7	4679	13.79
21	168.1	4439	13.09
22	173.1	3744	11.04
23	143.5	853	2.51
24	285.7	5593	16.49
25	194.3	3023	8.91
26	185.2	2172	6.40
27	286.9	2516	7.42

Table 10 shows the longest stoppage of the yaw direction signal (i.e. a fixed and constant yaw angle), the length of the stoppage and the percentage of the total operational time. From this table, it can be seen that turbines have a longest stoppage ranging from 2.5% (WTG13) to 48.7% (WTG8) of the respective entire operational time. More detailed results of each turbine are listed in Table 1a in Appendix-A showing stoppages that are longer than 10 time stamps. The longest stoppage can

reflect turbine nacelle direction sensor or yaw errors at certain angle, e.g. the “0” degree for WTG8, and therefore should be investigated in the actual site by the wind farm operator.

Generally, from the animation, as the example snapshot in Figure 15 (left) shown, WTG 8, 12, 17, 19 indicate a constant direction difference with the neighbouring turbine and turbines in the same row. Other turbines such as WTG 2, 15 and 24 have occasional apparent yaw angle difference compared with others in the same row. These turbines are suggested to have direction or yaw errors, and they are going to be analysed with emphasis in the further process, e.g. time series and power curve, in this chapter.

3.2.3 Time series of local wind speed, yaw angle and active power

The time series of local wind speed (measured by the nacelle anemometer), yaw angle and active power provide further important information on turbine operation, as shown in Figure 17 to Figure 19. The colour code is shown in Figure 17. These figures show an initial high level impression on the wind turbine performance in this wind farm, and more detailed analyses on individual turbines have been undertaken from here. Some turbines show abnormal records of local wind speed (most apparent as constant values over several days), but on the whole there is a high degree of correlation between turbines.

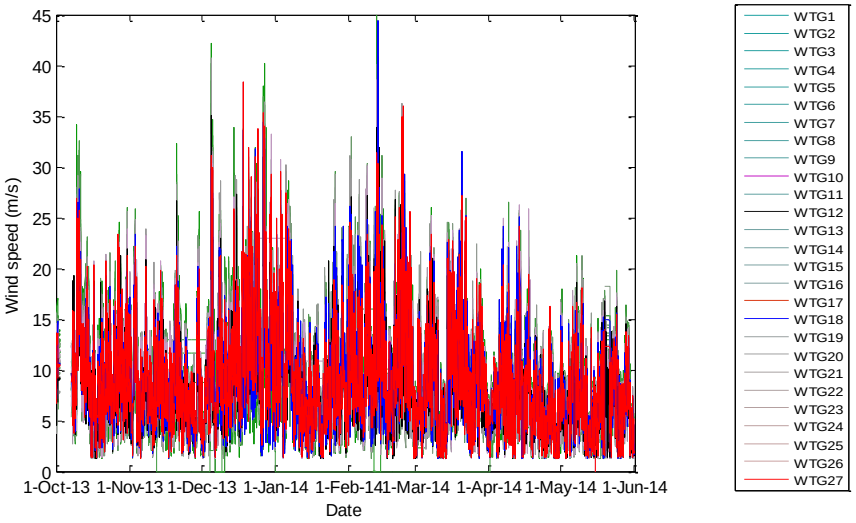

Figure 17. Time series of local wind speed with selected SCADA from wind farm T

The time series of yaw angle sees a range of angles for certain turbines, and also prolonged constant values. It is also clear that some wind turbine yaw angles are significantly offset from the whole group but follow the same broad temporal changes, suggesting possible wrong calibrations of the yaw sensors.

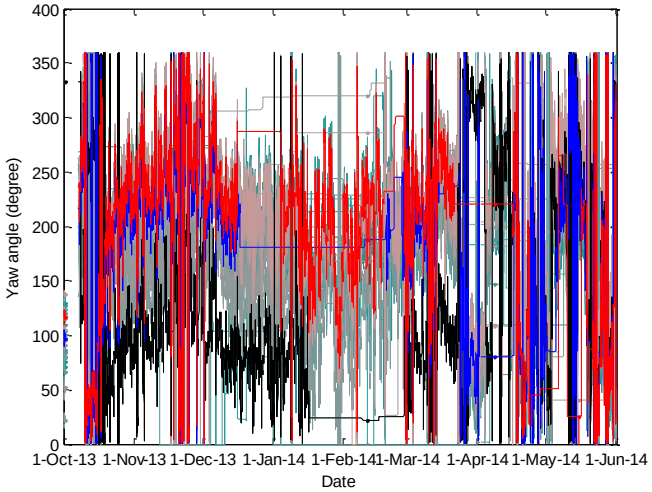

Figure 18. Time series of yaw angle with selected SCADA from wind farm T

Without curtailment flag available in the SCADA data, the time series of active power shows fluctuations with prolonged periods at rated power output that might be expected during high winds, but also extended periods of curtailment and also

stoppage (or loss of data). Separate time series graphs are shown in the later content and Figure 1a in Appendix-A.

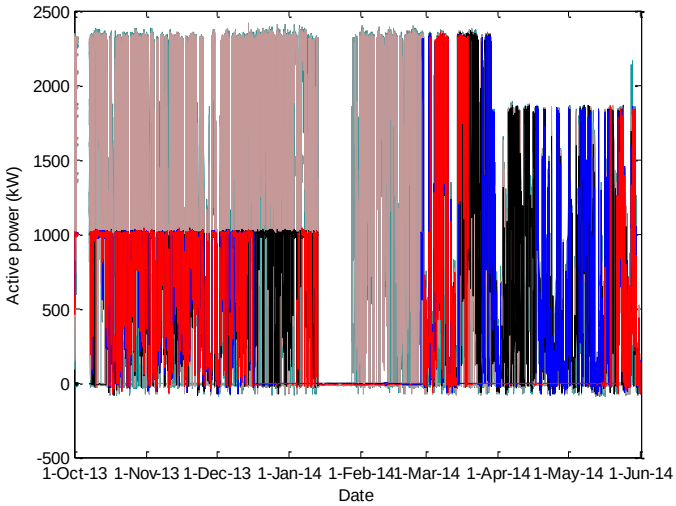

Figure 19. Time series of active power with selected SCADA from wind farm T

Figure 20 compares time series of local wind speed (top row), yaw angle (middle row) and active power (bottom row) of the selected WTG 8, 12, 17 and 19 (left to right column) which have been found with potential problems from the initial animation view. It indicates that WTG 8 has serious abnormal performance recorded in terms of both local wind speed and yaw direction. Its active power time series shows it experiences a long period of stoppage. It might have encountered a long period of shut down or loss of communication, which requires further investigation by the wind farm operator. WTG 12, 17 and 19, on the other hand, have relatively healthy records of local wind speed. WTG 12 has a relatively healthy yaw angle record and two levels of extensive curtailment and stoppage in power time series. As circled in red in Figure 20, the yaw time series shows WTG12 had yaw activity around mid of October 2013, whereas the power time series shows no power production during that period. Similar situation occurred at the end of January 2014 for WTG17. WTG 19 has abnormal records at the latter half of the yaw angle time series, one level of curtailment and

extensive stoppage in the power time series, but the consistency of yaw activity and power production suggests the health of its yaw and direction sensing systems.

Figure 1a in the Appendix-A shows the comparison graphs of WTG 2, 15, 20 and 24, where partially abnormal behaviour in the animation is shown. As circled in red, WTG2 shows yaw activity but no power production at the end of January 2014. WTG15 has three suspicious periods: from the end of December 2013 to beginning of January 2014, the end of January 2014 and the end of April 2014. WTG24 also shows this behaviour at the end of April 2014. These phenomena show that these turbines might have suffered yaw problem or turbine nacelle direction sensor errors, and need to be investigated in reality by the wind farm operator and be paid attention when applied with further methods presented in the later sections.

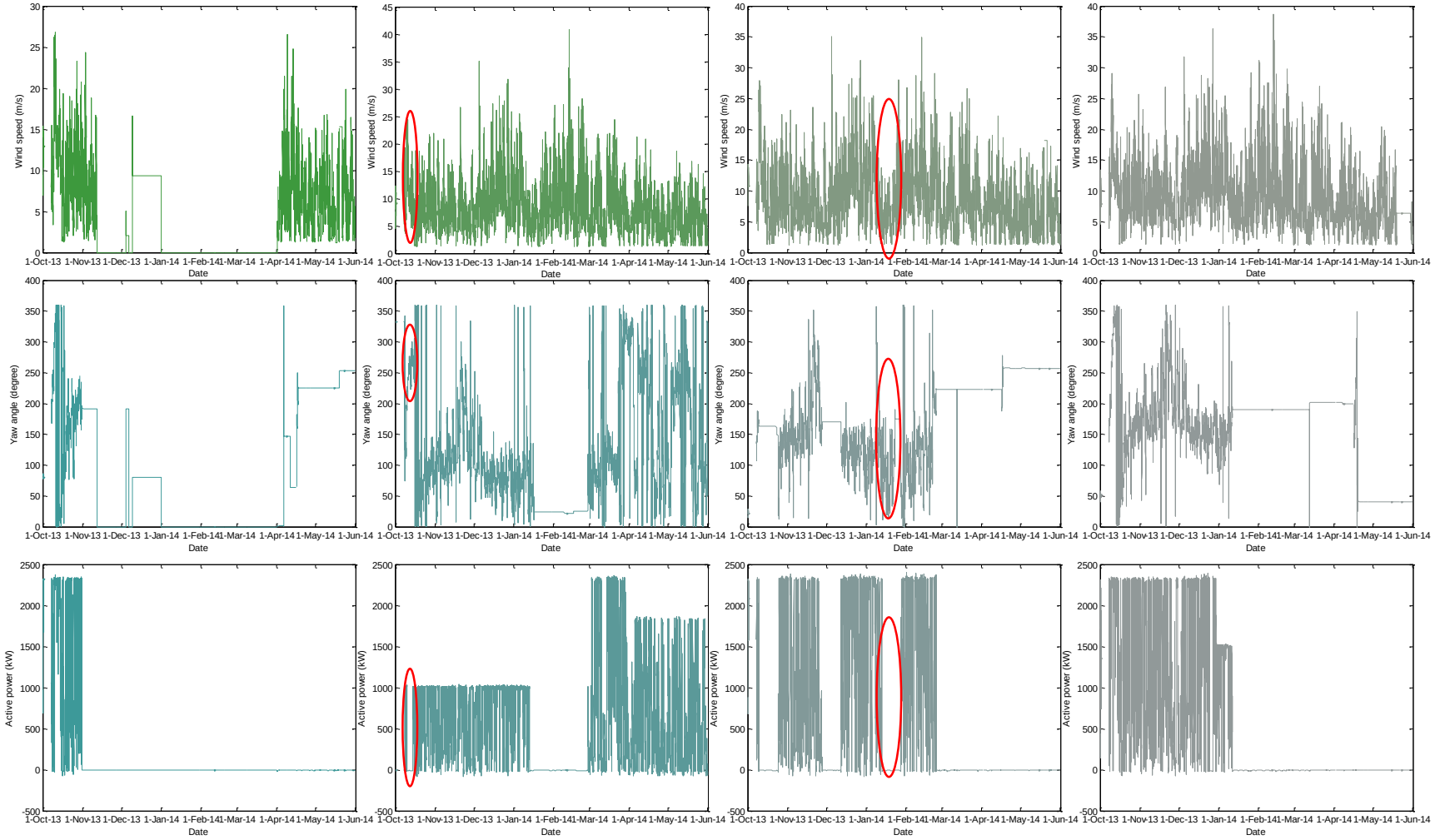

Figure 20. time series of local wind speed (top), yaw angle (middle) and active power (bottom) of WTG 8, 12, 17 and 19 (Left to right) in wind farm T

3.2.4 Power curve

The power curve shows the relationship between the local ten-minute averaged wind speed and the turbine power output. Figure 21 shows the nominal power curve of the turbine in use: the offshore wind turbine Siemens SWT-2.3 93, [132]. The cut-in wind speed is 4m/s, the rated wind speed is 14m/s, and the cut-out wind speed is 25m/s.

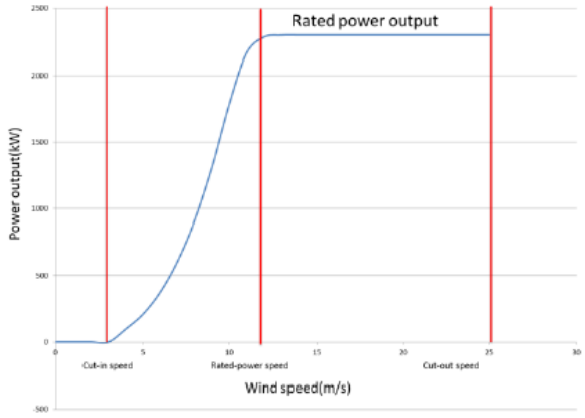

Figure 21. Nominal power curve of the Siemens SWT-2.3 93 turbine [132]

Within the wind farm, turbines in line with the wind direction encounter wakes. These wakes change the local wind speed to a certain extent. However, the correlation between local wind speeds measured by the nacelle anemometer and the power output of this individual turbine do not change, assuming the turbine is otherwise unhealthy. Therefore, even though the wind speed measured from nacelle anemometer is only a reference for starting and shutting down the turbine in the control system, the local wind speed used to plot the power curve of the individual turbine for comparison purposes should be the one measured from the wind anemometer set on the nacelle, rather than measured from the wind mast. Since met mast data are not available in this wind farm, an example of comparison of scatter plots of speed-power relationship using wind speed from turbine anemometer and wind mast from the wind farm L are

shown in Figure 22 [131]. In both diagrams, a red curve representing the nominal power curve is plotted. The left diagram is the plot using local wind speed measured from the anemometer on the nacelle, and the one on the right uses wind speed from a wind mast. The points in the plot using local wind speed are more concentrated and fit better to the nominal power curve when compared to the other plot.

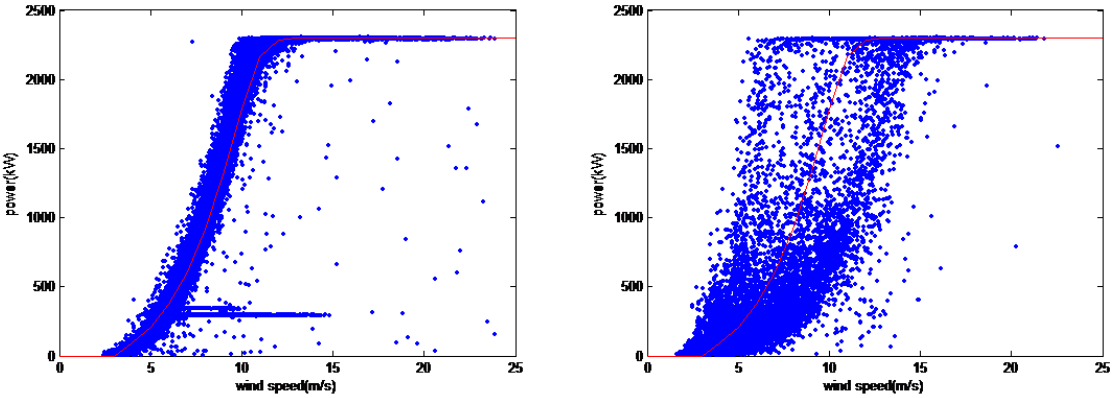

Figure 22. Example of comparison of scatter plots of speed-power relationship using wind speed from turbine anemometer (left) and wind mast (right) (Wind farm L, WTG17)[131].

As shown in Figure 2a in the Appendix-A, the selected SCADA data sees some stoppage of every turbine during the 6 month period. WTG 2, 3, 4, 5, 7, 15, 16, 19, 20 and 27 have obvious curtailment at one power level (mostly at just below 2000kW and others at around 1000kW and 1500kW). WTG 6, 10, 11, 12, 13, 14, 18, 21, 22, 23, 24, 25 and 26 have obvious curtailment at two different power levels (mostly one at 2000kW and the other at 1500kW or 1000kW). WTG 1, 8, 9 and 17 don't have any obvious periods of curtailment. Attention is paid to WTG8 whose power curve fits well with the nominal power curve. This result is in contrast to the abnormal performance apparent of WTG 8 in time series analysis.

3.2.5 Overall diagnosis

The overall diagnosis combines the above methods to identify turbines with anomalous performance. In general, if a turbine shows abnormal behaviour in animation and the calculated time series for yaw, but has a normal power curve, the turbine is diagnosed as having a turbine nacelle direction sensor error. In contrast, if a turbine shows abnormal behaviour in animation and time series, and has a significantly reduced power curve, the turbine is not considered to have a turbine nacelle direction sensor error, but rather, to be suffering from some form of yaw control problem.

Table 11 shows a comparison of the results from the statistical analyses of the time series and results from the calculated power curves. As stated above, every turbine has periods with invalid value (NaN) errors indicated ("Intf shut" and "I/O Timeout") taking around 1075 time stamps (approximately 3% of entire operation time). For easy reading, the column under "No.NaN" shows the number of invalid values in comparison of 1075. WTG 8, 7, 5, 6, 4 and 26 have "0" degree of direction for over 200 time stamps, which can also mean invalid values, as already discussed in previous section. Therefore, recommendations have been made to the maintenance team to check and confirm the "0" degree which is largely suspected to be a state of shut down (planned or unplanned) or loss of communications for WTG 8, 7, 5, 6, 4 and 26, and to investigate any extensive occurrence of invalid values.

Every turbine shows yawing stoppage at different times in the animation. As listed in Table 11, WTG8 has the longest stoppage at "0" degree taking 48.8% of the entire time period. WTG 1 has the 2nd longest stoppage taking around 28% time at the

nacelle yaw position of 213.3 degree. Even the shortest stoppage takes 2.5% of time (WTGs 23 and 13).

Table 11. The comparison of the potential problematic turbines from animation, time series and power curve with 6-month SCADA from wind farm T

Turbine No.	No. NaN (±1075)	No. 0	No. Yaw Activity			Curtailment Levels
			Direction(°)	Stamps	Percentage (%)	
1	4	2	213.3	9473	27.9	0
2	1	4	103.9	3030	8.9	1
3	0	4	146.7	1887	5.6	1
4	-1	409	199.7	2875	8.5	1
5	0	529	228.4	3530	10.4	1
6	-1	525	271.4	3530	10.4	2
7	0	528	273.9	3530	10.4	1
8	2	16539	0	16539	48.8	0
9	1	3	187.5	1331	3.9	0
10	4	4	230.1	3463	10.2	2
11	0	6	224. 9	4606	13.6	2
12	2	2	23.7	3403	10.0	2
13	-1	3	167.7	854	2.5	2
14	0	4	199.1	2728	8.0	2
15	1	3	156	1512	4.5	1
16	0	4	190.2	1742	5.1	1
17	2	3	222.8	6968	20.5	0
18	1	5	180.5	6454	19.0	2
19	1	3	190	7899	23.3	1
20	-1	4	319.7	4679	13.8	1
21	0	3	168.1	4439	13.1	2
22	1	4	173.1	3744	11.0	2
23	-1	5	143.5	853	2.5	2
24	0	4	285.7	5593	16.5	2
25	0	6	194.3	3023	8.9	2
26	0	265	185.2	2172	6.4	2
27	0	20	286. 9	2516	7.4	1

Without curtailment flag available in the SCADA data provided, it can be observed from the time series that most of the turbines have 2 curtailment levels apparent from the power curve analysis, whereas WTG 1, 8, 9 and 17 have no curtailment. WTG 2, 3, 4, 5, 7, 15, 16, 20 and 27 have 1 level of curtailment. This curtailment is understood to be for operational reasons rather than power system constraints.

WTG8 seems to have been out of operation for most of the time, and this is reflected in its low availability and capacity factor. However, it has a reasonable power curve

when it is in operation. From the power time series, it finishes its shut-down and operates well at the end of the selected investigation period. It is not known what the operational fault was but clearly it has been fixed and no further attention is required.

With all the information combined, WTG 1, 17 and 19 show a significant mismatch of the animation/time series and the power curve, where the former shows abnormal yaw performance but the latter shows reasonable power curves. WTG 2, 12 and 20 also show not so dramatic but still visible mismatch of the two. Therefore, these turbines have been recommended to have their turbine nacelle direction sensor errors checked.

3.2.6 Conclusion

Since the "yaw angle" in the SCADA data is sensed by the wind turbine nacelle direction sensor rather than the actual yaw direction fed in the control system, some of the apparent yaw errors are actually nacelle direction sensor errors without power production loss. These false yaw errors confuse the failure rate recording, and therefore are needed to be filtered out before the analyses undertaken in Chapter 4, 5 and 6. This section has provided a methodology of identification of yaw and nacelle direction sensor errors in comparison of power production. It draws on the results of animation of the yaw direction, time series of yaw angle, time series of power output and the power curve analysis. It provides methods useful for both engineers and non-technical staffs to recognize and diagnose nacelle direction sensor (or display) errors and other issues within wind farm T.

For having a general understanding of this main offshore wind farm investigated in this thesis, turbine environment statistics such as a wind rose and the Weibull distribution of local wind speed have been presented. Wind farm operational statistics

such as turbine availability, capacity factor, array efficiency and turbine operational rate are also calculated. These statistics not only present the basic operational status, but also provide basis for future wake analyses.

Specific turbines have been suggested to be inspected with particular attention to the nacelle direction sensors. The displayed “0” degree values should be investigated to assess whether this is a further sensor, data collection or communication issue.

The met mast data is important for the research and is not provided by the operator for this wind farm. In the future, the met mast data is expected to be provided and analysed with turbine data. Data with higher frequency (i.e. shorter record interval) is also expected to be helpful for accurate analysis and diagnosis. It is a beneficial basis for further study of wake losses. It would also be most useful to have data on the yaw error as measured by the nacelle wind vanes.

3.3 Yawing error and turbine nacelle direction sensor error identification for offshore wind farm L

Wind farm L is an established operational offshore wind farm that uses the same type of wind turbines as in wind farm T. It has the advantage, from an analysis point of view, of a longer operational time (3 years) and a more comprehensive data set, including met mast data, than the newly commissioned wind farm T. This makes it useful to investigate wind farm L with regard to yaw and turbine nacelle direction sensor errors. This section enriches the main methodologies outlined in section 3.2, with additional approach that applies correlation analyses and examines wake losses which helps to identify nacelle direction sensor errors by using turbulence information.

In this section, 10 minute SCADA data are used for the entire wind farm of 48 turbines, covering at total of 69115 time stamps. To maintain data confidentiality, the actual time period covered by the data is not disclosed. All time series are plotted in terms of the time stamp number. Over 80% of the time stamps show at least one error code -*999*. These data are removed. The data is further filtered to remove all those data points with wind speed lower than 6m/s (slightly higher than the cut-in wind speed) to ensure that the wind turbines are generating meaningful power. After this process, the total length of data remaining is 10543. Even though in theory the removal of this amount of data may incur large steps of data value changes, the result from later analysis shows a rather smooth data trend (can be observed from Figure 27 in Section 3.3.5).

3.3.1 Animation of wind farm L

Following the time series animation method described in Section 3.2, static angle investigation in this section makes use of animations showing apparent yaw direction

dependent on wind direction. This provides a general view of the manner in which the turbines respond to wind direction changes.

In the static angle analysis animation, the basic layout of the whole wind farm is kept and all the filtered SCADA data are sorted into 1 degree bins as given by the met mast wind vane. For each wind direction bin, the mean turbine directions and their standard deviations are calculated. The total achievable direction range is from 20 to 339 degree; however, considering the prevailing wind direction of this area, the analysed direction range focuses on the range from 190 to 330 degrees.

Figure 23 is a snapshot of the animation when the wind direction is 257 degrees. The turbines and the wind mast are represented by black dots. The arrow in red at the left bottom corner dot representing the wind mast is considered as the wind incoming direction, and the blue arrows of each turbine represent the turbine facing directions—ideally opposite to the wind incoming direction.

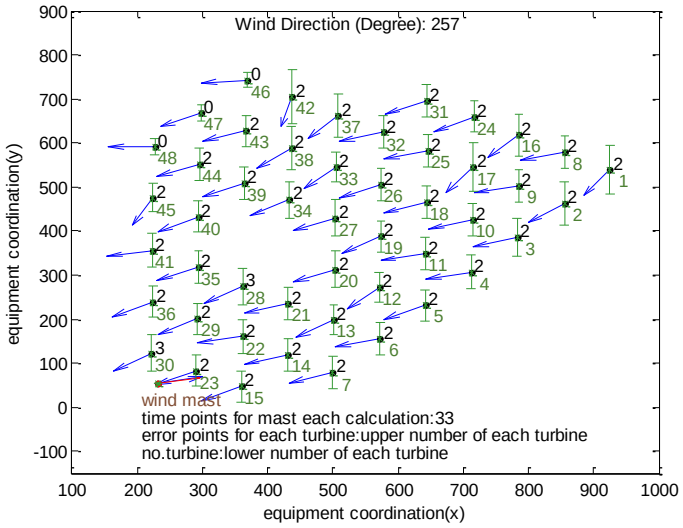

Figure 23. Snapshot of animation for nacelle direction dependent on wind direction in 1 degree steps with SCADA from wind farm L

The green number shown on the right bottom of each dot (each turbine) is the turbine serial number. The black number on the right top of each dot is the number of SCADA invalid values (*-999*) of each turbine that have been removed in the stated general data removal stage at each wind incoming direction. These removed time stamps are not taken into account in the calculations but it is useful to be aware of them. The error bar of each dot indicates the standard deviation of the mean direction of each turbine at each wind incoming direction.

For the wind mast, the number of data points used in calculation of the mean wind direction value for each direction step is shown in words under the wind farm map (33 in this case). Since the number of SCADA invalid values and the data sorted in each direction bin are different, the number of data for each direction bin is usually different.

As a result, the static angle analysis animation sees some turbines having abnormal average yaw performance, and most turbines show a significant standard deviation, particularly for certain wind directions, suggesting appreciable average yaw errors. WTG42 and WTG45 show very different average yawing directions compared to other turbines and the wind direction at the met mast constantly. This result is confirmed by the time series animation, where WTG45 shows poor direction match almost all the time, while WTG42 behaves normally most of the time but abnormally for approximately the last 10% of the time.

3.3.2 Basic analysis tools and theory

In addition to the methodology introduced in Section 3.2, two further mathematical tools are introduced here. These tools support investigation from a more analytical perspective.

3.3.2.1 Cosine-cubed law

Cosine-cubed law [133] provides a reasonably accurate and simple analysis of wind turbine yaw performance. It describes the relationship between the yaw angle and the power output:

$$P_{yaw} = cos^3(\delta) \cdot P \quad (3)$$

where δ is the yaw angle and P is the wind turbine power with flow perpendicular to the rotor.

This expression provides a reasonable estimation of how yaw error affects the power output. If there is a large difference between the nacelle yaw direction and the wind incoming direction measured at the met mast, according to this equation, the power output should be correspondingly high; if the power output measured from the turbine tends to be close to the nominal power output, it is then suspected that there is a nacelle direction sensor error rather than an actual yaw problem.

3.3.2.2 Correlation analysis of direction time series

Correlation analysis makes use of the cross-correlation and auto-correlation functions. This method provides a statistical view of the time series characteristics that proves to be useful in the study of turbine yawing performance. Cross-correlation describes the correlation between wind turbine yaw direction and wind incoming direction measured from the met mast and indicates the extent to which the turbine follows wind direction changes and any significant time delays in the response. The auto-correlation investigates the correlation of the turbine direction with itself as a function of time lag and provides an indication of how dynamically active the turbine yawing is.

The expression of cross-correlation coefficient [134] can be considered as a general correlation function. With different input vectors, this equation can generate the cross-correlation or the auto-correlation function.

$$corr(x,y) = \frac{1}{N-1}\sum_{i=1}^{N}\frac{(x_i - \bar{x})(y_i - \bar{y})}{\sigma x \sigma y} \quad (4)$$

where N is the total vector length. (x and y must have the same length).

When x and y are the same vector input, this equation becomes the auto-correlation function. The auto-correlation of yaw direction describes how quickly the yaw direction changes with time. If for a short time lag, the coefficient drops dramatically, this means there is no longer any significant temporal correlation and the yaw direction is then considered to have changed significantly over this time scale. Comparing the auto-correlation of yaw direction for each turbine and of wind direction from the met mast gives an indication of the turbine yawing speed in response to changes in wind direction. Excessively fast yawing could indicate a potentially faulty yaw control.

The cross-correlation function for each turbine has a same vector input—the wind incoming direction measured by the met mast. Considering the wake effect, turbines in each row and at different positions have a certain time lag between each other, but the general shape of the correlation function curve should be similar. If some particular turbines have very different curve shapes from the remainder, they are considered to have potential yaw problems or nacelle direction sensor errors. To avoid the impact of the rotational wind direction on data analysis, i.e. from 359° to 0° (360°), a de-trending process has been applied to the wind direction data before the correlation analyses in this section, presented in Section 3.3.5.

The potentially problematic turbines can then be investigated in term of power output. If the power output is close to the nominal expected value, this turbine is considered to have turbine nacelle direction sensor error.

3.3.3 Turbine time series

Time series analyses are undertaken for suspected turbines identified by the animations. From the animations, WTG45 and WTG42 show abnormal performance; thus in this section, emphases are made on these two turbines with a selected reference group of WTG43 and WTG44.

Figure 24 shows the direction time series of WTG42, 43, 44 and 45, and the wind measured from the met mast. The legend on the right applies to both graphs. From the figure, WTG43 and 44 show a good agreement with the wind direction from the met mast. WTG45 shows a consistent direction offset for all time stamps. WTG42 shows a direction offset at the last 7% of the time stamps. As shown in Figure 24 (right), WTG42 (in green) shows a higher direction range after 0.98×10^4 time points and wider direction range with lower direction reaching 200 degree after 1.04×10^4 time points.

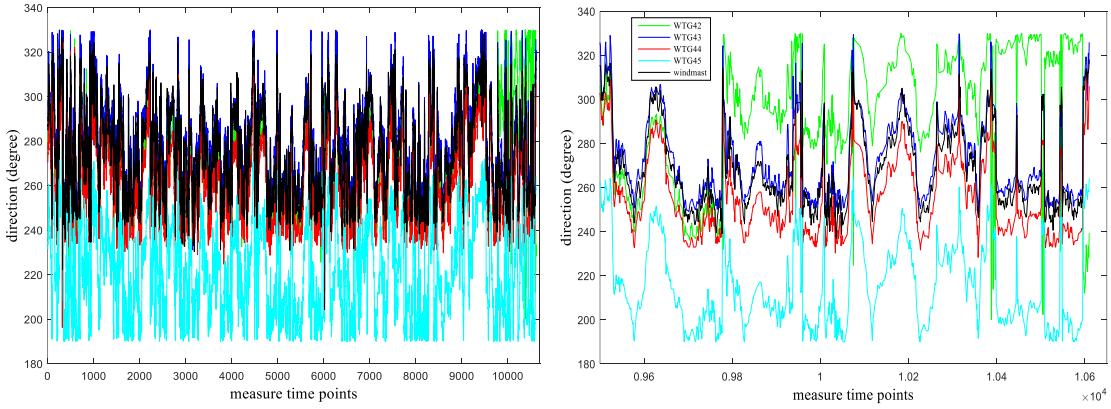

Figure 24. Direction time series of WTG42 to 45 and the wind at the met mast using 3-year 10-min SCADA from wind farm L with full length (left) and last 7% time series (right)

The relevant mean direction values are listed in Table 12. It shows that WTG45 has an offset of -53 degrees, and WTG42 has an offset of 31 degrees for the last 7% of the time, compared with the wind direction. WTG43 and WTG44 display a similar yaw direction to the wind, thus if WTG42 and WTG45 have yaw problems, they will show different power output from WTG43 and WTG44. This is investigated in Figure 25, which shows the power time series of WTG42 to WTG45 and indicates that all 4 turbines have similar power outputs. The legend on the right applies to both graphs. The last 7% time series on the right of Figure 25 clearly shows the consistency of the trends of all 4 turbines.

Table 12. Mean direction of WTG 42-45 and wind in whole time stamps and of WTG42 in last 7% time stamps from wind farm L

Device	WTG42		WTG43	WTG44	WTG45	Wind
	Entire time	last 7% time				
Direction(°)	270	305	279	261	221	274

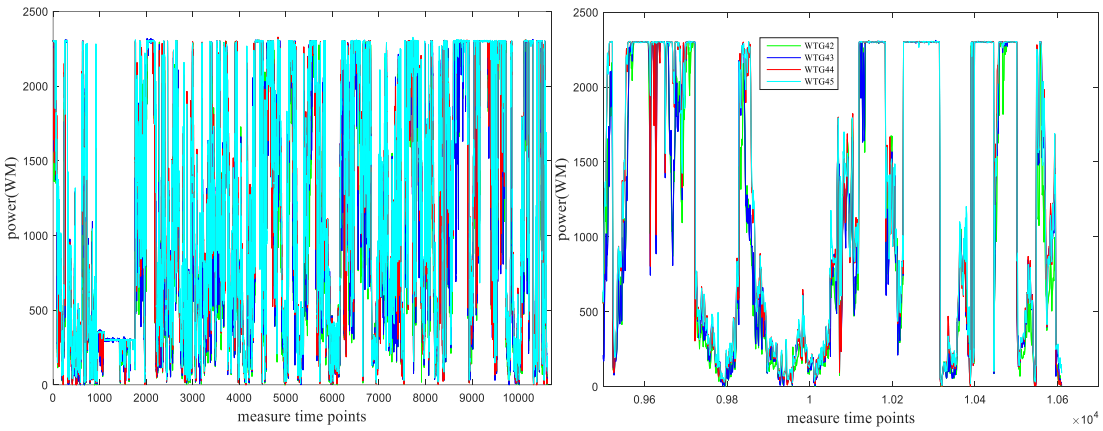

Figure 25. Power time series of WTG42 to 45 using 3-year 10-min SCADA from wind farm L with full length (left) and last 7% time series (right)

It can be concluded that WTG42 and WTG45 suffer from poorly aligned nacelle direction sensors, for all or part of the time period examined.

3.3.4 Wake losses alignment test

Wind can come from different directions depending on the prevailing weather systems and perhaps terrain features. In theory, when wind blows along the line of two turbines, the one behind suffers a wake loss in that it is operating in the reduced velocity wake of the first turbine, and thus has the lower power output. One way to identify a potential yaw problem or sensor error is to compare the measured wind incoming direction when the highest wake loss occurs with the theoretical geometric alignment of the two turbines. If the two angles match within a sensible resolution, the turbine of study is regarded as healthy; otherwise the turbine is suspected to have yaw problem or turbine nacelle direction sensor errors [135]. The wind incoming direction is measured from the turbine nacelle direction sensor at the nacelle of each turbine, so there is still a potential nacelle direction sensor error occur when theoretical and geometric direction do not agree. It needs further investigation such as power output time series. This analysis is practical not only to identify a potentially problematic turbine, but also to obtain the misalignment angle.

In this analysis, WTG43, 44 and 45 are located directly next to WTG48 but at different angles and without any other turbine in between. This does not apply to WTG42. Therefore this analysis only investigates WTG43, 44 and 45 with WTG48 as the reference turbine, as shown in Figure 26.

The relative power outputs of WTG43, 44 and 45 are plotted against wind direction measured at each turbine, so the curves present actual relative power with the same basis of WTG48. Figure 26 marks the measured wind direction of each turbine at which the largest power loss occur. In theory, when wind comes in the line of WTG48

and the turbine of study, the power loss should be maximum, thus it should show a point with minimum value in the power output plot as a function of wind direction.

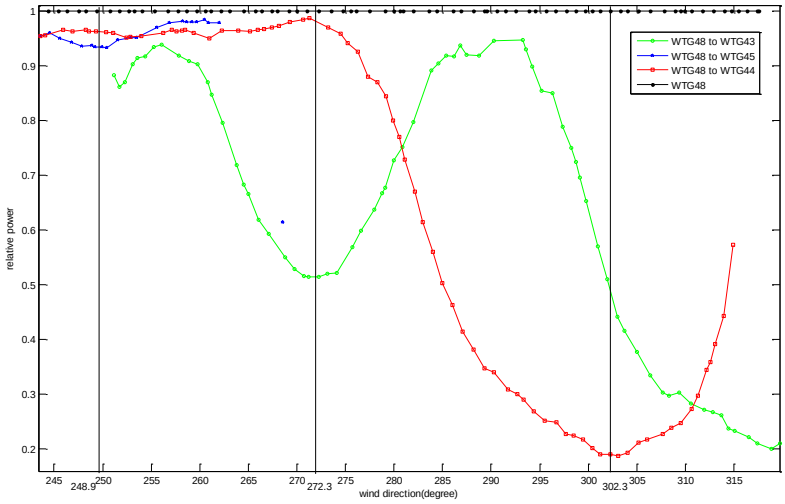

Figure 26. Relative power output of WTG43 to 45 compared with WTG48 against wind direction using 3-year SCADA from wind farm L

The theoretical geometric and measured alignment directions are listed in Table 13. WTG44 and WTG43 show fair agreements with the theoretical direction listed in the table, with offsets of 2˚ and 17˚ (this can be the product of the wake effect), respectively. WTG45 shows a deviation of 68˚, and this indicates a significant yawing problem or sensor error.

Table 13. The wind direction when the highest relative power losses occur in theory and reality in wind farm L

Turbine	WTG43	WTG44	WTG45
Theoretical geometric wind direction(˚)	256	301	181
Power output measured wind direction (˚)	272	302	249
Offset (˚)	17	2	68

3.3.5 Correlation analyses

The correlation analysis aims to investigate how quickly the yaw direction responds to changes in wind direction. In a wind direction time series, environmental conditions such as passing weather systems can result in a long term trend of direction increase

or decrease. This low frequency (seasonal) fluctuation of the direction time series is not of interest for the short term (up to an hour) correlation analysis, but has the negative influence that this common trend increases the correlation and lowers the resolution of this research.

To eliminate the impact of this low frequency trend of the direction change and remove the problems caused by repeated rotations, the data has been de-trended as follows. Taking points in time order, the second time when 0 degrees occurs, it and all angles after it have 360 added; the third time when 360 degrees occurs, it and all angles after have a further 360 added, and so on. The resulting direction time series is shown as the upper plot in Figure 27. A process of de-trending is then applied to it by deducting a least squares linear fit, with the result as shown in the lower plot of Figure 27.

After this angular pre-processing, the long term trend has been removed. The direction data can then be used to calculate the short term correlations.

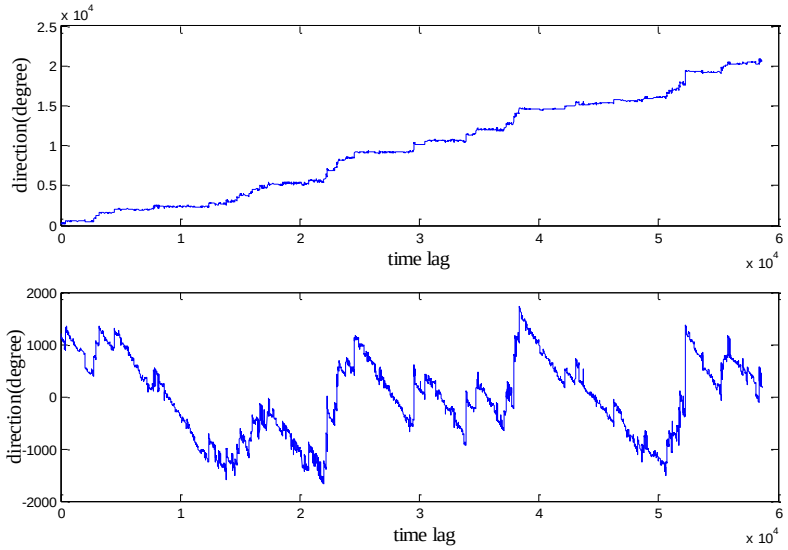

Figure 27. Example of direction time series pre-processing using SCADA from wind farm L: circularly adding-up for direction angles (upper), and de-trended angles processed from the circularly added directions (lower)

3.3.5.1 Autocorrelation

The autocorrelation function has been calculated for the de-trended direction time series for selected wind turbines WTG42 to 45 and the wind measured by the met mast. It indicates how quickly the direction changes in time with high values indicating high persistence, i.e. slow changes. As shown in Figure 28 where the first 700 lags are presented, the yaw direction of WTG45 (blue solid curve) decreases much more dramatically than the others and even more rapidly than the wind (red dashed line) over all time lags from the time lag around 460 onwards. Other turbines show smoother/slower trends for yaw angle than the wind as would be expected as most yaw controllers are design to respond to time averaged wind direction signals to reduce the amount of yaw activity. The suggestion is that turbine WTG45 is yawing excessively, perhaps due to noise in the yaw error signal (regrettably not available in the SCADA data set), or noisy turbine nacelle direction sensor.

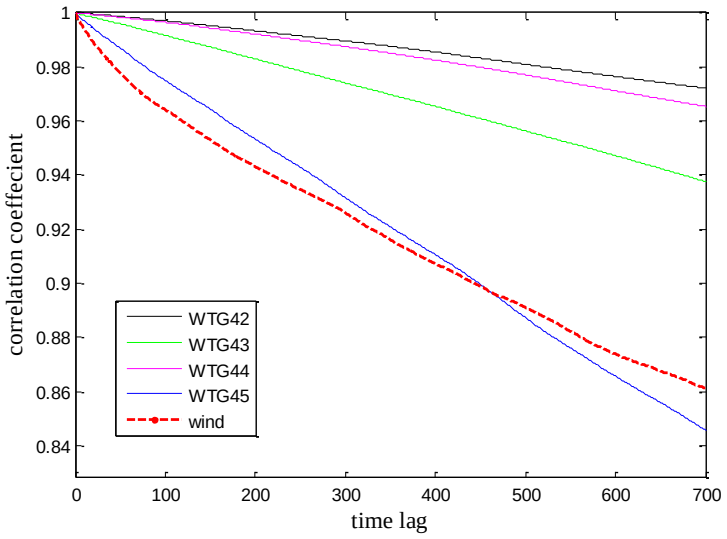

Figure 28. Autocorrelation of time series of WTG42 to 45, and wind measured from the met mast using 3-year SCADA from wind farm L

3.3.5.2 Cross-correlation

The cross-correlation shows how quickly the yaw direction of selected wind turbine changes relative to the wind direction measured at the met mast, as shown in Figure 29 where the first 500 time lags are presented. Because of the different location of each turbine in the wind farm and the wake effect, the turbine yaw responding time to the wind at the met mast is not the same. This explains the different cross-correlation coefficient ranges of these turbines. All turbines are in the same cross-correlation curve range except WTG45 which shows obviously lower coefficient than others at all time lags selected.

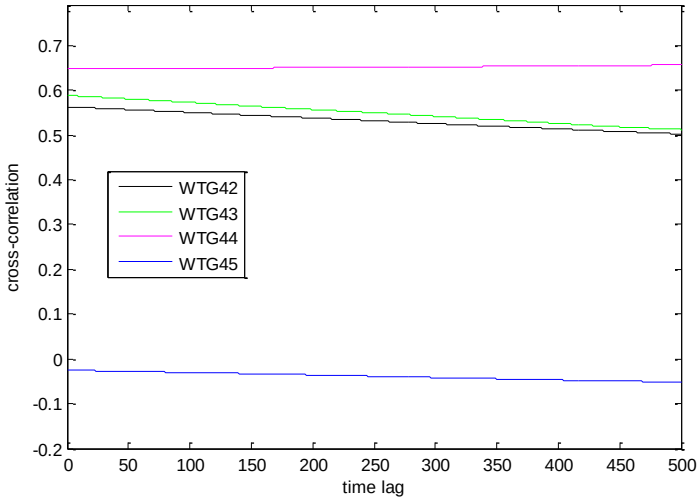

Figure 29. Cross-correlation diagram of WTG42 to 45 dependent on wind measured from the met mast using SCADA from wind farm L

3.3.6 Power curve

Power curves are used to show the relationship between the power output of turbines WTG42 to 45 and the wind speed. WTG43 and WTG44 are considered to be the reference healthy turbines. As described in Section 3.2.4, power curve analysis should use local wind speed measured by turbine nacelle anemometer rather than the one from

the met mast. A nominal power curve from the manufacturer for this type of turbine is also plotted.

As shown in Figure 30, all four turbines show fair agreement with the nominal power curve from the manufacturer (red curve). Between the cut-in speed and the rated speed, all four curves have high correlations to the manufacturer's curve. After the rated speed, potentially because of the de-rated operation, there are drops of the power output at certain wind speed. Despite of this, all four turbines show a high similarity of the power drop and this similarity also shows on the standard deviation. Furthermore, the standard deviation shows high values just above the rated wind speed and at very high wind speed where mostly the power drops occur. These high standard deviation values might suggest insufficient data in the bins. This indicates that WTG42 and WTG45 have normal power output dependent on local wind speed. Since turbine WTG45 has a respectable power curve, the earlier indications of yaw performance problems most likely indicate a noisy nacelle direction sensor, although excessive yaw activity cannot be ruled out as this could be consistent with good power production.

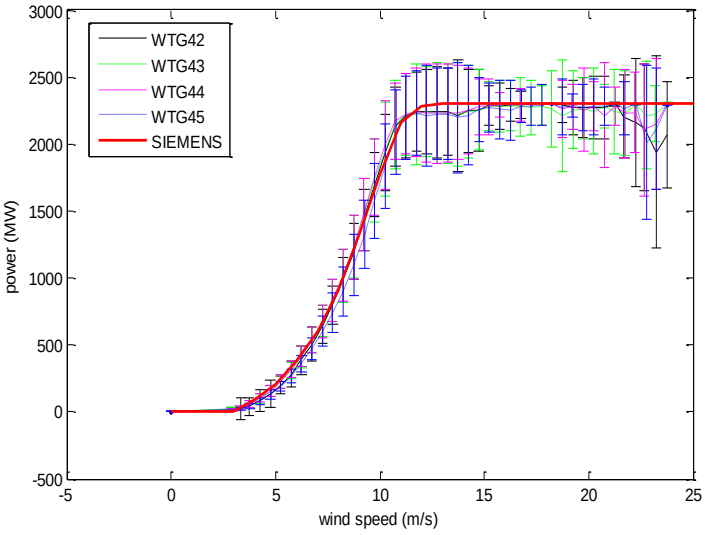

Figure 30. Power curve of WTG42 to 45 and nominal power curve from the manufacturer in wind farm L

3.3.7 Conclusion

Yaw effectiveness is an important consideration for good wind turbine operation; large yaw errors lead to power loss and higher fatigue loads, impacting both reliability and cost effectiveness. Further steps such as the maximisation of power output and the reduction of the wake effects are also of research interest in the context of improving wind farm operation. This study has shown that it is important to distinguish turbine nacelle direction sensor error from actual yaw problems that degrade power production, and methods to do this have been proposed.

In this section, the relatively long operational record for offshore wind farm L provides the opportunity of using additional mathematical techniques to those presented in section 3.2. To identify the potential problematic turbines in this wind farm, two types of animations are made. The animations are the tools that enable rapid focus on the potentially problematic turbine(s), even for a large wind farm. From these animations, WTG42 and WTG45 are found to have abnormal performance. Detailed time series analyses are then applied to these two turbines and compared with a reference group. The wake loss alignment test is an indirect method to explore direction measurement issues and provide misalignment angles.

The correlation analyses investigate the dynamics of turbine yawing. An angular pre-processing method is applied to the original direction data in order to remove the effect of long term trend.

A comparison of power curves is then made from data of WTG42 to 45 and the nominal power curve from the manufacturer. From this comparison, WTG42 and WTG43 show normal power outputs along with the local wind speed.

From these technical analyses, a conclusion can be provisionally drawn that WTG42 and WTG45 have turbine nacelle direction sensor errors and actually behave normally in terms of yawing and power generation. The analyses suggest that WTG45 is regarded to have a mean bias of -53.7 degree of all time and also has a noisy sensor as indicated by the low correlations and WTG42 is regarded to have a mean bias of 30.6 degree for the last 7% time.

The techniques in this section taken together enable yawing problems and sensor errors to be distinguished. The failure data used in next chapters are therefore filtered in this manner.

Chapter 4 Offshore wind turbine component reliability

After having the wind farm operating status investigated and the failure data filtered with the methodology developed in Chapter 3, this chapter starts the wind turbine reliability analysis based on these failure data. The failure rate of a wind turbine subsystem or component is key to any wind turbine reliability analysis, and to the assessment of the cost effectiveness of condition monitoring in Chapter 5 and 6.

The only failure data for wind turbines accessible in this thesis is from onshore, not offshore. Under this situation, this chapter introduces an innovative methodology applied to an onshore/offshore failure rate translation. This methodology has avoided the unreliable direct Kernel fitting used by other research, but developed a cumulative probability distribution (CPD) method with more credible fittings. Fitting functions have been compared in goodness, and one function with best fit has been chosen. The methodology has a wide potential of applications, among which an offshore wind turbine subsystem risk priority number (RPN) has been calculated from accessible onshore rankings. Even though the CPD method has largely improved the credibility of the translation, the limited length of the onshore failure rate has affected the accuracy of the translation results. Therefore, the methodology developed in this chapter has rather provided a train of thought in failure data translation and can be assessed and improved when more data are available.

This translation has also been applied to the cost modelling with condition monitoring in Chapter 5 and Chapter 6. Again, although not all subsystem failure rates have an accurate translated value; it has provided a train of thought of improving the failure

rate input from purely assumption or direct use of onshore data to offshore ones. Detailed description can be found in Chapter 5 and 6.

4.1. Component failure rate translation from onshore to offshore

The concept of translating the failure rate from onshore to offshore has been initially developed in the Wind CDT in University of Strathclyde by directly fitting a Kernel function to the failure rate likelihood in format of probability distribution function (PDF) and calculated the failure rate probability by dividing it with the probability of the environmental factor [136]. Because of the limited length of onshore failure rate data, the direct Kernel fitted PDF can hardly represent the generic onshore failure rate. It therefore results in limited the accuracy of the translation.

The failure rate translation developed in this chapter has followed this concept and applied a CPD method with a standard Bayes theorem to improve the genericity of the failure rate probability distribution. The core calculation is of the ratio of the expectation of the failure rate, offshore to onshore. The expectation of the failure rate is dependent on the prevailing environment.

Research into wind turbine reliability provides evidence of the effect of a maritime environment on failure modes and highlights the importance of undertaking further research in this field. [137] provides an overview of the available databases from German and Scandinavian wind farm projects. From this data, information on the most critical components and subassemblies, i.e. the ones that fail most frequently and/or cause the most downtime, can be established. A number of factors have been identified that could influence the failure frequency, modes, causes and cascading effects of the turbines. These are:

- *Weather*
- *Coupled wind and wave loading*
- *Turbulence and wake effects*
- *Maritime atmosphere*
- *Marine bio-fouling*
- *Ice flows*

A link has been established between wind speeds and the level of failure experienced of wind farms. The most recent series of analyses into this phenomenon [138], used the Scientific Measurement and Evaluation Programme (WMEP in German) of failure from three onshore sites with homogenous turbine types and weather data from those locations. The study extends previous investigations which use the database and finds a significant level of dependence of failure rates on weather patterns using cross-correlation methods. The study was able, to some extent, to identify the root causes of failure for both electrical and mechanical systems and considered wind speeds, humidity and turbulence. The study fell short of establishing a strong link other than a connection between one site's electrical failures and temperature; both mechanical and electrical failure was related to turbulence at another site, and electrical failure to humidity. None of these correlations were based on the data detected at more than one site. With reference of this study, this thesis considers onshore wind turbine failure rate for an extensive wind farm to explore the change in risk to wind turbine components.

Offshore turbine structures are subjected to loading from both wind and wave. The coupled wind and wave cyclical loadings on structures that support wind turbines are higher than on similar structures for traditional oil and gas installations [139]. In order to predict the largest waves for the design loads, a return period of 50 years is assumed.

However, loads on the turbine structures can increase beyond the 50 return period design load when in the wave breaking zone as noted by [140], in their demonstration of a solver to replicate the loads of offshore wind structures due to breaking waves for shallow water sites.

Failure of the structure can occur if the single extreme event loading exceeds the design loads or if a series of events induce fatigue loading. Failures that could occur from extreme overturning moments are deformation or collapse of the structure, causing complete and catastrophic loss of function and turbine.

Turbulence of the site is a key parameter in the fatigue loadings of wind turbine particularly for offshore wind farms where the majority of turbulent air flow originates from the wakes of other turbines. One of the studies of the effects of wakes on fatigue loading at the Vindeby wind farm, [141] explores the relationship between loading on components in the turbine, turbulence intensity brought on from other turbines and the ambient turbulence intensity. An aero elastic model was used to estimate the wind loads and it was found that fatigue loads increase 5% and 15% for a wind turbine within an array and a complete wind farm, respectfully, from a base line (a turbine in non-wake low turbulence free flow). Despite the importance, in this thesis, however, wind speed standard deviation is not available for the turbulence study.

In a more recent study by the National Renewable Energy Laboratory (NREL) an aero-elastic code FAST was used to model two 5MW turbines seven rotor diameters apart. Both the structural response and the blade bending moment were calculated. It was found that for the in-plane blade moment, there was a reduction in the damage equivalent loads in the downstream turbine due to reduction in wind speed for both

onshore and offshore wind cases. In the out-plane blade moment however, with onshore there is a reduction in damage equivalent loading and offshore there is an increase. This anomaly is also seen in the low speed shaft torque [142].

With cooperation of the operator of the large onshore wind farm W, fault reports covering a 3-year period have finally been made available and investigated in this thesis. The only accessible environmental time series data for both onshore and offshore sites, wind speed and temperature, are taken from the SCADA of onshore wind farm W and from offshore wind farm L.

This is not to say that there are no other factors that influence failure rate, but if that data was available, it could be included in a similar manner, e.g. wind turbulence (significant but not available for this thesis).

This method can be expanded to wind farms using the same type of wind turbine, amended and supplemented by different turbine types in future work.

4.1.1 Calculating the ratio of the expectation of the failure rate

The core calculation in the failure rate translation is the failure rate expectation dependent on the selected environmental factor, denoted $E[F_E]$. The environmental factor subscript E represents both the wind speed U and temperature T for the corresponding separate calculations. The failure rate probability given the environmental factor, $P(F|E)$, is derived per turbine per year. This failure rate probability is multiplied by the environmental factor probability distribution $p(E)$. The equation is shown below.

$$E[F_E] = \int_{-\infty}^{+\infty} P(F|E) \cdot p(E) dE \tag{5}$$

Assuming that the probability distributions of the environmental factors (wind speed and temperature is this case) are available both on and offshore, the ratio of expected failure rates can be expressed as:

$$Ratio_E = \frac{E_{offshore}[F_E]}{E_{onshore}[F_E]} \tag{6}$$

This assumes the expectations are linear and the ratio calculated is a single value, which is not the case in reality. This simplified mathematical model has provided an initial attempt of translating failure rate from onshore to offshore by expectations, and needs to be improved into a more complicated model.

4.1.2 Failure rate probability distribution

The wind turbine component failure rate probability is one of the core elements in the expectation calculation. According to Bayes' rule [143], shown in Eq.7, the probability of failure rate dependent on the environmental factor *P(F|E)*, considered as the posterior probability in Bayes' rule, is calculated from the product of the probability of the environmental factor given failure rate (the likelihood), *P(E|F)*, multiplied by the annual mean failure rate of the selected turbine component, $\overline{P(F)}$, which is considered as the prior probability in Bayes' rule for simplicity (which was neglected in [136]), and divided by the environmental factor distribution, *P(E)*.

$$P(F|E) = \frac{P(E|F) \cdot \overline{P(F)}}{P(E)} \tag{7}$$

The probability of environmental factor given failure rate is the information which can be directly obtained from failure record of the wind turbine operational data, where the failure type, location, date and the corresponding daily averaged weather statistics are recorded. It is important to note that the value used for wind speed and ambient temperature is the daily mean value since it is accepted that the impact of the environment on failure is not instantaneous. One-day averaging may well be insufficient and in future work, longer averaging periods should be investigated.

4.1.2.1 Fitting a suitable function to the failure probability distribution

The probability of the environmental factor given failure rate $P(E|F)$ is one of the core variables in the failure rate probability dependent on the environmental factor $P(F|E)$ calculation. The fitting of the data set for $P(E|F)$ directly affects the accuracy of $P(F|E)$ calculation. As introduced in previous chapters, the length of actual failure data is limited. This fact lowers the applicability of the estimated $P(E|F)$. In order to obtain a reasonable failure rate probability dependent on the environmental factor $P(F|E)$, a fitting process is developed and studied here to obtain a generic probability of the environmental factor given failure rate $P(E|F)$.

The common approach to estimate curves for the probability density function (PDF) is by using a non-parametric estimate of the density function, such as the Kernel function [144]. Although these fitted distributions look reasonable, as an example shown in Figure 31, for the limited size of the raw data, the records cannot cover all wind speed values. For some wind speed bins, high fault rates are apparent. These unexpected spikes most likely only reflect the limited data available, and are not

generic. This limitation lowers the precision of the distribution Kernel fit. It is difficult to derive smooth and reliable probability distributions through this method.

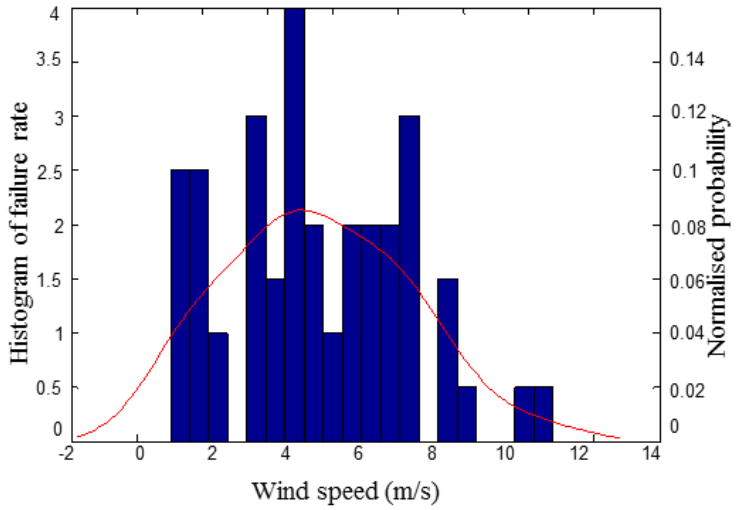

Figure 31. Failure rate histogram (left axis) and normalized probability (right axis) Kernel fitted distribution of drive train system in the onshore wind turbine from wind farm W

In order to obtain a smoother and more reliable distribution curve, a procedure related to cumulative probability distribution (CPD) has been applied in this research. This procedure finds a fit to the cumulative probability distribution of *P(E|F)* and then differentiates the result to regain the desired probability distribution function.

The first attempt of the fitting function of the CPD in this example is a 2nd order polynomial function, as shown in Eq.8, where *a* and *b* are the parameters required for the derivation of the function. The derivative of the fitted CPD function is the *P(E|F)*, as shown in Eq.9. The CPD fitting function is derived from the actual data, and the differentiation function is the standard function substituted for the parameters obtained from the fitting function.

$$f_{poly2} = a \cdot E^2 + b \cdot E + c \tag{8}$$

$$P(E|F) = \frac{df_{poly2}(E)}{dE} = 2 \cdot a \cdot E + b \tag{9}$$

The 2nd order polynomial function has suitable characteristics for the ascending curve with a flexible tangent. It provides reasonable fitting to the data and is easy to differentiate. However, the disadvantage is that the curve extends (extrapolates) at the two ends with high-value tangents, which creates significant error in the fitting of the tails to the original curve. This error will have exaggerated impact when differentiation is applied.

An alternative fitting function is a variation of exponential, as shown in Eq.10. In this equation, *a*, *C* and *k* are the parameters required for differentiation, as shown in Eq.11. The fitted exponential has well defined asymptotic behavior towards 0 and 1. The variation of exponential function can be derived to reflect this behavior and this makes the fitting of the tails much more reliable. The disadvantage of exponential fitting is the complexity of the function itself, which increases the difficulty of parameter estimation. The goodness of the two fitting functions is further investigated in Table 16 in Section 4.2.3.

$$f_{ex}(E) = 1 - a \cdot e^{-\left(\frac{E}{C}\right)^k} \tag{10}$$

$$P(E|F) = \frac{df_{ex}(E)}{dE} = a \cdot \frac{k}{C} \cdot (\frac{E}{C})^{k-1} \cdot e^{-(E)^k} \tag{11}$$

Once obtained from the fitting function, the parameters allow algebraic differentiation of the CPD function to give the required PDF function.

4.1.2.2 Fitting of failure probability distribution dependent on wind speed distribution

Figure 32 shows the staircase curve of the CPD dependent on wind speed (blue) with the fitting curves (red and green). The red line shows the exponential function fit, and

green dashed line represents the 2nd order polynomial fit. In this figure, the two fitted functions show good agreement with the main body of the staircase CPD curve.

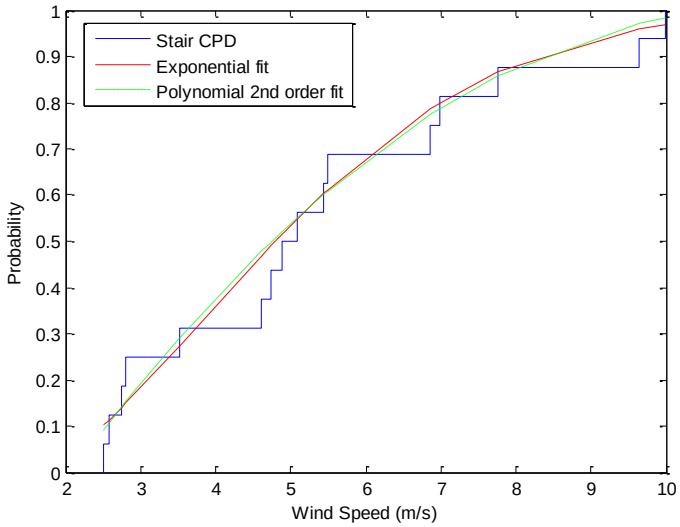

Figure 32. Staircase plot of failure CPD fitted by 2nd polynomial and exponential function of rotor system in the onshore wind turbine dependent on wind speed from wind farm W

The parameters obtained from the fitting functions are substituted into the expressions for *P(E|F)*. The failure rate probability function *P(F|E)* can then be calculated based on Bayes' rule (Eq. 7). Figure 33 shows the direct Kernel function obtained failure rate probability function curve, where a lump at the high wind speed is shown. This lump is likely the result of the limited data record and does not reflect an actual functional relationship.

Figure 34 shows the *P(F|E)* calculated from the exponential fitted *P(E|F)*. It retains the basic shape of the long term distribution but avoids the fluctuations in short term. Figure 35 (upper) presents the *P(F|E)* calculated from the 2nd polynomial fitted *P(E|F)*. Because of the issues concerned with extrapolation using the 2nd polynomial function, as stated above, a further process is applied on the curve which restricts the curve shape

within the two vertical bars, as shown in the lower figure in Figure 35. In the absence of any other indication, constant value extrapolation has been used outside these limits.

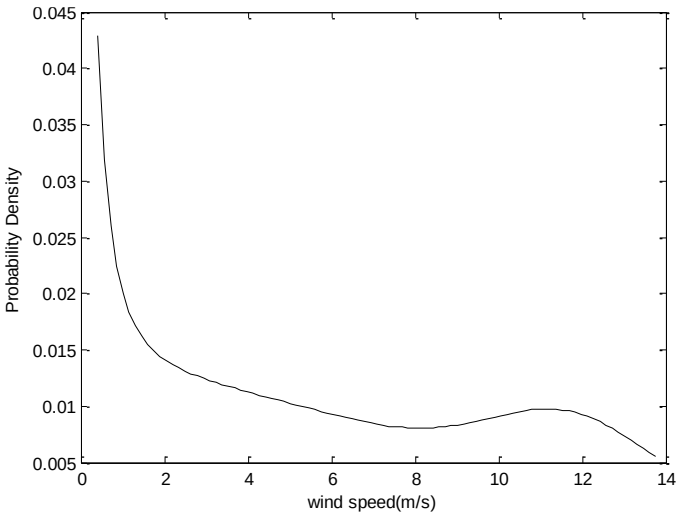

Figure 33. Failure rate PDF with non-fitted (Kernel function) method of rotor system in the onshore wind turbine dependent on wind speed from wind farm W

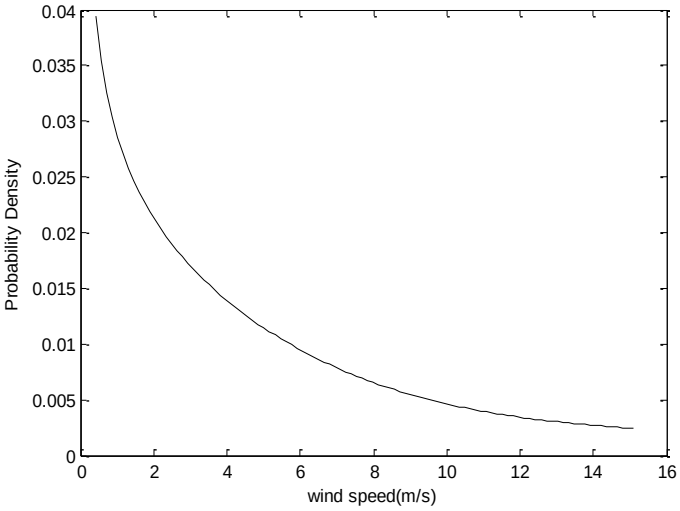

Figure 34. Failure rate PDF with exponential fitting function method of rotor system in the onshore wind turbine dependent on wind speed from wind farm W

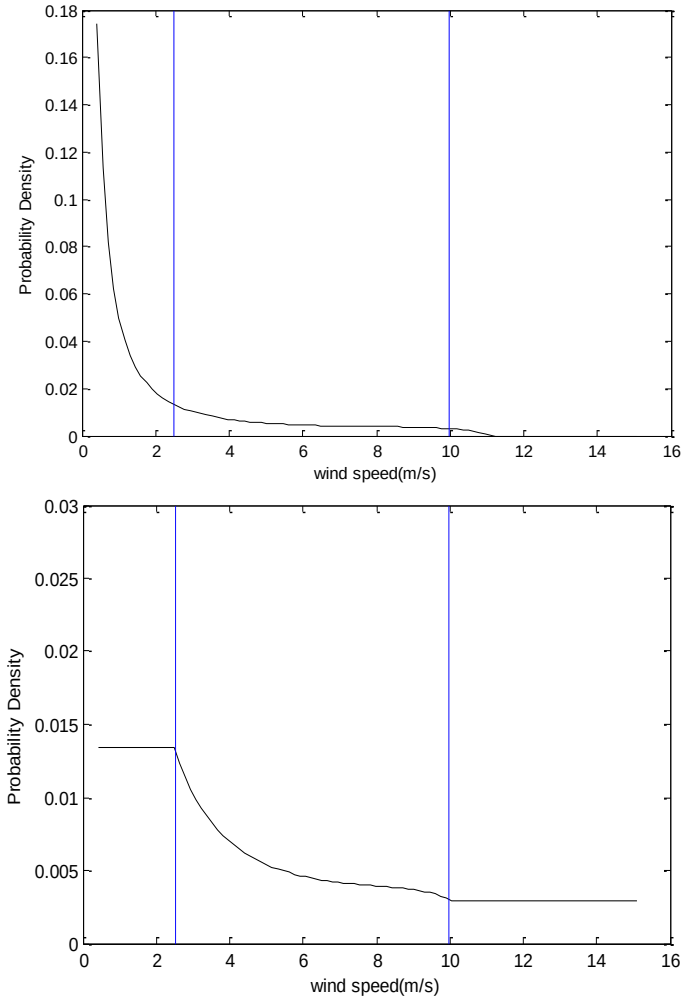

Figure 35. Failure rate PDF with 2nd order polynomial fitting function (upper) and processed function (lower) of rotor system in the onshore wind turbine dependent on wind speed from wind farm W

4.1.2.3 Fitting of failure probability distribution dependent on temperature distribution

The situation for temperature is slightly different. Unlike wind speed, temperature can have a negative value. This is an obstacle to fitting an exponential function to the temperature distribution because of the non-negative-x-value nature of the exponential function. The curves are offset to the right-hand side of the y axis, fit with exponential functions, and shifted back. In this way, the parameters are obtained in the offset stage and put in the PDF calculation after the restoration.

Figure 36 shows an example of the staircase curve of the CPD dependent on temperature (blue) with the fitting curves (red and green). In this figure, the 2nd order polynomial (green dashed) shows a high-value tangent at the high temperature values, which reflects its disadvantage stated above. This can be observed at the right hand side of the curve.

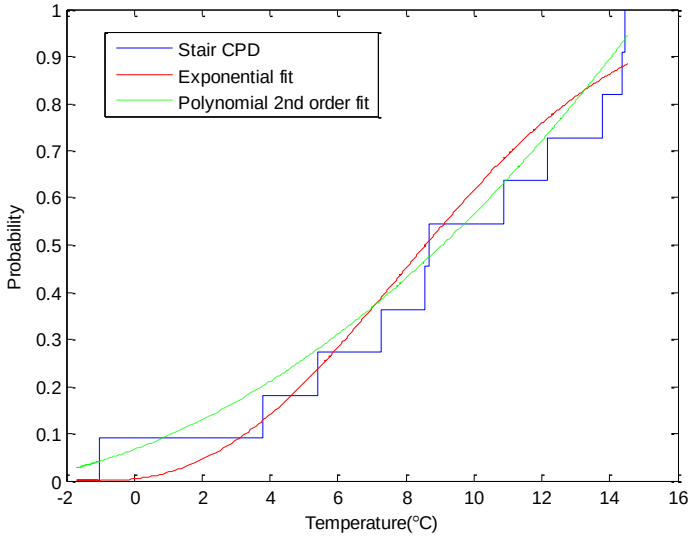

Figure 36. Staircase plot of failure CPD fitted by 2nd polynomial and exponential function for blade system dependent on temperature in the onshore wind turbine from wind farm W

Figure 37 (upper) shows the failure rate probability function *P(F|E)* based on the Bayes' rule. This figure clearly shows the high-tangent nature of the 2nd polynomial function (green dashed line). The high-temperature tail expands far above 1, which is not allowed for a probability function plot. Ignoring the illogical tails and zooming in on the middle range of temperatures (around 2-15°C), as shown in the lower figure, the three methods can be observed agreeing each other to a certain extent. The non-fitted method shows a peak in failure PDF at around -4 degree, in some agreement with the 2nd order polynomial method but with a much higher fluctuation; whereas the exponential method shows a peak at around 5-10 degrees.

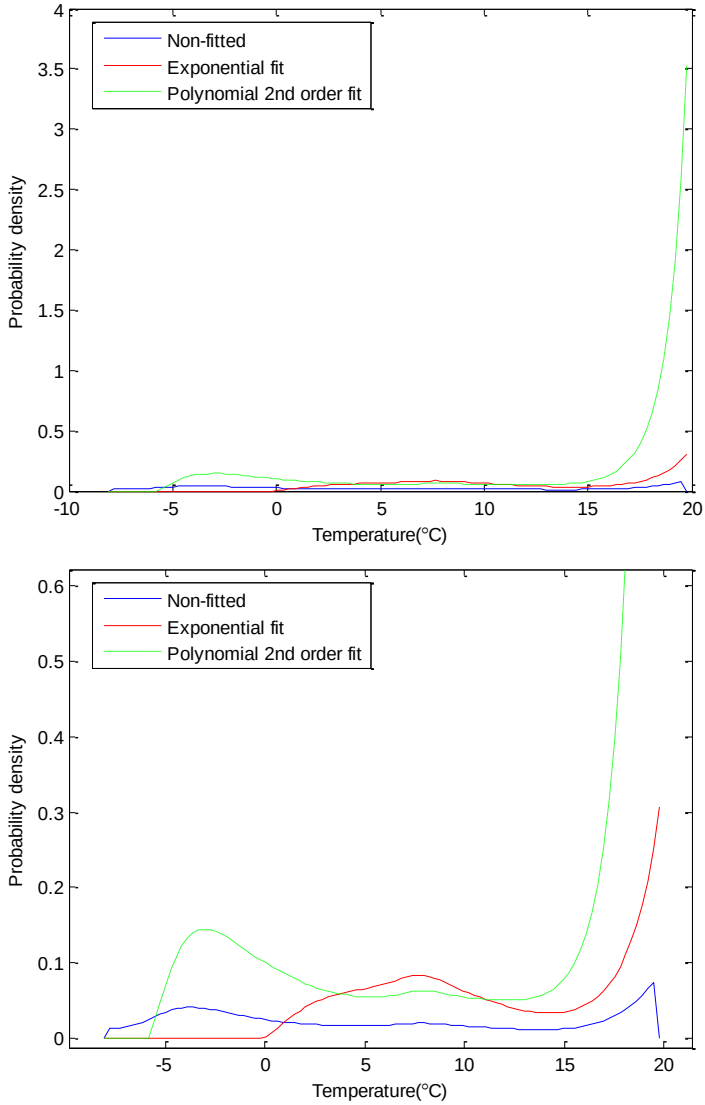

Figure 37. Failure rate PDF with non-fitted, exponential fitting function and 2nd order polynomial fitting functions for blade system dependent on temperature (upper) and zoomed-in figure (lower) in the onshore wind turbine from wind farm W

4.1.3 Environmental factor distribution

The environmental factor distribution is the other core element not only in the expectation calculation but also in the Bayes' rule equation for failure rate probability. For maximizing the accuracy with the limited accessible data, some environmental factor distributions are from the standard equation, others are elicited from the actual data.

4.1.3.1 Wind speed distribution

The wind speed distribution from both on and offshore sites conforms to the Weibull distribution. In the Bayes' rule, the environmental factor distribution *P(E)*, in this case the wind speed distribution *P(U)*, is calculated from real onshore data at the selected site, to be consistent with and cancel out the effect of the numerator *P(U|F)* which is calculated from real onshore data; whereas in the higher level expectation equation, the wind speed probability density distribution *p(U)* is derived from a standard Weibull probability density function for better flexibility and genericity.

The Weibull probability density function is shown in Eq.12. The shape parameter, *k*, has been assumed to be 2. Since this gives $k \in [1.6, 3.0]$ for both onshore and offshore sites, according to the standard of the Weibull distribution equation, the scale parameter, *C*, is given by Eq.13 to be within 1%.

$$P(U) = \frac{k}{C} \cdot (\frac{U}{C})^{k-1} \cdot e^{-(\frac{U}{C})^{k}} \tag{12}$$

$$C = \frac{2 \cdot \overline{U}}{\pi^{0.5}} \tag{13}$$

It is generally understood that offshore wind speeds are higher than those in onshore in comparable locations. For simplicity an empirical annual mean wind speed $\overline{U}$= 7m/s has been assumed to be typical of onshore sites and a mean value of $\overline{U}$=10m/s has been set to represent a typical offshore site. Figure 38 shows the Weibull distribution from the standard equation of wind speeds for both onshore (black line) and offshore (red dashed line). Note that since this is based purely on *k* and the annual mean wind speed, and not data, the probabilities can be interpreted as being for daily mean wind speeds and are thus consistent with the conditional distributions derived from operational data.

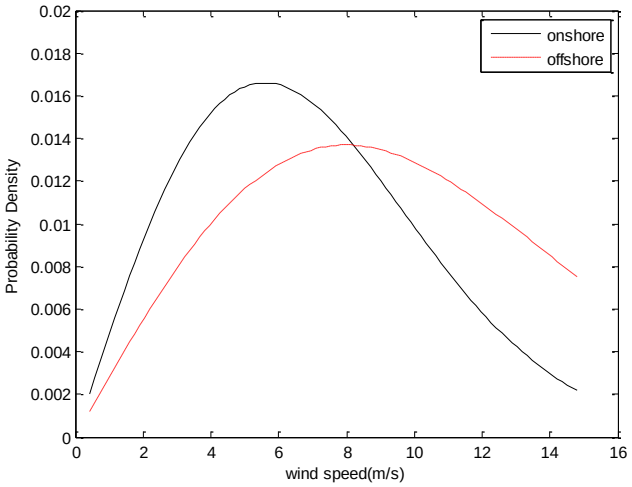

Figure 38. Standard Weibull probability distribution for 7m/s (onshore) and 10m/s(offshore) annual mean wind speed.

The wind speed distribution has a general shape of Weibull distribution, and thus a Weibull distribution function should be fitted to the data for the site in question (presented as a histogram). An example is shown in Figure 39. Histograms are plotted from wind speed data from onshore (wind farm W) and offshore (wind farm L). Both of them are fitted by the Weibull distribution with the same size of the bins, which gives good shaped probability distribution function curves. Compared to the standard Weibull distribution function derived from Eq. 12, whose curve shapes are shown in Figure 38, the distributions with real onshore and offshore data provide slightly different probability range and shapes, as shown in Figure 40. Therefore, it is meaningful to offset this difference in the Bayes' rule by using wind speed probability distribution from real onshore data for both the probability of the environmental factor given failure rate $P(E|F)$ and the environmental factor distribution $P(E)$.

Because of the different recording format and therefore different length of the recording data, the onshore and offshore histogram frequencies are not in the same range of magnitudes. The highest onshore frequency reaches less than 160, whereas

the offshore frequency reaches about 1500. For this reason, the distribution is calculated in the probability density function, so it will not be affected by the total size of the data. Figure 40 shows a typical relationship between actual onshore and offshore wind speed distribution.

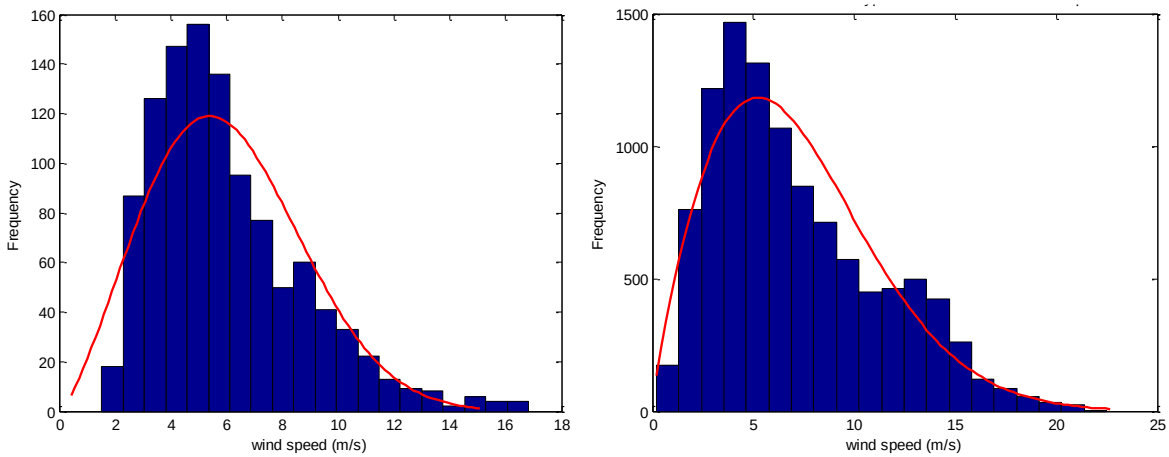

Figure 39. Example of wind speed histograms and Weibull distribution fits of data from onshore wind farm W (left) and offshore wind farm L (right).

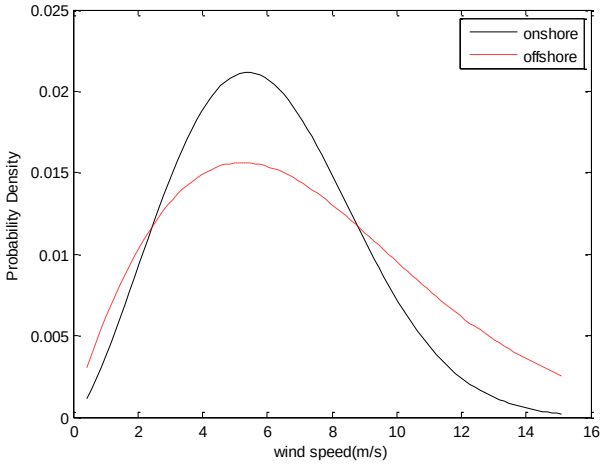

Figure 40. Wind speed Weibull distribution function extracted from real data from onshore wind farm W (black line) and offshore wind farm L (red dashed line).

4.1.3.2 Temperature distribution

Not like wind speed, the temperature distribution does not follow a specific standard distribution function such as Weibull distribution function. In this situation, a Kernel function, as used above, is applied to the histogram to obtain the temperature distribution; and not like the application of the standard wind speed Weibull distribution function for genericity reason, both the Bayes' rule and the expectation function are using real data temperature distribution.

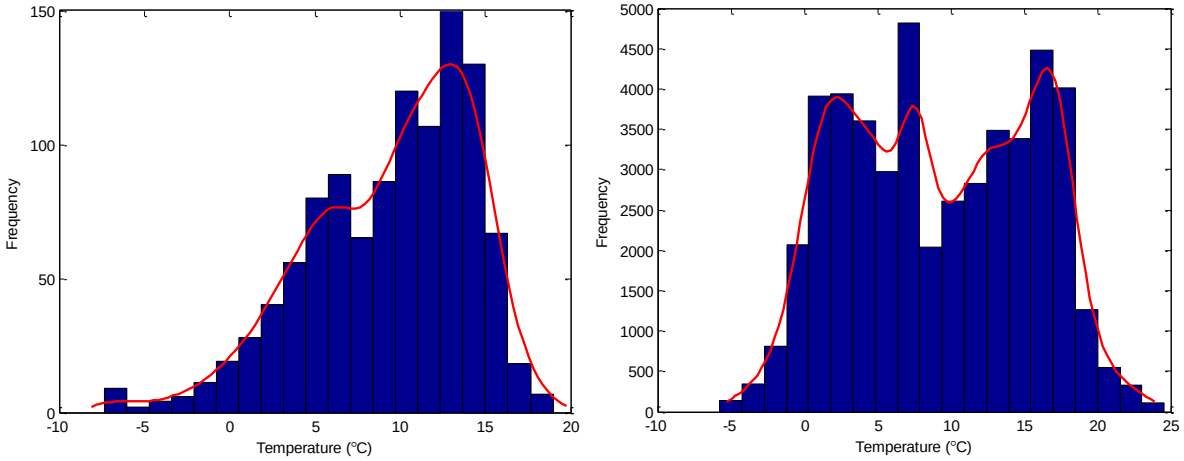

Figure 41. Examples of temperature distribution histograms and Kernel function fits of onshore wind farm W (left) and offshore wind farm L (right).

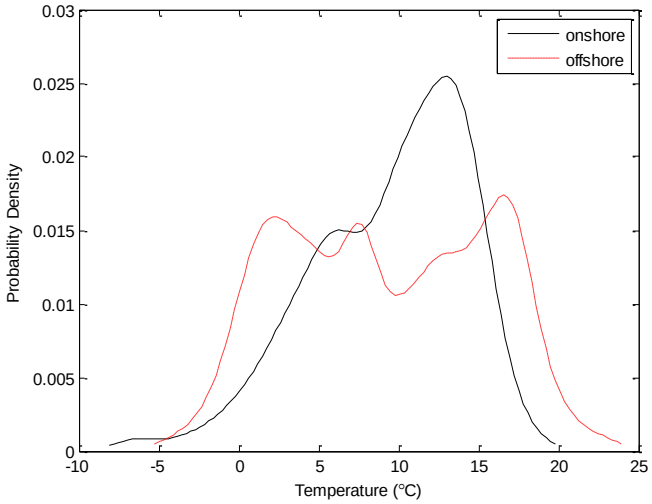

Figure 42. Temperature distribution function by Kernel function extracted from real data from onshore wind farm W (black line) and offshore wind farm L (red dashed line).

Figure 41 shows the temperature histograms from onshore wind farm W (left) and offshore wind farm L (right). The probability distributions derived from the histograms by Kernel function are shown in Figure 42. Same as wind speed, the lengths of recording data of onshore and offshore are not in the same range of magnitude; therefore Figure 42 is plotted to compare the probability density of temperature of the two wind sites.

4.1.4 Conclusion

This section presents an initial analysis that attempts to estimate failure rate probabilities for offshore wind turbines based on the onshore values. Even though it shows in practice wind speed, turbulence, moisture and corrosive air have the most impact on the reliability of offshore wind turbine components, for the limited data access, this chapter only applies correction factors dependent on wind speed and temperature to the failure rate probability distribution. The correction factors are calculated by comparing the failure rate expectations from on and offshore wind farms. The failure rate probabilities obey Bayes' rule. A range of fitting functions are applied from the failure rate probability distribution to environmental factor distributions in an attempt to obtain the more generic function to make up the limitation of the data available.

A method of using CPD to derive the failure rate probability distribution is developed in order to get more generic results. 2nd order polynomial and exponential function are proved to fit the failure rate function in order to give a smoother and more generic function. Environmental factor distributions are used from both the actual data and standard distribution equations for maximizing the precision with the limited data. This

method can be packaged and extended to wind farms using same type of wind turbine, amended and supplemented by different turbine types in future work. A wide range of applications such as FMEA and O&M cost modelling are discussed in the later content.

4.2 Translation of onshore FMEA to offshore operational conditions

It has been increasingly accepted in the industrial field that Failure Modes Effect Analysis (FMEA), or a step further, Failure Modes Effect and Criticality Analysis (FMECA) is an effective tool for assisting in the identification, evaluation and reporting of component failure modes and their severity and impact on systems. FMEA has been applied to onshore wind turbines [146]-[150], but fewer has been published on offshore wind turbine applications [152][153]. FMEA is generally based on expert assessment; however, a metric is in common use known as the Risk Priority Number (RPN) that quantifies the risk.

One of the few existing FMEA applications for onshore wind turbines is available in [146]. It provides a list of RPNs for selected onshore wind turbine components and applies these RPN values to an offshore setting by estimating correction factors calculated from the onshore data. The research behind this research can be traced back to [154]. It is an important application and extension of the offshore/onshore failure rate translation.

As stated in Section 4.1, the large onshore wind farm W has been used as the reference onshore wind farm, and environmental data from offshore wind farm L has been used as the offshore reference site. Although both the wind farms use similar Siemens 2.3 MW rated wind turbines, it is accepted that turbines for offshore operation are often configured differently and may use different components (for example to resist corrosion better offshore). Nevertheless, in the absence of actual offshore component failure data, it is considered that a first attempt of offshore rates can be estimated in the manner proposed here in which the differences between onshore and offshore

operational conditions can be to an extent captured by the differences in ambient temperature and wind speed.

4.2.1 FMEA and FMECA for wind turbine systems in general

FMEA is driven by the failure mode of the components and then mapping the effects throughout the system in tabular form. It is normally used as one of a number of steps towards producing an informed maintenance plan. For each component, the functions are identified and listed. The FMEA process used here follows the hardware approach of the MIL-STD-1629A (1980) standard [151] and scaling tables have been adapted for wind turbines.

The criticality part of the FMECA is introduced through adding a metrics to the FMEA with a quantifiable ranking structure to identify the critical failures. A common method is through determining levels of *severity*, *occurrence frequency* and *detectability* [*S, O, D*] and multiplying these to establish a risk priority number (RPN). These factors are individually rated using numerical scales ranging from 1 to 10. Alternatively, other criticality parameters are costs, environment or safety. An example of cost priority number (CPN) is given in the last column in Table 14. Once a ranking has been established, maintenance and mitigating activities can be added to form part of reliability centred maintenance (RCM) schemes. In this research, RPN calculation follows the [S, O, D] criteria, as shown in Eq.14.

$$RPN\ [S, O, D]\ = Severity\ \times\ Occurrence\ \times\ Detection \tag{14}$$

In this equation, *severity* (*S*) expresses the consequences of component failure, *occurrence* (*O*) indicates the component failure rate, and *detection* (*D*) represents the

likelihood of early fault identification. In this provisional analysis, adjustment of RPN values from onshore to offshore conditions is undertaken only with regard to the occurrence of faults for a selection of key components.

Even though RPN is the numerical tool in FMEA, the initial value for *S*, *O* and *D* is still based on the expert evaluation. In order to reduce the "subjectivity" of the FMEA system, an additional parameter is introduced in [147] to the calculation of the *severity*, *occurrence* and *detectability* scale, where a weighting based on expert opinion is considered and the values of *S*, *O* and *D* are given as:

$$S, O, D = \sum (W_i \cdot x_i) / \sum W_i \tag{15}$$

In this expression, W is the weight value of the experts, x is the rank and i is the number of experts. In order to identify the most significant risks to the turbine, an arbitrary threshold value is decided on to identify the failure modes which should receive additional improvements.

It has been found in the research domain that, in most cases, an FMECA is conducted and a ranking procedure used, but often referred to as an FMEA. The ranking of onshore wind turbine subcomponents for the FMECAs reviewed here are shown in Table 14. The RPN numbers cannot be directly compared as the criticality criteria are different but the resulting ranks are shown in Table 14. The classification of what component fitting into which subsystem is often not fully defined in the journal articles and conference proceedings. For example, it is unknown how much overlap there may be between the "electrical system" and "electrical controllers." Generators appear as the number one or two most at risk components of the list in most cases. Not all of the sources have published the individual severity, occurrence and detection values, but

the ones that have, [149] and [152], show that the values found for the generator are high in all respects. The blade assembly, electrical and control systems also feature in the most critical subsystems but they are interchangeable within the different cases.

Table 14. Critical ranking for onshore wind turbine components for different research criteria

Evaluation	RPN [146]	RPN[149]	RPN[147]	RPN[152]	CPN[149]
Turbine Type / Rank	R80 2MW pitch controlled geared drive	Direct Drive	2MW variable speed geared drive	2 MW geared drive	Direct Drive
1	Rotor and Blade Assembly	Generator	Crowbar Protection	Generator	Generator
2	Generator	Control System	Gearbox	Hydraulic System	Electrical System
3	Electrical Controls	Mechanical Brake	Low Speed Shaft	Gearbox	Blades
4	Hydraulics	Electrical System	Pitch Controller	Mechanical Brake	Converter
5	Gearbox	Converter	Current Controller		Control System
6	Grid and Electrical Systems	Tower and Structure	High Speed Shaft		Mechanical Brake
7	Yaw System	Blades	Utility Grid		Hydraulic System
8	Pitch Control System	Pitch Mechanism	Generator		Yaw System
9	Tower, Foundations, Nacelle	Main Shaft	Turbine Rotor		Tower and Structure
10	Mechanical Brake	Other Parts	Blade Assembly		Pitch Mechanism
11	Main Shaft	Hydraulic System	Transformer		Main Shaft
12		Yaw System	Frequency Controller		Other Parts

Among all the references listed, the ReliaWind project in [146] was a Framework Program 7 funded EU project that was run between component manufacturers, research institutions, wind turbine manufacturers and operators in order to increase the reliability of wind turbines. Work Package 2 was to develop a complete reliability model of a generic wind turbine using information from the project partners. The Whole System Reliability Model was constructed from a reliability block diagram (RBD) and FMECA. The reliability information was sourced from common reliability references and information from project partners. This thesis mainly follows the

onshore RPN results from the ReliaWind project, not only because the turbine type and list of components are close to the turbine in this research; but also because the ranking evaluation in the project comes from prestigious experienced experts in this research area.

4.2.2 FMEA and FMECA for offshore wind application

As stated above, a few publications are available with the topic of the application of FMEA or FMECA for offshore wind farms [152]-[154], and this field is still to be explored. As an attempt of applying FMEA to the offshore application from the published onshore RPN with onshore/offshore failure rate translation developed in this chapter, a number of assumptions have been made here to adjust the RPN values in the way expressed in Eq. 14. The onshore RPN values are multiplied by the ratios of expected offshore failure rates to the corresponding onshore rates in the previous section for the selected components to give values appropriate to offshore conditions, and these ratios are considered as linear. The severity and detection indices are unaffected at this stage, but results in Chapter 5 Section 5.5 and Chapter 6 Section 6.1.3.2 provide the potential of having these two aspects considered. In particular differences in turbine downtime as a result of specific component failures onshore and offshore are ignored. In addition, as mentioned at the beginning of this section, wind speed and ambient temperature only are considered as the environmental factors influencing failure rate with the current data availability in this research. Finally, the offshore RPN can be derived from the onshore RPN as:

$$RPN_{offshore}=RPN_{onshore}\cdot Ratio_{windspeed}\cdot Ratio_{temperature} \quad (16)$$

The derivation of the ratio of the two environmental factors follows the technique introduces in Section 4.1. This also assumes the factors are uncorrelated. The RPN, as seen by Eq.14, is an aggregate of severity, occurrence and detection of a failure mode. Therefore, as mentioned above, in this adjustment, severity and detection are regarded as unchanged. The ratio of failure rate expectations dependent on temperature and wind speed are multiplied directly to give the onshore RPN. It is assumed that wind speed and temperature have equal weighting although this is an area requiring further investigation.

This attempt of offshore RNP calculation is still rather simple and to be upgraded. In future work, apart from the additional environmental factors that could be incorporated in failure rate translation stated in previous section, e.g. wind and wave turbulence, and application of weights on the ratios; the RPN simplification will be examined in more detail, in which for example, suitable proxies for the severity could be the downtime and for detection could be the condition monitoring detection effectiveness associated with a failure.

4.2.3 Results and Discussion

Table 15 shows the RPN translation from onshore to offshore. Because of few unmatched component names from the publications and the actual data from the wind farms, components are processed separately in the middle stage and averaged at the end. Take rotor and blade assembly in the onshore RPN publication as an example, the actual record system in wind farm W records them as rotor system and blades system respectively. Thus the ratios dependent on wind speed and temperature using the different translation methods in previous section are calculated separately. The two

translated offshore RPN are finally averaged as the weighting of the two subcomponents is regarded as the same. The same strategy is applied to the assembly of tower, foundations and nacelle.

It can be seen that the non-fitted method of translation shows that the riskiest component is rotor and blades assemblies which stays the same as the onshore ranking. The exponential fitting method shows that the onshore 3rd riskiest component control system becomes to the 1st riskiest offshore. The 2nd polynomial fitting method indicates the largest difference between onshore and offshore: the high voltage system which is the 6th riskiest component jumps to the 1st position in the offshore system.

With the RPN ranking, the wind farm operator can have a quantified reference of the risky components for operation and maintenance resources allocation, in both personnel and budget. The accuracy of the ranking therefore directly affects the O&M planning and decision making. Theoretically, the exponential function has well defined asymptotic behavior towards 0 and 1 on each end which meets the general shape of the CPD curve; whereas the polynomial function has both ends toward infinity which could not fit the tails of CPD curve. The goodness of the fits is therefore discussed later.

Table 15. Ratios of selected wind turbine subcomponents with normalised onshore RPNs and rank and adjusted offshore RPNs

Onshore			$Ratio_{WindSpeed}$			$Ratio_{Temperature}$			Offshore RPN			
Order	code	Normalised RPN	Non Fitted	Poly2 Fitted	Exp Fitted	Non fitted	Poly2 Fitted	Exp Fitted	Non fitted	Poly2 Fitted	ExpFitted	
											RPN	order
1	Rotor	1609	0.9408	0.8350	0.7889	1.2460	0.6929	1.1853	1926.4	1329.7	1270.0	2
	Blades		0.9994	1.0148	0.82	1.2231	1.0586	0.7811				
2	Main Generator	1204	0.9189	0.7391	0.6336	1.6859	0.7357	0.5164	1865.2	654.7	393.9	9
3	Control system	925	1.2632	1.1809	1.1716	0.9459	1.7393	1.2113	1105.2	1899.9	1312.7	1
4	Hydraulic system	921	1.0869	0.8418	0.8702	1.4600	0.9324	0.5887	1461.5	722.9	471.8	6
5	Main Gearbox	909	0.9968	1.3303	0.9396	1.0383	1.8378	1.3969	940.8	2222.3	1193.1	3
6	High voltage system	872	1.0405	1.2974	0.8136	0.8506	2.5943	1.1702	771.7	2935.0	830.2	4
7	Yaw system	813	1.2682	0.9197	1.0447	1.0368	2.3428	0.8838	1069.0	1751.7	750.6	5
8	Blade Pitch system	692	0.8701	0.7938	0.6893	1.2635	1.5275	0.8911	760.8	839.1	425.1	8
9	Tower	508	1.0990	1.2823	0.9621	0.8224	1.3407	0.8911	637.9	623.1	469.8	7
	Nacelle		1.6958	1.1514	0.8431	0.9480	0.6376	1.1768				
10	Mechanical brake system	336	0.9592	0.6049	0.7437	0.7665	3.4995	1.1819	247.1	711.3	295.3	10
11	Main shaft assembly	246	0.8993	0.7007	0.6929	1.2622	0.7702	1.4381	279.2	132.8	245.1	11

Table 16 shows the goodness of the fits from 2nd polynomial and exponential functions using R-squared and root-mean-square error (RMSE). R-squared is a statistical measure of how close the data are to the mean. Between 0% - 100%, the higher the value is, the better the fit is. The RMSE is another frequently used measure of the goodness of fit. The lower the value is, the better the fit is. In this table, for simplicity of comparison between the two fits, it calculates the difference from the exponential to the 2nd polynomial function for both goodness assessment tools, under the named column "Exp-Poly2". The positive value of the difference indicates the exponential function has a higher value of goodness-of-fit, and vice versa. For convenience of reading, the positive values of the difference for R-squared are highlighted in light green and the negative values of the difference for RMSE are highlighted in light blue.

Table 16. Goodness of the exponential and 2nd polynomial fit using R-Squared and RMSE

	R-squared			RMSE		
component	Exp	Poly2	Exp-Poly2	Exp	Poly2	Exp-Poly2
Rotor 8	0.928	0.972	-0.044	0.058	0.058	0.000
Blades 9	0.969	0.985	-0.015	0.072	0.079	-0.007
Main Generator 27	0.940	0.899	0.042	0.091	0.140	-0.049
Control system 24	0.998	0.970	0.028	0.013	0.020	-0.006
Hydraulic system 23	0.966	0.975	-0.009	0.025	0.038	-0.012
Main Gearbox 14	0.989	0.966	0.023	0.032	0.045	-0.013
High voltage system 1	0.979	0.966	0.013	0.063	0.114	-0.050
Yaw system 18	0.994	0.972	0.022	0.021	0.025	-0.003
Blade Pitch system 11	0.969	0.994	-0.025	0.036	0.039	-0.003
Tower 33	0.975	0.929	0.046	0.041	0.053	-0.012
Nacelle 32	0.842	0.906	-0.064	0.063	0.104	-0.041
Mechanical brake system 15	0.500	0.750	-0.250	0.354	0.280	0.073
Main shaft assembly 13	0.939	0.963	-0.024	0.135	0.136	-0.001
high speed shaft transmission 17	0.950	0.915	0.035	0.131	0.128	0.003

It can be clearly seen that with R-square, exponential function fits better in half of the subsystems (7 out of 14), and with RMSE, exponential function fits better in almost all the subsystems (11 out of 14). Therefore, it can be concluded that in general exponential function fits better to the CPD curve.

This suggests the result of RPN ranking from exponential fitted method is more convincible to be treated as the final result for the failure rate onshore to offshore translation method, where control system overrides rotor and blades assemblies becoming the highest risky wind turbine subsystem in the offshore context. The rotor and blades assemblies become the second highest risky subsystem followed by the main gearbox. The least risky subsystems the mechanical brake and the main shaft assembly remain the same from onshore to offshore. It suggests the wind farm operator can have a more convincing reference of the risky component ranking by the exponential fitted translation method, and therefore can pay more attention and allocate the most important maintenance resources towards the riskiest components in wind turbine O&M.

4.2.4 Conclusion

Failure Modes Effect Analysis (FMEA) or Failure Modes Effect and Criticality Analysis (FMECA), an effective tool of reliability analysis, assists to identify, evaluate and report component failure modes and the severity of potential impacts on the system so that fault tolerance mechanisms can be designed and trained to control the failure impact on operational availability. It has been applied in industries including onshore wind turbines successfully but as yet it is still a new topic and to be explored in an offshore wind context.

Different from a few published literatures working on the failure modes in the research domain, this thesis focus on the only numerical method in FMEA, the Risk Priority Number (RPN). It uses two of the possible failure root causes that change for offshore wind; increase in wind speed and temperature, to demonstrate the effect on the

outcome of an FMECA for offshore wind projects. It provides a novel way of assessing the risk ranking of offshore wind turbine components.

In order to obtain a more reliable failure rate of each wind turbine subsystem, an innovative method has been applied to the limited length of failure data. This method calculates the cumulative probability distribution function of the failure rate, fits a smooth function curve, and differentiates it. The core step is finding a proper fit to the CPD. In this thesis the CPD has been fit and compared with 2^{nd} polynomial and a variation of exponential function. It can be concluded that exponential function is a more reliable method to fit the CPD curve theoretically and actually fits the curve better. Therefore, exponential function is chosen to be the fitting function and the results from the exponential fitting will be applied to the analyses in next chapters.

This chapter focuses on the failure occurrence in the RPN translation, however the failure severity and detection are also key inputs. The simple sole consideration in this chapter has led limited creditability of the translated offshore RPN results. Some side results in Chapter 5 and Chapter 6 provide potential train of thought of having these two aspects considered.

In conclusion, as an important application of the onshore/offshore failure rate CPD translation method, the RPN translation using exponential fitted CPD method shows that control system becomes the highest risky wind turbine subsystem in the offshore context. The rotor and blades assemblies become the second highest risky subsystem followed by the main gearbox. The least risky subsystems the mechanical brake and the main shaft assembly remain the same from onshore to offshore. The onshore/offshore failure rate CPD translation method is further used in the cost

modelling in Chapter 5 and Chapter 6, aiming to help improve the credibility of the failure rate input for the offshore wind farm O&M estimations.

Chapter 5 Strathclyde Probabilistic Cost Model (Plus) for offshore wind farm

Compared to onshore, offshore wind has the advantage of generally higher mean wind speed, less temporal variation and lower turbulence. In addition, negative impact on the landscape is reduced and noise is a less critical issue. On the other hand, some of these advantages come at a cost. The low disturbance to human population is the result of a substantial distance between the offshore wind farm and shoreline where the port where the operation and maintenance (O&M) centre is located. Moreover, marine conditions restrict access for maintenance which depends on the prevailing wind and wave conditions. The result is that O&M accounts for a much larger proportion of total costs than for onshore wind farms. A NREL cost of wind energy review shows that typical OPEX for a 1.94MW onshore wind turbine is $51/kW/yr or $15/MWh, and $138/kW/yr or $37/MWh for a 3.39MW offshore wind turbine [155]. This characteristic of offshore wind farm operations motivates the interest in condition monitoring.

Compared to reactive maintenance, as already discussed in Chapter 2, condition based maintenance is based on data providing an indication of the real time condition of certain turbine subsystems or components. The O&M team can arrange the maintenance considering both component condition and vessel access. In this way, major failures of the turbine can often be circumvented; at the same time, the cost of maintenance should be reduced due to a more effective maintenance regime.

For quantifying the cost effectiveness of O&M, and condition monitoring in particular, failure rate is a key input. The accuracy of the failure rate directly affects the accuracy of any O&M cost estimation. However, as stated in the previous chapter, offshore component failure rate data is not publically available as it has been commercially protected by manufacturers and operators. This results in failure rate data in the public domain being very limited, especially for offshore. The translation of component failure rates from onshore to offshore developed and explained in Chapter 4 can be used to fill this gap.

A cost effectiveness analysis between reactive and condition-based maintenance is presented in this chapter and next chapter to quantify the benefit and discuss the drawbacks of condition monitoring for offshore wind farms. As another important application of the onshore/offshore CPD translation method developed in Chapter 4 apart from the RPN calculation, the research presented in this chapter has applied the translation method to an existing cost model and improved the credibility of the cost model results.

In this chapter, the existing cost model is introduced comprehensively with mathematical methodology in Section 5.1. A wide literature review of other offshore wind farm O&M cost models with comparison discussion of the existing model is then presented in Section 5.2. After gaining the knowledge of the advantages and disadvantages of the existing cost model from the first two steps, a series of improvements have then been undertaken and resulted in the upgraded model. The improvements are presented in Section 5.3. In order to investigate the performance of the improved model, a benchmark against a number of accessible other cost models

introduced in Section 5.2 has been undertaken and is discussed in Section 5.4. Since condition based maintenance is an innovative highlight of this cost model and the core research concern of this thesis, a condition monitoring system detection effectiveness analysis is presented in Section 5.5. Section 5.6 provides a detailed sensitivity analysis against eight key parameters of the improved cost model.

This improved cost model has been used for two real site case studies presented in Chapter 6.

5.1 Strathclyde probabilistic cost model (StraPCost)

The existing cost model adapted and used in this research was initially developed for an Energy Technologies Institute (ETI) condition monitoring project undertaken by the University of Strathclyde, [124][156]. The purpose of the development of this cost model is to assess the maintenance of offshore wind turbines, and the impact of condition monitoring. Access probabilities, expected delays and the associated costs are all calculated using a probabilistic approach.

Unlike onshore, offshore O&M costs are largely due to the vessel usage. For the safety and legal reasons, vessel accessibility relies strictly on the sea state (e.g. wave conditions) and wind conditions. Delays will happen if the sea state does not allow the vessel to approach the turbine and offload maintenance staff, and there will be a considerable amount of revenue loss due to the stoppage of the turbine and extra rental fees if the delay is not predicted. The delay for different types of vessels is therefore significant for the cost effectiveness of the wind farm operation.

In the Strathclyde probabilistic cost model (StraPCost), expected delay time to the turbine repairs due to the sea state and/or wind condition is estimated, together with the costs associated with the repairs and delays. Sensitivities to key factors, e.g. vessel access limits and time required, can be estimated as well.

This cost model is still in its development stage. This provides the opportunity to look into each calculation step and the correlation of different parameters. The cost model consists of two main parts using Matlab codes and Excel spreadsheets, respectively. Outputs from Matlab are manually extracted and set as input of the Excel spreadsheet with additional pre-processing.

5.1.1 Statistical Output

An example of the final output interface of the entire cost model (Excel Spreadsheet) is shown in Table 17. It lists the calculated total downtime (in days), together with the availability, capacity factor, energy lost, mean power generated over a year, total annual energy generated, annual revenue. It calculates revenue lost and annual maintenance cost for an individual wind turbine and for the entire wind farm. It also provides the vessel cost, wage cost, component costs, and the total O&M cost (with and without revenue loss) for an individual wind turbine and the entire wind farm.

A strength of this model is that it allows comparison of results for reactive maintenance and condition based maintenance in neighbouring columns, and lists the difference between the results from these two maintenance strategies together with the percentage change relative to the baseline.

Table 17. StraPCost final output with example statistics

WITH DOWNTIME based on	Reactive Maintenance	Condition-based Maintenance	Change due to CM
downtime	26.5days	24.3 days	-2.1 days
availability	92.7 %	93.3 %	0.6 %
capacity factor with downtime	36.3 %	36.6 %	0.4 %
energy lost	845.1MWh	752.3 MWh	-92.8 MWh
mean power generated over year with downtime	1.09MW	1.10 MW	0.01 MW
total annual energy generated with downtime	9527.2MWh	9620.0 MWh	92.8 MWh
annual revenue with downtime	857.4£k	865.8 £k	8.4 £k
revenue lost	76.1£k	67.7 £k	-8.4 £k
annual maintenance cost	329.9£k	295.8 £k	-34.1 £k
vessel cost	£0.021/kWh	£0.018 /kWh	-£0.003 /kWh
wage cost	£0.0016/kWh	£0.0020 /kWh	£0.0004 /kWh
component cost	£0.0121/kWh	£0.0111 /kWh	-£0.0010 /kWh
Total O&M cost (w/o revenue loss)	£0.0346/kWh	£0.0310 /kWh	-£0.0036 /kWh
revenue lost	£0.0080/kWh	£0.0071 /kWh	-£0.0009 /kWh
Total O&M cost (with revenue loss)	£0.0426/kWh	£0.0382 /kWh	-£0.0045 /kWh

5.1.2 Requirements of input and middle stage function spreadsheets

As the cost model puts emphasis on the vessel characteristics and in particular the sea states in which the vessel can access the turbines, the input requires wave and vessel information. Considering the sometimes limited accessibility of the actual sea state data, alternative methods are provided in the cost model. Inputs covering four main aspects are: wave statistics of the given site; the vessel operational limits mainly in terms of the threshold of the wave height and required access time which comprises vessel waiting time; travel time; and repair time. Through appropriate probability distributions, the expected maintenance delay time can be estimated, and thus the turbine operational downtime and the related cost of lost generation can be calculated. A comprehensive list of model inputs is given below:

From met mast, wave sensing device and turbine:

- *Actual wind speed time series from the met mast, or alternatively the calculated wind Weibull parameters.*
- *Actual significant wave height time series; alternatively, significant wave height duration characteristics in term of graphs/tables/statistics, in terms of wave location parameter, wave shape parameter, wave scale parameter.*
- *Wind turbine power curve—nominal.*

From wind farm operator:

- *Personnel total hourly rate (including salary, tax, holiday cost etc.).*
- *Electricity sale price per unit.*
- *Renewables Obligation Certificate (ROC) price per unit.*
- *Shift length.*
- *Delay charge for unscheduled vessel.*
- *Delay charge for scheduled vessel.*
- *The types of vessels required for each category of repairs.*
- *How many people required for each category of repairs.*
- *Day rate for each type of vessels.*
- *Component replacing/repairing cost.*
- *Vessel waiting/travel time.*
- *Repair time for each turbine component.*
- *Component failure rates*
- *Condition monitoring successful fault identification and advance warning time.*
- *Condition monitoring false-positive rate.*

The analysis process begins with the Matlab programme. The inputs for the Matlab codes are the wind speed and significant wave height time series and the corresponding time stamps for the selected wind farm sites. Outputs from the Matlab calculations are shown in Table 18. They provide a statistical characterisation of the wave climate for use by the Excel spreadsheet.

Table 18. Statistical output table from Matlab part of the cost model

wave location parameter (m)	Ho
wave shape parameter	Kh
wave scale parameter (m)	Hc
characteristic wave duration (hrs)	Ah
wave duration exponent	bh
duration parameter scaling	acgh
wave exponent	akh

The remaining inputs to the Excel spreadsheet were detailed below. Examples of input sheets are given in Table 19 and Table 20. Other input sheets cover "Vessels" and "Sites". The "Vessels" sheet covers vessel type, maximum wave height, maximum wind speed, vessel speed, positioning time, day rate, etc. Once the list of vessel information by types is set, it can be called directly from the "Input & Output" sheet. Wind and wave accessibility, accessible days per year and day rate (£) are then calculated.

Table 19. Site metocean characteristics input table in StraPCost

	SITE METOCEAN CHARACTERISTICS		
	Site name (Windsite)	**Land**	**0%**
distance to shore	ds	1	km
Wave Weibull Parameters (3 para)	(read from sheet 'Sites')		
wave location parameter	Ho	0.000	m
wave shape parameter	kh	2.000	
wave scale parameter	Hc	0.001	m
mean wave height	Hbar (derived)	0.00	m
	Site name (Windsite)	**Land**	**0%**
Wind Weibull Parameters (2 or 3 para)	(read from sheet 'Sites')		
wind location parameter	U0	0.000	m/s
wind shape parameter	kU	2.000	
wind scale parameter	Uc	7.899	m/s
mean wind speed	Um (derived)	7.00	m/s

Similarly, the "Sites" sheet takes the wind farm information, with geographical data such as location, source of database, grid point, latitude, longitude and distance from shore; basic wind statistics of mean and standard deviation of wind speed; wind speed Weibull parameters in terms of location, shape and scale parameters, which are

required to be calculated from the wind farm time series data outside the Excel spreadsheet; similarly with the wave statistics and wave height Weibull parameters; Kuwashima-Hogben parameters for wave height duration calculation can be estimated when the duration statistics is unknown. Once the wind farm site information is set in the "Sites" sheet, it can be called directly by the site name, as shown in Table 19.

With the input of access limits, required access times and the site wind and wave data, the expected delay time can be estimated, and thus the cost due to this delay can be calculated and added to the O&M cost in the final output.

In order to do this, another important input information is required from the wind farm operators. Table 20 shows the turbine basic information inputs, in terms of rated power, rated wind speed, cut-in wind speed, cut-out wind speed, and drive train efficiency. The financial inputs are also listed in terms of personnel hourly rate (salary and all the other costs for the personnel), electricity sale price per unit, ROC price per unit, year length, and shift length. Delay charges for unscheduled and scheduled vessel usage is also required to be taken into account in the vessel cost calculations.

Table 20.Turbine characteristics and financial assumptions input table in StraPCost

TURBINE CHARACTERISTICS			
rated power	Prate	**2.3**	MW
rated wind speed	Urate	**12**	m/s
cut-in wind speed	Uci	**4**	m/s
cut-out wind speed	Uco	**25**	m/s
drive train efficiency	eff	**96.5%**	
FINANCIAL ASSUMPTIONS			
personnel hourly rate	rh	**25**	£/hr
electricity sale price per unit	pe	**40**	£/MWh
ROC price per unit	pr	**45**	£/MWh
year length	yr	**8760**	hr
shift length	tshift	**12**	hr
delay charge for unscheduled vessel	puves	**25%**	
delay charge for scheduled vessel	psves	**0%**	

Assumes £45 / ROC, 2 ROC / MWh offshore

5.1.3 Methodology for delay time calculation

Many of the wind turbine maintenance cost models in the research domain make use of Monte Carlo simulation [157]-[160], where repeated long runs are required and continuous time-series data are essential for the full length of each run. Considering this, StraPCost just as its name implies, uses a more direct probabilistic approach instead to undertake the modelling. This much enhances the speed and simplicity of the computation and the transparency for exploring trends and sensitivity by adjusting input parameters. An event tree is constructed in this approach, as shown in Figure 43. Conceivable events and alternatives are joined in a branched sequence (event tree).

5.1.3.1 The Event tree

Since this model is in its initial development stage, the event tree only captures the main variables of interests and relies on a number of assumptions. A fault is considered to occur randomly in time, governed by the appropriate failure rate. All operations are carried out once for one operation, avoiding multiple trips. At this stage, only a single condition applies to the timing of the repair: significant wave height. Wind speed could provide a further restriction on access, however, since studies show a good correlation between significant wave height and wind speed, only significant wave height is considered at this stage. This correlation and related process will be presented in detail later. Accurate short term forecasts of sea state are assumed to be available with enough look-ahead time to complete the required operation; in the model as in reality, an operation would only be initiated when the sea state is forecasted to be suitable for a sufficient period of time. For simplicity, the term “storm” is used in this model to represent any period when waves are too high for the vessel to access the turbine and

undertake the repair. In a similar manner, “calm” is used to represent the period when the wave height is low enough for the purpose of repair.

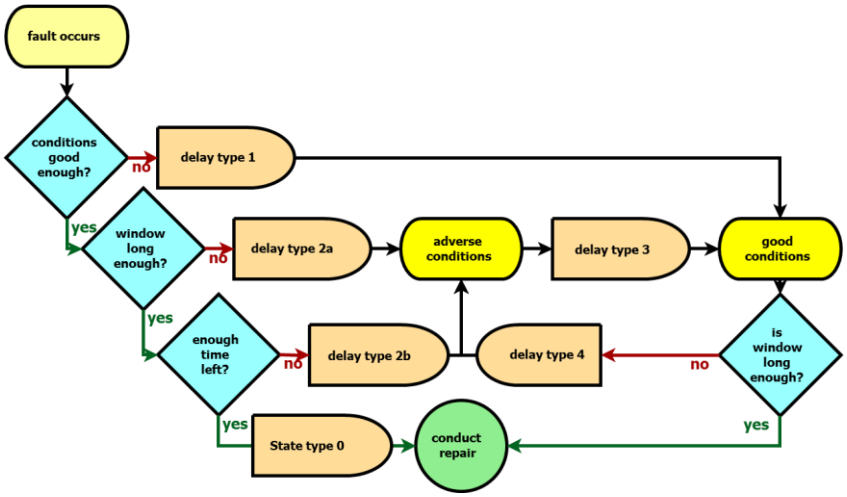

Figure 43. Model of the event tree in the StraPCost algorithm, with modification from [156]

5.1.3.2 Modelling definitions

As shown in Figure 43, sea states are categorised into delay types when a fault occurs. Sea state type 0 represents the situation when the sea state is low enough, which is a “calm” duration, and there is sufficient time for the maintenance operation to be completed. First order delay (Delay type 1) is when the sea state is too high to access, which is a “storm” period, and the operation needs to wait for the next “calm” duration. Second order delay type “a” (Delay type 2a) is when the sea state is low enough but the prediction shows there is too short a time available to affect repair, and the operation still needs to wait for the sufficient “calm” duration. Second order delay type “b” (Delay type 2b) represents the situation when the sea state is low enough and the predicted duration is long enough, but the fault occurs too late in the weather window, and in this case the operation still needs to wait for the next Sea state 0. These four states are enough for a simplified event tree model, and are illustrated in a fictional

example in Figure 44. Delay type 4 is derived after Delay type 1 occurs, which represents when the sea state finally "calm" following a "storm" state, but there is not enough time for the repair to be undertaken. This type of delay looks similar to Delay type 2 but has a different calculation. Similarly, after suffering Delay type 2 or 4, there is still a period of "storm" and this derives Delay type 3. Again, even though it is similar to Delay type 1, the calculation is different.

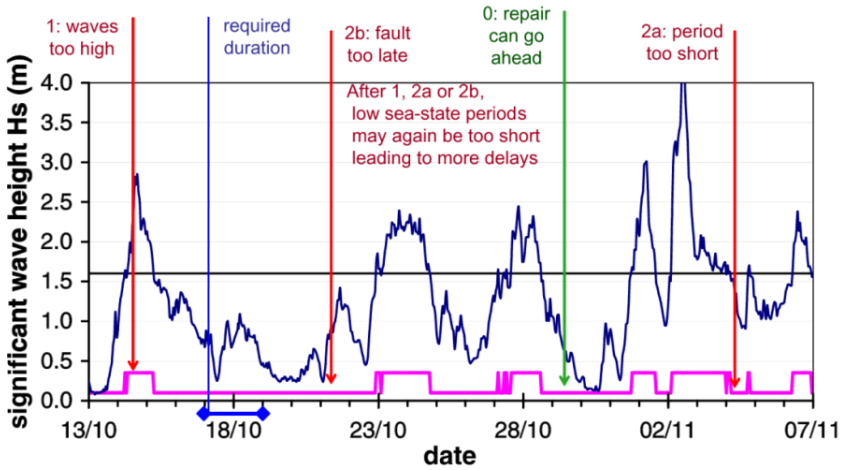

Figure 44. Example of 4 types of delay dependent on significant wave height time series as used by the StraPCost model algorithm [156]

5.1.3.3 Wave and wind correlation

Wind speed and significant wave height are found to be well correlated at most sites, both temporally and spatially. As shown in Figure 45, from [161], the strong wind is over 15 m/s, which is shown in the left graph, can be found in the region near the South Pole. This region also has an extreme wave climate with an average significant wave height of over 5 m, shown in the right graph. Similarly, around the equator, where the wind is the lowest (lower than 5m/s) can be found the lowest significant wave height at less than 2 m. Other less extreme values also show a highly correlated spatial distribution.

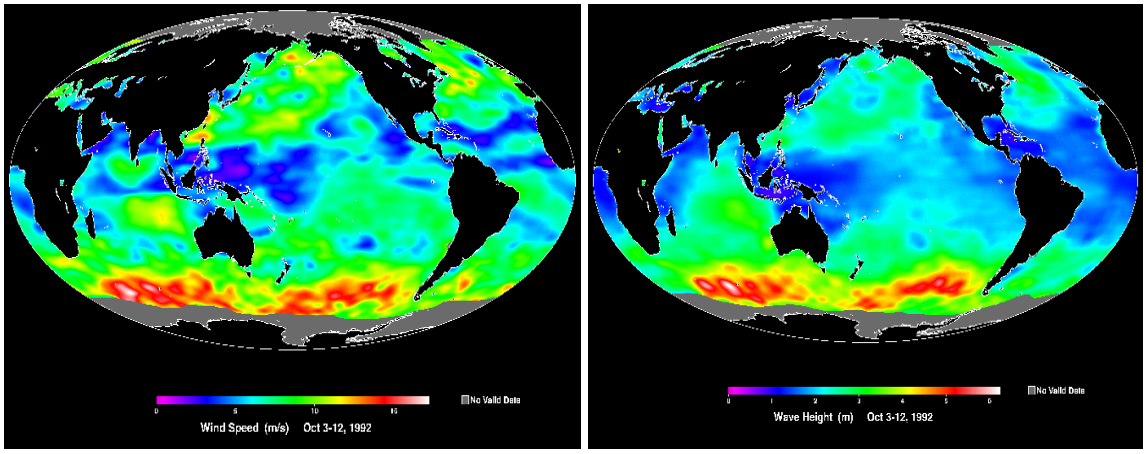

Figure 45. Global distribution of wind speed (left) and significant wave height (right) recorded by NASA [161]

A time series record comparison also shows that wave height and wind speed are highly correlated temporally at the same location, as shown in Figure 46 [162]. Even though the wind speed time series exhibits higher frequencies of fluctuation, the two time series have highly correlated trends. When the first peak occurs in the significant wave height, the wind speed time series also shows a peak at time stamp of around 151. Similarly, when the second peak in the significant wave height occurs at the time stamp around 155, it also shows a peak in the wind speed time series.

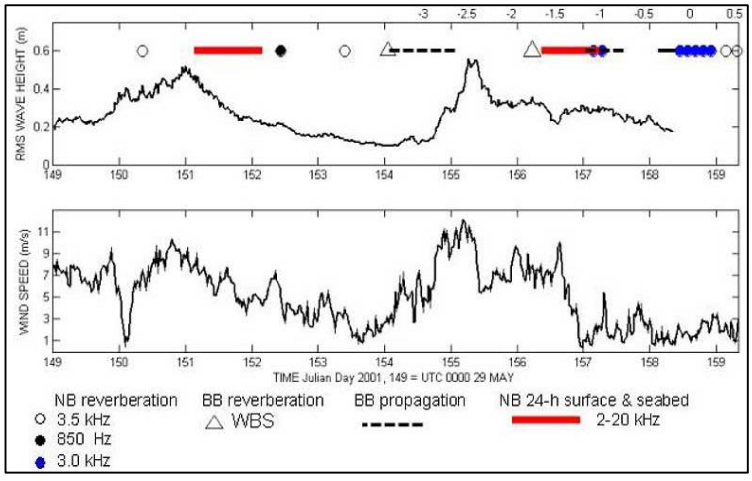

Figure 46. Time sequence of the wave height (top) and wind speed (bottom) from ASIAEX, East China Sea [162]

Statistically, a correlation analysis has been done on the NEXT database grid point 15631. The Pearson correlation** coefficient for annual figures is 0.88, [163].

A translation calculation of significant wave height and wind speed is built in the Matlab part of the cost model. It is used to transfer the significant wave height threshold into the corresponding wind speed threshold for use in generation loss calculation. The average power can be calculated from above and below the translated wind speed threshold, as shown in equations below.

$$\overline{P_{below}} = \int_{U=0}^{threshold} p(U) \cdot P(U) dU \tag{17}$$

$$\overline{P_{above}} = \int_{threshold}^{\infty} p(U) \cdot P(U) dU \tag{18}$$

It shows the Weibull distribution of the wind speed and the idealised power curve as an example. As shown in Figure 47, the translated wind speed threshold from the significant wave height is set as red line at approximately 9m/s. Both curves are cut into two parts: below threshold (left) and above threshold (right). The capacity factors can then be calculated in equations below, respectively. These give the threshold turbine capacity factor of 44.5% and mean power of 2.22MW, as shown in Figure 48.

$$CF_{below} = \frac{\int_{U=0}^{threshold} p(U) \cdot P(U) dU}{P(U) \cdot \int_{U=0}^{threshold} p(U) dU} \tag{19}$$

$$CF_{above} = \frac{\int_{threshold}^{\infty} p(U) \cdot P(U) dU}{P(U) \cdot \int_{threshold}^{\infty} p(U) dU} \tag{20}$$

**The Pearson product-moment correlation coefficient is a measure of the linear correlation (dependence) between two variables X and Y, giving a value between +1 and −1 inclusive, where 1 is total positive correlation, 0 is no correlation, and −1 is total negative correlation.

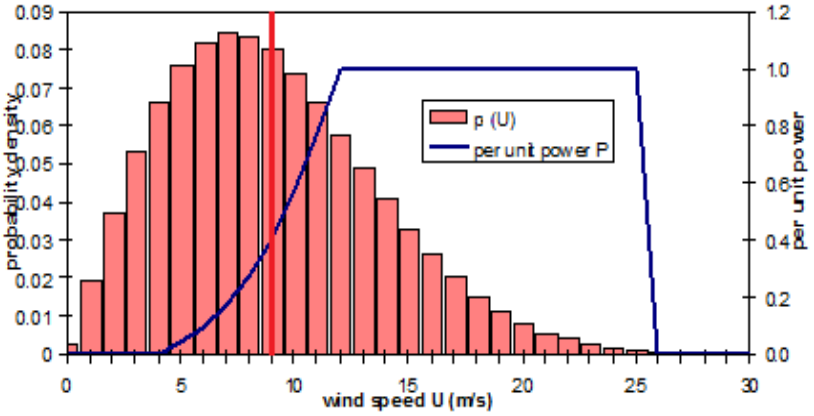

Figure 47. Idealised wind turbine power curve with Weibull probability density function curve in [156]

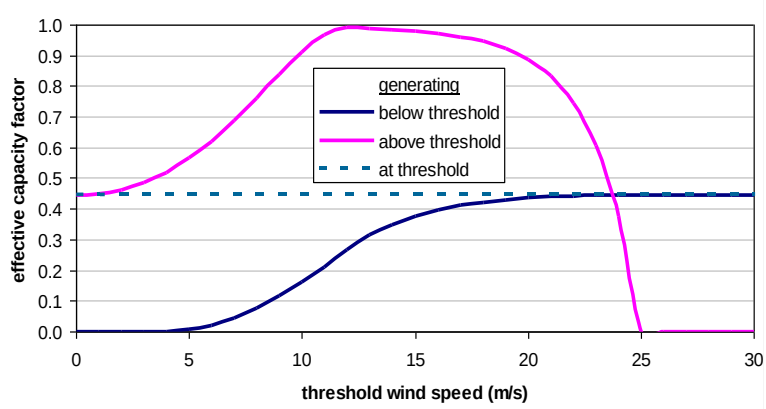

Figure 48. Variation of effective capacity factor with threshold wind speed for above and below threshold generation [156]

5.1.3.4 Basic mathematical tool

As a probability based statistical cost model, the core calculations are for the probability distribution and the expected values of the corresponding delay.

The calculation starts from the significant wave height exceedance probability, P_H. The distribution fitting function is chosen from the standard three-parameter Weibull distribution, as shown in Eq. 21, where H_{th} represents the significant wave height for a given threshold; H_0, H_C and k_H are the location, scale and shape parameter of the three-parameter Weibull distribution, respectively.

$$\mathrm{P_H} = \mathrm{P}(H_{th}) = \exp\left(-\left(\frac{H_{th} - H_0}{H_C}\right)^{k_H}\right) \tag{21}$$

In a similar manner, the calm state can be expressed by the Weibull distribution for the probability of occurrence of the required time:

$$\mathrm{Q_n}(H_{th}, t_{req}) = \exp\left(-g_n \cdot \left(\frac{t_{req}}{\tau_n}\right)^{\alpha_n}\right) \tag{22}$$

The corresponding probability density function is the differentiation of Q_n in Eq.22:

$$q_{\mathrm{n}}(H_{th}, t_{req}) = \frac{g_n \alpha_n}{\tau_n} \cdot \left(\frac{t_{req}}{\tau_n}\right)^{\alpha_n - 1} \exp\left(-g_n \cdot \left(\frac{t_{req}}{\tau_n}\right)^{\alpha_n}\right) \tag{23}$$

where $\alpha_n$is the shape parameter of the Weibull distribution for calm duration and is a function of H_{th}; t_{req} is the required duration for an operation to be completed; and g_n is the normalization factor:

$$g_n = \Gamma(1 + \frac{1}{\alpha_n})^{\alpha_n} \tag{24}$$

For this calm duration, a definition of partial first moment of the distribution with normalization to the mean is given:

$$\mathrm{M_{qn}}(H_{th}, t_{req}) = \frac{1}{\tau_n} \cdot \int_0^{t_{req}} t \cdot \mathrm{q}_n(t)\, dt \tag{25}$$

When the storm duration is given as t, a fault can occur at any instant during t with equal probability, thus a delay of t/2 is expected. This can be seen in Delay type 1. The normalized complete second moment of the storm duration is given:

$$\mathrm{M_{qqx}}(H_{th}) = \frac{1}{2\tau_x^{\,2}} \cdot \int_0^{\infty} t^2 \cdot \mathrm{q}_x(t)\, dt \tag{26}$$

When a calm duration is shorter than the required repair time, delay is still expected (can be seen in Delay type 2a).

The probability for a fault occurring is given by the normalized partial first moment:

$$\mathrm{M}_{\mathrm{qq}\,n}\left(H_{th}, t_{req}\right) = \frac{1}{2\tau_n^{\,2}} \cdot \int_0^{t_{req}} t^2 \cdot \mathrm{q}_n(t)\,dt \qquad (27)$$

An important example of the application of this algorithm is the expression of the Sea state type 0. The probability P_0 expresses the state when the wave height is predicted to be below the set threshold and remain so for a long enough window of time, as shown in the equation below, where $\tau_n(H_{th})$ is the mean calm duration. Similarly, $\tau_x(H_{th})$ is the mean storm duration.

$$P_0(H_{th},t_{req}) = [1-P(H_{th})] \cdot [1-M_{qn}(H_{th},t_{req})-Q_n(H_{th},t_{req}) \cdot t_{req}/\tau_n(H_{th})] \qquad (28)$$

For the Delay type 1, the significant wave height is above the set threshold. The probability of this type is the same as Eq.21.

$$\mathrm{P}_1\left(H_{th}\right) = \mathrm{P}_H = \exp\left(-\left(\frac{H_{th}-H_0}{H_C}\right)^{k_H}\right) \qquad (29)$$

When the wave height is below the set threshold (calm) but for an insufficient duration, the probability of Type 2a delay is given:

$$P_{2a}(H_{th},t_{req}) = [1-P(H_{th})] \cdot M_{qn}(H_{th},t_{req}) \qquad (30)$$

For the Delay type 2b, where sea sees a calm duration with enough long time t, however the fault occurs too late in this calm window. The probability of the occurrence of the enough long calm duration is Q_n (Eq. 22). The probability of the occurrence of this type of delay is given:

$$P_{2b}(H_{th},t_{req}) = [1-P(H_{th})] \cdot Q_n \cdot t_{req}/\tau_n = P(H_{th}) \cdot Q_n(H_{th},t_{req}) \cdot t_{req}/\tau_x(H_{th}) \qquad (31)$$

For higher order delays, Delay type 3 has two possible occurrences.

When it occurs after Delay type 2a, Delay type 3 is similar to this second order delay, with probability of:

$$P_{3'}(H_{th},t_{req}) = P_{2a}(H_{th},t_{req}) = [1-P(H_{th})] \cdot M_{qn}(H_{th},t_{req}) \quad (32)$$

Similarly, when Delay type 3 occurs after Delay type 2b, this additional delay has probability of:

$$P_{3''}(H_{th},t_{req}) = P_{2b}(H_{th},t_{req}) = [1-P(H_{th})] \cdot Q_n \cdot t_{req}/\tau_n \quad (33)$$

After Delay type 1 and 3 following type 2a or 2b, there is still certain possibility that the calm duration is not long enough. Delay type 4 or higher thus is simply calculated as the probability of a calm insufficient duration, given as:

$$P_4 = 1 - Q_n \quad (34)$$

In this type of delay, two additional delays in terms of waiting out the insufficient calm duration and waiting out the subsequent storm are considered in the expected delay time.

With all the types of delays, Eq.35 gives the general simplified expression of the expected delay. The stated algorithm gives the routine calculation for given probability distribution. More detailed calculation can be found in [124].

$$\begin{aligned} \mathrm{E}\left[\mathrm{t}_{\mathrm{delay.total}}\left(H_{th},t_{req}\right)\right] = {} & \mathrm{P}\left(H_{th}\right)\cdot \mathrm{M}_{\mathrm{qqx}}\left(H_{th}\right)\cdot \tau_x\left(H_{th}\right) \\ & + \frac{\left(1-\mathrm{P}\left(H_{th}\right)\right)^2}{\mathrm{P}\left(H_{th}\right)}\cdot \mathrm{M}_{\mathrm{qqn}}\left(H_{th},t_{req}\right)\cdot \tau_x\left(H_{th}\right) \\ & + \mathrm{P}\left(H_{th}\right)\cdot \mathrm{Q}_{\mathrm{n}}\left(H_{th},t_{req}\right)\cdot \frac{t_{req}^{\ 2}}{2\tau_x\left(H_{th}\right)} \\ & + \mathrm{P}\left(H_{th}\right)\cdot \mathrm{Q}_{\mathrm{n}}\left(H_{th},t_{req}\right)\cdot t_{req} \\ & + \left(1-\mathrm{P}\left(H_{th}\right)\right)\cdot \mathrm{M}_{\mathrm{qn}}\left(H_{th},t_{req}\right)\cdot \tau_x\left(H_{th}\right) \\ & + \left[\mathrm{P}\left(H_{th}\right)+\left(1-\mathrm{P}\left(H_{th}\right)\right)\cdot \mathrm{M}_{\mathrm{qn}}\left(H_{th},t_{req}\right)\right]\cdot t_{req} \\ & + \frac{\left[\mathrm{P}\left(H_{th}\right)+\left(1-\mathrm{P}\left(H_{th}\right)\right)\cdot \mathrm{M}_{\mathrm{qn}}\left(H_{th},t_{req}\right)\right]^2}{\mathrm{P}\left(H_{th}\right)\cdot \mathrm{Q}_{\mathrm{n}}\left(H_{th},t_{req}\right)}\cdot \tau_x\left(H_{th}\right) \end{aligned} \quad (35)$$

5.1.4 Assumptions

At its initial development stage, this cost model estimates the output based on a series of assumptions, from the failure rate setting to the maintenance categories.

5.1.4.1 Reliability and failure rate allocation

As mentioned, there is almost no accessible data for offshore failure rates or down times and very limited onshore data in the public domain. The accessible reliability data are relatively old and mainly reflect smaller onshore wind turbines. It is certainly not ideal for the cost model for offshore O&M.

Another problem with the published data is the lack of consistent subsystem/component categories. Studies based on data collected by the Land Wirtschafts Kammer Schleswig-Holstein (LWK) show a general relationship of the failure rate dependent on turbine size, however these failure rates are based on the whole turbine with no detailed subsystem breakdown at all, [164]. It can be observed from the scatter graph of the turbine failure rate with size, that a power law trend can be fitted with reasonable correlation, as shown in Figure 49. The power law trend fit derivation is as shown in Eq.36. This enables the estimation of failure rate for turbine sizes of e.g. 2.75MW and 5MW, at 5.4 and 7.9 failures per turbine per year, respectively.

$$Failure\ rate = 0.0395 \cdot \left(\frac{Power}{kW}\right)^{0.621} \cdot \frac{failures}{yr} \qquad (36)$$
$$R^2 = 0.735$$

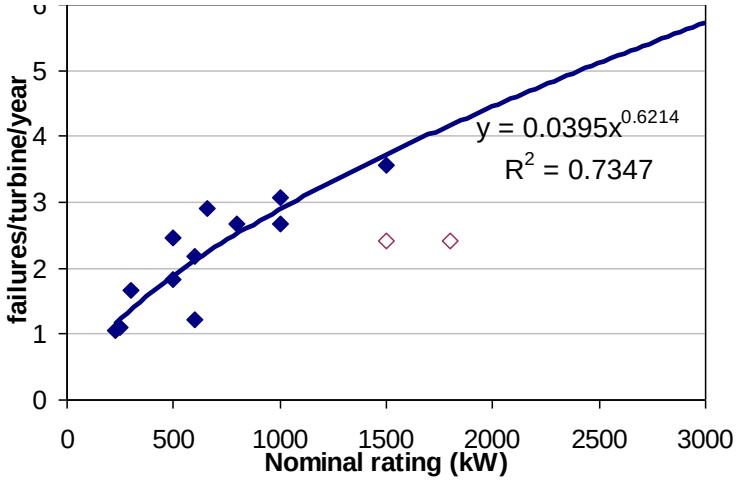

Figure 49. Power law trend of turbine failure rate with turbine nominal size [156]

When it comes to a more detailed breakdown of failure rates and down time, the ReliaWind project study comprised 290 wind turbines for varying operating time over 240 wind-farm months, [165]. Results from this study have been presented in Chapter 2, Section 2.3. Leaving aside the fact the analysed turbines are for onshore application and the question whether the types are up to date, what is noticeable is that the data presented are normalised relative to the overall failure rate or down time, which shows the percentage contribution to the overall failure rate or down time and gives the cumulative contribution 100% in total. This means the results do not give actual failure rates and cannot be used as direct input in the cost model.

For the allocation of the failure rate, the cost model in this thesis uses the power law trend gained from the failure rate with turbine size in [164] as the total failure rate, and takes the breakdown of failure rate for different components and subsystems from the percentage in [165], shown in Table 21. Thus total failure rate changes automatically with the size of the turbine used. The division of failure rate contribution based on component/subsystem from [165] is set as the percentage of all faults for each

component/subsystem. The percentage of detailed failure rate is then multiplied by the total failure rate in order to give the assumed failure rate of each component/subsystem. As highlighted in colour in the table, components with different condition monitoring (CM) types are calculated only once, as one general value.

$$Subsystem\ failure\ rate = Total\ failure\ rate \cdot Falure\ rate\ percentage \quad (37)$$

Table 21. Example of failure rate allocation in StraPCost, first row given the total value of failure rate and its total percentage (close but not equal to 100%)

CM error margins	CMtype	% fail.rate	fail. /yr /turbine
Total		99.5%	3.479
Gearbox Assembly		**5.1%**	0.179
Gearbox Assembly	Vibration		
Gearbox Assembly	Particles		
Gearbox Assembly	Strain		
Gearbox Assembly	SCADA		
Generator Assembly		**7.2%**	0.250
Generator Assembly	Vibration		
Generator Assembly	Current		
Generator Assembly	SCADA		
Blades	Strain	**1.5%**	0.051
Pitch System	SCADA	**21.3%**	0.745
Yaw System	SCADA	**11.3%**	0.394
Frequency Converter		**13.0%**	0.453

5.1.4.2 Maintenance categories

Division on failures dependent on repair categories was undertaken by study on the WMEP programme, [166]. The relevant graph is shown in Figure 10 in Chapter 2, Section 2.3. In the programme in [166], the failures are categorised into two schemes considering the down times with actual failure rate values. Failures with downtimes less than a day are assumed to be minor, and of those with down time of more than a day are assumed to be major. Even though this categorization is fairly simple and rough, it contains actual failure rate values and provides a train of thought of dividing failures with economic impact and reflects the nature of the repair required.

The maintenance categories are further split into four schemes in the DOWEC project and applied in the ECN O&M cost model [167]. As shown in Table 22, in this model, Category 1 is when replacing core components up to 300 tonne (t) requiring heavy lift, external crane; Category 2 is when replacing large parts over 50t where a built up internal crane is sufficient; Category 3 is when replacing small parts less than 1t and where a permanent internal crane is sufficient, with repair time no more than 48 hours; and Category 4 is when replacing small or no parts, repair time no more than 24 hours, including inspection or cleaning inside (A) or outside (B).

Table 22. Division of maintenance categories and their definition in DOWEC project and ECN O&M cost model [167]

Maintenance Categories		**Fault type class classification**	
Nr	**Description**	**Description**	**Nr.**
4A	Repair, Cleaning Reset Inside	No materials	1
4B	Repair, Cleaning Reset Outside	Consumables	2
3	Replacement small parts (<1 MT)	low priced parts, small crew	3
			4
2	Replacement large parts (>50 MT)	med. priced parts, med. crew	5
		low priced parts, med. crew	6
			7
1	Replacement rotor and nacelle, shaft, main bearing and yaw gear (<300MT)	high priced parts, med crew	8
		med. priced parts, med crew	9
			10
			11
			12
			13
			14
			15
			16

Referring to the categorizations stated above, StraPCost mainly allocates three maintenance categories for the unscheduled (reactive) and scheduled (condition-based) maintenance, together with one remote reset scheme, as shown in Table 23.

Table 23. Example of maintenance categories in StraPCost

Procedure Category	**reactive maintenance**			**condition-based maintenance**			
	Heavy components, external crane	Small parts, permanent internal crane	Inspection and repair (outside)	Heavy components, external crane	Small parts, permanent internal crane	Annual service	Manual reset
	unscheduled			scheduled			
Repair type	Au	Cu	Du	As	Cs	Ds	E
weight limit	**500**	**10**	**10**	**500**	**10**	**10**	**10**
repair time	**52**	**22**	**7.5**	**52**	**22**	**60**	**3**
lead time	**1440**	**0**	**0**	**48**	**24**	**1440**	**0**
people reqd	**5**	**3**	**3**	**5**	**3**	**3**	**2**
vessel	**HLV1**	**CTV1**	**CTV1**	**HLV1**	**CTV1**	**CTV1**	**CTV1**
subsystem							
Generator Assembly	10%	26%	64%	0%	0%	0%	0%
Gearbox Assembly	10%	26%	64%	0%	0%	0%	0%
Blades	5%	13%	82%	0%	0%	0%	0%
Pitch System	0%	32%	68%	0%	0%	0%	0%
Yaw System	0.5%	27.5%	72%	0%	0%	0%	0%

Comparing to the ECN model, some categories are omitted. The maintenance category A is equivalent to Category 1 in the ECN model, with heavy components replacement and external crane hire; the maintenance category *C* can be referred to Category 3 in the ECN model, with small parts replacement and permanent internal crane use; the maintenance category *D* can be referred to Category *4B* in the ECN model, with inspection and minor repair outside. The subscript *u* represents *unscheduled* which refers to the assumption that the vessel usage in the reactive maintenance is always unscheduled, as opposed to the *s* in *scheduled* in condition based maintenance. The value of each turbine component under each maintenance category under the unscheduled maintenance category is assumed based on empirical knowledge to expand the minor-major categorization in the WMEP programme [166] into three categories. The value under scheduled maintenance category is assumed based on the condition monitoring effect indicators adjusting scheduled values.

5.1.4.3 Condition monitoring effect

An important innovation of StraPCost is that its takes into account of the effect of condition monitoring. The application of condition monitoring is categorized in terms of three possibilities: general detection (*Detectability*) is where a fault is detected before failure occurs; early detection (*Pre-Empt*) is where a fault is detected early enough allowing suitable advance planning and maintenance to degrade the fault level; and false alarm (*False-Positive*) is where the condition monitoring indicates a fault where none exists. An example of condition monitoring performance for selected systems is given in Table 24. It is important to note that these numbers are estimates rather than actual data. Despite model assumptions, these numbers can be varied to explore the way that the performance of the condition monitoring affects the economic value.

Table 24. Example of assumptions of condition monitoring effect in StraPCost

Subsystem	**CM type**	detectability	Pre-empt	falsepos
Generator Assembly		40%	20%	10%
Generator Assembly	Vibration	**25%**	**12%**	**4%**
Generator Assembly	Current	**10%**	**8%**	**4%**
Generator Assembly	SCADA	**5%**	**0%**	**2%**
Gearbox Assembly		50%	25%	10%
Gearbox Assembly	Vibration	**30%**	**14%**	**4%**
Gearbox Assembly	Particles	**10%**	**6%**	**2%**
Gearbox Assembly	Strain	**5%**	**3%**	**2%**
Gearbox Assembly	SCADA	**5%**	**2%**	**2%**
Blades	Strain	**20%**	**10%**	**5%**
Pitch System	SCADA	**35%**	**10%**	**5%**
Yaw System	SCADA	**35%**	**10%**	**5%**

Detectability describes the general state that a fault is detected before it runs to complete failure. This excludes the early detection presented by *Pre-empt*, which is when a fault is detected before it escalates in severity so the maintenance can be scheduled with enough time and the repair category can be downgraded. For example,

the failure rate from the unscheduled heavy repair category can be transfer to the scheduled light repair category. *False-Positive* represents a negative effect by the condition monitoring system, which is when a non-existent fault is detected and that results in an unnecessary scheduled repair visit which increases the O&M cost.

It needs to be noted that the overall condition monitoring detection value of each subsystem is simply assumed to be added from each CM type without interconnections. This means it assumes different CM systems have independent detection effect to the subsystem, and the more types of CM systems are used in the subsystem, the higher the detection effect the subsystem has. In the case of generator assembly in Table 24, for example, the overall detection state = vibration + current + SCADA. The *detectability* value, for example, is 25%+10%+5%=40%. This simple assumption could be improved in future work.

When it comes to the impact of condition monitoring system, the affected unscheduled maintenance categorized failure rate of each turbine component is transferred from its corresponding original unscheduled value input without consideration of the CM detection effectiveness in Table 23, denoted as *Au, Bu* and *Du*, by the suitable condition monitoring detection parameters. Again *Au* stands for unscheduled heavy components requiring external crane, *Bu* stands for unscheduled small parts with permanent internal crane, and *Du* stands for unscheduled inspection and small outside repair. These inputs are used in the calculation of the unscheduled categorized failure rate *Au', Cu'* and *Du'* with consideration of the CM detection characteristics, *detectability* and *pre-empt* in this case, and scheduled categorized failure rate, *As, Cs*

and *Ds* with consideration of the CM detection characteristics, *detectability*, *pre-empt* and *falsepos*.

In this existing cost setting, simple assumptions are made for the unscheduled maintenance with consideration of CM detection where only the heavy components replacement *Au'* is affected by both the condition monitoring system general detection (*detectability*) and early detection (*pre-empt*), while small parts repair *Bu'* and inspections *Du'* are only affected by the *detectability*, as listed below:

$$\mathrm{A}'_U = A_U \cdot (1 - detectability - preempt) \quad (38)$$

$$\mathrm{C}'_U = C_U \cdot (1 - detectability) \quad (39)$$

$$\mathrm{D}'_U = D_U \cdot (1 - detectability) \quad (40)$$

The scheduled maintenance categorized failure rate values of each turbine component, *As*, *Cs* and *Ds*, are transferred from their corresponding original unscheduled values, *Au*, *Bu* and *Du*, by the suited CM effect indicators, where *As* is only affected by the *detectability*, *Cs* is affected by both *detectability* and *pre-empt*, and *Ds* is affected by *detectability* and *falsepos*, as shown below:

$$A_S = A_U \cdot detectability \quad (41)$$

$$C_S = C_U \cdot detectability + A_U \cdot preempt \quad (42)$$

$$D_S = D_U \cdot detectability + (A_U + C_U + D_U) \cdot falsepos \quad (43)$$

5.1.4.4 Component costs

The component costs are assumed based on two sources. The first breakdown into individual components is from a confidential source. Since this source is quite recent, its cost values are maximally used. Where this source does not cover the particular components, a second source is used, taken from the WindPACT study hosted by

NREL [168]. This study reports a broad breakdown by subsystem including a scaling study where a scaling of component cost with turbine size is presented, as shown in Table 25. The turbine size is limited to 750kW, 1.5MW, 3.0WM and 5.0MW. This limitation is fitted and extended by a power scaling law. The convergence gives the closest value of index by the scaling value, as shown in Eq.44, where *a*, *b* and *index* are coefficients to be obtained. However, the component names in StraPCost cannot always match with [168], which often happens among different study authorities. If the scaling value is not listed, the index value will be set as 0.7.

$$Cost = a + b \cdot (Rated\ Power)^{index} \tag{44}$$

Table 25. Costs of all wind turbine components for baseline case [168]

Rating	kW	750 kW	1.5 MW	3.0 MW	5.0 MW
Rotor	$	**101,897**	**247,530**	**727,931**	**1,484,426**
Blades	$	64,074	147,791	437,464	905,903
Hub	$	21,617	64,191	213,027	429,307
Pitch mechanism and bearings	$	16,205	35,548	77,440	149,216
Drive train, nacelle	$	**255,631**	**562,773**	**1,282,002**	**2,474,260**
Low-speed shaft	$	8,433	19,857	56,263	120,903
Bearings	$	3,794	12,317	41,436	101,834
Gearbox	$	64,919	150,881	357,224	697,062
Mechanical brake, HS coupling, etc.	$	1,492	2,984	5,968	9,947
Generator	$	48,750	97,500	195,000	325,000
Variable-speed electronics	$	50,250	100,500	201,000	335,000
Yaw drive and bearing	$	5,268	12,092	28,213	109,705
Main frame	$	21,452	63,992	192,115	433,627
Electrical connections	$	30,000	60,000	120,000	200,000
Hydraulic system	$	3,375	6,750	13,500	22,500
Nacelle cover	$	17,898	35,901	71,283	118,682
Control, safety system	$	**10,000**	**10,200**	**10,490**	**10,780**
Tower	$	**69,660**	**183,828**	**551,415**	**1,176,152**
Balance of station	$	**217,869**	**388,411**	**873,312**	**2,458,244**
Foundations	$	34,919	48,513	76,765	108,094
Transportation	$	26,586	51,004	253,410	1,312,150
Roads, civil works	$	44,896	78,931	136,359	255,325
Assembly and installation	$	24,374	50,713	112,714	224,790
Electrical interface/connections	$	71,304	126,552	224,196	431,500
Permits, engineering	$	15,790	32,698	69,868	126,385
Initial capital cost (ICC)	$	**655,057**	**1,392,741**	**3,445,150**	**7,603,862**
Initial capital cost (ICC)	$/kW	873	928	1,148	1,520
Net annual energy production	kWh	**2,254,463**	**4,816,715**	**10,371,945**	**18,132,994**
Rotor	¢/kWh	0.477	0.543	0.741	0.864
Drive train	¢/kWh	1.197	1.234	1.305	1.441
Controls	¢/kWh	0.047	0.022	0.011	0.006
Tower	¢/kWh	0.326	0.403	0.561	0.685
Balance of station	¢/kWh	1.021	0.852	0.889	1.432
Replacement costs	¢/kWh	0.499	0.467	0.434	0.414
O&M	¢/kWh	0.800	0.800	0.800	0.800
Total COE	¢/kWh	**4.367**	**4.321**	**4.741**	**5.642**

5.1.4.5 Vessel costs

As stated earlier, vessel usage is a major contribution to cost. At this stage of the development of the cost model, vessel costs are calculated on a per day basis and assumed to be charged during unscheduled delays but not scheduled ones. The cost starts to be counted from travelling, positioning and carrying out repair operations. The assumption of vessel hire is based on the DOWEC project [167] and the project of Cost Modelling of Lightning Damage for Offshore Wind Farms [169], as shown in Table 26 and Table 27.

Table 26. Breakdown on vessel usage information [167]

Nr	Desription	Weather window	H_{max}	V_{max}	T logistic equip.	T travel (+access)	Cost equipment for mission (MOB/DEMOB) and travel [Euro]	Cost equipment during waiting and repair period [Euro/unit]
			m	m/s (For inrformation only)	hr value	hr value	Euro/mission value	Euro/unit value
1	Supplier with OAS (personnel)	6	2.00	12.0	6.0	1.0	0.0	1100.0
2	Supplier with OAS (equipment)	2	1.50	8.0	6.0	1.0	0.0	1210.0
3			0.00	0.0	0.0	0.0	0.0	0.0
4			0.00	0.0	0.0	0.0	0.0	0.0
5			0.00	0.0	0.0	0.0	0.0	0.0
6	Jumping Jack with crane (positioning)	4	2.00	8.0	48.0	8.0	147000.0	45000.0
7	Jumping Jack with crane (operation)	12	5.00	10.0	0.0	0.0	0.0	45000.0
8	Crane ship (positioning)	2	1.50	8.0	48.0	8.0	160000.0	70000.0
9	Crane ship (operation)	2	1.50	8.0	0.0	0.0	0.0	70000.0
10	Internal crane, hoisting outside (1MT)	3	2.00	6.0	0.0	0.0	0.0	0.0
11	Internal crane, hoisting outside (Intermediate)	3	2.00	6.0	0.0	0.0	0.0	0.0
12	Internal crane, hoisting outside (50MT)	3	2.00	6.0	0.0	0.0	0.0	0.0

Table 27. Vessel usage information [169]

Nr	Desription	H_{max}	V_{max}	Fixed costs for mission (MOB/DEMOB)			Variable costs during waiting and repair period		
		m	m/s	Euro/mission			Euro/hr		
				min	ML	max	min	ML	max
1	Supplier with zodiac	0.50	6.0	0	0	0	850	1,100	1,700
2	Supplier with MOB	1.00	12.0	0	0	0	850	1,100	1,700
3	Supplier with OAS	2.00	12.0	0	0	0	1,000	1,100	1,300
4	Helicopter	-	15.0	300	775	1,250	3,400	3,750	4,100
5	Pontoon with tug	1.00	6.0	8,000	9,000	10,000	1,000	1,100	1,200
6	Jack-up with crane (positioning)	0.50	6.0	90,000	100,000	120,000	1,400	1,600	2,000
7	Jack-up with crane (operation)	-	6.0	0	0	0	1,400	1,600	2,000
8	Crane ship (positioning)	1.50	6.0	80,000	90,000	110,000	5,700	7,800	11,400
9	Crane ship (operation)	1.50	6.0	0	0	0	5,700	7,800	11,400
10									
11									
12									

Take all references into account; StraPCost makes assumptions of vessels as in Table 28. It should be noted that vessels are assumed to be always available when required. Some studies include waiting time for suitable vessels to become available and this will be examined in later sections to the cost models.

Table 28. Example of StraPCost vessel assumptions, with modification from [156]

VESSELS		max wave height	max wind speed	speed	positioning time	day rate	Wave Accessibility	Wind Accessibility	Limit
		M	m/s	knots	hrs	£			
	Type	Hv	Uv	Vv	tv	vessel rate	1-Ph	1-Pu	VLimit
supplier with MOB	M	1.5	14	25	1	12000	30%	75%	H
crane vessel (severe wind limit for bulky lifts)	J	2	9	8	2	160000	67%	54%	W
self-propelled jack-up	S	2	11	10	3	160000	67%	69%	H
none	0	10	50	5000	0		100%	100%	W

5.2 Review of cost models in the research domain, analyses and comparison with StraPCost

Even though wind energy is a relatively new source of power production, Operation and Maintenance (O&M) cost effectiveness is of concern to the wind farm owner and operator. This urges the development of cost estimation models in the research domain. There are a few developed commercially packaged cost models in the industry. The best know ones are ECN O&M [170], OMCE [171], ECUME [158] and NOWIcob [160]. The cost model developed in this thesis, StraPCost, as in traduced in Section 5.1, has used these commercial cost models as references. Other models are still under development and have different methodologies and emphases, such as UiS Offshore [179], Strathclyde OPEX [159] and Strathclyde Structural Health Monitoring model [178]. The emphases can be, for example, the vessel costs and approachability, maintenance strategy (or wind turbine components repair categories), and structure health assessment etc. The main techniques used by the cost models are discrete-event, time-sequential modelling and Monte Carlo simulation. Since wind farm data are still not quite transparent, especially when the offshore wind energy is still in its developing stage, real operation data are not easily accessible in the public domain. Therefore, the validation and verification of these simulation-based models is limited, and a comparison among the simulation models is necessary.

For a better understanding of the main cost models, Section 5.2.1 introduces the basic mathematical theories used in these cost models in detail, and Section 5.2.2 presents a review of main cost models in the research domain, with theoretical comparison of StraPCost used in this thesis.

5.2.1 Basic mathematical tools and theory

The cost models developed by each group of researchers are based on different algorithms as outlined above. The majority of the mathematical tools used are Monte Carlo methods, Hidden Markov Model (HMM) and Bayesian network (BN). These mathematical tools are introduced here for a better understanding of the methodology applied within the cost models under consideration.

5.2.1.1 Monte Carlo methods

In scientific computation Monte Carlo methods play an important role. As a computational algorithm, it relies on repeated random samplings from probability distributions to obtain numerical results. It is especially useful when modelling large - dimensional phase space and phenomena with significant uncertainty regarding inputs such as the likelihood of failures, costs, and external constraints etc. When it is used for solving complex probability distributions representing multiple random variables, advanced techniques such as Marko Chain modelling, can be used.

Monte Carlo methods require the generation of large quantities of random numbers in order to provide a good representation of the relevant probability distributions. This procedure generally makes use of pseudorandom number generators.

Monte Carlo methods start from defining a domain of possible inputs and generating random inputs conforming to a given probability distribution, the target density function, *P(x)*, over the domain, where x is an N-dimensional vector with real components x_i. The expectation estimator is given by [172] :

$$\widehat{\Phi} = \frac{1}{R}\sum_{r} \Phi(x^{(r)}) \tag{45}$$

where *R* is the number of samples *r = {1, 2, … , R}*, and $\{x^{(r)}\}_{r=1}^{R}$ is the sample group to be generated.

In order to solve the target density *P(x)*, a function of *P*(x)* is introduced:

$$P(x) = \frac{P^*(x)}{Z} \tag{46}$$

where *Z*, the normalizing constant, is given by:

$$Z = \int d^N x P^*(x) \tag{47}$$

One example of *P*(x)* is given for the Ising model (other called Boltzmann machine, or Markov field [173]), whose probability distribution is proportional to:

$$P^*(x) = exp[-\beta E(x)] \tag{48}$$

where $x_n \in \{\pm 1\}$ and the Boltzmann energy function [173]:

$$E(x) = -[\frac{1}{2}\sum_{m,n} J_{m_n} x_m x_n + \sum_{n} H_n x_n] \tag{49}$$

where J_{m_n} is the connection strength between unit *m* and unit *n*, and H_n is the bias of unit *n* in the global energy function. However, this simple model requires extensive computation.

A sequence of Monte Carlo method sampling models is established for more efficient sampling such as: importance sampling, rejection sampling, the Metropolis method and Gibbs sampling.

In these samplings, a simpler density function including a multiplication constant, the sampler density, *Q(x)*, is assumed, with *Q*(x)* in the same manner:

$$Q(x) = \frac{Q^*(x)}{Z} \tag{50}$$

Importance sampling and rejection sampling only work well when the assumed *Q(x)* is similar to *P(x)*. In large complex situations, Metropolis algorithm is more efficient.

A further assumption of x' which can be derived from the proposed density function $Q(x'; x^{(t)})$ is made. In addition, a state indicator is computed:

$$a = \frac{P^*(x')}{P^*(x^{(t)})} \frac{Q\left(x^{(t)}; x'\right)}{Q(x'; x^{(t)})} \tag{51}$$

if $a \geq 1$ then the new state is accepted, and $x^{(t+1)} = x'$ is set;
otherwise the new state is accepted with probability a, and $x^{(t+1)} = x^{(t)}$.

The Metropolis method is an example of a Markov chain Monte Carlo (MCMC) method for which the time development is represented by a Markov process. In this model, each sample $x^{(t)}$ is dependent on the previous value $x^{(t-1)}$. Because of this correlation of the successive samples, the Markov chain may have to run for a considerable time.

In general, Monte Carlo methods can generally solve any problem related to *P(x)*. High-dimensional problems can be successfully solved by MCMC method: in particular, using the Metropolis method and Gibbs sampling. The Metropolis method is widely used for high-dimensional sampling. However, the "random walk" probability distribution makes this method quite time consuming.

5.2.1.2 Hidden Markov Model (HMM)

An HMM is a doubly stochastic process with unobservable (hidden) stochastic process, that can only be observed using another stochastic method which produces the

sequence of observable symbols [173][174]. A typical probabilistic parameter structure diagram is given in Figure 50.

In a HMM, there are a series of model parameters as given below:

- *T = length of the observation sequence;*
- *N = number of states;*
- *M = number of observation symbols;*
- *I = {$i_1, i_2, \dots, i_N$}, the state sequence;*
- *Q = {$q_1, q_2, \dots, q_N$}, states;*
- *V = {$V_1, V_2, \dots, V_N$}, discrete set of possible symbol observations;*
- *A = {a_{ij}}, transition probability distribution of state j at t+1 following state I at t;*
- *B = {$b_j(k)$}, observation symbol probability distribution k in state j;*
- *π = {π_i}, initial state distribution;*
- *λ = (A, B, π), the compact notation for the three parameters are the core of the algorithm.*

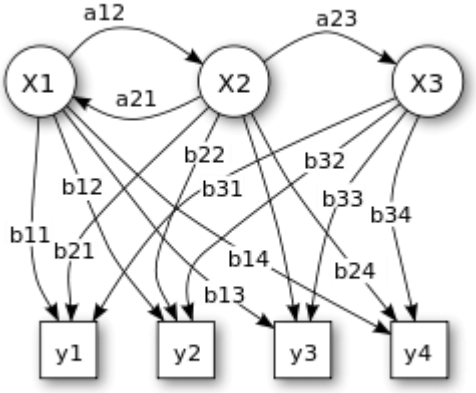

Figure 50. Example of typical probabilistic parameters of a HMM [173]

When an HMM is being established, it starts by choosing the following parameters: an initial state i_1, according to the initial state distribution π at *t*=1; O_t according to $b_{i_t}(k)$,

the symbol probability distribution at state i_t; i_{t+1} according to $\{a_{i_t i_{t+1}}\}$. Once the initial parameters are set, it can be iterated from *t*=*t*+1until *T*.

The probability of the observation sequence *O* given the model λ is obtained by the following equation over all possible state sequences:

$$P(O|\lambda) = \sum_{I} P(O|I,\lambda)\, P(I|\lambda) = \sum_{i_1, i_2, \ldots, i_T} \pi_{i_1} b_{i_1}(O_1) \cdot a_{i_1 i_2} b_{i_2}(O_2) \cdot \cdots \cdot a_{i_{T-1} i_T} b_{i_T}(O_T) \tag{52}$$

Since this contains numerous items and calculation, a more efficient computational procedure is used: the Forward-backward procedure, where the following variables are defined.

For the forward procedure, the forward variable is given by:

$$\alpha_{t+1}(j) = [\sum_{i=1}^{N} \alpha_t(i) a_{ij}] b_j(O_{t+1}) \tag{53}$$

where *t*=1, 2, … , *T*-1 and initial setting $\alpha_1(i) = \pi_1 b_j(O_1)$.

For the backward procedure, the backward variable is given with *t*= *T*-1, *T*-2, …, 1, and initial setting $\beta_T(i) = 1$:

$$\beta_t(i) = \sum_{j=1}^{N} a_{ij} b_j(O_{t+1}) \tag{54}$$

Once the probability of the observation sequence is defined, the associated optimal state sequence can be determined using different criteria. The probability of being in state q_i at time *t*, given the observation sequence *O* and the model λ can be expressed as:

$$\gamma_t(i) = P(i_t = q_i|O, \lambda) = \frac{\alpha_t(i)\beta_t(i)}{P(O|\lambda)} \quad (55)$$

The individually most likely state at $t \in [1, T]$ can be obtained by finding the argument of the maximum:

$$i_t = \underset{1 \le i \le N}{argmax}[\gamma_t(i)] \quad (56)$$

A mature technique of finding the single best state sequence is the Viterbi algorithm.

After the most likely state has been found, the model parameter $\lambda = (A, B, \pi)$ can be adjusted to maximize the probability of the observation sequence given the model. The probability of a path being in state q_i at time t making a transition to state q_j at time t+1 can be express as:

$$\xi_t(i,j) = P\left(i_1 = q_i, i_{t+1} = q_j \middle| O, \lambda\right) = \frac{\alpha_t(i)a_{ij}b_j(O_{t+1})\beta_{t+1}(i)}{P(O|\lambda)} \quad (57)$$

Since there is no known way to solve the maximum likelihood model analytically, an iterative procedure, usually the Baum-Welch algorithm or gradient techniques, have to be used, and the HMM parameters can be estimated.

The HMM is a useful tool for estimation with unobservable conditions. It is of such importance that many practical transformations are derived to solve the problem and simplified from it, such as dynamic Bayesian network (DBN) and simpler Markov models like the Markov chain.

5.2.1.3 Bayesian belief network (BBN) and Dynamic Bayesian network (DBN)

A Bayesian network (BN), or Bayesian belief network (BBN), is a discrete or continuous probability model joining sets of variables with mutually exclusive states. The directed nature of the variables ensures no feedback cycles exist. A conditional

probability table (CPT) is required for each variable state. Figure 51 shows an example structure of a Bayesian network.

As stated in the above subsection, the BN is a simplified version of the HMM, and the calculation follows a similar approach. The joint probability distribution (JPD) can be expressed as below [175]:

$$P(X_1, X_2, \cdots, X_n) = \prod_{i=1}^{n} P(X_i|\pi_i) = \prod_{i=1}^{n} \theta_{X_i|\pi_i} \tag{58}$$

where $X_1, X_2, \cdots, X_n$ denote the random variables; θ represents the set of parameters of the network; π_i is the set of parents of X_i for the directed acyclic graph (DAG).

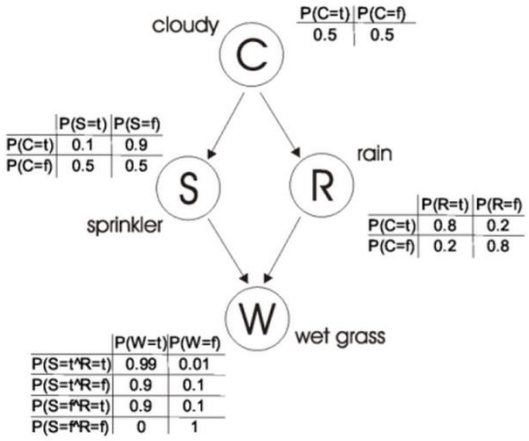

Figure 51. Example of Bayesian network [176]

The Dynamic Bayesian network (DBN) is a Bayesian network where the variables are linked over adjacent time slices. An example of two variables is shown in Figure 52. The two variables *A* and *B* each contain *i* states. At each time slice, the two variables are connected with solid lines. There is also a connection of *A* at each time slices with dashed lines [177].

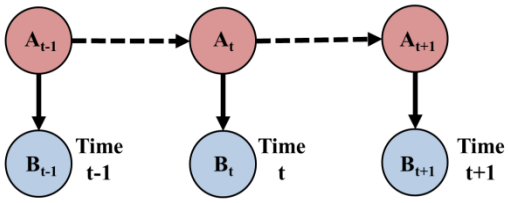

Figure 52. Example DBN with two variables [178]

Since a DBN is a BN with additional time slices, the expression is similar but with an additional parameter *t*:

$$P(U_t|U_{t-1}) = \prod_{i=1}^{n} P\left(X_i^t \middle| \theta_{X_i|\pi_i}^{t-1}\right) \quad (59)$$

Its straightforward concept and accuracy makes Bayesian network (both BBN and DBN) increasingly of interest for wind farm O&M cost modelling, for recent research see [178].

5.2.2 Existing cost models

After gaining the knowledge of the basic mathematical tools and theory used in the main cost models in the public domain, this subsection presents a detailed review of these cost models. The cost models reviewed are ECN cost models, ECUME Model, NOWIcob, UiS Offshore wind logistics decision support model, Strathclyde OPEX model and Strathclyde Structural Health Monitoring model. While reviewed, these models are compared with StraPCost from all aspects.

5.2.2.1 ECN cost models

The cost models developed by Energy research Centre of the Netherlands (ECN) are treated as the standard by the European industry. The best known ones are the ECN O&M tool and the ECN OMCE, as introduced in Section 5.2.2.1.1 and Section 5.2.2.1.2, respectively.

5.2.2.1.1 ECN O&M tool

The ECN O&M tool is a relatively well developed cost model. It has been in used by more than 20 leading project developers and manufacturers. Due to its success, this model is also considered as an industry model for O&M analysis for offshore wind farms in the early planning phase [173]. This model, from the main concept, the category settings to the form of presentation of results have influenced the development of the cost model StraPCost in this thesis.

The ECN O&M tool mainly focuses on reactive maintenance with little considering condition based maintenance and is largely based on the repair process, as shown in Figure 53.

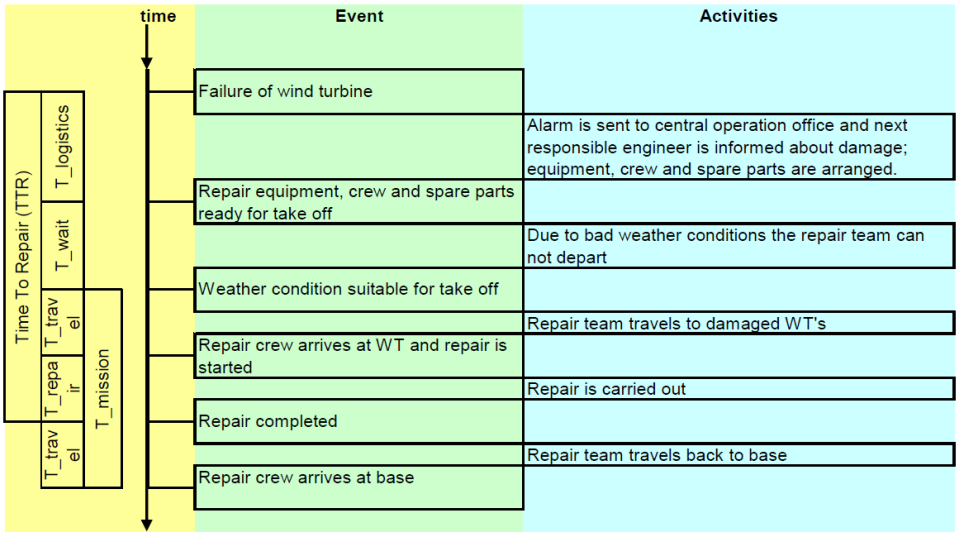

Figure 53. Repair process in ECN O&M tool [170]

In contrast to the waiting, travel and repair time categories in StraPCost, the Time to Repair (TTR) in the ECN O&M tool is split up into 4 stages. T_logistics represents the period after the wind turbine is shut down and while repair crew is assigned and ready to travel to the turbine. T_wait is triggered if the weather is not suitable,

according to the weather forecast, for the vessel to depart. This period is followed by the T_travel and T_repair when the repair process can finally proceed.

Apart from the mean and standard deviation of the failures, the ECN O&M tool determines the statistical uncertainty of the failures using a Poisson process and determines the results through convergence of the Monte Carlo method. This is different from the probabilistic analysis applied by StraPCost.

The ECN O&M tool is developed in two MS-Excel sheets. The first Excel sheet WaitingTime.xls determines the suitable time for the repair operation and estimates the average waiting time before a suitable weather window occurs. The program uses time series with three hourly wind and wave data as input. In contrast to the power law in StraPCost, the ECN method fits the original scatter data with second or third order polynomials to estimate the mean value and standard deviation of waiting time as a function of the duration of the maintenance activity [170].

The second Excel sheet CostCal.xls determines the long term annual or seasonal O&M costs and the associated downtime. Apart from the weather window and waiting time polynomial fitted function from the WaitingTime.xls and a series of basic wind farm information, this program requires failure occurrence rates and the associated repair actions as input. As stated repeatedly, such data are rarely available. An alternative approach available with this model is to use data from similar turbine type, or from generic databases.

The maintenance categories were defined in Section 5.1.4.2 while introducing StraPCost. As a mature commercial model, it also gives step-by-step instructions regarding each maintenance category. In addition, the maintenance class is split up

into Fault Type Classes (FTC's) which provide the detailed costs: labour costs, costs of spare parts and consumables, cost of equipment and revenue losses.

In contrast to the StraPCost, as shown in Table 29, the output of the ECN O&M tool divides the downtime into 4 stages: logistics, waiting, travel and repair. It splits the equipment cost into MOB/DEMOB, waiting and repair. It also lists the cost for each season as well as an annual total. In the same way as StraPCost, the ECN O&M model provides a pie chart of the cost drivers with downtime. StraPCost provides a bar chart of cost drivers divided into scheduled and unscheduled O&M, while the ECN O&M presents the turbine availability per season.

Table 29. Example of ECN O&M tool output [170]

1 Wind Turbine			Winter	Spring	Summer	Autumn	Total	Year
Downtime per year								
	Logistics	hr	190	141	124	164	618	618
	Waiting	hr	107	28	13	56	204	160
	Travel	hr	2	2	1	2	7	7
	Repair	hr	14	10	9	12	44	44
	TOTAL	hr	313	181	148	233	874	829
Availability		%	86%	92%	93%	89%	90,0%	90,5%
Loss of production per year		kWh	370528	158611	114579	238240	881957	808224
Energy production per year		kWh	2224140	1765284	1586460	2002090	7577974	7727863
Revenue losses per year		Euro	29642	12689	9166	19059	70557	64658
Costs of repair per year								
Material costs		Euro	16236	12038	10644	14018	52936	52936
Labour costs								
	Wages	Euro	1758	1303	1152	1518	5731	5731
	Daily allowance	Euro	0	0	0	0	0	0
	TOTAL	Euro	1758	1303	1152	1518	5731	5731
Costs equipment								
	MOB/DEMOB	Euro	9506	7048	6232	8208	30994	30994
	Waiting	Euro	29281	9367	6413	15550	60612	53055
	Repair	Euro	9522	7060	6242	8221	31046	31046
	TOTAL	Euro	48309	23475	18888	31979	122651	115095
Total costs of repair per WT		Euro	66302	36817	30684	47515	181318	173762
Total cost per kWh		Euro Cent/kWh	2,98	2,09	1,93	2,37	2,39	2,25

5.2.2.1.2 ECN OMCE

The ECN Operation and Maintenance Cost Estimator (OMCE) consists of two main modules: the OMCE Building Blocks and the OMCE-Calculator, in order to monitor O&M actions and to control and optimise the future costs, as shown in Figure 54. In

the first module (the red dashed rectangle in the middle of the figure), Four OMCE Building Blocks (BB) are established in order to process operational data. The outcomes of these blocks are for monitoring as well as the input for the next module. The OMCE-Calculator (the red dashed rectangle on the right hand side of the figure) synthesizes the information from the previous blocks to exam the existing O&M action and associate costs. The OMCE-Calculator is largely based on the ECN O&M tool and is a Matlab based time-domain simulation program.

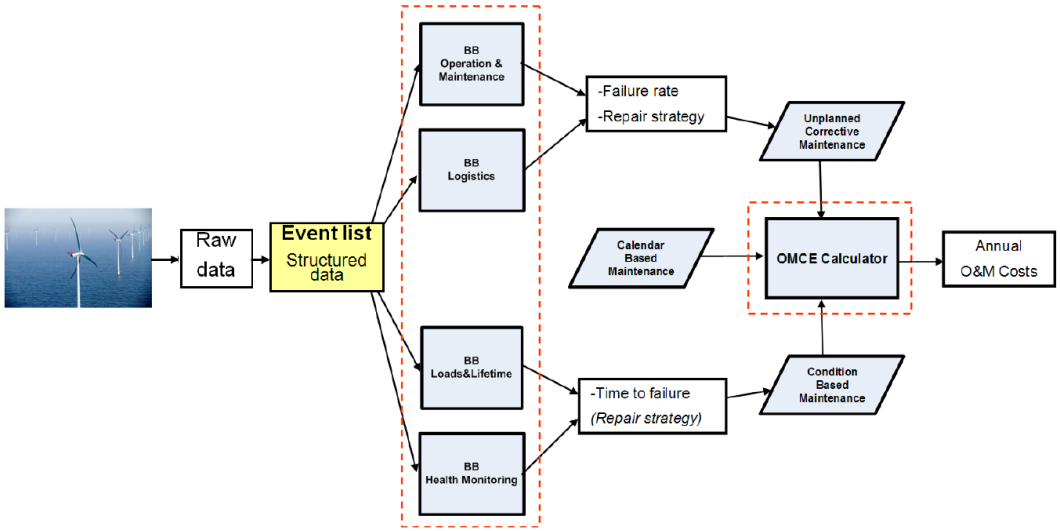

Figure 54. OMCE concept with two major modules: Building Blocks and OMCE-Calculator [171]

Similar to StraPCost, OMCE has an additional module to process the time domain operational data and provide the calculated parameters as input to the cost and effects estimation module. As a more mature model, OMCE also provides split blocks in the module for monitoring purposes. The simulation process of OMCE-Calculator is shown in Figure 55.

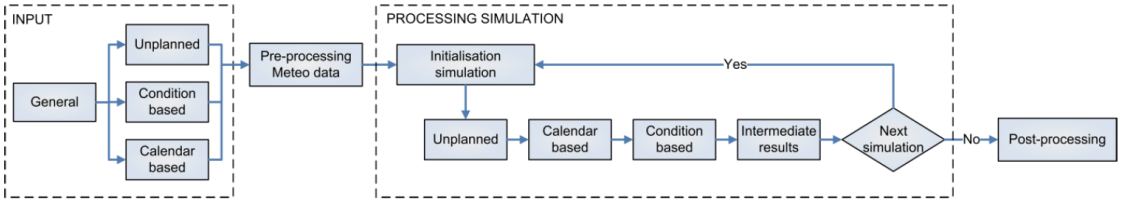

Figure 55. Simulation process of OMCE-Calculator [171]

The weather window of the OMCE-Calculator is similar to StraPCost; however, instead of having one threshold for significant wave height, the OMCE-Calculator splits the threshold into different levels as well as considering wind speed. It also accepts repairs that do not need to be completed in one operational visit. Figure 56 shows the weather window with both wind speed and significant wave height. In this example, the maintenance can be carried out when significant wave height is no more than 1.5m and wind speed no more than 12m/s and the duration is 20hr (left box) and 40hr (right box).

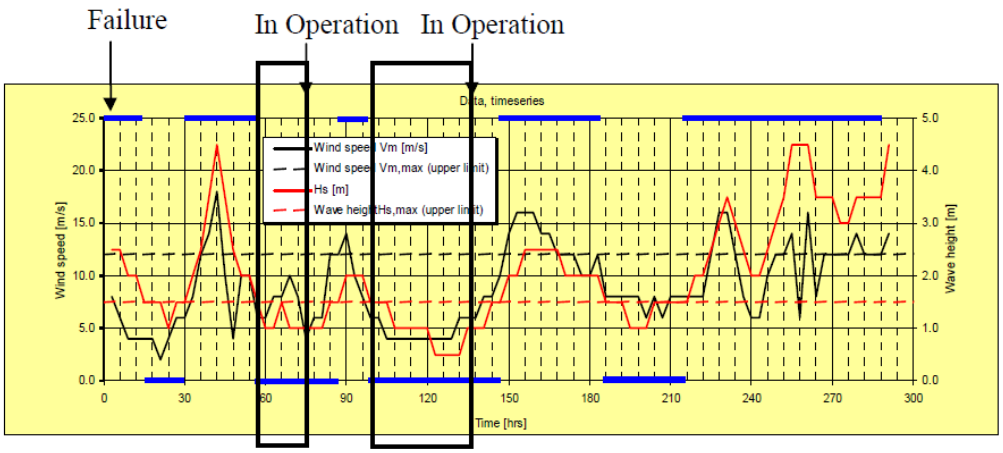

Figure 56. Example of determination of waiting time for a maintenance action to be carried out [171]

In general, ECN models are quite mature packaged commercial cost models. The core algorithm synthesizes weather conditions and has multi-levels of thresholds for repair operations that can be completed in more than one visit. It provides the model output

for different seasons and a breakdown of the downtime. It determines the statistical uncertainty of the failures using a Poisson process and determines the results through convergence of the Monte Carlo method. It provides more detailed and accurate estimation when it comes to the reactive maintenance, whereas StraPCost allows assessment of condition based maintenance.

5.2.2.2 ECUME Model

The ECUME model is developed by and used within EDF in recent years supporting the group company in making investment decisions, turbine selection, life cycle logistics and O&M strategies for its growing portfolio of offshore wind farms [158]. The model evaluates the total mean cost of the operation of an offshore wind farm project at the design phase. This model adapts a cost estimator which has been used in EDF to help investment decision making for traditional power plants. It also makes use of inputs used by the ECN O&M tool [170][171].

Capital operational costs, including fixed costs, preventive periodical maintenance costs, standard costs for condition based maintenance are input. Deterministic cash flows are set by the user. The probabilistic cash flows, which are due to corrective maintenance after the occurrence of a failure and condition based maintenance after the detection of component degradation, are estimated by the model.

ECUME used to largely depend on another combined EDF model, AMER. With set thresholds of wind speed and significant wave height, AMER calculates the mean waiting time per season for the appropriate meteorological window for the selected maintenance. The improvement in ECUME is based on a Monte-Carlo-based event model for the modelling of failure risk, and a Hidden Markov Model (HMM) is used

for obtaining and the evaluation of the risk of accessibility dependent on meteorological and marine parameter, as shown in Figure 57.

The hidden states in the HMM model are considered to be temperature, sun position, etc., as established by Baum-Welch algorithm [173][174].

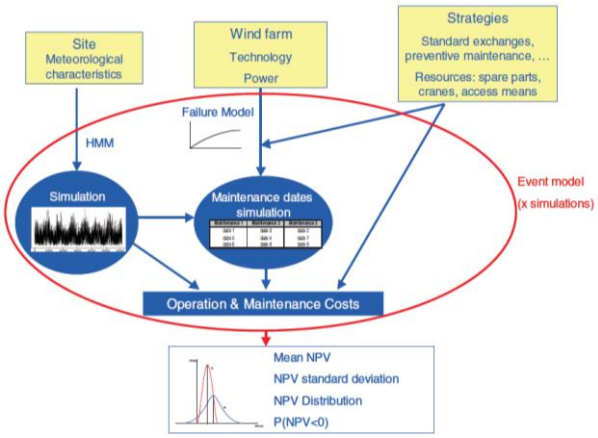

Figure 57. ECUME event model structure [158]

The failure rate evolution follows the bathtub curve, as shown in Figure 58, where the failure rate is decreasing during the infant mortality period; the failure rate is constant during the useful life period; and the failure rate towards end of life period is increasing reflecting cumulative damage to components. Each of the three failure rate periods is represented by a two parameter Weibull distribution, where $\beta_i$is the shape parameter and $\eta_i$is the scale parameter:

$$F_i(t) = \beta_i \cdot \frac{t^{\beta_i - 1}}{\eta_i^{\beta_i}} \tag{60}$$

These two parameters are determined by an inbuilt questionnaire covering the component failure mechanism, component minimal life duration, and mean failure over the life of the wind farm operation. The parameters are then calculated according

to three constraints: continuity, mean value and the upper and lower limit of the failure starting and ending dates.

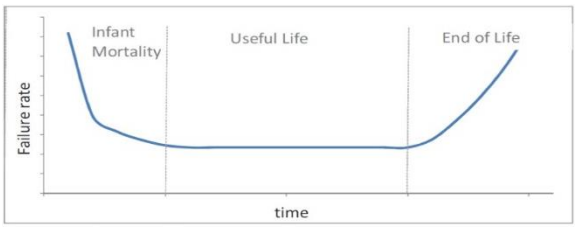

Figure 58. Evolution of failure rate Bathtub curve [158]

With the failure distribution function determined by fixing the two Weibull parameters, the Monte Carlo event model simulation is then applied to each maintenance strategy. The failure times are estimated by inverse transformation sampling, which is another of EDF's internal tools for asset management.

Generally speaking, this model uses a Hidden Markov model to estimate the environmental inputs for the waiting time of each maintenance action, and the Monte Carlo method to estimate the failure risk for each maintenance strategy simulation. The failure rate estimation is based on Bathtub curve and Weibull distribution function fit. Compared to the developer's purely empirical assumption on the failure rate in the original StraPCost, this failure rate estimation is supported by evidence to a certain extent. This model considers multiple risk indicators, which makes this O&M cost estimator more realistic. On the other hand, this model contains a number of parameters requiring calculation. In addition, the complex combination of two methodologies increases the modelling time and the chance of the error in the computation procedure as well as increasing the cost of the modelling.

5.2.2.3 NOWIcob

The Norwegian offshore wind cost and benefit (NOWIcob) model is another commercially developed cost estimator for offshore wind farms. This decision support tool is developed and owned by SINTEF providing sensitivity analysis of the O&M costs mainly due to the maintenance and logistic strategy, and thus assists optimal strategy choice [160].

This model is also based on the Monte Carlo method with Markov chain process in the time sequence for weather and relevant uncertainty. The highlight of the model is the vessel selection concept based on simulation of time-based, condition-based and corrective maintenance. The results from the model include availability, life cycle profit, O&M cost, electricity produced etc.

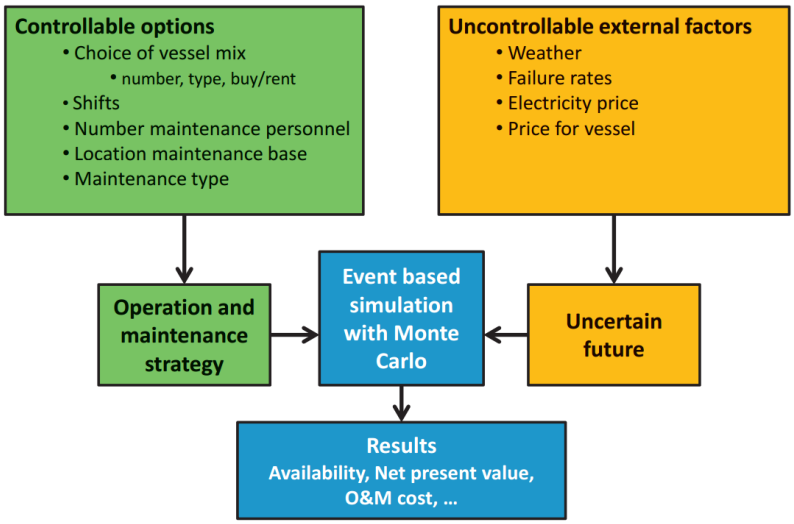

Figure 59. General structure of the NOWIcob model with controllable and uncontrollable factors [160]

This model categorizes the input data for the Monte Carlo estimator into controllable and uncontrollable factors, as shown in Figure 59. The controllable factors are basic O&M choices, and uncontrollable factors reflect by external conditions. What is

noticeable is that failure rates are treated as uncontrollable factors and it is assumed that maintenance actions do not affect the failure rates.

For condition based maintenance, similar to StraPCost, this model also breaks down condition based fault diagnosis into three categories, with a slight difference in names rather than the concepts: *detectability*, *efficiency* and *false alarm*, equivalent to *Detectability*, *Pre-Empt* and *Falsepos* in StraPCost, respectively.

The simulation of this model makes a few assumptions. The Markov chain process used in this model assumes that future weather is only dependent on the current weather situation and isolated from historical weather. The transition matrices are based on both significant wave height and wind speed. Similar to every cost model, this model assumes perfect weather forecasting.

As stated, this model places emphasis vessel selection. From a stoppage perspective, among the three maintenance types, time-based and condition-based maintenance only lead to turbine stoppage for the time when transporting starts, in contrast to the immediate stop at the moment the failure results in corrective maintenance. This provides more detailed stoppage dependent on the maintenance strategies than StraPCost. In NOWIcob, motherships are considered for locating personnel.

Similar to some of other cost models, NOWIcob allows multiple visits for one maintenance task, as shown in Figure 60 [160]. In addition, access vessels can serve several maintenance operations in parallel, as well as the sequential maintenance by other vessels. This model defines different routes for these two types of vessel tasks.

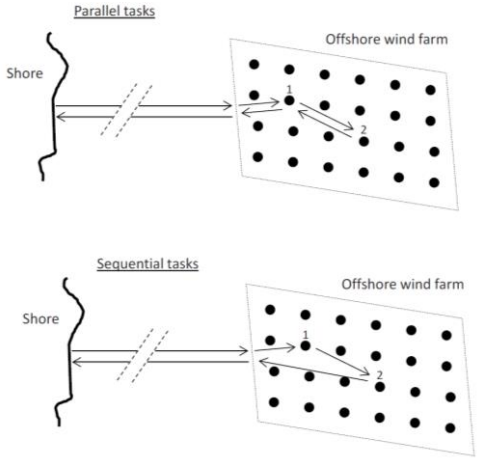

Figure 60. Travel strategies for multiple tasks in the wind farm in NOWIcob [160]

In terms of maintenance tasks in parallel requiring vessel and personnel resources at the same time, this model also determines priorities. The highest priority goes to the ongoing maintenance, followed by maintenance that can be undertaken by an already ordered vessel. Corrective maintenance is given the highest priority among the three strategies, followed by condition-based maintenance and finally time-based maintenance. The vessel cost comprises yearly fixed costs and variable costs for usage.

The estimation of the availability in this model also takes a fairly comprehensive approach to internal and external factors. It takes account of the downtime of the wind turbine, as well as the downtime of the electrical infrastructures such as inner cables, substations and export cables.

Since this model considers both the wind speed and significant wave height in the weather condition simulation, power production is based on the simulated wind speed in the time domain and the power curve. It also considers the wake loss from the wind farm perspective as well as the electrical losses in the electrical infrastructure.

In general, this model can be considered a fairly mature packaged commercial model. It uses Monte Carlo methods with Marko chain process for weather simulation. It has put considerable emphases into vessel conditions and choices. It considers multiple tasks for one vessel seagoing, which is useful and realistic for light maintenance, but for heavy maintenance, the weather window is usually only enough for one task. Even though it does not output results for condition based maintenance as in StraPCost, this model does consider condition based maintenance with regard to vessel use, and categorizes the condition monitoring performance into three similar categories.

5.2.2.4 UiS Offshore wind marine logistics decision support model

The UiS Marine logistics decision support model developed by researchers at the University of Stavanger (UiS) is a simulation-based O&M strategy making tool for offshore wind farm operators. It absorbs the core concept from the ECN O&M tool, which is as stated, treated as the standard by the European industry. However, unlike the above cost models; this simulation model has its own development environment using Java programming language and the commercial simulation software AnyLogic, as shown in *Figure 61* [179].

This model has a combination of agent-based and discrete event modelling, for modelling operation actions and working processes, respectively. This model only considers 19 wind turbine components which covers the main body of the turbine, but are less detailed than StraPCost.

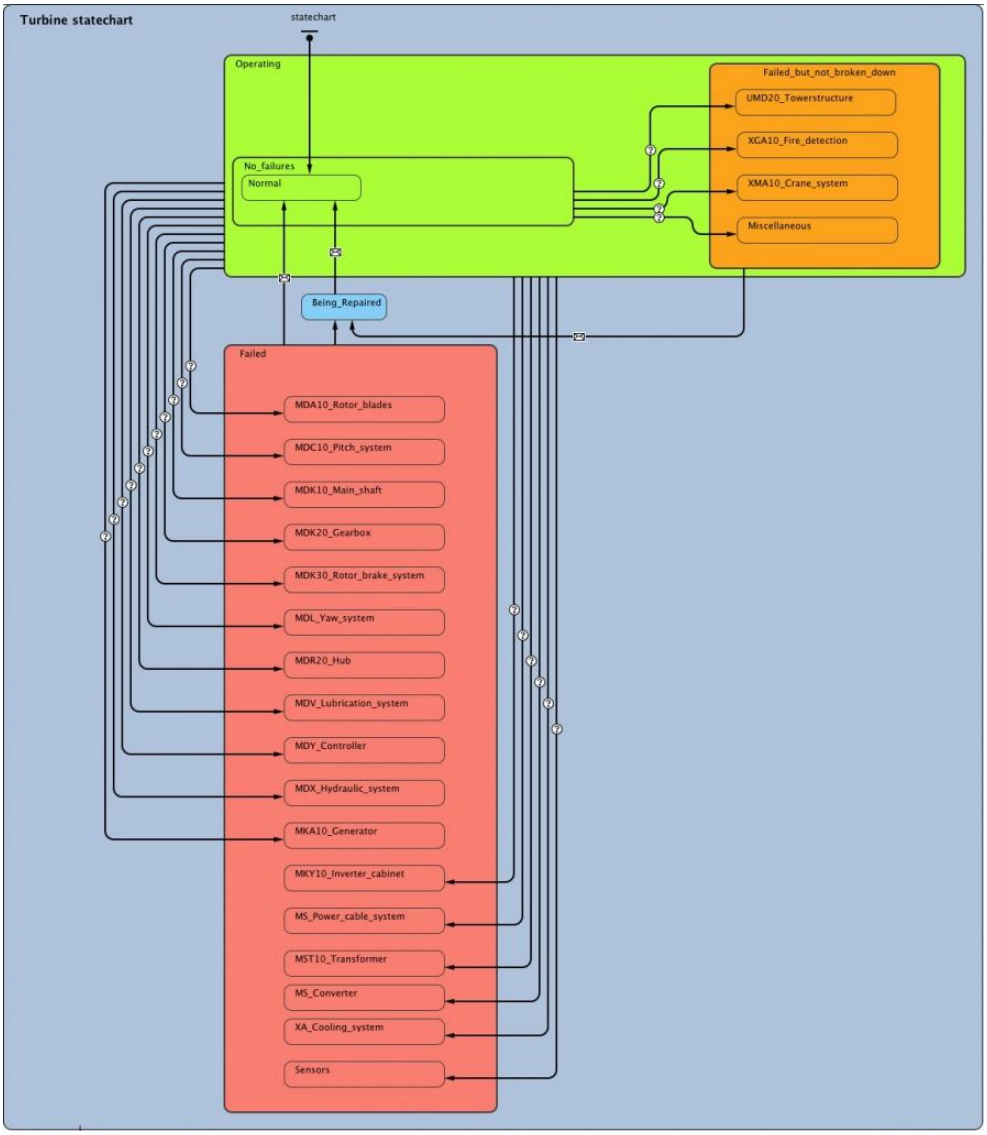

Figure 61. Simulation statechart of the UiS Offshore wind marine logistics decision support model [179]

Similar to ECN O&M tool, this model processes the probability of failure occurrence dependent on time *P(N(t))* through a non-homogenous Poisson process where the failure intensity $\lambda(t)$ is represented by a Power law process following a Weibull-function, as shown in the equations below.

$$P(N(t) = i) = \frac{(\lambda(t) \cdot t)^i}{i!} e^{-\lambda(t) \cdot t}, i = 0,1,2, \cdots \quad (61)$$

$$\lambda(t) = \lambda \beta t^{\beta - 1} \quad (62)$$

where λ is the annual failure intensity, β is the Weibull distribution shape parameter.

The simulation module takes into consideration preventive maintenance and corrective maintenance, but not condition based maintenance. This is its major shortcoming when compared with other cost models, especially the StraPCost.

On the other hand, this model considers failure severity more comprehensively. It classifies the severity with the failure type classification (FTC) scale, with indexes from 1 to 20, where 1-16 represents severity low to high, and 17-20 denotes service, inspection and routine preventive maintenance tasks. When carrying out maintenance actions, the AnyLogic model enables agent-to-agent communication, where a message from the vessel to a technician is added to a Java file on the vessel and initiates a transition in the technician's statechart.

An innovative assumption in this model is that the technicians are assumed to require less time for a given repair with accumulation of the experience, and of course, the increase of the gain in experience diminishes with times. The assumption treats all technicians, e.g. electrical and mechanical technicians, in the same manner, although it is already more detailed in this aspect than all other cost models.

From a vessel chartering perspective, this simulation-based model allows various strategies for different wind farms or projects. It is possible to choose the contract type, e.g. spot or long term, contract duration and if the charter rate is fixed or variable; whereas in StraPCost the vessel charter only considers extra costs for unscheduled maintenance in contrast to scheduled maintenance. However, the vessel classification in this model is less comprehensive than StraPCost, with only heavy lift vessels (HLV), crew transfer vessels (CTV) and service operation vessels (SOV).

The simulation and decision making progress in this model has four main steps. The first step is to define all the possible decisions and scenarios. The second step is to define output metrics which are to be used for evaluating the decision alternatives. The next step is to repeat *n* simulation runs. Finally, the most advantageous decision is selected according to the output metrics. Since StraPCost does not provide a decision making function, when compared with other cost models, this model's simultaneous metrics of decisions improves simulation efficiency and its multiple runs provide a certain level of accuracy.

In common with most other cost models, this model treats both significant wave height and mean wind speed at hub height as two weather parameters. This model also uses Markov chain Monte Carlo approach for processing weather data.

In the way as StraPCost, this model refers to the NREL Wind Pact project for the default cost of spare parts. It also assumes that the electricity price is constant with a government supplement such as the Renewable Obligation Certificate (ROC) [180] or Contract for Differences (CfD) [181].

As in StraPCost, the decision maker is expected to input the preferred number of technicians and vessels, the type of vessels, and in what situation a certain type of vessel should be used. What is noticeable, in the UiS Marine logistics decision support model the location of the onshore supply base is specified by longitude and latitude, rather than distance to the wind farm.

In common with some other cost models but not StraPCost, the outputs of this model distinguish availability into time-based and energy-based. It also provides the technical availability which states the available time as a fraction of the theoretical available

time. It lists the marine logistics cost and vessel utilization which represents the days used as a proportion of the days actually chartered.

In general, this model is a simulation based decision support cost model with Markov chain Monte Carlo approach for the weather data processing. This model is a combination of agent based and discrete event modelling. It treats marine logistics as critical. Its use of metrics for possible decision scenarios and multiple runs provides a relatively efficient and accurate algorithm. Its critical shortcoming is that it considers only preventive and corrective maintenance.

5.2.2.5 Strathclyde OPEX model

The Strathclyde OPEX model has been developed in the University of Strathclyde for operational and strategic decision support for offshore operation. It is a Matlab based model with Bayesian Belief Networks and decision trees for the decision making algorithm [159]. This model relies on expert knowledge to a certain degree, as inputs to the operational module. The output from the operational model is then fed into a decision support module for the final analyses.

One of the strengths of this model is that it is based on a comprehensive study of offshore jack-up vessels for different maintenance strategies. Being developed within the same university, the author of OPEX model had the benefit of being able to access the vessel database, including the capital expenditures (CAPEX), from the University of Strathclyde department of Naval Architecture, Ocean & Marine Engineering (NAOME).

It lists the available jack-up vessels and established a methodology for the estimation of the charter rates dependent on different charter periods from the spot market to up

to a 20-year charter. However, as stated, this charter rate estimation is generally based on judgment of the vessel market and the offshore wind operators. This highlights the lack of available charter rates for specific charter periods due to the opaque negotiation between the vessel owner and the charterer, and the excessive protection of information within the immature offshore wind market. These limited data are processed through a ready-made regression analysis model, and vessel charter rates are plotted against CAPEX for different charter durations and fitted with a polynomial function, as shown in Figure 62. Another important assumption in this model is that a mean value of £400,000 mobilization cost is assumed for every vessel commissioned regardless of the actual cost, taken from [159].

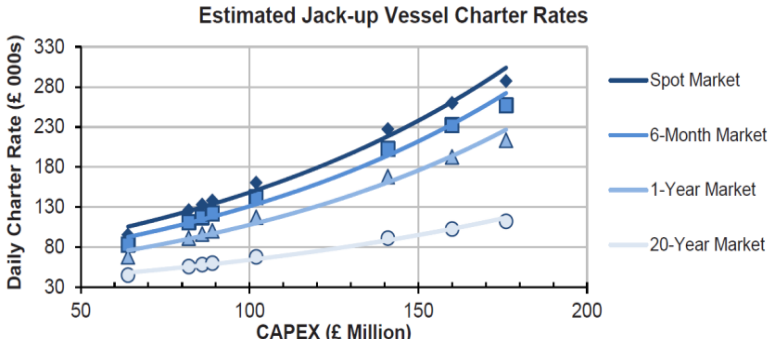

Figure 62. Vessel charter rates under different operational scenarios in the Strathclyde OPEX cost model [159]

In common with the UiS Marine logistics decision support model, the failure behaviour in this model uses Weibull probability density function, and each subsystem is described by a binary state value of operating or failed. The transition probability is compared with a random number R in the interval [0,1]. If for one case the condition in Eq.63 is satisfied, the repair times are considered to be deterministic and are further used in the weather model.

$$R < \lambda(t) \cdot \frac{\Delta t}{8760} \tag{63}$$

In the weather parameter simulation, this model uses a correlated Multivariate Auto-Regressive (AR) approach to process wind speed and significant wave height. Since the standard AR model contains a Gaussian noise term, which means the standard AR equation is only suitable for process including a Normal (Gaussian) distribution. However, neither wind speed nor significant wave height follows such distribution. The Box-Cox transformation [182] is used to remove the non-stationary trends and transform the distribution to Gaussian form. The correlation is captured by substituting a Gaussian pseudorandom vector. The final de-trended and transformed expression for significant wave height Hs_t, with the transform coefficient Λ, is shown below.

$$Y_t = \frac{Hs_t^{\Lambda-1}}{\Lambda} - \hat{\mu}_{\frac{Hs_t^{\Lambda-1}}{\Lambda}} \tag{64}$$

The determination of the AR coefficients and modelling is implemented using the "arfit" algorithm [183] in Matlab with order chosen by optimizing Schwarz's Bayesian Criterion and coefficients identified by stepwise least squares estimation. This pre-processing of the weather time series data provided is closer to reality to a certain extent than StraPCost but requires more calculation space and is more time consuming.

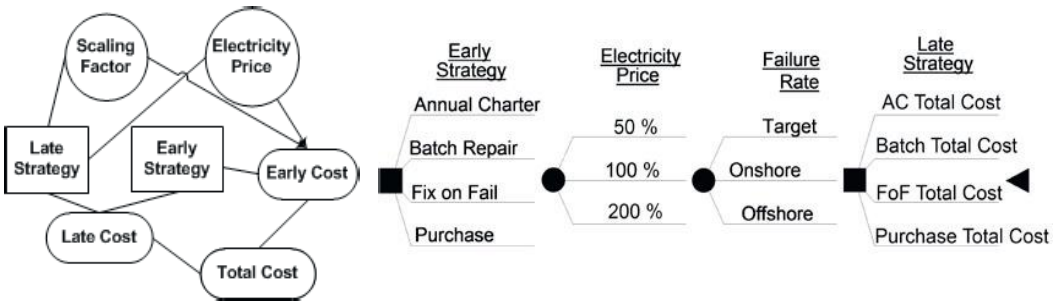

Figure 63. BBN modelling and decision tree for an example site in OPEX model [159]

In this model, Bayesian Belief Networks and decision trees are used as decision making algorithm, as shown in Figure 63. As introduced in 5.2.1.3, a Bayesian network is a variant of HHM and suitable for high-dimensional probability distributions. To evaluate BBN, a decision tree is constructed and solved by dynamic programming. One advantage of BBN is that it gives the decision maker a framework to update their beliefs based on new evidence as it appears.

In general, the OPEX model is an offshore wind farm decision support model using a Multivariate Auto Regressive weather model with a Markov chain Monte Carlo failure simulation repair process for the cost estimation. The decision making algorithm is a conjunction of BBNs and decision trees. This model accurately represents jack-up vessel usage and provides a more realistic way to process environmental data, when compared with StraPCost and other cost models.

5.2.2.6 Strathclyde Structural Health Monitoring model

The Strathclyde Structural Health Monitoring model is another model developed at the University of Strathclyde. As suggested by its name, this model aims to investigate the benefit of using structural health monitoring as a complement to condition monitoring system. Similar to the OPEX model, this model is based on Dynamic Bayesian networks (DBN) with Monte Carlo simulation [178].

Structural health monitoring (SHM) is a process involving observation of a structure or mechanical system over time using periodic measurements, elicitation of the damage features from the measurements, and statistical analysis of these features. With these three steps, the current state of the system can be assessed [184].

The deterioration of mechanical components is used to determine failure rates. In this model, failure rates are calculated as a simple mean value from 3-year operational data from the Efmond aan Zee offshore wind farm, with 36 Vestas V90 3MW wind turbines. Even though this wind turbine sample group is fairly limited in size, it still provides statistical evidence to a certain level, rather than the purely assumption used in StraPCost.

As introduced in 5.2.1.3, a DBN is a BN with time slices. With failure rate defined as the number of failures expected to occur over a given time period:

$$\lambda = \frac{f}{N} \tag{65}$$

The deterioration which is assumed to follow an exponential function can be expressed as the probability function below. A simple 2×2 CPT is given referring the "Major" and "Minor" failure mode categories, as introduced in Section 5.1.

$$P_t = 1 - e^{-\lambda t} \tag{66}$$

$$CPT = \begin{pmatrix} 1 - P_t & P_t \\ 0 & 1 \end{pmatrix} \tag{67}$$

The structural components are modelled with fatigue limit state equations and solved by Monte Carlo sampling, which is previously done by one of the authors and his team [185]. As expressed below, the fatigue limit state g is a function defined as the difference between the structural resistance Δ, and the fatigue loading which consists of the annual number of stress cycles v, the year of service t and the expected value of stress cycles $E[\Delta\sigma^m]$, where m and K are the relevant S-N curve constants.

$$g = \Delta - v \cdot t \cdot \frac{E[\Delta\sigma^m]}{K} \tag{68}$$

In the cost modelling perspective, this model considers the costs as a Net Present Value (NPV), as with the ECN O&M tool and the majority of the commercial cost models. A discount rate of 4% is applied in this model.

$$NPV = \sum_{i=1}^{y} \frac{C(i)}{(1+r)^i} \tag{69}$$

where C(i) is the cost of year *i* within the number of years *y*.

One strength of this model is the evaluation of the benefit of the SHM system, as expressed of the structure costs expectation $E[C_R]$, and the expected benefit from risk reduction E[B].

$$E[C_R] = P_F C_F \tag{70}$$

$$E[B] = E[C_R] - E[C_{MR}] \tag{71}$$

The cost caused by failure is taken as £3,780,000 based on the generic costs of £1,260,000 per MW converted from the original currency Euros [186]. Again this value has a certain meaning in the barren environment of the cost research field, but only to a level. This model finally gives an evaluation of 6% of levelised costs reduction due to the SHM system application with the case study of the stated wind farm [186].

In general, this model is based on Dynamic Bayesian networks (DBN) with Monte Carlo simulation. It emphasizes the fatigue on the structure of the turbine and estimates the structure costs. It suggests a final 6% of cost reduction due to the SHM system in addition to the condition monitoring system. However, compared to StraPCost, this model only investigates the cost at a turbine level rather than a subsystem or

component level. It only considers the failure rate of the turbine as a whole, whereas in reality the failure rate in each subsystem can vary dramatically.

5.2.3 Conclusion

This section has reviewed the state-of-the-art cost models for offshore wind farms, introduced the mathematical tools and theories behind them, analysed their strength and shortcoming, and compared them with StraPCost.

This research area is still at a development stage reflecting the immaturity of the industry itself. There are no cost models at this time able to investigate any environmental factors other than significant wave height and wind speed. The majority of the cost models use Markov methods or a simplified derivative in a Monte Carlo simulation. The regression manner of these algorithms provides higher accuracy but requires a fairly long calculation time. Among these models, some are quite mature commercially packaged models, where others are still in their development or improvement stage. Each model has its own strengths and emphases, and this somehow enriches the understanding in this newly rising and data-protected research area. This review section provides a close view of other cost models for comparison with StraPCost. This gives an important train of thought of improving the existing StraPCost which will be discussed in the next section.

Currently, none of the existing offshore O&M cost models uses actual offshore failure rates as estimation inputs, and these inputs are purely assumptions mainly from onshore wind farms. Since Chapter 4 in this thesis has developed an onshore to offshore translator, it provides a train of thought of applying this translator to

StraPCost for an attempt to fill this gap of having translated offshore failure rates as inputs.

From this review and comparison, it can be seen that the majority of the cost models have at least four levels of maintenance categories which describe the maintenance activity in more detail. This urges the extension of the original three maintenance-category setting in StraPCost. The extension also eases the benchmark study in Section 5.4.

Currently wind and wave are equally important concerns of all the existing cost models. However, in StraPCost, there is only a wave parameter calculator set. This urges the installation of the wind parameter calculator which derives the parameters from the wind speed time series in StraPCost.

As wind farm O&M cost estimators, the majority of the models provide estimations based on the entire wind farm level, whereas the original StraPCost provides estimations on averaged wind turbine level without considering the number of wind turbines installed in the wind farm. The urges the improvement of adding an input window for the number of wind turbines. Cost models such as NOWIcob consider multiple visits with one vessel seagoing. This can be useful and realistic for small maintenance but not heavy maintenance which usually requires long weather window for its own, therefore at this stage this multi-visit function will not be considered for StraPCost.

It can be seen that all existing cost models considers technician basic cost including salary, utilities, taxes and well-beings, while StraPCost only counts individual technician cost when the maintenance is undertaken which is not realistic. The single

technician estimation of StraPCost also unrealistic while other cost models considers the number of technicians available per working shift and the cost per technician per day. These two technician inputs are urged to be installed in StraPCost.

It can be seen that all of the reviewed cost models are simulation-based models with no more than two modelling software, and all functions are packaged which enables the modelling on one go. This urges the packaging of the original StraPCost with more user friendly functions and the correction of some uncorrelated inputs through all calculations within StraPCost.

Currently none of the existing cost models provides easy sensitivity analysis access, which is important for understanding of the impact of the key parameters for a wind farm. This provides a train of thought of installing sensitivity analysis percentage adjustment coefficients for the key parameters in StraPCost.

Based on this conclusion, a series of improvements are done to StraPCost and upgraded into StraPCost+ in Section 5.3.

5.3 Improvements and updated model StraPCost+

This section presents the improvements to the existing cost model StraPCost based on the research and comparison results with other cost models explored in the previous sections in this chapter. Here calls the updated model StraPCost+.

The improvements made are the application of the failure rate translation developed in Chapter 4, expending maintenance categories, application of wind speed Weibull distribution parameter calculator, expending the cost estimation to the wind farm level, consideration of the technician cost, correlation of the delay information, and application of sensitivity analysis percentage adjustment coefficients.

5.3.1 Failure rate translation application to StraPCost+

The accuracy of failure rate data directly affects the accuracy of the cost estimation. As already mentioned, failure rate data are not available to researchers from offshore wind farms and data from onshore wind plant is limited. As discussed in 5.1, the breakdown failure rate of individual wind turbine components is an important input to StraPCost, and as it pointed out, this part in the original model uses empirical data for a number of onshore wind turbines, albeit with relatively low ratings. Even though this classic onshore failure rate breakdown still has meaning, as an offshore wind cost model it is important to use as much offshore data as possible. Therefore, one meaningful application of the failure rate translation procedure introduced in Chapter 4 is to generate “offshore” subsystem failure rates for input to the updated model.

There are still problems to be solved in making this application, among which is the naming of the wind turbine subsystems and components. Since there is no standard for

naming the wind turbine subsystems or components, each manufacturer, operator and research authority has its own way approach to naming. This often results in a mismatch of the names of some subsystems. One subsystem might have different names in different recording systems, be assembled with different other subsystems, or might not be recorded at all in some of the recording systems. Because of this, there is not always a value available for each subsystem in this research, and some pre-processing is required. When introducing the failure translation method in Chapter 4, the rotor and blades are treated as separate components in the onshore and offshore real data recorded from Siemens wind turbines, but are recorded as just one subsystem in the existing onshore RPN publication [146]. This mismatch results in a certain loss of accuracy.

Before applying the methodology to the failure rate data, it takes a step to correlate the failure rate for the input page of the entire model, as presented in subsection 5.3.1.1. The methodology of the application of the failure rate translator is presented in subsection 5.3.1.2. Results and discussion can be found in subsection 5.3.1.3.

5.3.1.1 Pre-processing: failure rate correlation within StraPCost+

In the original model, when the failure rate data is to be changed, it has to be changed on every related sheet. This is not only inconvenient but also risks leaving out some of the subsystems on some sheets. Once this step is completed, the failure rate needs only be set once in the *Input&Result* sheet.

5.3.1.2 Methodology

In the original model StraPCost, the failure rate breakdown is taken from two different references, [164] and [165], and the compromise formed by mixing the two data sets makes the naming of the subsystem more difficult to match up with the real data recorded by the wind farms investigated in this thesis. What is worse, because of the complicated model structure, the failure rate module is highly used and closely related to the maintenance category in most of the sheets in the model. The subsystems used cannot be easily removed or changed.

In this situation, a remedy is to, as far as possible, apply the failure rate translation technique for subsystems which are in both the original cost model and the real data recorded from the wind farms, and calculate failure rates for the remaining subsystems by multiplying the percentage failures of the subsystem taken from [165] and the total failure rate of the entire turbine. The total failure rate can be a set to a default value for a specific application or a mean value determined from the breakdown failure rate by subsystem. The subsystem specifications common to both sources constitute the main parts of a turbine and cover the majority of failures, while the rest of the subsystems account for only a small part of the total failures. This approach is not perfect but it provided an acceptable estimate of the offshore failure rate breakdown by component and subsystem for application to cost modelling.

To implement the offshore translation in the cost model, three middle-stage calculation columns are used instead of the original failure rate column in *Input&Result* sheet: the original onshore failure rate, onshore to offshore ratio for wind speed and temperature.

The updated subsystem failure rate equals the original onshore failure rate multiply the two ratios (assuming statistical independence), as shown in the equation below.

$$Failure\ rate_{translated} = Failure\ rate_{original\ onshore} \cdot Ratio_{wind\ speed} \cdot Ratio_{temperature} \quad (72)$$

If the subsystem does not have a matched translation, the ratios are set to be 1. An example of the updated settings of StraPCost+ is shown in Table 30. Compare to Table 15, it can be seen that different naming systems are adopted from different companies.

Table 30. Example snapshot of the updated failure rate allocation in StraPCost+, first row given total failure rate and its percentage (close but not 100%)

Subsystem	% fail. rate	Fail./yr/ turbine	Failure rate processing		
Total failure rate	99.5%	10.461	Onshore Original	Ratio WindSpeed	Ratio Temperature
Gearbox Assembly	5.1%	0.801	0.610	0.9396	1.3969
Blades	1.5%	0.111	0.172	0.8239	0.7811
Pitch System	21.3%	1.556	2.532	0.6893	0.8911
Yaw System	11.3%	1.239	1.342	1.0447	0.8838
Transformer	1.7%	0.194	0.203	0.8136	1.1702
Generator Assembly	7.2%	0.279	0.852	0.6336	0.5164
Frequency Converter	13.0%	1.542	1.542	1	1
L.V. Switchgear	5.9%	0.699	0.699	1	1
M.V. Switchgear	3.3%	0.395	0.395	1	1
Power Module Other	1.6%	0.194	0.194	1	1

5.3.1.3 Results and Discussion

Table 31 shows the failure rate translation from onshore to offshore for the subsystems shown in both data sources with a set default total failure rate of 11.895. As concluded in Chapter 4, the exponential fitting method is used in the translation. The second and third columns in the table show the original onshore failure rate percentage from [165] and the corresponding onshore failure rate derived from multiplying the set total failure rate with the system failure rate percentage, as the failure rate input used in the original version of the cost model, StraPCost. The rightmost column lists the translated

offshore failure rate derived using exponential fitting method. This table lists different subsystems in the order that suits the StraPCost+ failure rate module. The middle stages—the ratio of the wind speeds and the ratio of the temperatures— are also shown in the table separately.

Table 31. Failure rate translation from onshore to offshore for the matched subsystems for StraPCost+

Subsystem	Original Onshore failure rate%	Original Onshore failure rate	Ratio WindSpeed	Ratio Temperature	Translated Offshore failure rate
Gearbox Assembly14	5.10%	0.610	0.9396	1.3969	0.801
High Speed Shaft transmi	0.40%	0.049	0.9531	2.4941	0.116
Controller H/W	2.40%	0.289	1.1716	1.2113	0.410
Controller S/W	1.40%	0.169	1.1716	1.2113	0.240
Control & Comms Other	0.50%	0.056	1.1716	1.2113	0.079
Main Shaft13	0.30%	0.034	0.6929	1.4381	0.034
Rotor Other8	0.10%	0.007	0.7889	1.1853	0.007
Mechanical Brake15	0.50%	0.056	0.7437	1.1819	0.049
Blades9	1.50%	0.172	0.8239	0.7811	0.111
Yaw System18	11.30%	1.342	1.0447	0.8838	1.239
Transformer(HighV)1	1.70%	0.203	0.8136	1.1702	0.193
Generator Assembly27	7.20%	0.852	0.6336	0.5164	0.279
Pitch System11	21.30%	2.532	0.6893	0.8911	1.555
Hydraulic System23	1.20%	0.142	0.8702	0.5887	0.073
Tower33	2.70%	0.316	0.9621	0.8911	0.271

What is worth to be noticed is that the total percentage of all subsystems listed is only 99.5% rather than 100% from the best match between the subsystem failure reference [165] and the maintenance categorized failure rate reference [166], as introduced in Section 5.1.4. As the mismatch between the references, the dermatology used in the translation method also has unmatched subsystems with the original onshore failure rate values from the reference [165] in Table 31. Therefore, in StraPCost+, the matched subsystems are set to the translated offshore failure rates, and the unmatched subsystems are set to be the original onshore failure rate values (with environmental ratios equal to 1).

Higher wind speed in the marine condition can incur more loads and fatigue to a wind turbine, whereas the higher temperature offshore reduces the ice damage. Under the circumstance that these are the only two environmental factors considered and treated with equal weight, it is unsure whether the failure rate goes up with the translation to offshore. In general, the translated offshore failure rates dependent on the main subsystems are higher than the onshore original failure rate, but there are still exceptions. As already discussed in Chapter 4, apart from the mismatch of the subsystem terminology, the unexpected results can also come from the inaccurate (or can be wrong) shape derived from the limited length of the only accessible real failure rate data, and the simple assumptions that only wind speed and temperature are considered as the environmental factors with equal weight, etc.. Because of these limitations, the results from the translator cannot at this stage be assumed to be as reliable as would be wished. The translation method can be treated rather to provide a train of thought at this stage. The method can be expected to be improved when more real failure rate data available. On the other hand, it cannot be affirmed that the original onshore failure rates from reference [165] used in the original cost model are absolute accurate and the generic values for all onshore wind farms. The failure rate of some subsystems can be unrealistically high which show higher values than the offshore ones in this table.

Despite the limitations, in this way, the failure rate input of this cost model is made for the offshore application rather than the original onshore assumptions. It can be treated as a step closer to the realistic modelling. This improved failure rate setting algorithm is applied and further compared in the next sections. Because of the uncertainty, the benchmark in Section 5.3.4 uses both onshore original failure rates and the translated

offshore ones, with an additional comparison of a one value setting which applies only one general failure rate for the entire wind turbine and neglects the breakdown subsystem failure rate.

5.3.2 Expanding maintenance categories within StraPCost+

The maintenance category is an important aspect of cost modelling. Proper categorized maintenance groups provide suitable maintenance data for the corresponding cost calculation for the wind turbine and the entire wind farm level. As introduced in Section 5.1, the original StraPCost model selected three categories from the ECN O&M tool settings for unscheduled (denoted *Au*, *Cu* and *Du*) and scheduled maintenance (denoted *As*, *Cs* and *Ds*), and one separate category *E* for "remote reset". Even though it satisfies the requirements of basic estimation, it can be improved by adding more categories for more detailed estimation and with uniformity of other cost models benchmarked in Section 5.4.

The updated maintenance category in StraPCost+ is extended to five groups (*A*, *B*, *C*, *D* and *E*) for unscheduled (*u*) and scheduled (*s*) maintenance separately and *F* for "annual service". An example is given in Table 32. The parameters in this table are also used for the comparison with other cost models in the next section. The level of maintenance is listed in descending order. The updated *A* stands for "major replacement", *B* represents "major repair", *C* represents "medium repair", *D* stands for "minor repair", and *E* stands for "manual reset"—the original separate state "manual reset" is now listed as one of the categories under both maintenance strategies, and the separate state now becomes filled by "annual service". As shown in this table, the percentage value under each maintenance category shows the percentage of failure

occurrence associated with the maintenance activity. Thus the total percentage of every row in the table remains 100%.

Table 32. Example of extended maintenance categories in StraPCost+ input setting

Procedure Category	**Reactive maintenance**					**Condition-based maintenance**					Annual service
	Major Replacement	Major Repair	Medium Repair	Minor Repair	Manual Reset	Major Replacement	Major Repair	Medium Repair	Minor Repair	Manual Reset	
	unscheduled					scheduled					
Repair type	Au	Bu	Cu	Du	Eu	As	Bs	Cs	Ds	Es	F
weight limit	**500**	**50**	**10**	**10**	**10**	**500**	**50**	**10**	**10**	**10**	**10**
repair time	**52**	**26**	**22**	**7.5**	**3**	**52**	**26**	**22**	**7.5**	**3**	**60**
lead time	**1440**	**504**	**0**	**0**	**0**	**1440**	**504**	**0**	**0**	**0**	**1440**
people reqd	**5**	**4**	**3**	**3**	**2**	**5**	**4**	**3**	**3**	**2**	**3**
vessel	**HLV1**	**FSV1**	**CTV1**	**CTV1**	**CTV1**	**HLV1**	**FSV1**	**CTV1**	**CTV1**	**CTV1**	**CTV1**
Subsystem											
Generator Assembly	0.67%	0.34%	2.31%	25.22%	63.05%	0%	0%	0%	0%	0%	8.41%
Gearbox Assembly	0.67%	0.34%	2.31%	25.22%	63.05%	0.00%	0.00%	0.00%	0.00%	0.00%	8.41%
Blades	0.67%	0.34%	2.31%	25.22%	63.05%	0.00%	0.00%	0.00%	0.00%	0.00%	8.41%
Pitch System	0.67%	0.34%	2.31%	25.22%	63.05%	0.00%	0.00%	0.00%	0.00%	0.00%	8.41%
Yaw System	0.67%	0.34%	2.31%	25.22%	63.05%	0.00%	0.00%	0.00%	0.00%	0.00%	8.41%

Similar to 5.3.1.1, it is significant for this sheet to correlate the data with the relevant internal calculation sheets of the model. The values of breakdown failure rates under maintenance categories in the sheet *Difference* has been correlated to the sheet *Input&Result*. The information table in this window has also been expanded to cover the five maintenance categories.

With this extension of the categories, StraPCost+ can provide a more detailed estimation with respect to different maintenance operations.

The extension of the maintenance categories also affects the condition monitoring system detection effectiveness. Originally, the formula of each condition based maintenance category is shown as in Section 5.1.4.3. It is often interesting to investigate the effectiveness of condition monitoring systems at the entire wind turbine level. Normally, this investigation can only be realised by setting the condition

monitoring system effectiveness percentage one by one of each subsystem. For the convenience of condition monitoring system detection sensitivity analysis, the existing but not well functioning window of total detection effectiveness adjustment coefficients in the *Input&Result* sheet is correlated to the maintenance category tables in each relevant sheet, as shown in Table 33. In addition to Section 5.1.4.3, the coefficients are noted as: *edet* for *detectability*, *epre* for *pre-empt* and *efalse* for *false positive*. The percentages of this table show the additional percentages added to the detection effectiveness of every subsystem, e.g. 10% *detectability* means the detectability of the condition monitoring systems of every subsystem with condition monitoring systems becomes 110% of their original settings. In this way, it is straightforward to adjust each of the three detection effectiveness parameters for the entire wind turbine system in one go. The formulae are applied with the CM detection sensitivity coefficients *edet*, *epre* and *efalse, as shown from Eq.*73 to 82.

Table 33. Snapshot of the window of detection effectiveness adjustment coefficients in Input&Result *in StraPCost+*

detectability	Pre-empt	falsepos
10%	0%	0%

This condition monitoring system detection effectiveness sensitivity adjustment window is effectively connected to every variable in the cost model. The formula for each category is also adjusted and expanded to suit the new settings. Apart from the sensitivity coefficients, for unscheduled maintenance, *Cu'* is extended to be affected with not only *detectability* of *Cu*, but also *pre-empt*, same with *Bu'* and *Du'*. For scheduled maintenance, *Cs* is no longer over-optimistically estimated to be reduced to the two-level-lower *Au* due to *pre-empt*, but to be reduced to the next lower scheduled category *Bu*, and same concept has been applied to *Bs* and *Ds*.

When it comes to the false positive (*falsepos*), as introduced in Section 5.1.4.3, the original StraPCost version on its early stage assumes that when an alarm occurs, the maintenance team immediately sends out the corresponding level of vessel and technicians and stop the turbine when the level of failure requires, and this incurs the false positive having a severe impact on the loss of revenue and wind turbine availability. The published paper of this version of StraPCost [156] shows that *falsepos* has high sensitivity with results including revenue lost and O&M cost. This assumption over-estimates the negative economic impact of *falsepos*.

After consulting with the wind farm reliability engineers, the *falsepos* should have much less impact on the entire system. In reality, with current technology, the response to alarm is much less impetuous. When an alarm occurs, the maintenance centre will send the size of vessel and the number of technicians in the lower level category to check the turbine before the relatively heavier vessels and certain size of maintenance team. In some wind farm, the maintenance team would rather reduce the sensitivity of the condition monitoring system to avoid false positive. In some extreme examples, the maintenance team tend to only react when more than one alarm occurs at the same time, rather than immediately send out the checking team with one single alarm. However, for remote offshore wind farm, it is impossible to send small vessel to check the validity of the alarm. Therefore, improvement of the reliability of condition monitoring system is under the call for the development of the remote offshore wind farm.

With the sensitivity analysis of the condition monitoring system detection effectiveness including *falsepos* which is further discussed in Section 5.5, the final

regime is selected between two attempts. The first attempt assumes the impact of false positive of all levels from *Au* to *Eu* are all added to the manual reset *E* in the scheduled maintenance category. This makes *Es* in the scheduled maintenance consists of the *detectability* failure rate impact from *Eu*, the *pre-empt* failure rate impact from *Du* and the false positive failure rate impacts from *Au* to *Eu*. This regime incurs an under-estimation impact on *falsepos*, where the results such as loss of revenue do almost no change with the adjustment of *falsepos*. The formulae of regime1 are shown in Appendix-B Equation 1b and 2b.

Regarding to the further consulting with the engineers, in reality, when a major fault occurs and with decision to react, the maintenance team will send enough number of technicians with relatively long checking time, which matches the maintenance category *D* in this case. Therefore the regime is modified with having the impact of *falsepos* from *Au* and *Bu* (rather than the original *Au*, *Cu* and *Du* in Eq. 43) into *Ds*, as shown in Eq. 81, and the impact of *falsepos* from *Cu*, *Du* and *Eu* into *Es*, as shown in Eq.82. The formulae of unscheduled maintenance categories with the adjustment coefficients are listed as below.

$$\mathrm{A}'_U = A_U \cdot (1 - detectability \cdot (1 + edet) - preempt \cdot (1 + epre)) \quad (73)$$
$$\mathrm{B}'_U = B_U \cdot (1 - detectability \cdot (1 + edet) - preempt \cdot (1 + epre)) \quad (74)$$
$$\mathrm{C}'_U = C_U \cdot (1 - detectability \cdot (1 + edet) - preempt \cdot (1 + epre)) \quad (75)$$
$$\mathrm{D}'_U = D_U \cdot (1 - detectability \cdot (1 + edet) - preempt \cdot (1 + epre)) \quad (76)$$
$$\mathrm{E}'_U = E_U \cdot (1 - detectability \cdot (1 + edet)) \quad (77)$$

The scheduled maintenance categorized failure rate formulae are listed as:

$$A_S = A_U \cdot detectability \cdot (1 + edet) \quad (78)$$
$$B_S = B_U \cdot detectability \cdot (1 + edet) + A_U \cdot preempt \cdot (1 + epre) \quad (79)$$
$$C_S = C_U \cdot detectability \cdot (1 + edet) + B_U \cdot preempt \cdot (1 + epre) \quad (80)$$
$$D_S = D_U \cdot detectability \cdot (1 + edet) + C_U \cdot preempt \cdot (1 + epre) + (A_U + B_U) \cdot falsepos \cdot (1 + efalse) \quad (81)$$

$$E_S = E_U \cdot detectability \cdot (1 + edet) + D_U \cdot preempt \cdot (1 + epre) + (C_U + D_U + E_U) \cdot falsepos \cdot (1 + efalse) \quad (82)$$

where *Au, Bu, Cu, Du* and *Eu* are the maintenance categorized failure rate input setting under unscheduled maintenance category scenarios without consideration the CM detection; *Au', Bu', Cu', Du'* and *Eu'* are the estimated failure rate under unscheduled maintenance category scenarios with consideration of CM detection and *As, Bs, Cs, Ds* and *Es* are the estimated failure rate under scheduled maintenance category scenarios with consideration of CM detection.

5.3.3 Wind speed Weibull distribution parameter calculator

As described in the previous sections, wind speed parameters are significant initial inputs for the cost model since they are used to estimate lost generation due to turbine downtime. Pre-processing to obtain the wind speed parameters is not part of the original model, and this is inconvenient when the input data are in the form of a raw time series. This section improves the Matlab module by adding the wind Weibull distribution parameter calculation in StraPCost+.

5.3.3.1 Methodology

A linear fitting based calculation is an effective method to obtain the parameters in a way that is accurate as well as computationally efficient. Even though with a time series simulation, it can have a better precision with consideration of both mean value and the standard deviation (whereas the linear analytical method only considers the mean), the time- and computational-space-consuming characteristics are the main drawbacks of time series simulation, and the linear fitting method is finally chosen for the additional wind speed parameter calculator.

To linearize the Weibull distribution function, a log-log plot of the wind speed exceedance probabilities is used. The methodology starts from the calculation of the natural logarithm value of wind speed *U*, *lnU*, as shown below.

$$lnU = ln(U) \tag{83}$$

The occurrence frequency at each wind speed bin is obtained. The summation of frequencies at each wind speed bin, *totalfreq*, is then calculated, as shown below.

$$totalfreq = \sum(freq) \tag{84}$$

The exceedance of the frequency, *exfreq*, is then obtained by subtracting the frequency value of the wind speed less than or equal to the calculated wind speed from the total frequency value, as shown below.

$$exfreq(U) = totalfreq - freq(\leq U) \tag{85}$$

The log-log value of the frequency at each wind speed bin is obtained in below, and this gives the first part of the entire method:

$$loglogfr = ln(ln(totalfreq) - ln(exfreq)) \tag{86}$$

After obtaining the log-log values as above, the best linear fit can be calculated by least squares. The log-log graph of frequency against each natural logarithm value of wind speed is plotted as the red curve in Figure 64. A linear fitting with parameters of *a* and *b* is applied to the original curve, as shown below.

$$y(lnU) = a \cdot lnU + b \tag{87}$$

where *a* represents k_{est} and *b* is equal to $ln(\sqrt[k_{est}]{C_{est}})$. Solving these equations gives the initial values of k_{est} and ${C_{est}}^{k_{est}}$.

A convergence process is then done based on the equation below in the programme, where k_{est} and ${C_{est}}^{k_{est}}$ are obtained as the wind shape parameter and wind scale parameter, respectively.

$$lnlnfr(lnU) = k_{est} \cdot lnU + ln(\sqrt[k_{est}]{C_{est}}) \tag{88}$$

5.3.3.2 Case study and Results

This case study uses 10-year hourly wind data from FINO [187], which is also the environmental data used in the cost model comparison of the next section. The wind Weibull parameter calculator is realised in Matlab. It processes the wind speed time series data, produces its Weibull distribution, fits the middle stage log-log linearization, and calculates the shape parameter *k* and scale parameter *C*. As shown in Figure 64, even though the actual log-log value of the frequency (red) shows anomalous shaped tail at low *lnU* values (this relates to the extremely low wind speeds, below 1m/s) below the fitted curve (blue), the majority of the data is well fitted.

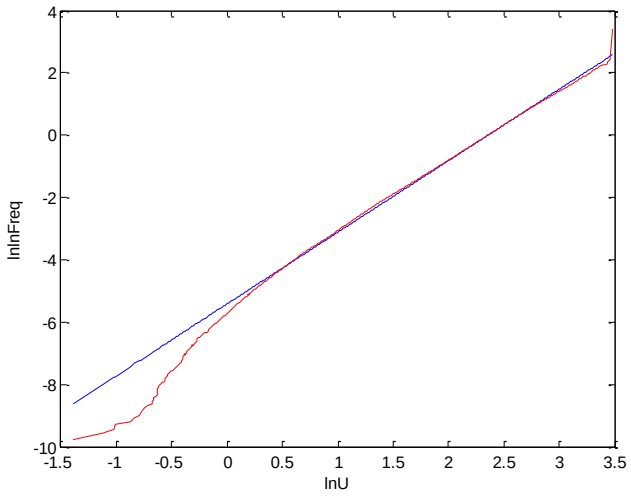

Figure 64. Wind speed Weibull distribution parameter k and C calculation from fitting to log-log linearized format

The wind Weibull parameters are then computed. For this data set, the shape parameter is 2.30 and the scale parameter is 10.63.

These results are also used as the pre-processed wind speed parameter input in StraPCost+ for the comparison analyses in Section 5.4.

5.3.4 Wind farm level cost estimation

One of the most significant limitations of the original model is that even though the cost model requires inputs of wind farm information such as wind and wave data, distance to shore, and financial and personnel characteristics, StraPCost only provides the cost estimation for O&M on an individual wind turbine level, which cannot represent that for the whole wind farm.

In StraPCost+, the improvement adds an input for the "number of wind turbines" in the wind farm basic characteristics setting in the *Input&Result* sheet, and uses this with other input data in order to provide a wind farm level estimation. Items of "entire wind farm annual maintenance cost", "Entire wind farm total O&M cost (with revenue loss) per unit" and "Entire wind farm total O&M cost (without revenue loss) per unit" are also added in the result table. It clearly shows the annual maintenance cost and the total O&M cost at a wind farm level, compares the results between reactive and condition based maintenance, and provides the result differences between the two types of maintenance.

This is the first attempt of extending the cost estimation of StraPCost+ into a wind farm level under the current model algorithm and structure. The model estimation is based on the individual turbine reliability, and it assumes linear relationship for all

turbines in the wind farm, which is simply the multiplication of the individual turbine estimation and the number of turbines. This simple assumption also causes linear relationship for wind farm availability estimation. It assumes the maintenance proceed for one failure per turbine per visit. However as stated in the previous sections, in reality the wind farm operator would integrate the maintenance requirement and deal with multiple failures and turbines in one visit to maximize the vessel usage with minor maintenances, which would need modifications further made to the internal calculations, in this example, the vessel cost. In future work, the algorithm can be further improved so that the estimation can be done at wind farm level as an entirety. For example, a vessel travel strategy for multiple tasks similar to NOWIcob [160] can be added to StraPCost+.

Another issue for the wind farm level cost estimation that can be addressed in future work is seasonality, i.e. the significant differences between summer and winter. The sea-state parameters, the numbers of hours of operation, the corresponding failure rates and the unavailable hours can be treated separately for these two main seasonal states (or more seasons of required). Thus the overall availability can be calculated in summer and winter separately and this will add accuracy. Alternatively, if sufficient data is available the analysis could be undertaken month by month.

5.3.5 Technician cost

In the original model, it is assumed that the number of technicians depends on the maintenance category, and that the estimated cost of technician only considers the time required for the maintenance operation itself. However, in reality, the wind farm operator has to employ and ensure a certain number of permanent technicians available

every day during the year preparing for the daily operation, reactive, preventative, condition-based and emergency maintenance. The cost of the technicians from the operator point of view includes not only wages but also training, national insurance contribution (NIC), pension, life assurance, etc. Company cars, software licences, IT support and all other general overheads are also relevant.

Therefore, the improved cost model adds the technician inputs of "the number of technicians available per working shift" and "the cost per technician per day". The cost of permanent available technicians required, as an elementary expenditure from the wind farm perspective, is in addition to the wage calculation during the actual maintenance working time in StraPCost+. This first attempt provides linear relationship that affects the cost related estimations in StraPCost+ but not the wind farm performance estimation such as availability and capacity factor. The linear relationship between the number of technician and the wind turbine availability causes the unchanged results for StraPCost+ with the sensitivity benchmark in Section 5.4.1.2.1.

5.3.6 Delay information correlation

As in its original form, the StraPCost model has some correlation problems. One example is given in the failure rate correlation discussed above in Section 5.3.1.1. There is additional information that is not correlated between sheets in the Excel document in the original model. One significant correlation omission is in the sheet *Delay*. The information window "SITE METOCEAN CHARACTERISTICS" which is supposed to have the same values in the window under the same name in the sheet *Input&Result* did not show the information correctly. This severely affected

calculations in every step dependent on this information, and the accuracy of the estimation of the final results. In StraPCost+, the information correlation omission has been corrected.

5.3.7 Sensitivity analysis percentage adjustment coefficient

Similar to the CM detection percentage adjustment coefficients, *edet*, *epre* and *efalse*, for *detectability*, *pre-empt* and *falsepos* respectively, as shown in Table 33 in Section 5.3.2, more sensitivity percentage adjustment coefficients are set correlated in the entire StraPCost+. Some of the coefficients were already set in an embryonic form in the old version StraPCost, and this section improves the correlations of them to allow more comprehensive applications in StraPCost+ for the ease of the sensitivity analysis as discussed in Section 5.6.

The coefficients are set for distance to shore, default total turbine annual failure rate, wind and wave parameters, and weather window threshold for heavy maintenance (*A* and *B*) and light maintenance (*C*, *D* and *E*).

Table 34 shows the percentage adjustment coefficient added for distance to shore. It adjusts the base value with the additional percentage in the rightmost yellow cell and shows the adjusted exact value in the orange cell on the left hand side. In this case, the base value is 50km, and the adjusted value is: 50 × (1+200%) = 150 km.

Table 34. Snapshot of the percentage adjustment coefficient for distance to shore

Distance to shore(km)	ds	150	200%

A similar concept is applied to the default total turbine annual failure rate. The adjustment affects the related calculations that use this value including breakdown

subsystem failure rates and the corresponding maintenance category failure rate calculations. As shown in Table 35, the example base case of the default total turbine annual failure rate is 11.895, and the adjusted value is: 11.895 × (1+10%) = 13.085.

Table 35. Snapshot of the percentage adjustment coefficient for default total turbine annual failure rate

Total turbine annual failure rate	13.085	10%

Since the wind and wave conditions are highly correlated, the wind and wave parameter percentage coefficients in Table 19 in Section 5.1.2 are here set to be adjusted at the same time. In order to keep the basic shape of the wave distribution, the wave Weibull parameters adjusted are only the wave location and scale parameter; and since the wind location parameter is set to be 0 all the time, the adjustment only applies to the wind scale parameter.

The weather window threshold is as introduced in Figure 44 in Section 5.1.3.2. Adjustment of the threshold affects the corresponding "storm" and "calm" period definitions, and thus affects the vessel usage estimation. This group of adjustments are highly affected by the weather window threshold. The adjustments are divided into two parts: heavy maintenance related (maintenance category *A* and *B*, with use of heavy lift vessels and the longer "calm" period required) and light maintenance related (maintenance category *C*, *D* and *E*, with use of light vessels and shorter associated "calm" periods). Table 36 shows the snapshot of the percentage adjustment coefficients for these two maintenance category groups. In this example, it shows that the adjustment for repair time, *krep*, is set to be 10% more of the original setting for heavy maintenance *A* and *B*; the on land lead time per failure, *klead*, is set to be 10% more of the original setting for light maintenance *C*, *D* and *E*; the weather window

threshold (both wind and wave), *kthr*, is set to be 20% less of the original setting for heavy maintenance *A* and *B*; and the vessel travel speed, *kspd*, is set to be 10% less of the original setting for light maintenance *C*, *D* and *E*. Each percentage adjustment coefficient is applied to all StraPCost+ calculations on one go.

Table 36. Snapshot of the interface of the percentage adjustment coefficient for heavy maintenance (A and B) and light maintenance (C, D and E)

	A & B	C, D & E
krep	10%	0%
klead	0%	10%
kthr	-20%	0%
kspd	0%	-10%

5.3.8 Conclusion

This section has outlined the improvements made to the original model that result in the updated version, StraPCost+. It discusses the possibility of enhancing the reliability of failure rate breakdown value of each wind turbine subsystem by applying the failure rate on/offshore translation procedure developed in Chapter 4.

Before doing so, the failure rate data have been internally correlated within the cost model in order to provide more developer-friendly interface in StraPCost+. This enhances the convenience of changing the failure rate data and reduces the risk of leaving out of any item in any of the Excel sheets.

Following Chapter 4, the exponential function is used as the fitting function in the onshore/offshore translation method. Even though the translation method does not provide lower failure rate values to all subsystem components compared with the default onshore failure rate, it cannot be concluded that the translation method has lower reliability than the onshore default setting which is taken from empirical onshore

data. For the cost model's offshore scope, it is theoretically closer to the reality to use the translated offshore data. A further comparison of different sources of failure rate data with other cost models will be undertaken in the Section 5.4.

The maintenance categories in the original model covered three situations that determine vessel type and usage. This has been refined with five categories for both unscheduled and scheduled maintenance and one separate category of annual service in StraPCost+.

A wind Weibull parameter calculator is also built into the StraPCost+ model package. The analytical wind parameter calculator is realised by using a log-log linear fitting algorithm which provides the accuracy as well as simplicity of calculation.

One significant disadvantage of the original model is that it only provides the cost estimation in an individual wind turbine level. An initial attempt in the improvement makes up for this disadvantage by adding as an input the number of wind turbines in the wind farm which complements the wind-turbine-level calculations to provide an analysis at wind farm level in StraPCost+. This function affects the cost related cost model results and does not affect the wind farm performance results such as availability and capacity factor, as discussed in Section 5.4.

Another unrealistic assumption of the original model is that it only calculates staff wages during the maintenance activity. The improvement adds technician inputs into the financial assumptions window for the estimation of the cost due to the daily available permanent technicians in StraPCost+. Again, the number of technician's only affects the cost related results but not the wind arm performance results, as discussed in Section 5.4.

More percentage adjustment coefficients are set in StraPCost+ for easier sensitivity analysis as presented in Section 5.5 and Section 5.6.

With the stated improvements, StraPCost+ presents a theoretically more accurate and realistic estimation of O&M cost and is to be assessed by real data. Before further analyses and applications to the real wind farm case studies, StraPCost+ is compared in the Section 5.4 with a selection of available other cost models introduced in the previous section. In theory, StraPCost+ is expected to present similar estimation results with other cost models to a certain extent. Since all other cost models are time-series simulation based while StraPCost+ is an analytical model, it can also be expected differences in estimated results, especially the time based ones such as wind farm availability. Cost models such as NOWIcob which put emphasis on the vessel travel conditions (both wind and wave) are expected to have higher cost related estimation. StraPCost+, on contrast, which is a relatively simple model in terms of e.g. the assumption of one visit per vessel task, dispersed event assumption, linear impact of the technician settings on the model results, linear impact of the number of turbines to the entire wind farm estimation, is expected to have quite optimistic estimations among all the cost models compared in terms of both wind farm availability and the O&M cost. These predictions are assessed and discussed in Section 5.4.

5.4 Comparison of StraPCost+ with other O&M cost models

This section presents the result comparison between StraPCost+, the updated cost model, with other cost models introduced in Section 5.2. It is important to cross-check the cost model performance in this way. Because of the lack of offshore wind farm operational data, one approach is to compare the results among the existing cost models. The mean results of the other cost models will be used as the performance indicator against StraPCost+ in this Section.

This investigation is based on the results from the comparison of ECUME, NOWIcob, the UiS cost model and Strathclyde OPEX model as documented in [188]. As introduced in Section 5.2, not all cost models consider condition based maintenance and every few lists specific results under this maintenance strategy. Therefore, the comparison is concerned only with reactive maintenance.

According to [188], the entire wind farm *time-based availability* and *annual maintenance cost* are the parameters compared for baseline reactive maintenance strategy with uniform settings also applied to all cost models as far as possible. This investigation also compares the results from different failure rate scenarios including the aggregated total failure rate, the default onshore failure rate and translated offshore failure rate. In the future, when more actual data are available, the results can be inspected more comprehensively.

This section begins with the introduction of the comparison scenarios, which consist with the baseline analysis and the sensitivity analyses in Section 5.4.1. In baseline analysis, because the other cost models only consider the overall failure rate on the wind turbine level, three methods modifying StraPCost+ failure rate settings are

applied, with Method 1 of one value, Method 2 of the same values for original onshore subsystem failure rate setting, and Method 3 of the same values for translated failure rate setting. In the sensitivity analyses, the number of technicians, failure rates, vessel usage and maintenance categories are adjusted and the corresponding modelling results are cross-checked. The results are discussed in detail in Section 5.4.2.

5.4.1 Comparison scenarios

The comparison scenarios consist of the baseline analysis and the sensitivity analyses. Both analyses only compare the reactive maintenance.

5.4.1.1 Baseline analysis

The baseline comparison is for a fictitious offshore wind farm consisting of 80 Vestas V90 3.0MW wind turbines with a hub height of 90m. Instead of the actual wind farm layout and other logistic details, it sets the distance from the closest turbine to the onshore maintenance base at 50km. The environmental data is dependent on the FINO 1 offshore research platform [187] which is located approximately 45km off the coast of Germany in the German development zone for offshore wind farms. The site provides the representative environment for the Central North Sea nearby to the existing Alpha Ventus wind farm. The wind and wave data are pre-processed in the updated cost model built-in parameter calculator, in which the wind speed Weibull parameters are calculated according to method introduced in Section 5.3.3.

The original comparison was done by [188] without StraPCost+. In the virtual wind farm, the wind speeds were recorded at 90m, as a typical hub height for an offshore wind turbine. The significant wave heights were measured by a wave buoy. The data

covers 8 years from 2004 to 2012 whereas the simulated time duration is 10 years for the purpose of model comparison. Thus a pre-processing including division of hourly resolution and a time extension has been done to the data by filling gaps with the average values of data over other months and keeping the basic fluctuations with time.

The vessel types in use are set as: Crew Transfer Vessels (CTV), Field Support Vessels (FSV) and Heavy-Lift Vessels (HLV). They are defined with specific operational and environmental criteria, as shown in Table 37.

Table 37. Vessel inputs for the FINO virtual wind farm comparison in [188]

VESSEL INPUT	Crew transfer vessel	Field support vessel	Heavy-Lift vessel
Number of vessels	3	1	1
Governing weather criteria	Wave	Wave	Wave/Wind
Weather criteria	1.5 m	1.5 m	2.0 m / 10.0 m/s
Mobilisation time	0 weeks	3 weeks	2 months
Mobilisation cost	£ 0	£ 0	£ 500 000
Speed of vessel	20 knots	12 knots	11 knots
Technician capacity	12	60	100
Day rate	£1750/day	£9500/day	£150 000/day
Maximum offshore time	1 shift	4 weeks	No limit
Comment	Hired on a long-time charter so that the vessel always is available at the maintenance base.	Hired. Charter period 1 month. Has external crane.	Hired. Charter period 1 month. Wave height for jack-up operation, wind speed for crane

As stated, the comparison only concentrates on reactive maintenance. Failure data in [188] are empirically provided from a group of experts from wind farm developers at a wind farm level, i.e. there are only five failure rate values for the five maintenance categories and one value for the annual service, as shown in Table 38. The data is considered to represent the current generation of offshore wind turbines. The failure rate is calculated in a summation value and percentage for the format of StraPCost+ input. The summed value for the six categories gives an overall failure rate of 11.895 in this case.

Table 38. Failure input for the five maintenance categories and the annual service, with modification from [188]

FAILURE INPUT	Major replacement	Major repair	Medium repair	Minor repair	Manual reset	Annual service	SUM
Repair time	52 hours	26 hours	22 hours	7.5 hours	3 hours	60 hours	
Required technicians	5	4	3	2	2	3	
Vessel type	HLV	FSV	CTV	CTV	CTV	CTV	
Repair cost	£334,500	£73,500	£18,500	£1,000	0	£18,500	
Failure rate	0.08	0.04	0.275	3.0	7.5	1.0	11.895
Failure rate %	0.67%	0.34%	2.31%	25.22%	63.05%	8.41%	100%

In contrast to models that only use an overall failure rate, StraPCost+ has an innovative subsystem level structure of the failure rate input. For consistency of the one value overall failure rate setting, there are two modified ways of setting in StraPCost+.

Method 1 is to set the overall failure rate in one of the subsystems for the maintenance categories, set the percentage of the breakdown failure rate of this subsystem 100%, and set 0% for the rest subsystems, as shown in Table 39 (partially). This method bypasses the subsystem breakdown failure rate of StraPCost+ and is useful for inspecting performance of the entire model except for the breakdown failure rate window comparing with other models.

Table 39. Snapshot of part of comparison setting Method 1: Overall failure rate value for the entire turbine system set in subsystem failure rate input and maintenance categories in StraPCost+

Failure rate				**reactive maintenance**					Annual service
				Major Replacement	Major Repair	Medium Repair	Minor Repair	Manual Reset	
Failure rate database used			Reliawind	Unscheduled					
			failure rate/yr	Au	Bu	Cu	Du	Eu	F
				500	**50**	**10**	**10**	**10**	**10**
Defaults total turbine annual failure rate			**11.895**	**52**	**26**	**22**	**7.5**	**3**	**60**
Subsystem	CM type	Subsystem% failure rates	Subsystem failure rates	**1440**	**504**	**0**	**0**	**0**	**1440**
				5	**4**	**3**	**3**	**2**	**3**
Total		100.0%	11.895	**HLV1**	**FSV1**	**CTV1**	**CTV1**	**CTV1**	**CTV1**
Generator Assembly		100.0%	11.895	0.67%	0.34%	2.31%	25.22%	63.05%	8.41%
Gearbox Assembly		0.0%	0.000	0.00%	0.00%	0.00%	0.00%	0.00%	0.00%
Blades	Strain	0.0%	0.000	0.00%	0.00%	0.00%	0.00%	0.00%	0.00%
Pitch System	SCADA	0.0%	0.000	0.00%	0.00%	0.00%	0.00%	0.00%	0.00%
Yaw System	SCADA	0.0%	0.000	0.00%	0.00%	0.00%	0.00%	0.00%	0.00%

The other way is to set the same maintenance categorized failure rate values for every listed turbine subsystem, and apply the failure rate breakdown to each subsystem. Practically, in the cost model, all maintenance categorized failure rate percentages are set equal to the first line for the convenience of changing the values. The failure rate breakdown of each subsystem follows the stated two streams: Method 2 uses the original onshore failure rate shown in Table 40 (partially), and Method 3 uses the translated offshore failure rate shown in Table 41 (partially).

Table 40. Selection of failure rates comparison setting Method 2 with original onshore subsystem failure rate (shown partially)

Failure rate				**reactive maintenance**					Annual service
				Major Replacement	Major Repair	Medium Repair	Minor Repair	Manual Reset	
Failure rate database used			Reliawind	Unscheduled					
			failure rate/yr	Au	Bu	Cu	Du	Eu	F
				500	**50**	**10**	**10**	**10**	**10**
Defaults total turbine annual failure rate			**11.895**	**52**	**26**	**22**	**7.5**	**3**	**60**
Subsystem	CM type	Subsystem% failure rates	Subsystem failure rates	**1440**	**504**	**0**	**0**	**0**	**1440**
				5	**4**	**3**	**3**	**2**	**3**
Total		99.5%	11.833	**HLV1**	**FSV1**	**CTV1**	**CTV1**	**CTV1**	**CTV1**
Generator Assembly		**7.2%**	0.852	0.67%	0.34%	2.31%	25.22%	63.05%	8.41%
Gearbox Assembly		**5.1%**	0.610	0.67%	0.34%	2.31%	25.22%	63.05%	8.41%
Blades	Strain	**1.5%**	0.172	0.67%	0.34%	2.31%	25.22%	63.05%	8.41%
Pitch System	SCADA	**21.3%**	2.532	0.67%	0.34%	2.31%	25.22%	63.05%	8.41%
Yaw System	SCADA	**11.3%**	1.342	0.67%	0.34%	2.31%	25.22%	63.05%	8.41%

Table 41. Selection of failure rates comparison setting Method 3 with exponential translated offshore data (shown partially)

Failure rate				**reactive maintenance**					Annual service
				Major Replacement	Major Repair	Medium Repair	Minor Repair	Manual Reset	
Failure rate database used			Reliawind	Unscheduled					
			failure rate/yr	Au	Bu	Cu	Du	Eu	F
				500	**50**	**10**	**10**	**10**	**10**
Defaults total turbine annual failure rate			**11.895**	**52**	**26**	**22**	**7.5**	**3**	**60**
Subsystem	CM type	Subsystem% failure rates	Subsystem failure rates	**1440**	**504**	**0**	**0**	**0**	**1440**
				5	**4**	**3**	**3**	**2**	**3**
Total		99.5%	10.460	**HLV1**	**FSV1**	**CTV1**	**CTV1**	**CTV1**	**CTV1**
Generator Assembly		**7.2%**	0.279	0.67%	0.34%	2.31%	25.22%	63.05%	8.41%
Gearbox Assembly		**5.1%**	0.801	0.67%	0.34%	2.31%	25.22%	63.05%	8.41%
Blades	Strain	**1.5%**	0.111	0.67%	0.34%	2.31%	25.22%	63.05%	8.41%
Pitch System	SCADA	**21.3%**	1.555	0.67%	0.34%	2.31%	25.22%	63.05%	8.41%
Yaw System	SCADA	**11.3%**	1.239	0.67%	0.34%	2.31%	25.22%	63.05%	8.41%

The complete original onshore failure rate values follow the settings in Section 5.1, and the full length translated offshore failure rate values are obtained in Section 5.3.1. These three methods provide a good opportunity to check the performance of the onshore/offshore failure rate translator installed in StraPCost+. Results are discussed in the later content.

The technician cost settings filled in StraPCost+ are £80,000 per technician per year, 20 technicians required per shift, and 12 hours per shift. At the same time, for the additional StraPCost+ maintenance task wage calculation, an hourly rate of £80,000 / (12*365) = £18.26 is also set as input.

Other detailed settings can be found in [188].

5.4.1.2 Sensitivity analyses

In order to further investigate and compare all three failure setting methods for StraPCost+ and the selected other cost models, a series of sensitivity analyses are applied based on the baseline case in terms of adjusting the number of technicians, failure rates and maintenance category settings, as initially proposed in [188]. The sensitivity analyses are following the control variable scientific method, i.e. when comparing one aspect; other settings remain the same as in the baseline.

5.4.1.2.1 Number of Technicians

The sensitivity of the number of technicians is inspected on both sides of the baseline assumption: increase and decrease the number from the baseline of 20 by 10, i.e. for the more technicians case set the number of technicians to 30 and the fewer technicians' case set the number of technicians to 10 [188].

5.4.1.2.2 Failure rates

The sensitivity of the failure rates is inspected in a similar manner: a decrease to 50% of all maintenance categorized failure rates in the corrective maintenance, and an increase to 200% of the original maintenance categorized failure rate values. The failure rate value of annual services remains the same as the baseline. These analysis settings affect the total turbine failure rate which is the summation of the six failure rate values as well as the maintenance categorized failure rate percentage which is calculated by the exact value and the summation [188]. Table 42 shows the calculated exact values, the percentage and the summation of the failure rate under the three scenarios.

Table 42. Overall maintenance categorized failure rates and percentages for failure rate sensitivity scenarios, with modification from [188]

Failure Rate	Major replacement	Major repair	Medium repair	Minor repair	Manual reset	Annual service	SUM
Baseline	0.08	0.04	0.275	3	7.5	1	11.895
Baseline %	0.67%	0.34%	2.31%	25.22%	63.05%	8.41%	100%
Failure down	0.04	0.02	0.1375	1.5	3.75	1	6.4475
Failure down %	0.62%	0.31%	2.13%	23.26%	58.16%	15.51%	100%
Failure up	0.16	0.08	0.55	6	15	1	22.79
Failure up %	0.70%	0.35%	2.41%	26.33%	65.82%	4.39%	100%

5.4.1.2.3 Vessel usage

Among the three vessels used in this investigation setting, the heavy-lift vessel (HLV) takes the longest mobilisation time, and has the highest day rate and mobilisation cost. It is important to investigate the impact of the HLV on the entire cost model. The sensitivity analysis sets the HLV-related maintenance category, i.e. major replacement Au, to zero influence on the entire model in order to compare the results with and without the heavy-lift vessel influence. In practise, it sets all failure rates under this

maintenance category into zero, which changes the overall maintenance categorized failure rates and percentages, as shown in Table 43 [188].

Table 43. Overall maintenance categorized failure rates and percentages for vessel usage sensitivity scenario, with modification from [188]

Failure Rate	Major replacement	Major repair	Medium repair	Minor repair	Manual reset	Annual service	SUM
No HLV	0	0.04	0.275	3	7.5	1	11.815
No HLV %	0.00%	0.34%	2.33%	25.39%	63.48%	8.46%	100%

5.4.1.2.4 Maintenance categories

To investigate the impact of each maintenance category on the entire cost model, the sensitivity analysis sets the cost model into the "selected maintenance category only" mode. In practice, the failure rates under all maintenance categories except the selected maintenance category are set to zero, as shown in Table 44 [188].

Table 44. Overall maintenance categorized failure rates and percentages for maintenance categories sensitivity scenarios, with modification from [188]

Failure Rate	Major replacement	Major repair	Medium repair	Minor repair	Manual reset	Annual service	SUM
Major replacement only	0.08	0	0	0	0	0	0.08
Major replacement only%	100%	0%	0%	0%	0%	0%	100%
Major repair only	0	0.04	0	0	0	0	0.04
Major repair only%	0%	100%	0%	0%	0%	0%	100%
Medium repair only	0	0	0.275	0	0	0	0.275
Medium repair only%	0%	0%	100%	0%	0%	0%	100%
Minor repair only	0	0	0	3	0	0	3
Minor repair only%	0%	0%	0%	100%	0%	0%	100%
Manual reset only	0	0	0	0	7.5	0	7.5
Manual reset only%	0%	0%	0%	0%	100%	0%	100%
Annual service only	0	0	0	0	0	1	1
Annual service only%	0%	0%	0%	0%	0%	100%	100%

5.4.2 Results

The results from StraPCost+ with the overall failure rate, original onshore failure rate, and the translated failure rate are shown in Table 45. The red edged boxes highlight the two main objects of comparison.

Table 45. Comparison of the reactive outputs with different failure rate inputs for StraPCost+

WITH DOWNTIME based on	Overall one value	Original Onshore	Exp-translated
downtime	26.8 days	26.7 days	23.6 days
Time-based availability	92.6 %	92.7 %	93.5 %
capacity factor	45.1 %	45.2 %	45.8 %
energy lost	1389.4 MWh	1382.2 MWh	1221.8 MWh
mean power generated over year	1.35 MW	1.35 MW	1.37 MW
total annual energy generated	11860.8 MWh	11868.1 MWh	12028.5 MWh
annual revenue	1067.5 £k	1068.1 £k	1082.6 £k
revenue lost	125.0 £k	124.4 £k	110.0 £k
annual maintenance cost	226.1 £k	187.7 £k	165.7 £k
entire wind farm annual maintenance cost	19.7 £m	16.6 £m	14.9 £m
vessel cost per unit	£0.012 /kWh	£0.012 /kWh	£0.010 /kWh
wage cost per unit	£0.0021 /kWh	£0.0021 /kWh	£0.0018 /kWh
component cost per unit	£0.0052 /kWh	£0.0020 /kWh	£0.0017 /kWh
Total O&M cost (w/o revenue loss) per unit	£0.0191 /kWh	£0.0158 /kWh	£0.0138 /kWh
revenue lost per unit	£0.0105 /kWh	£0.0105 /kWh	£0.0091 /kWh
Total O&M cost (with revenue loss) per unit	£0.0296 /kWh	£0.0263 /kWh	£0.0229 /kWh

The annual O&M cost and time-based availability comparison of all three failure rate setting methods using StraPCost+ and ECUME, NOWIcob, UiS and OPEX, which are grouped as the other cost models in the later context, with both baseline and all sensitivity analyses are shown in Figure 65 and Figure 66. With data protection, the exact values are not available directly from the cost model owners; therefore extraction from the publication [188] has been done for the other four cost models.

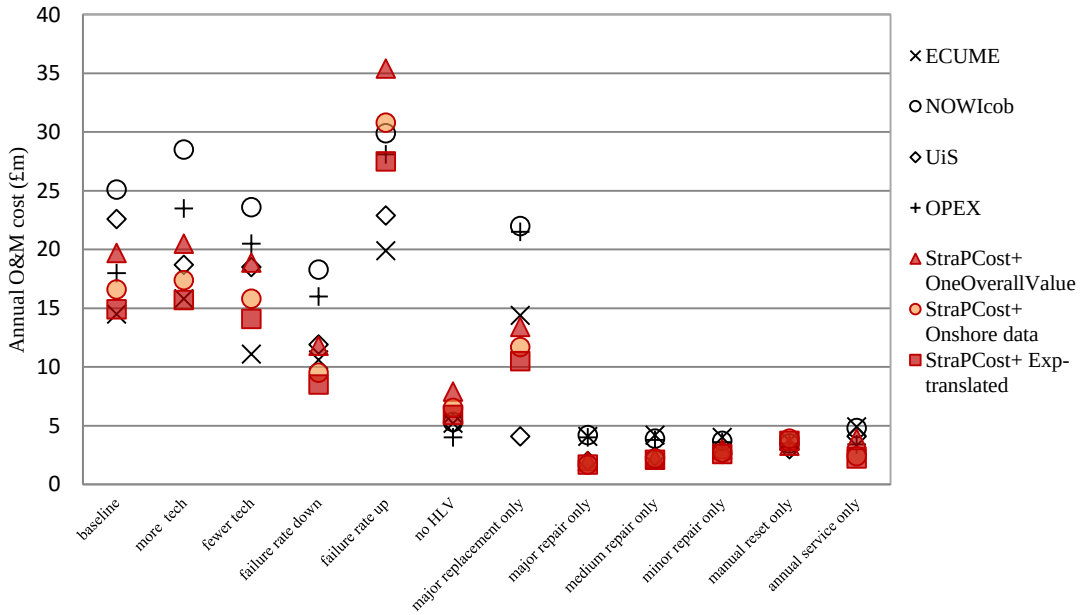

Figure 65. Annual O&M cost baseline and sensitivity analyses for all cost models in the comparison study

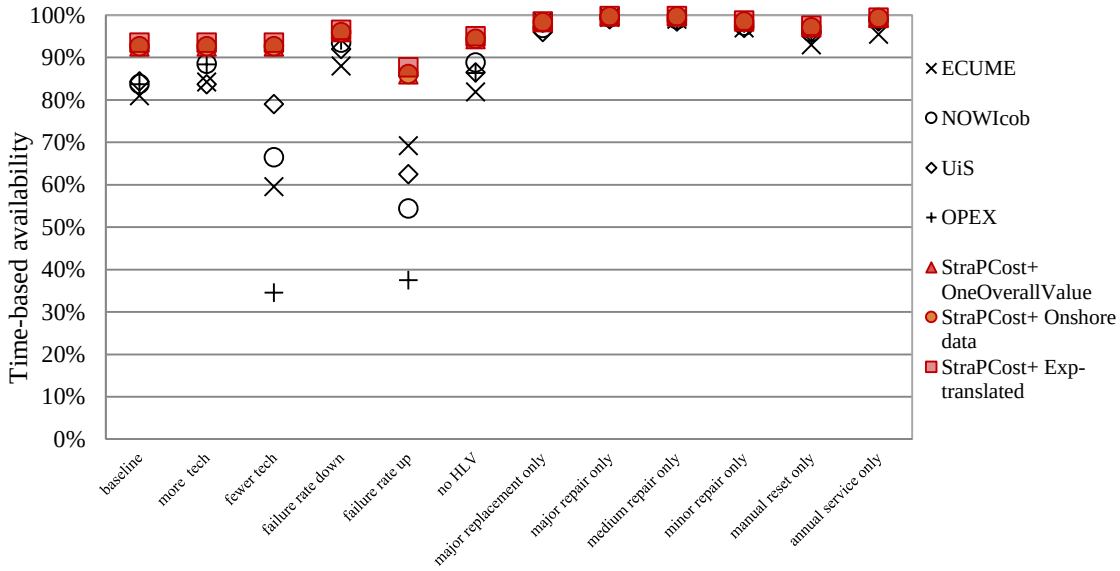

Figure 66. Time-based availability baseline and sensitivity analyses for all cost models in the comparison study

5.4.3 Discussion

The discussion is given in baseline and sensitivity analyses, in Section 5.4.3.1 and Section 5.4.3.2 respectively.

5.4.3.1 Baseline comparison

Table 45 shows that the overall one value approach gives a time-based availability of 92.6%; the original onshore data in method 2 gives an availability of 92.7%; and the translated offshore data in method 2 gives an availability of 93.5%. From the entire wind farm annual maintenance cost perspective, the overall one value method gives £19.7m; the original onshore failure rate gives £16.6m; and the translated offshore data gives £14.9m. It can be seen that the translated subsystem failure rate settings result in generally optimistic estimations in both availability and annual O&M cost. As stated repeatedly, this translator is very limited with lack of reasonable length of real data for its training process which might have led to incorrect failure rate distribution functions

and result in the underestimation of the annual O&M cost and the overestimation of the availability. The compromised translated environmental factor ratio setting of "1" for unmatched subsystems also reduces the differences among the three methods especially in the availability estimation results.

The results of these three failure rate assumptions using StraPCost+ compared with the other cost models are at the leftmost marked as *baseline* in Figure 65 and Figure 66. It can be seen that even the one overall value method gives a quite high availability estimation. It can be initially deduced that the original StraPCost algorithm is more optimistic than other cost models in this aspect and to be assessed when more real data are available. Since this wind farm setting is from a virtual wind farm and the lack of real operational data to prove the estimation, even though all other cost models give the availability estimation at the same rage, it cannot be concluded that those are the correct results for the fact that they all apply the Monte Carlo method while StraPCost+ uses analytical method. For better assessment of the validation of the estimation, these StraPCost+ results from this virtual wind farm are compared with two real offshore wind farms with ECUME in Chapter 6.

The annual O&M cost results from StraPCost+ in Figure 65 locate at the lower range among all the cost models, but higher than the lowest one from ECUME. The average value of results from all methods using StraPCost+ is £17.07m, with a -£2.98m difference from the average value of £20.05m using the other four cost models. This difference is even smaller than the difference of the average value with the other cost models ECUME (-£5.55m) and NOWIcob (£5.05m), both of which are developed commercially packaged cost models.

The annual O&M cost from the four other cost models are fairly scattered. A surprising result from ECUME is that even with its low availability estimation (as shown in Figure 66), it provides the lowest estimation of cost, with £14.5m annually. NOWIcob presents the highest estimated annual O&M cost, with £25.1m. The difference between the lowest and highest estimation is as much as £10.6m. UiS and OPEX give values in between, with £22.6m and £18m, respectively. The lowest deviation among other cost models comes from the Strathclyde OPEX model, with -£2.05m. This deviation is not far from the second lowest, UiS, with £2.55m.

Among the three StraPCost+ results, the closest to the average value of the four other cost models is from the overall one value method, with -£0.35m difference. The original onshore data gives a difference of -£3.45m, and the translated offshore failure rate gives a difference of -£5.15m. The translated offshore failure rate presents a similar result to the commercial model ECUME, with only £0.4m difference. Because of the failure rate in the one overall value method is set regardless of the breakdown into subsystem values, which is the closest setting to that used in the other cost models, the one overall value implementation of StraPCost+ can be viewed as closest in its representation to the other four cost models. The implementation using the translated offshore failure rate data has a difference from the one overall value method of £4.8m, and this difference is still in a reasonable range (smaller than the ECUME difference with the other cost model mean value of £5.55m).

Similarly, the baseline comparison of the time-based availability values are at the leftmost of Figure 66. It can be seen that all three StraPCost+ results are at the higher range among all the cost models. The difference between the average of StraPCost+ results and the other cost models is 9.77%. The fact that StraPCost+ with all three

failure rate resources are close with each other but relatively far from the other methods highlights the difference of cost model algorithms between StraPCost+ **(**using analytical method) and the other cost models (using Monte Carlo Markov methods). In addition, as stated, the fact that StraPCost+ does not consider multiple tasks in one vessel visit and the seasonality could also increase the difference (e.g. the wind and wave condition are dramatically different in summer and winter season, thus the wind turbine failure rates and vessel usage are affected).

The deviation between the three StraPCost+ results and their average value is within 0.57%, much lower than the highest deviation between the other cost models and their average value 2.35% (ECUME). It shows ECUME gives a clearly lower value than the other three, with 81%. The other three are in a closer range, with 83.74%, 84.40% and 83.70% in the stated order. Even though ECUME gives estimation results with high deviation from the mean of the four other cost models, it is a commercial-trusted cost model, and with real operational data training from EDF, its results are highly valued. It shows from another angle that it cannot be concluded the estimation from one cost model is not accurate when it is not the same with the other cost models. More estimation comparisons between StraPCost+ and ECUME for real offshore wind farms are shown in Chapter 6 with assessment of empirical operational result range.

It is not possible to judge which group of methods has the higher accuracy and is closer to the reality, but the gap in the calculated time-based availability cannot be ignored.

In general, from the results of annual O&M costs comparison, it is shown that the differences among the three failure rate sources using StraPCost+ are not large compared with the differences among the other cost models. The translated offshore

failure rate provides the closest O&M cost estimation with the commercial cost model ECUME. For its theoretically preferable algorithm discussed in Chapter 4, the exponential translated failure rate is further inspected as the failure rate input of StraPCost+ in later analyses.

The performance of the time-based availability of StraPCost+ for the three sources of failure rate are quite close and but higher than the other cost models, which highlights essentially different basic algorithms used by StraPCost+. It cannot be concluded which group is closer to reality because of lack of actual data as a reference. However, the range of the availability shown by StraPCost+ is rather high. The fact that the current StraPCost+ model does not consider multiple tasks in one maintenance visit or seasonality may explain some of the difference. These aspects could be explored in future work.

5.4.3.2 Sensitivity analyses of the comparison

The results from the sensitivity analyses are shown from the second column in Figure 65 and Figure 66, for annual O&M cost and time-based availability, respectively. As stated the results from other cost models are extracted from the figures in [188], and these are brought together with the direct statistical results from StraPCost+, as shown in Table 46 and Table 47. The original figures of each cost model in these tables have already been presented in the graphic manner in Figure 65 and Figure 66, and are presented here with clear mean value and difference calculation.

Generally, from these figures and tables, the time-based availability results from StraPCost+ are quite uniform and higher than those from the rest of the cost models for sensitivity analyses with number of technicians, failure rate and heavy-lift vessel

usage, but the sensitivity adjustments of the maintenance categories see uniformity across all the models. In the annual O&M cost estimations, the results from StraPCost+ are generally within the range of the results from the other cost models. On the other hand, the other cost models show rather scattered results for both aspects, especially for fewer technicians and failure rate up in time-based availability sensitivity analyses and more and fewer technicians, failure rate up and down and major replacement only in annual O&M cost sensitivity analyses.

For clear expression of the comparisons, average values of the group of StraPCost+ analyses using the different failure rate sources and average values of the group of all other cost models are listed in Table 46 and Table 47. Also presented are the maximum differences between the highest and the lowest values from the different cost models for each scenario, as shown below:

$$Max\ difference = highest\ value - lowest\ value \tag{89}$$

This difference is equivalent to the value range for each scenario setting in Figure 65 and Figure 66. It helps to assess the degree of dispersion of all results from the cost models. The results from these tables are used in every specific sensitivity analysis, from Section 5.4.3.2.1 to Section 5.4.3.2.4.

Table 46. Time-based availability with all sensitivity scenarios in comparison of the baseline

Time-based availability	baseline	more tech	fewer tech	failure rate down	failure rate up	no HLV	major replacement only	major repair only	medium repair only	minor repair only	manual reset only	annual service only
ECUME	81.0%	84.2%	59.5%	88.0%	69.2%	81.9%	98.5%	99.5%	99.0%	97.0%	93.0%	95.5%
NOWIcob	83.7%	88.5%	66.5%	93.5%	54.4%	88.8%	97.0%	99.5%	99.0%	97.5%	96.0%	99.0%
UiS	84.4%	83.7%	79.0%	92.0%	62.5%	86.5%	96.0%	99.0%	98.5%	97.0%	96.0%	98.5%
OPEX	83.7%	88.4%	34.5%	94.0%	37.5%	86.3%	98.0%	99.0%	98.5%	98.0%	95.0%	98.5%
StraPCost+ OneOverallValue	92.6%	92.6%	92.6%	96.0%	86.0%	94.3%	98.3%	99.7%	99.7%	98.5%	97.1%	99.3%
StraPCost+ Onshore data	92.7%	92.7%	92.7%	96.0%	86.1%	94.4%	98.3%	99.7%	99.7%	98.5%	97.1%	99.3%
StraPCost+ Exp-translated	93.5%	93.5%	93.5%	96.5%	87.7%	95.0%	98.5%	99.8%	99.8%	98.7%	97.5%	99.4%
average of four other model	83.2%	86.2%	59.9%	91.9%	55.9%	85.9%	97.4%	99.3%	98.8%	97.4%	95.0%	97.9%
average of StraPCost+	92.9%	92.9%	92.9%	96.2%	86.6%	94.6%	98.4%	99.7%	99.7%	98.6%	97.2%	99.3%
Max difference	12.5%	9.8%	59.0%	8.5%	50.2%	13.1%	2.5%	0.8%	1.3%	1.7%	4.5%	3.9%

Table 47. Annual O&M cost with all sensitivity scenarios in comparison of the baseline

Annual O&M cost (£m)	base line	more tech	fewer tech	failure rate down	failure rate up	no HLV	major replacement only	major repair only	medium repair only	minor repair only	manual reset only	annual service only
ECUME	14.5	15.8	11.1	10.6	19.9	5.2	14.4	4.1	4.2	4.0	3.7	4.9
NOWIcob	25.1	28.5	23.6	18.3	29.9	5.3	22.0	4.2	3.9	3.7	3.5	4.8
UiS	22.6	18.7	18.5	11.9	22.9	5.2	4.1	2.0	2.4	2.6	3.0	4.1
OPEX	18.0	23.5	20.5	16.0	28.1	4.0	21.5	4.0	3.8	3.6	3.5	3.4
StraPCost+ OneOverallValue	19.7	20.5	18.9	11.8	35.4	7.9	13.4	2.0	2.2	3.0	3.3	3.9
StraPCost+ Onshore data	16.6	17.4	15.8	9.5	30.8	6.5	11.7	1.7	2.2	2.7	3.9	2.4
StraPCost+ Exp-translated	14.9	15.7	14.1	8.5	27.5	5.9	10.5	1.7	2.1	2.6	3.7	2.2
Average of four other model	20.1	21.6	18.4	14.2	25.2	4.9	15.5	3.6	3.6	3.5	3.4	4.3
Average of StraPCost+	17.1	17.9	16.3	9.9	31.2	6.8	11.9	1.8	2.2	2.8	3.6	2.8
Max difference	10.6	12.8	9.4	7.5	15.5	3.9	17.9	2.5	2.1	1.4	0.9	2.7

Table 48 and Table 49 show the percentage change of each sensitivity scenario for time-based availability and annual O&M cost, respectively. The calculation for each cost model result is shown below:

$$Percentage\ change = \frac{scenario\ value - baseline}{baseline} \times 100\% \qquad (90)$$

The percentage change shows the degree of the change of the sensitivity adjustment from the baseline value. The results from these tables are used in every specific sensitivity analysis, from Section 5.4.3.2.1 to Section 5.4.3.2.4.

Table 48. Time-based availability percentage change to baseline of each sensitivity scenario

Time-based availability	more tech	fewer tech	failure rate down	failure rate up	no HLV	major replacement only	major repair only	medium repair only	minor repair only	manual reset only	annual service only
ECUME	4%	-27%	9%	-15%	1%	22%	23%	22%	20%	15%	18%
NOWIcob	6%	-21%	12%	-35%	6%	16%	19%	18%	16%	15%	18%
UiS	-1%	-6%	9%	-26%	2%	14%	17%	17%	15%	14%	17%
OPEX	6%	-59%	12%	-55%	3%	17%	18%	18%	17%	14%	18%
StraPCost+ OneOverallValue	0%	0%	4%	-7%	2%	6%	8%	8%	6%	5%	7%
StraPCost+ Onshore data	0%	0%	4%	-7%	2%	6%	8%	8%	6%	5%	7%
StraPCost+ Exp-translated	0%	0%	3%	-6%	2%	5%	7%	7%	6%	4%	6%

Table 49. Annual O&M cost percentage change to baseline of each sensitivity scenario

Time-based availability	more tech	fewer tech	failure rate down	failure rate up	no HLV	major replacement only	major repair only	medium repair only	minor repair only	manual reset only	annual service only
ECUME	-9%	23%	27%	-37%	64%	1%	72%	71%	72%	74%	66%
NOWIcob	-14%	6%	27%	-19%	79%	12%	83%	84%	85%	86%	81%
UiS	17%	18%	47%	-1%	77%	82%	91%	89%	88%	87%	82%
OPEX	-31%	-14%	11%	-56%	78%	-19%	78%	79%	80%	81%	81%
StraPCost+ OneOverallValue	-4%	4%	40%	-80%	60%	32%	90%	89%	85%	83%	80%
StraPCost+ Onshore data	-5%	5%	43%	-86%	61%	30%	90%	87%	84%	77%	86%
StraPCost+ Exp-translated	-5%	5%	43%	-85%	60%	30%	89%	86%	83%	75%	85%

Table 50 and Table 51 show the impact of the result for each sensitivity scenario setting from the baseline value for time-based availability and annual O&M cost, respectively. This calculation is especially useful for analysing the sensitivity to the different maintenance categories, where only one maintenance category is set for each scenario.

The calculation for each cost model result is shown below. Again, the results from these tables are used in every specific sensitivity analysis, from Section 5.4.3.2.1 to Section 5.4.3.2.4.

$$Impact = \frac{scenario\ value}{baseline} \times 100\% \quad (91)$$

Table 50. Time-based availability impact of each sensitivity scenario

Time-based availability	more tech	fewer tech	failure rate down	failure rate up	no HLV	major replacement only	major repair only	medium repair only	minor repair only	manual reset only	annual service only
ECUME	104.0%	73.5%	108.6%	85.4%	101.1%	121.6%	122.8%	122.2%	119.8%	114.8%	117.9%
NOWIcob	105.7%	79.4%	111.7%	65.0%	106.0%	115.8%	118.8%	118.2%	116.4%	114.6%	118.2%
UiS	99.2%	93.6%	109.0%	74.1%	102.5%	113.7%	117.3%	116.7%	114.9%	113.7%	116.7%
OPEX	105.6%	41.2%	112.3%	44.8%	103.1%	117.1%	118.3%	117.7%	117.1%	113.5%	117.7%
StraPCost+ OneOverallValue	100%	100%	103.7%	92.9%	101.8%	106.2%	107.7%	107.7%	106.4%	104.9%	107.2%
StraPCost+ Onshore data	100%	100%	103.6%	92.9%	101.8%	106.0%	107.6%	107.6%	106.3%	104.7%	107.1%
StraPCost+ Exp-translated	100%	100%	103.2%	93.8%	101.6%	105.3%	106.7%	106.7%	105.6%	104.3%	106.3%

Table 51. Annual O&M cost impact of each sensitivity scenario

Annual O&M cost (£m)	more tech	fewer tech	failure rate down	failure rate up	no HLV	major replacement only	major repair only	medium repair only	minor repair only	manual reset only	annual service only
ECUME	109%	77%	73%	137%	36%	99%	28%	29%	28%	26%	34%
NOWIcob	114%	94%	73%	119%	21%	88%	17%	16%	15%	14%	19%
UiS	83%	82%	53%	101%	23%	18%	9%	11%	12%	13%	18%
OPEX	131%	114%	89%	156%	22%	119%	22%	21%	20%	19%	19%
StraPCost+ OneOverallValue	104%	96%	60%	180%	40%	68%	10%	11%	15%	17%	20%
StraPCost+ Onshore data	105%	95%	57%	186%	39%	70%	10%	13%	16%	23%	14%
StraPCost+ Exp-translated	105%	95%	57%	185%	40%	70%	11%	14%	17%	25%	15%

5.4.3.2.1 Number of Technicians

As shown in Figure 66, Table 46 and Table 48, it can be seen that at current stage, StraPCost+ does not correlate the number of technicians with the time-based availability, while as shown Figure 65, Table 47 and Table 49, the three failure rate input methods have different sensitivity reactions to the annual O&M cost estimation.

The setting of more technicians brings the results from all cost models closer compared to the baseline. Since StraPCost+ has no time-based availability sensitivity with the number of technicians, here compares the results from other cost models relative to

StraPCost+. From Figure 66 and Table 46, the results from other cost models are divided into two groups with a small distance: the results of NOWIcob and OPEX are close to 89%, and the results of ECUME and UiS are close to 84%. The group of results from NOWIcob and OPEX are closer to model results from StraPCost+ with average of 93%. In this sensitivity setting, as shown in Table 46, the difference between the highest value (StraPCost+ exponential translated) and the lowest value (UiS) reduces to 9.8% from the maximum difference of 12.5% in baseline.

In contrast, setting fewer technicians results in a scatter in time-based availability. From Figure 66 and Table 46, UiS shows the highest and the closest value to the results from StraPCost+, with around 79%. The lowest value comes from OPEX, with around 35%. The commercial cost models NOWIcob and ECUME scatter in the middle, relatively closer to the UiS value. In this sensitivity setting, as shown in Table 46, the difference between the highest value (StraPCost+ group) and the lowest value (OPEX) is as large as 59%, 5 times the baseline difference value.

In the annual O&M cost comparison, as shown in Figure 65, Table 47 and Table 49, the degree of dispersion does not change as much as with setting fewer technicians for the time-based availability. In the more technicians setting, the exponential translated StraPCost+ value shows good agreement with the result from ECUME, with around £16m. The onshore original StraPCost+ is slightly higher than the exponential translated, with £17.4m, and lies below the UiS value. The one overall value is just above £20m, and locates below the OPEX value. The maximum difference (NOWIcob, exponential translated StraPCost+) is around £13m. This difference is £2.2m larger than the baseline maximum difference (NOWIcob, ECUME) of just over £10m.

In the fewer technicians setting, all the results from StraPCost+ locate between OPEX and ECUME, with the one overall value result slightly exceeding the UiS result. The maximum difference (NOWIcob, ECUME) is just over £9m. While the degree of fluctuation of StraPCost+ remains the same (£0.8m), the degree of fluctuation of ECUME is around £3m.

Generally speaking, the sensitivity analysis on the number of technicians highlights the different internal calculation algorithms used for each of the cost models. The algorithms tend to provide more uniform time-based availability estimations when there are more technicians, while more scattered estimation results with the decrease of the number of technicians. StraPCost+ shows no sensitivity of time-based availability to the number of technicians which is because calculation of the cost of technicians is simply the multiplication of the single technician results, and the improvement of the interconnection can be put on the agenda in the future work.

In the annual O&M cost perspective, StraPCost+ shows a linear fluctuation along with the adjustment of the number of technicians. This is again because of the simple multiplication calculation of the cost of technicians. Nevertheless, the results from StraPCost+ agree closely with the commercial cost model ECUME and academic model UiS. The cost estimation from the commercial cost models ECUME and NOWIcob drops more dramatically when decreasing than increasing the number of technicians by the same proportion (10), and OPEX has a converse performance pattern. In contrast to a proportional relationship between annual O&M cost estimate and the number of technicians in almost all the cost models, UiS shows insensitivity to the number of technicians.

These sensitivity analyses show that the time-based availability and annual O&M cost estimation of ECUME, NOWIcob and OPEX are various non-linearly interconnected with the number of technicians. However, it is not obvious in real wind farm operation how the number of technicians directly affects the time-based availability and annual O&M cost. This could indicate a further investigation when more real data available.

5.4.3.2.2 Failure rates

From Figure 66, Table 46 and Table 48, it can be seen that the time-based availability estimations from all cost models are quite sensitive to the failure rate. All cost models show an increase of the availability when the failure rates are set lower, and decrease when the failure rates are increased. The changes are not linear.

From Figure 66, all the cost models align quite closely with the maximum difference (StraPCost+ exponential translated, ECUME) of around 8.5% (exact value of availability). This is smaller than the 12.5% maximum difference from the baseline. It shows that when the failure rates decrease, the time-based availability estimations from StraPCost+ are closer to the other cost models, simply because the range is compressed.

When the failure rates are increased, the estimations of all cost models are more scattered. The maximum difference (StraPCost+ exponential translated, OPEX) is over 50% (exact value of availability). OPEX has the highest percentage change of over 55% of the baseline value, which is almost inversely proportional to the doubly increased failure rates. NOWIcob has the second highest increase rate of around 35%, followed by UiS of around 26%. ECUME has the lowest increase rate among the four other cost models, with nearly 15%, which is still higher than the 7.13% from StraPCost+ with one overall value.

As shown in Table 48, among all the cost models, StraPCost+ has relatively low time-based availability sensitivity to failure rates. For StraPCost+ with all failure rate sources, the percentage changes are within 4% for setting the failure rate 50% down, and 7.13% for setting failure rate 100% up (i.e. 200% of the original value). All StraPCost+ results are located closely together in this sensitivity analysis. Other cost models show higher sensitivities. When the failure rates are reduced, the group of NOWIcob and OPEX increase more than 10% from the baseline value, and the group of ECUME and UiS present an increase of just below 10% of the baseline value.

From an annual O&M cost perspective, as shown in Figure 65, Table 47 and Table 49, all cost models present decreased results of different degrees with reduced failure rate. StraPCost+ presents relatively low estimations among all the cost models and the results locate closely around ECUME and UiS. The exponential translated StraPCost+ replaces ECUME presenting the lowest value with £8.5m, followed by the onshore original StraPCost+ with £9.5m. ECUME has the third lowest value with just above £10m. StraPCost+ one overall value method result is £11.8m, which is just below the UiS result value. NOWIcob and OPEX give higher estimations. NOWIcob result remains the highest value among all cost models, with £18.3m, followed by OPEX with £16m.

From the annual O&M cost estimation sensitivity aspect, as shown in Table 49, all StraPCost+ estimations have decreased 40% or more compared with the baseline results, among which the onshore original and exponential translated methods have 43% decrease, and the one overall value has a 40% decrease. This decrease rate can be compared by UiS, which has the largest decrease among all the cost models with over

47%. ECUME and NOWIcob have almost the same decrease of around 27%. OPEX has the lowest decrease of just 11%.

When the failure rates are increased by 100%, StraPCost+ shows dramatic increases in cost of 80% or more. The results from one overall value and onshore original StraPCost+ exceed NOWIcob presenting the highest values, with £35.4m and £30.8m, respectively. The increase rates of the StraPCost+ results are 80% and 86% compared to the baseline, whereas the increase rate of NOWIcob is less than 20%. Even though, as shown in Table 47, NOWIcob still presents the third highest estimation among all cost models, with almost £30m. The results from the exponential translated StraPCost+ and OPEX are similar in this analysis, with around £28m. However, the increase rates are different, with 85% and less than 60%, separately. Different from its dramatic percentage change in the failure rate down case, UiS almost stays the same in the failure rate up case. ECUME remains the lowest estimation of near £20m, with 37% increase.

Generally speaking, the sensitivity analysis for failure rate percentage change highlights the different algorithms related to the failure rates of all cost models. When the failure rates are reduced, the time-based availability estimations from all other cost models tend to be uniform and closer to the results from StraPCost+ than the baseline. This suggests that StraPCost+ has a closer estimation of time-based availability along with the decrease of the failure rates if the four other cost models are treated as the reference. However, when the failure rates are increased, the estimates are scattered. This phenomenon suggests the uncertainty of the time-based availability estimation of all cost models when the failure rates increase.

The sensitivity analysis shows that the annual O&M cost estimations from all StraPCost+ methods are sensitive to the failure rate changing both up and down, and the other cost models show various degree of sensitivity to these changes. More specifically, UiS is sensitive to reducing failure rate, and has no sensitivity to an increased failure rate. OPEX has a low sensitivity to failure rate reduction, and is quite sensitive to increasing failure rate.

5.4.3.2.3 Vessel usage

The results of the sensitivity to vessel use shows closer agreement between StraPCost+ and some of the other cost models in both the time-based availability and annual O&M cost perspectives.

For the time-based availability perspective, as shown in Figure 66 and Table 46, the results from StraPCost+ with all failure rate resources remain close, with an average value of 94.57%. This value is closer to the results from NOWIcob, UiS and OPEX, and slightly further to ECUME than the baseline. The maximum difference (Exponential translated StraPCost+, ECUME) is about 13%.

For all cost models the increase rates for this change are not significant. As shown in Table 48, all StraPCost+ results have around a 2% increases. This rate is similar to the increased rates from UiS and OPEX. ECUME has the lowest increase, with only around 1%. NOWIcob has the highest increase at around 6%.

For the annual O&M cost perspective, as shown in Figure 65 and Table 47, results from StraPCost+ with an average value of £6.77m locate much closer to each other and other cost models than the baseline. In contrast to the relatively low estimations in

the baseline, results from StraPCost+ show higher estimations than other cost models. The highest estimation comes from StraPCost+ **(**using one overall failure rate value) with £7.9m, and the maximum difference with the lowest estimation model OPEX is £3.9m. This value is much smaller than the £10m maximum difference from the baseline. The differences between the other cost models and the average value from StraPCost+ are less than £3m.

All cost models show a high sensitivity to this adjustment, as shown in Table 49, with an over 60% decrease compared to the baseline. The decreased values from StraPCost+ for all three failure rate sources are between 60% and 61%. This decrease degree is similar to ECUME. NOWIcob, UiS and OPEX have decrease degree around 78%.

This sensitivity analysis shows that all cost models have similar sensitivity to the HLV usage for both time-based availability and annual O&M cost estimations, and it shows that all the cost models tend to have close estimates, especially on the annual O&M cost without HLV usage.

5.4.3.2.4 Maintenance categories

Time-based availability sees high uniform from all cost models in this analysis. As shown in Figure 66 and Table 46, the highest maximum difference of 4.5% comes from the manual reset only, for the translated failure rate version of StraPCost+ and ECUME presenting the highest and lowest estimates respectively. Annual service has the second highest maximum difference (translated StraPCost+, ECUME) of near 4%. This difference value is followed by major replacement of 2.5%, with the translated StraPCost+ and ECUME presenting the equally highest values and UiS presenting the

lowest estimate. The remaining three give less than 2%, among which major repair only has less than 1%, with translated StraPCost+ presenting the highest and UiS and OPEX equally the lowest. The differences are much smaller than for the baseline which has a maximum difference of 12.5%.

All of the settings see the average time-based availability estimates over 95%, among which major repair and medium repair are over 99% and 98.5%, respectively. These results suggest that requirements for major repair and medium repair have the least impact on dragging down the wind farm time-based availability, followed by annual service (except ECUME). As shown in Table 50, manual reset seems to have the lowest impact among the 6 maintenance adjustments on increasing the overall availability for all cost models.

The maintenance category sensitivity rates of all the other cost models are higher than the rates from StraPCost+. StraPCost+, as shown in Table 48, with all three failure rate sources shows similar increase degrees with an average of 6%; whereas other models show an average increase degree of around 17%.

From the cost perspective, as shown in Figure 65 and Table 47, all maintenance category adjustments bring the annual O&M cost estimates from all cost models much closer together than the baseline except for major replacement. Compared to the baseline, major replacement only has a distinctly different impact on each of the cost models: all cost models show decreased costs except for OPEX. The results from StraPCost+ are closely grouped (with £13.4m, £11.7m and £10.5m for one overall value, onshore original and translated methods, respectively). The degrees of decrease are close as well, as shown in Table 49, with 32%, 30% and 30% in the stated order.

This group of results is located in between of ECUME and UiS. ECUME stays at almost the same value as for the baseline, with the lowest rate responding to this setting; whereas UiS has a dramatic 82% decrease from its baseline value, which brings the estimate below £5m. NOWIcob has a moderate decrease of around 12% to £22m. In contrast to all the other models, OPEX has a noticeable increase of almost 20% which brings the estimation up to around £22m, close to NOWIcob. This result is not logically correct, and thus OPEX, which is still at the development stage, cannot be fully trusted in this particular regard.

All other maintenance categories have lower impact on the overall annual O&M costs. As shown in Table 51, the highest impact comes from the translated StraPCost+ with manual reset, at 25% of the baseline cost. The average result from the last five scenarios is 15.6% for StraPCost+ using all failure rate sources. All StraPCost+ results are highly uniform, especially for major repair only, medium repair only and minor repair only.

The results from StraPCost+ are much closer to the other cost models. The highest difference between the average value of StraPCost+ and the average value of the other four cost model results is £1.8m which is for major repair only. Manual reset only has the lowest difference value, with only £0.2m between the two groups.

This sensitivity analysis shows that for one single maintenance category taken on its own; all cost models tend to present high degree of agreement regarding the time-based availability estimation. All maintenance categories show little impact on lowering the time-based availability for all cost models. This demonstrates that major replacement is the main cause of the annual O&M cost for the majority of the cost

models in this thesis (as might be expected), especially for ECUME, whose major replacement cost accounts for almost all the overall annual O&M cost. UiS model, however, shows only around 18% impact with a dramatic 82% drop of the value on the major replacement only assumption. This shows that the sensitivity to major replacement costs for all StraPCost+ methods are reasonably consistent with the range for the other cost models except OPEX which is not reliable in this instance.

5.4.4 Conclusion

This section has presented sensitivity comparisons between the improved model, StraPCost+, with three failure rate input assumptions and the other cost models mainly reviewed in Section 5.2. This section not only compares the baseline setting for all cost models selected, but also presents the sensitivity to: number of technicians; failure rate assumption; vessel usage and maintenance categories. Because of lack of data, this section mainly focuses on the analyses of the time-based availability and annual O&M cost from an existing cross-check literature. Since there is no actual O&M data available, analyses were undertaken to identify for which scenarios the results from specific cost models can be treated as a reference, and the cases for which particular other cost models are not reliable.

The analyses on the time-based availability show that the results from StraPCost+ with all failure rate resources closely locate with each other and generally higher than the results from other cost models. Specifically, more number of technicians brings the availability estimation from other cost models closer to that of StraPCost+, and fewer number of technicians changes the estimation of other cost models dramatically. Decreasing the failure rate brings the results from all cost models together and higher

than their baseline values, whereas increasing the failure rate lowers and separates the results. For the most important vessel usage of HLV, the time-based availability shows little impact from all cost models. All maintenance category settings have little impact on bringing the availability down, especially for major repair and medium repair.

The analyses on the annual O&M cost show that the results from StraPCost+ with all failure rate resources generally locate in the lower range of the results from other cost models. For adjusting the number of technicians and the failure rate each cost model has different sensitivity reflected on the cost estimation. Generally, the estimation from StraPCost+ are close to the commercial cost model ECUME, except the increase of failure rate makes the results from StraPCost+ closer to the results from the other commercial cost model NOWIcob which constantly shows a relatively high estimation on the annual O&M cost. The sensitivity analysis on HLV reveals the low impact for HLV on the O&M cost estimation of all cost models. Apart from major replacement, all maintenance categories show low impact on the O&M cost estimation. For the major replacement only setting, except UiS, all cost models present high result values which suggest the major replacement takes account the majority of the entire annual O&M cost.

From the annual O&M cost baseline and sensitivity analyses, the exponential translated method tends to produce the lowest value among the three different method of StraPCost+ which is closer to the results from ECUME. The results meet the expectation of improving the accuracy of StraPCost+ by using the exponential translated failure rate.

This section shows that StraPCost+ produces reasonable estimations compared with other cost models for O&M cost, but further improvement including better interconnection of the number of technicians with the entire model is expected to be done in future work.

For further investigation of the validation of the translation improved StraPCost+, condition monitoring system detection effectiveness analyses are presented in Section 5.5 and a series of sensitivity analyses are presented in Section 5.6.

5.5 Condition monitoring system detection effectiveness analyses on StraPCost+

As stated in previous sections, one of the innovations of StraPCost+ is its emphasis on condition monitoring (CM) system effectiveness, not only in the module of condition-based maintenance categories, but also through an assessment of the dependency of O&M performance on the detection effectiveness of the CM system.

In this section, analyses are focused on condition based maintenance based on the same settings introduced in Section 5.4, i.e. the FINO virtual wind farm settings, using the translation improved StraPCost+, i.e. Method 3 in Section 5.4. To establish more generic results and minimise the impact of one specific wind farm, this analysis compares the levelised cost model outputs at wind turbine level. Outputs selected from StraPCost+ to be compared in this section are wind turbine availability, capacity factor with downtime, annual maintenance cost per turbine, total O&M cost (without revenue loss) per kWh per turbine and revenue loss per kWh per turbine. As improvements, the expansion of maintenance categories and the corresponding formulae of StraPCost+ follow the discussion in Section 5.3.

Further sensitivity analyses focusing the changes due to condition-based maintenance in comparison of reactive maintenance with eight sensitivity aspects have been undertaken and are presented in Section 5.6.

5.5.1 Comparison scenarios

Since CM detection sensitivity adjustment has been effectively integrated in StraPCost+, as discussed in Section 5.3.2, the comparison at the wind turbine level can

be realised by adjusting the total percentages of each of the three CM detection coefficients, *edet, epre* and *efalse*, for CM detection parameters, *detectability*, *pre-empt* (i.e. advance warning of failure) and *falsepos* (i.e. false positive) respectively, as shown in Table 33 in Section 5.3.2.

At this stage, the scientific control variable method is applied to derive the sensitivity. The coefficient adjustment of *detectability*, *pre-empt* and *false-positive* are set separately from -50% to 50% in steps of 10%. While adjusting one effectiveness coefficient, the others remain constant at the base case values (i.e. 0% adjustment).

This analysis starts with the attempt of using regime 1 which is modified from Eq. 43 as described in Section 5.3.2, where the assumed false positive rate only affects the lightest maintenance category *Es* (was *Ds* in Eq. 43) transferred from the heavier reactive maintenance categories, *Au* (major replacement), *Cu* (major repair), *Du* (medium repair) and *Eu* (manual reset), as shown below:

$$E_S = E_U \cdot detectability + D_U \cdot preempt + (A_U + C_U + D_U + E_U) \cdot falsepos \quad (92)$$

The results are shown in Appendix-B Table 2b and Figure 3b. With this attempt of regime 1, the number of decimal places used in Table 2b are limited for easily-reading: 1 decimal place for *availability*, *capacity factor* and *annual maintenance cost*, and 4 decimal places for t*otal O&M cost* and *revenue loss* for the fact that the significant figures from those two columns start from the second or third decimal places. However, even with 4-decimal-place resolution, the graphs in Table 3b which are plot based on Table 2b show rough steps in the curve, and in almost every graph, the value of *falsepos* stays unchanged, which indicates insufficient accuracy with the resolution in the corresponding columns in Table 2b.

As stated in Section 5.3.2, this regime cannot reasonably describe the reality where the falsepos has at least two levels of impacts. According to the actual operational experience from the offshore wind farm R&D team, when a major fault (mainly the major replacement *Au* and major repair *Bu*) alarm is triggered, the maintenance team will send enough number of technicians with relatively long checking time (longer than the manual reset *Eu*), which matches the maintenance category *Du*; and the lighter fault alarm only results in the level of technician and vessel usage equivalent to the manual reset *Eu*. The finally selected maintenance category regime shows impact of falsepos for both *Ds* and *Es*, with *Ds* transferred from *Au* and *Bu*, and *Es* transferred from *Cu*, *Du* and *Eu*.

The formulae of this regime are shown in Eq. 81 and Eq. 82 in Section 5.3.2, and are extracted with modification as below:

$$D_S = D_U \cdot detectability + C_U \cdot preempt + (A_U + B_U) \cdot falsepos \quad (81)$$

$$E_S = E_U \cdot detectability + D_U \cdot preempt + (C_U + D_U + E_U) \cdot falsepos \quad (82)$$

For enhancing the accuracy and smoothing the curves, more decimal places are taken for these values until there are no unchanged values between the neighbour adjustments. To make values with less decimal places, the unit of total O&M cost and revenue loss are also changed from pound (£) to pence (p). This change results in 3 decimal places for all 3 types of CM detection adjustments with availability and annual maintenance cost, and the adjustment of *detectability* and *pre-empt* with capacity factor and total O&M cost. It takes 4 decimal places for capacity factor and total O&M cost to see the results for the adjustment of the false positive sensitivity analysis. The revenue loss values have lower order of magnitude; therefore, more decimal places are

building during the test in order to avoid repeating values between neighbour adjustments: 4 significant figures are taken for the adjustments of *detectability* and *pre-empt*, with 7 decimal places, and 5 significant figures are taken for the adjustments of *falsepos*, with 8 decimal places in presentation.

Along with the analysis of the exact value, it is more important to compare the percentage changes in comparison of the 0% adjustment value. In this way, it enables the comparison not only within one selected cost model parameter, but also comparison between different factors. The equation is shown below:

$$Percentage\ change = \frac{adjusted\ value\ (x\%) - original\ value(0\%)}{original\ value\ (0\%)} \times 100\% \qquad (93)$$

Since CM detections only affect the results in the condition-based maintenance, this section compares the percentage change of the condition-based maintenance values; whereas in the next section, wider sensitivity analyses are undertaken for the result changes due to the application of condition-based maintenance in comparison of the reactive maintenance.

5.5.2 Results and discussion

Table 52 shows the percentage change to each value to the selected cost model results in comparison of the baseline (i.e. 0% adjustment) of the CM detection effectiveness with the stated three comparison adjustment scenarios. The exact values are shown in Appendix-B Table 3b and Table 4b.

Table 52. Percentage changes in comparison of 0% adjustment (baseline) of CM detection effectiveness sensitivity analysis with regime transferring falsepos from maintenance category A to E into D and E in condition-based maintenance; baseline figures given in the top row.

Detectability	Pre-empt	Falsepos	Availability	Capacity factor with downtime	Annual maintenance cost per turbine	Total O&M cost (without revenue loss) per kwh per turbine	Revenue loss per kwh per turbine
0%	0%	0%	94.43%	46.51%	144.90(£k)	1.21(p)	0.77(p)
-50%	0%	0%	-0.40%	-0.67%	5.02%	5.01%	7.94%
-40%	0%	0%	-0.32%	-0.54%	4.01%	4.02%	6.36%
-30%	0%	0%	-0.24%	-0.40%	3.01%	3.02%	4.77%
-20%	0%	0%	-0.16%	-0.27%	2.01%	2.03%	3.17%
-10%	0%	0%	-0.08%	-0.13%	1.00%	1.03%	1.59%
0%	0%	0%	0.00%	0.00%	0.00%	0.03%	0.00%
10%	0%	0%	0.08%	0.13%	-1.00%	-0.96%	-1.58%
20%	0%	0%	0.16%	0.27%	-2.01%	-2.04%	-3.18%
30%	0%	0%	0.24%	0.40%	-3.01%	-3.04%	-4.77%
40%	0%	0%	0.32%	0.53%	-4.01%	-4.03%	-6.35%
50%	0%	0%	0.40%	0.67%	-5.02%	-5.03%	-7.95%
0%	-50%	0%	-0.09%	-0.13%	2.43%	2.44%	1.48%
0%	-40%	0%	-0.07%	-0.10%	1.95%	1.94%	1.18%
0%	-30%	0%	-0.05%	-0.08%	1.46%	1.44%	0.89%
0%	-20%	0%	-0.03%	-0.05%	0.97%	0.95%	0.60%
0%	-10%	0%	-0.02%	-0.02%	0.49%	0.53%	0.30%
0%	0%	0%	0.00%	0.00%	0.00%	0.03%	0.00%
0%	10%	0%	0.02%	0.03%	-0.49%	-0.46%	-0.30%
0%	20%	0%	0.03%	0.05%	-0.97%	-0.96%	-0.60%
0%	30%	0%	0.05%	0.07%	-1.46%	-1.46%	-0.89%
0%	40%	0%	0.07%	0.10%	-1.95%	-1.96%	-1.19%
0%	50%	0%	0.09%	0.12%	-2.43%	-2.46%	-1.48%
0%	0%	-50%	0.0064%	0.0032%	-0.252%	-0.25%	-0.0364%
0%	0%	-40%	0.0053%	0.0026%	-0.202%	-0.20%	-0.0299%
0%	0%	-30%	0.0032%	0.0019%	-0.151%	-0.15%	-0.0221%
0%	0%	-20%	0.0021%	0.0013%	-0.101%	-0.10%	-0.0143%
0%	0%	-10%	0.0011%	0.0006%	-0.050%	-0.05%	-0.0065%
0%	0%	0%	0.0000%	0.0000%	0.000%	0.00%	0.0000%
0%	0%	10%	-0.0011%	-0.0006%	0.050%	0.06%	0.0078%
0%	0%	20%	-0.0021%	-0.0013%	0.101%	0.11%	0.0156%
0%	0%	30%	-0.0032%	-0.0019%	0.151%	0.16%	0.0234%
0%	0%	40%	-0.0042%	-0.0026%	0.202%	0.21%	0.0299%
0%	0%	50%	-0.0053%	-0.0032%	0.252%	0.26%	0.0377%

For better comparison, figures presenting each result item with the three CM detection adjustments are shown from Figure 67 to Figure 71. The legends are the same as in Figure 67.

After the enhancement of the resolution as discussed above and the re-setting of the scheduled maintenance regime, it can be seen that all selected comparison items present smooth curves. These figures indicate small sensitivity to *falsepos* rate in

comparison of *detectability* and *pre-empt*. The small sensitivity to *falsepos* rate is improved from the maintenance category regime 1 but still seems too optimistic, considering *falsepos* has a negative impact on CM system performance and should be minimised.

The curves in Figure 67 to Figure 71 show almost linear changes of the selected parameter as a function of the percentage variation of CM detection. In order to show a straightforward view of the gradient comparison, all figures from Figure 67 to Figure 71 have a zoomed-in graph showing ±0.5% around the 0% adjustment points, with vertical axis resolution in step of 0.1%, presented at the right-hand side next to the full scale graphs. Since the functions are considered linear, they have been fitted by least squares in order to calculate the gradient. Table 53 lists the calculated gradient for each parameter. Because of the small-value nature of the figures and their different order of magnitudes, all the gradient values are given to 3 significant figures.

Figure 4b follows the linear pattern and is magnified in a similar manner with resolution of step of 0.02 (for whatever unit) in exact value. Table 4b lists the gradients calculated from Table 4b.

The absolute value of the gradient shows positive correlation of the selected result sensitivity to the corresponding CM detection effectiveness, i.e. the higher the absolute gradient value is, the more sensitive the result is towards the corresponding CM detection effectiveness. From Figure 67 to Figure 71, all selected results show steadily increasing gradients and the highest sensitivity with *detectability*.

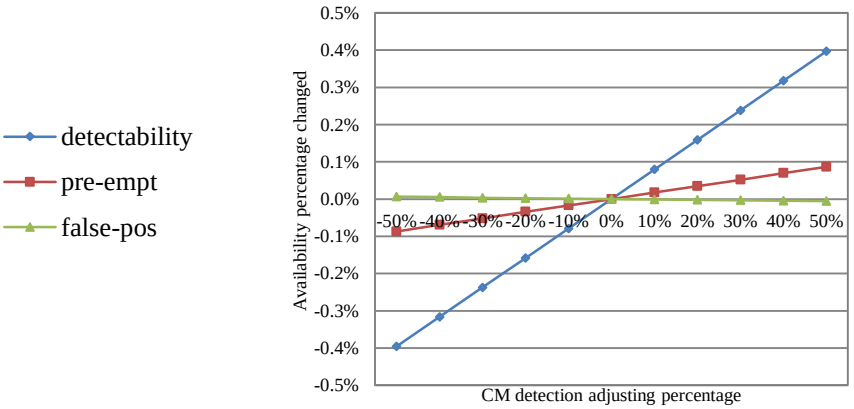

Figure 67. CM detection effectiveness sensitivity in percentage change of condition-based maintenance on availability with full scale in step of 0.1%

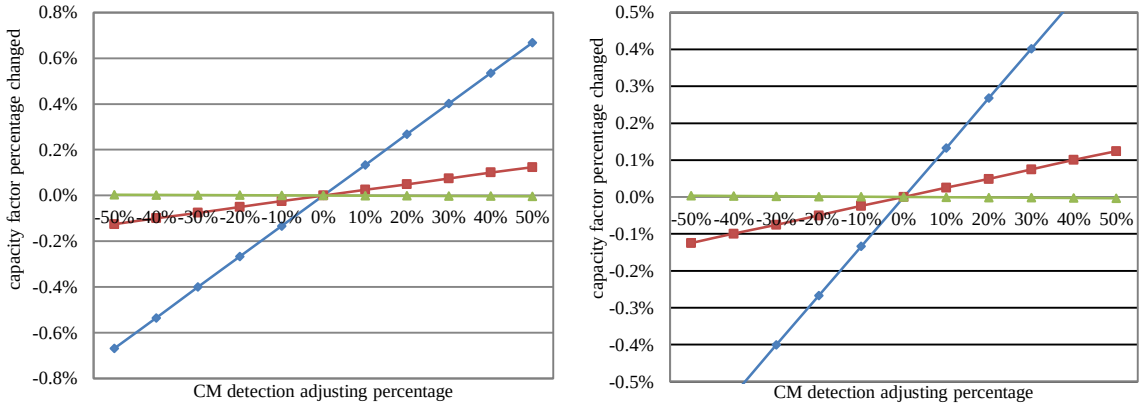

Figure 68. CM detection effectiveness sensitivity in percentage change of condition-based maintenance *on capacity factor with full scale and zoom-in in step of 0.1% (left) (right)*

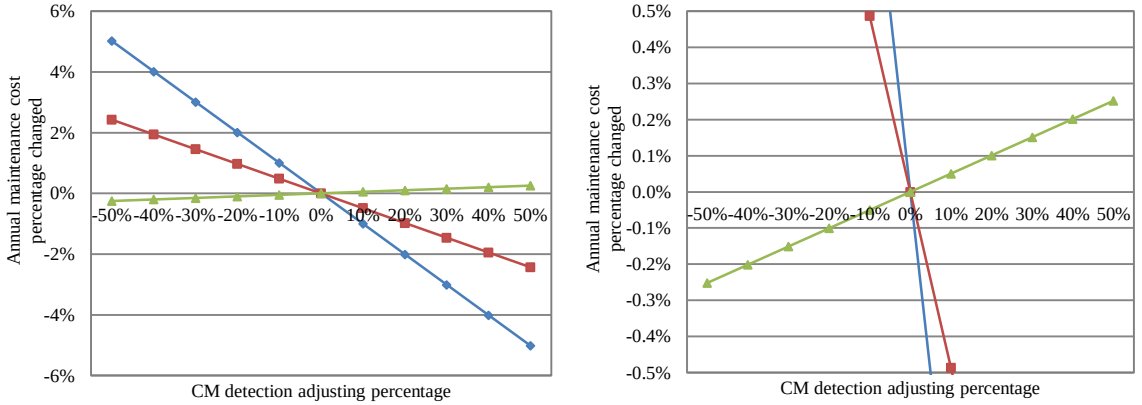

Figure 69. CM detection effectiveness sensitivity in percentage change of condition-based maintenance on annual maintenance cost per turbine with full scale (left) and zoom-in in step of 0.1% (right)

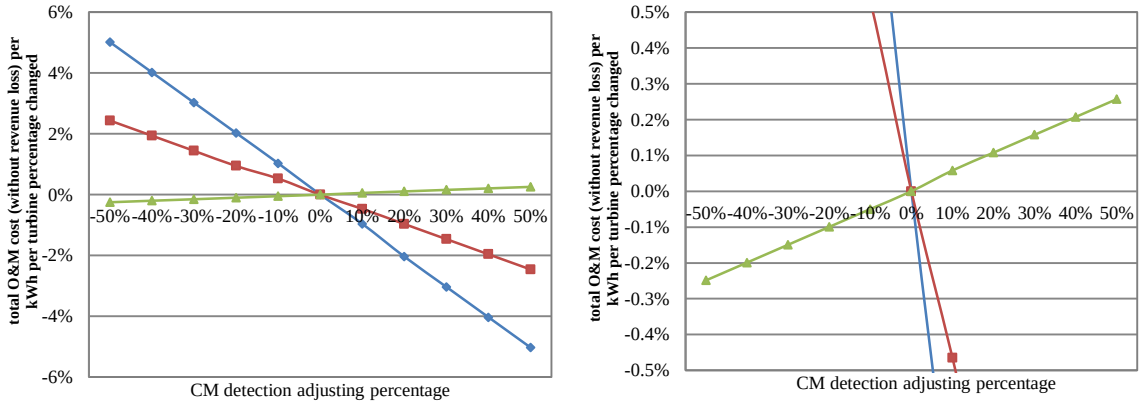

Figure 70. CM detection effectiveness sensitivity in percentage change of condition-based maintenance on total O&M cost (without revenue loss) per kWh per turbine with full scale (left) and zoom-in in step of 0.1% (right)

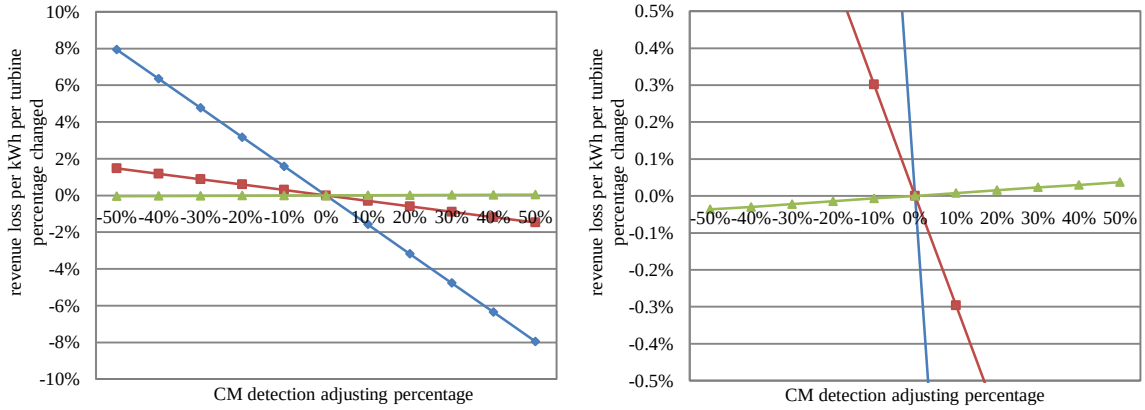

Figure 71. CM detection effectiveness sensitivity in percentage change of condition-based maintenance on revenue loss per kWh per turbine with full scale (left) and zoom-in in step of 0.1% (right)

All the selected results show the lowest sensitivity to the *falsepos* rate variation. The trends of sensitivity to *detectability* and *pre-empt* are in the same direction, while the trends of *falsepos* are in the opposite direction. As mentioned, this phenomenon can be easily understood as the *detectability* and *pre-empt* having a positive impact on the wind turbine system and thus are expected to be enhanced, while *falsepos* have a negative impact on the system and should be minimised.

Among the sensitivity of the five results, availability and capacity factor show positive correlation with *detectability* and *pre-empt* adjustment and negative correlation with

falsepos variation, while the remaining three selected cost model results show negative correlation with *detectability* and *pre-empt* adjustment and the positive correlation with the *falsepos* adjustment. This phenomenon can be understood as the availability and capacity factor show wind turbine operational performance and are expected to be maximized, while the remaining three selected results show cost performance which are expected to be minimized. The CM *detectability* and *pre-empt* are designed to improve the wind turbine performance that are expected to be maximized, while *falsepos* has the opposite effect.

It can be seen that the same detection sensitivity fits in Figure 69 and Figure 70 have very similar trends. Table 53 confirms the values of the gradients are very close (differences only shown after the second or third decimal places). Even though there are significant differences between the two selected cost model results in their exact values in Figure 4b, it shows that the algorithm in StraPCost+ highly correlates the change of the annual maintenance cost and the total O&M cost. Although among the exact value figures in Figure 4b the annual maintenance cost has the steepest curves, and revenue loss has the most gradual curves for all three detection adjustments, the corresponding parameters do not have the steepest and most gradual curves in the percentage change figures in Figure 69 and Figure 70. In fact, revenue loss is the most sensitive to *detectability* among all the sensitivity curves.

According to Table 53, among all the absolute values of the gradients, the impact of *falsepos* on capacity factor shows the lowest gradient with 0.0000745, and *detectability* impact on revenue loss shows the highest gradient with -0.159. The steepest trends for the sensitivity to *pre-empt* and *falsepos* both occur in total O&M

cost, with –0.0488 and 0.00509, respectively. The most gradual trends of *detectability* and *pre-empt* both occur for availability, with 0.00793 and 0.00173, separately.

The orders of the magnitudes of the gradient values vary across a wide range. The values of the gradients of *detectability* and *pre-empt* can have difference of less than 10 times with the same sign, while those between *detectability* and *falsepos* can be in hundreds of times with opposite signs. The multiples between *pre-empt* and *falsepos* can be tens also with opposite signs. More specifically, *detectability* can have a sensitivity from 2.07 (total O&M cost) to 5.36 (capacity factor) times the number of *pre-empt* and from -19.8 (total O&M cost) to -213.2 (revenue loss) times the number of *falsepos*. The multiples between *pre-empt* and *falsepos* vary from -9.57 (total O&M cost) to -39.83 (revenue loss). This phenomenon shows the close value difference and positive correlation between the sensitivity of the selected cost model results to *detectability* and to *pre-empt*, and the large value difference and negative correlation between that to *detectability* (and *pre-empt*) and to *falsepos*.

Since availability and capacity factor have the same nature of showing the wind turbine operational performance and have the same trend orientation with the same CM detection adjustments, and the remaining three selected cost model results have the same nature of showing the cost performance with same trend orientation, they can be divided and compared in two groups. The gradient values in capacity factor are 1.69, 1.44 and 0.56 times for availability, with *detectability*, *pre-empt* and *falsepos*, respectively.

While having comparison of each parameter in Table 53, revenue loss which has the highest absolute gradient value (-0.159) against *detectability* adjustment is around 1.58

times the number of both annual maintenance cost (-0.100) and total O&M cost (-0.101). Total O&M cost which has the highest absolute gradient value (-0.0488) for *pre-empt* adjustment is almost as same as annual maintenance cost (-0.0486) and 1.64 times the number of revenue loss (-0.0297). Total O&M cost which has the highest gradient value against *falsepos* (0.00509) is almost as same as annual maintenance cost (0.00504) and 6.83 times the number of revenue loss (0.000745). From these figures, the percentage changes are quite similar with the same CM detection adjustment among the selected cost model results with the same trend group (horizontal in the table), different from the wide range of the three CM detection variables with the same cost model parameters (vertical in the table).

Table 53. Curve gradients of the selected cost model results with detectability, pre-empt and falsepos in percentage changes (%) from Figure 67 to Figure 71.

Adjustment	Availability	Capacity factor with downtime	Annual maintenance cost per turbine	Total O&M cost (without revenue loss) per kWh per turbine	Revenue loss per kWh per turbine
Detectability	0.00793	0.013	-0.100	-0.101	-0.159
Pre-empt	0.00173	0.00250	-0.0486	-0.0488	-0.0297
Falsepos	-0.000115	-0.0000645	0.00504	0.00509	0.000745

5.5.3 Conclusion

This section has presented CM detection effectiveness sensitivity analyses for StraPCost+ at the wind turbine level. It gives a high level view of the impact of the CM system detection effectiveness. It lists the corresponding values of five selected main results for StraPCost+ covering the three CM detection variables This section has compared the percentage changes for the five selected cost model results with zoomed-in graphs.

The analyses show that the cost model results are the most sensitive to *detectability* and least sensitive to the false positive rates. Among the five selected cost model results, the availability and capacity factor have a positive correlation, while the remainder of the three cost model results have negative correlation.

Annual maintenance cost and total O&M cost have been shown to be highly correlated according to the StraPCost+ algorithm. According to these analyses, the influence of the false positive rate in the current cost model is quite low, and this is perhaps too optimistic. In the future, detailed analyses applying to each subsystem and each type of CM system might be undertaken, and a further improvement of the algorithm including having more realistic *false-positive* effectiveness to the system might also be undertaken.

This condition monitoring detection effectiveness analysis methodology has also provided an indicative train of thought to complete the FMEA RPN calculation as the *detectability* in RPN [O,S,D] method. This requires more accessible condition monitoring data for each component in the future.

For a deeper validation of StraPCost+, a series of sensitivity analyses in addition to the CM detection effectiveness have been undertaken and presented in Section 5.6.

5.6 StraPCost+ Sensitivity analyses

This section follows Section 5.5 and expands the sensitivity analysis of StraPCost+ with the exponential translation method using the same wind farm (FINO) input settings. In this section, eight sensitivity parameters are analysed and compared including the three CM detection parameters introduced in Section 5.5. The parameters added in this section are the wind and wave parameters, the weather window threshold for heavy maintenance (*A* and *B*), the weather window threshold for light maintenance (*C*, *D* and *E*), overall turbine annual failure rate and distance to shore. The first four key model parameters are varied from their base case values from -50% to 50% in steps of 10%. Distance to shore is varied from 10km up to 150km, which is from -80% to 200% from its base case (50km) in step of 20% (10km) reflecting the diversity of this parameter for proposed offshore wind farms. The different scales make the comparison figures difficult to read. To solve this problem, a zoomed-in scheme is applied for both x and y axis.

In the previous section, since CM detection parameters only affect the condition-based maintenance, the results compared in section 5.5 are only from the condition-based maintenance; while in this section, the expanded parameters affect both reactive and condition-based maintenance, and the results compared are the percentage difference due to the application of condition-based maintenance in comparison of reactive maintenance, as shown below:

$$Difference\ due\ to\ CM = \frac{condition\ based\ maintenance\ -\ reactive\ maintenance}{reactive\ maintenance} \times 100\% \quad (94)$$

5.6.1 Parameters assessed for sensitivity

This section uses the entire wind turbine level sensitivity percentage adjustment coefficients in StraPCost+ that have been introduced in Section 5.3.7. Scientific control variable method is applied to the adjustments and the comparisons are presented for the percentage changes calculated in the way stated in the previous section. That is to say, this section compares the percentage changes (in comparison of 0% adjustment) of the percentage difference due to the application of condition-based maintenance, i.e. the percentage of the percentage, as shown is listed below:

$$Percentage\ change = \frac{change\ due\ to\ CM\ (x\%) - change\ due\ to\ CM\ (0\%)}{change\ due\ to\ CM\ (0\%)} \times 100\% \quad (95)$$

As discussed in Section 5.3.7, the wind and wave parameter percentage adjustment coefficients are linked. The wave Weibull parameters adjusted are only the wave location and scale parameter; and since the wind location parameter is set to be 0 all the time, the adjustment only applies to the wind scale parameter. The maintenance category adjustments focus on the weather window threshold, *kthr*, for the heavy and light maintenances. The coefficient for the total turbine annual failure rate percentage adjustment is in reference to the default overall failure rate value. The percentage adjustment is also applied to distance to shore from base case values.

5.6.2 Results and discussion

Selected results in percentage changes are shown in Table 54, and the original percentage difference values due to condition-based maintenance are shown in Table 5b in the Appendix-B. For its particularity, distance to shore is listed after the first seven parameters.

Table 54. Percentage change in comparison of 0% adjustment of StraPCost+ sensitivity analysis for the ratio of difference due to condition-based maintenance to reactive maintenance; baseline figures given in the top row.

Adjustment		Availability	Capacity factor with downtime	Annual maintenance cost per turbine	Total O&M cost (without revenue loss) per kWh per turbine	Revenue loss per kWh per turbine
Baseline value	0%	0.96%	1.61%	-12.58%	-12.58%	-15.81%
Wind and wave parameters	-50%	-63.54%	-65.22%	-71.78%	-71.78%	-14.55%
	-40%	-57.29%	-52.80%	-60.41%	-60.41%	-7.91%
	-30%	-46.88%	-40.37%	-45.23%	-45.23%	-4.11%
	-20%	-34.38%	-27.33%	-29.09%	-29.09%	-2.02%
	-10%	-18.75%	-14.29%	-13.75%	-13.75%	-0.76%
	0%	**0.00%**	**0.00%**	**0.00%**	**0.00%**	**0.00%**
	10%	22.92%	14.91%	12.00%	12.00%	0.63%
	20%	48.96%	31.68%	22.18%	22.18%	1.14%
	30%	80.21%	50.93%	30.52%	30.52%	1.71%
	40%	118.75%	73.91%	37.28%	37.28%	2.40%
	50%	166.67%	103.73%	42.53%	42.53%	3.29%
Weather window threshold for heavy maintenance (*A* and *B*)	-50%	691.67%	560.87%	54.69%	54.69%	18.53%
	-40%	163.54%	135.40%	49.44%	49.44%	12.21%
	-30%	67.71%	59.01%	39.67%	39.67%	7.78%
	-20%	31.25%	28.57%	26.87%	26.87%	4.62%
	-10%	12.50%	11.18%	13.12%	13.12%	2.15%
	0%	**0.00%**	**0.00%**	**0.00%**	**0.00%**	**0.00%**
	10%	-7.29%	-8.70%	-11.69%	-11.69%	-1.90%
	20%	-12.50%	-15.53%	-21.70%	-21.70%	-3.67%
	30%	-16.67%	-20.50%	-30.13%	-30.13%	-5.06%
	40%	-19.79%	-24.22%	-37.04%	-37.04%	-6.26%
	50%	-22.92%	-26.71%	-42.61%	-42.61%	-7.21%
Weather window threshold for light maintenance (*C*, *D* and *E*)	-50%	175.00%	147.20%	4.69%	4.69%	-2.78%
	-40%	102.08%	90.68%	3.18%	3.18%	-2.09%
	-30%	59.38%	55.28%	2.07%	2.07%	-1.45%
	-20%	32.29%	31.68%	1.19%	1.19%	-0.89%
	-10%	13.54%	13.66%	0.56%	0.56%	-0.38%
	0%	**0.00%**	**0.00%**	**0.00%**	**0.00%**	**0.00%**
	10%	-9.38%	-11.18%	-0.40%	-0.40%	0.32%
	20%	-15.63%	-19.88%	-0.72%	-0.72%	0.57%
	30%	-21.88%	-26.71%	-0.95%	-0.95%	0.76%
	40%	-25.00%	-31.68%	-1.11%	-1.11%	0.95%
	50%	-28.13%	-35.40%	-1.27%	-1.27%	1.08%
Default overall failure rate	-50%	-51.04%	-52.80%	0.00%	0.00%	0.00%
	-40%	-41.67%	-42.24%	0.00%	0.00%	0.00%
	-30%	-31.25%	-32.30%	0.00%	0.00%	0.00%
	-20%	-20.83%	-21.74%	0.00%	0.00%	0.00%
	-10%	-10.42%	-11.18%	0.00%	0.00%	0.00%
	0%	**0.00%**	**0.00%**	**0.00%**	**0.00%**	**0.00%**
	10%	11.46%	10.56%	0.00%	0.00%	0.00%
	20%	21.88%	22.36%	0.00%	0.00%	0.00%
	30%	33.33%	33.54%	0.00%	0.00%	0.00%
	40%	44.79%	45.34%	0.00%	0.00%	0.00%
	50%	56.25%	57.76%	0.00%	0.00%	0.00%
CM Detectability	-50%	-41.46%	-42.33%	-34.85%	-34.83%	-42.28%
	-40%	-33.15%	-33.90%	-27.88%	-27.91%	-33.84%
	-30%	-24.83%	-25.33%	-20.91%	-20.99%	-25.40%
	-20%	-16.63%	-16.89%	-13.94%	-14.07%	-16.89%
	-10%	-8.31%	-8.46%	-6.97%	-7.15%	-8.45%
	0%	**0.00%**	**0.00%**	**0.00%**	**0.00%**	**0.00%**
	10%	8.31%	8.41%	6.97%	6.69%	8.43%
	20%	16.63%	16.97%	13.94%	14.18%	16.93%

	30%	24.94%	25.41%	20.91%	21.10%	25.37%
	40%	33.26%	33.84%	27.88%	28.02%	33.81%
	50%	41.57%	42.27%	34.85%	34.94%	42.32%
CM Pre-empt	-50%	-9.09%	-7.92%	-16.90%	-16.95%	-7.90%
	-40%	-7.21%	-6.28%	-13.52%	-13.49%	-6.31%
	-30%	-5.43%	-4.79%	-10.14%	-10.03%	-4.72%
	-20%	-3.55%	-3.16%	-6.76%	-6.57%	-3.20%
	-10%	-1.77%	-1.52%	-3.38%	-3.69%	-1.60%
	0%	**0.00%**	**0.00%**	**0.00%**	**0.00%**	**0.00%**
	10%	1.88%	1.61%	3.38%	3.23%	1.58%
	20%	3.66%	3.10%	6.76%	6.69%	3.17%
	30%	5.43%	4.73%	10.14%	10.15%	4.76%
	40%	7.32%	6.37%	13.52%	13.61%	6.35%
	50%	9.09%	7.86%	16.90%	17.07%	7.87%
CM Falsepos	-50%	0.67%	0.20%	1.75%	1.73%	0.19%
	-40%	0.55%	0.16%	1.40%	1.38%	0.16%
	-30%	0.33%	0.12%	1.05%	1.04%	0.12%
	-20%	0.22%	0.08%	0.70%	0.69%	0.08%
	-10%	0.11%	0.04%	0.35%	0.35%	0.03%
	0%	**0.00%**	**0.00%**	**0.00%**	**0.00%**	**0.00%**
	10%	-0.11%	-0.04%	-0.35%	-0.40%	-0.04%
	20%	-0.22%	-0.08%	-0.70%	-0.75%	-0.08%
	30%	-0.33%	-0.12%	-1.05%	-1.10%	-0.12%
	40%	-0.44%	-0.16%	-1.40%	-1.44%	-0.16%
	50%	-0.55%	-0.20%	-1.75%	-1.79%	-0.20%
Distance to Shore	-80%	-9.34%	-9.53%	-1.65%	-1.65%	-0.40%
	-60%	-7.05%	-7.16%	-1.24%	-1.24%	-0.30%
	-40%	-4.67%	-4.79%	-0.83%	-0.83%	-0.20%
	-20%	-2.39%	-2.43%	-0.41%	-0.41%	-0.09%
	0%	**0.00%**	**0.00%**	**0.00%**	**0.00%**	**0.00%**
	20%	2.49%	2.49%	0.42%	0.42%	0.09%
	40%	4.88%	4.98%	0.84%	0.84%	0.18%
	60%	7.37%	7.53%	1.27%	1.27%	0.27%
	80%	9.85%	10.15%	1.70%	1.70%	0.36%
	100%	12.34%	12.76%	2.14%	2.14%	0.45%
	120%	14.94%	15.44%	2.57%	2.57%	0.53%
	140%	17.53%	18.18%	3.00%	3.00%	0.61%
	160%	20.12%	20.92%	3.44%	3.44%	0.70%
	180%	22.82%	23.72%	3.89%	3.89%	0.78%
	200%	25.52%	26.59%	4.32%	4.32%	0.85%

The cost model results with the eight sensitivity parameters in Table 54 are shown in curves in Figure 72 to Figure 76. The legends are as same as in Figure 72. As stated above, because of the different span of each factor in the full scale graph, zoomed-in graphs are shown at the right-hand side of the full scale graph for each selected cost model result. In the zoomed-in graphs, the x axis is shown from -50% to 50% in step of 10%. For the y axis, the same zoomed-in span of from -80% to 200% with resolution of step of 20% is taken for Figure 72 and Figure 73; the same zoomed-in span of from -80% to 60% with resolution of step of 10% is chosen for Figure 74 and Figure 75;

and the zoomed-in span of from -50% to 50% with resolution of step of 10% is chosen for Figure 76. To emphasize again, these figures are the percentage change of the result difference due to condition based maintenance. Take the availability as an example, as the wind and wave parameter percentage adjustment increases, the percentage change of the result difference due to condition based maintenance (CBM) from reactive maintenance also increases. This means the condition based maintenance has more impact on the availability result when the wind and wave parameters increase (can be generally understood as the wind and wave become stronger).

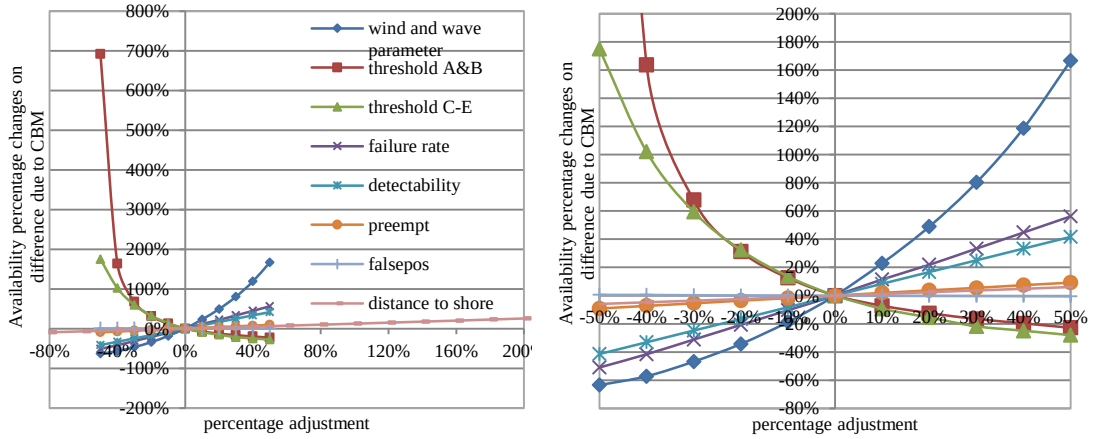

Figure 72. Eight sensitivity analyses in percentage changes of difference due to condition based maintenance on availability with full scale (left) and zoomed-in scale of [-50%, 50%, -80%, 200%] for x and y axis (right)

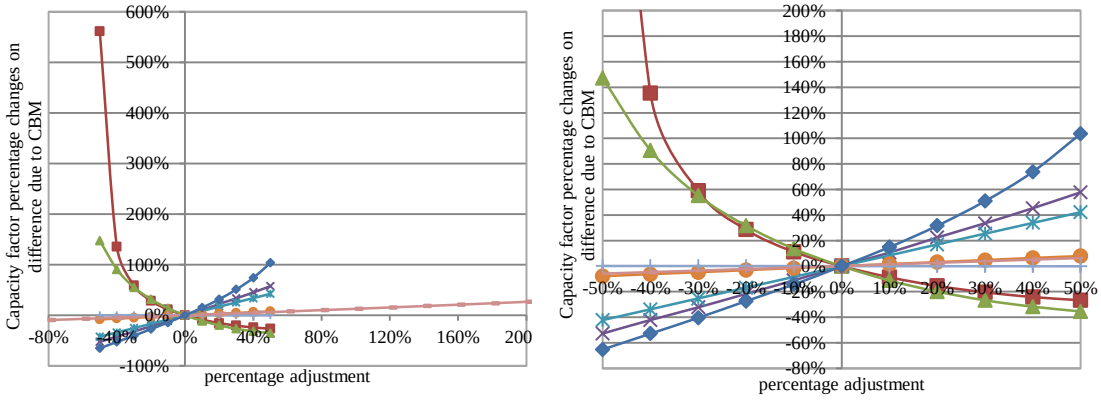

Figure 73. Eight sensitivity analyses in percentage changes of difference due to condition based maintenance on capacity factor with full scale (left) and zoomed-in scale of [-50%, 50%, -80%, 200%] for x and y axis (right)

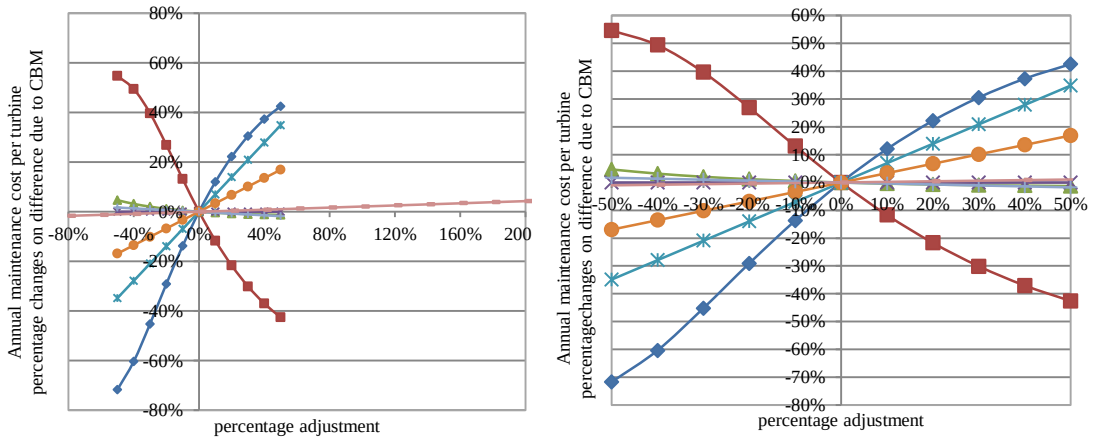

Figure 74. Eight sensitivity analyses in percentage changes of difference due to condition based maintenance on annual maintenance cost per turbine with full scale (left) and zoomed-in scale of [-50%, 50%, -80%, 60%] for x and y axis (right)

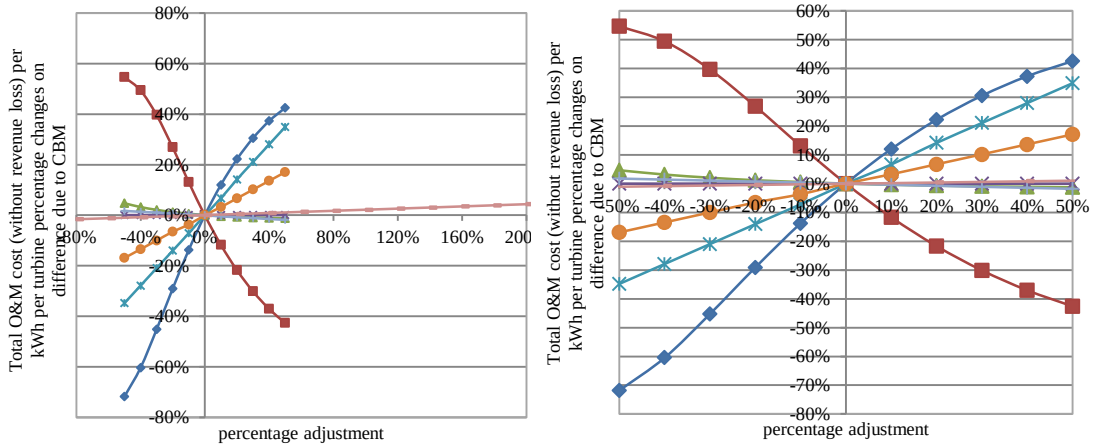

Figure 75. Eight sensitivity analyses in percentage changes of difference due to condition based maintenance on total O&M cost (without revenue loss) per kWh per turbine with full scale (left) and zoomed-in scale of [-50%, 50%, -80%, 60%] (right)

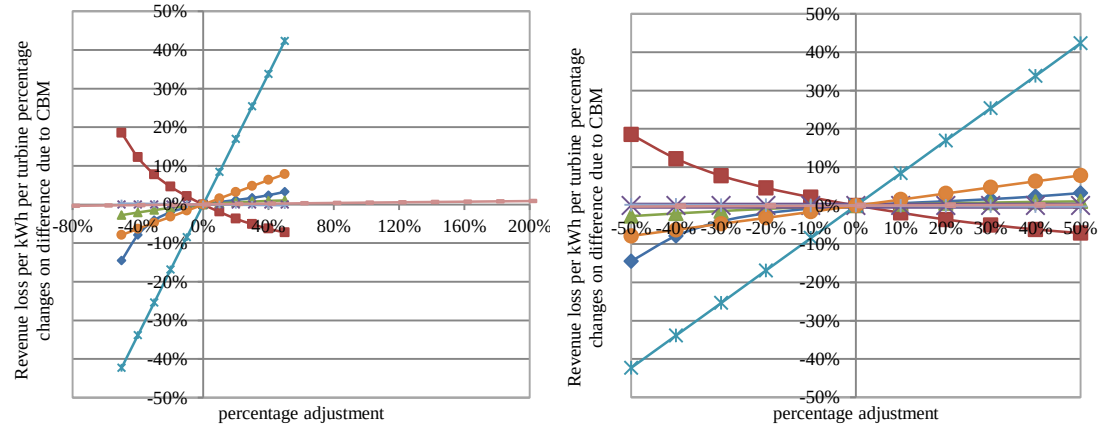

Figure 76. Eight sensitivity analyses in percentage changes of difference due to condition based maintenance on revenue loss per kWh per turbine with full scale (left) and zoomed-in scale of [-50%, 50%, -50%, 50%] for x and y axis (right)

Unlike the almost linear reactive maintenance sensitivity curves with CM detections discussed in the previous section, some of the results show non-linear relationships. The wind and wave parameters, the weather window threshold for heavy maintenance (*A* and *B*) and the weather window threshold for light maintenance (*C*, *D* and *E*) show exponential shaped curves for the selected cost model results.

Table 55 lists the calculated gradient of each curve around 0% adjustment (treated as tangents at 0% adjustment) in the figures. Because of the different order of magnitudes, in this table, the gradient values from first three rows are given to 2 decimal places, and the row of overall turbine annual failure rate is given 3 decimal places. As in the previous section, those from the three CM detection sensitivity factors and distance to shore use 3 significant figures.

Table 55. Curve gradients around 0% of the selected of StraPCost+ results with all seven sensitivity items in percentage changed values from Figure 72 to Figure 76.

Adjustment	Availability	Capacity factor with downtime	Annual maintenance cost per turbine	Total O&M cost (without revenue loss) per kWh per turbine	Revenue loss per kWh per turbine
Wind and wave parameters weather window	2.08	1.46	1.29	1.29	0.07
Threshold for heavy maintenance (*A* and i)	-0.99	-0.99	-1.24	-1.24	-0.20
Weather window threshold for light maintenance (*C*, *D* and *E*)	-1.15	-1.24	-0.05	-0.05	0.03
Overall turbine annual failure rate	1.094	1.087	0.00	0.00	0.00
Detectability	0.831	0.843	0.697	0.692	0.844
Pre-empt	0.183	0.156	0.338	0.346	0.159
Falsepos	-0.0111	-0.00408	-0.0350	-0.0375	-0.00380
Distance to shore	0.122	0.123	0.0209	0.0209	0.00474

The weather window threshold for heavy maintenance (*A* and *B*) shows fairly high sensitivity (and negative relationship) to all selected cost model results, especially for the adjustment below -30%; whereas distance to shore shows low sensitivity (and linear relationship) to all selected cost model results. The wind and wave parameter

shows high sensitivity to the first four cost model results. The weather window threshold for light maintenance (*C*, *D* and *E*) shows significant sensitivity to the first two cost model results and quite low sensitivity to the rest three cost model results, and it has negative relationship to the first four cost model results. CM *detectability* shows observable sensitivity for all cost model results and presents the highest sensitivity to the last cost model result, the revenue loss. CM *falsepos* shows negative and the lowest sensitivity to most of the cost model results. What is noticeable is that, the cost related results show no sensitivity to the default overall failure rate. The unexpected results highlight imperfections within the algorithm used in StraPCost+, and would be an interesting topic to be explored in future studies.

More specifically, Figure 72 and Figure 73 show similarity of the trends. The availability and capacity factor show a descending exponential type relation along with the increase of the adjustment of the weather window threshold for heavy maintenance (*A* and *B*) and light maintenance (*C*, *D* and *E*). The rest sensitivity parameters show positive impact along with the increase of the adjustment on these two selected cost model results, among which the wind and wave parameter shows an exponential-like relation and others show a roughly linear relation.

The stated three sensitivity curves newly investigated in this section have much steeper curves than the CM detection sensitivity curves in these two figures. The wind and wave parameters show the highest tangents at 0% adjustment in both figures. As shown in Table 55, the tangents at the 0% adjustment for both figures with the wind and wave parameters are 2.08 and 1.46, respectively. Despite of the relatively lower absolute values of the tangents at the 0% adjustment point (-0.99 for both figures), the weather

window threshold for heavy maintenance (*A* and *B*) shows dramatic increases with adjustment below -30%. The overall turbine annual failure rate also shows a slightly higher tangent (and thus higher sensitivity) than the CM *detectability* which is the most sensitive parameters among the three CM detection factors for all cost model results. Distance to shore, on the other hand, shows little sensitivity to the wind turbine availability and capacity factor, with tangent lower than CM *pre-empt*. CM *falsepos* shows the lowest sensitivity to the selected two cost model results.

Figure 74 and Figure 75 show very similar (and for some parameters are the same) trends for the sensitivity curves analysed in this section. This could be because that the in-built algorithm in StraPCost+ considers the percentage change of annual maintenance cost equals to that of the total O&M cost without revenue loss, and would be an interesting aspect to be explored.

Apart from the discussed 0% sensitivity impact on the failure rate adjustment, the weather window threshold for light maintenance (*C*, *D* and *E*), CM *falsepos* and distance to shore also show little sensitivity to the selected cost model results. Distance to shore has the lowest impact on these two selected cost model results.

The weather window threshold for heavy maintenance (*A* and *B*) and wind and wave parameters show variations of the exponential-like curves with the highest gradients in both figures around the 0% adjustment. The order of magnitude for these two types of sensitivity curves are up to 62 times the other sensitivity curves (the highest magnification is the wind and wave parameters to distance to shore). The weather window threshold for light maintenance (*C*, *D* and *E*) also shows a decreasing exponential-like curve, but with much lower gradient (thus low sensitivity).

The annual maintenance cost and the total O&M cost show more obvious sensitivity to CM *detectability* and CM *pre-empt* than wind turbine availability and capacity factor. These two parameters are among the four highest sensitive parameters following the weather window threshold for heavy maintenance (*A* and *B*) and wind and wave parameters.

Figure 76 shows different trends of the selected cost model parameters for revenue loss from those in the other figures. In this figure, CM *detectability* becomes the most sensitive parameters. The absolute gradient value for CM *detectability* is up to 222 times the other sensitivity parameters (in this extreme case, CM *falsepos*). The second most sensitive parameter, weather window threshold for heavy maintenance (*A* and *B*), has a negative relation and shows a descending exponential-like relation curve. CM *pre-empt* also has a negative relation and shows the third most sensitive to revenue loss. Unlike in the above four cost model results, wind and wave parameters show quite low sensitivity, with gradient slightly higher than the weather window threshold for light maintenance (*C*, *D* and *E*). CM *falsepos* has the lowest sensitivity, and its gradient value is close to distance to shore.

When compared from the angle of each parameter, the five selected cost model results show variable sensitivity towards the sensitivity parameters covered in this section.

The wind and wave parameters show always positive impacts on the cost model results, among which its highest impact happens on the availability, lowest impact on the revenue loss, and similar intermediate impact on the remaining three cost model results. It has simple exponential shaped relation to the availability, capacity factor, a variation

of exponential shaped relation to annual maintenance cost and total O&M cost, and a 3rd order polynomial shaped relation to revenue loss.

The weather window threshold for heavy maintenance (*A* and *B*) shows always negative impacts on the five selected cost model results. It has high impact on the first four cost model results along with the entire adjustment scale and shows the dramatically highest impact on the availability and capacity factor for adjustment of lower than -30%. When compared with the impact around 0% adjustment, its highest impact happens on the annual maintenance cost and the total O&M cost, followed by on the availability and capacity factor, and the lowest impact on the revenue loss. The tangent of the highest impact is 6 times as much as the lowest one. It has simple exponential shaped relation to the availability and capacity factor, a variation of exponential shaped relation to annual maintenance cost and total O&M cost, and shows a trend of a 3rd order polynomial shaped relation to revenue loss.

The weather window threshold for light maintenance (*C, D* and *E*) has a negative impact on the first four cost model results and positive impact on the revenue loss (which needs to be investigated in the future work). Among the first four cost model results, capacity factor shows the highest sensitivity, followed by availability. The remaining three results have similar low sensitivities. The tangent of the highest impact is more than 41 times as much as the lowest one. The weather window threshold for light maintenance (*C, D* and *E*) has simple exponential shaped relation for all five selected cost model results.

The failure rate only has similar positive impact at around 1% for availability and capacity factor and as stated already, no impact on the others.

The three CM detection parameters show similar linear impact as discussed in Section 5.5 with different magnitudes.

Distance to shore shows always positive, low and linear impact on all five cost model results. Among the five cost model results, distance to shore shows its highest sensitivity to availability and capacity factor, and the lowest sensitivity to revenue loss. The highest tangent value is 26 times the lowest.

5.6.3 Conclusion

This section presents further sensitivity analyses for percentage changes due to condition based maintenance from reactive maintenance with wind and wave parameters, weather window threshold for heavy maintenance (*A* and *B*), weather window threshold for light maintenance (*C*, *D* and *E*), overall turbine annual failure rate and distance to shore, together with the CM detection parameters, *detectability*, *pre-empt* and *falsepos*, initially analysed in Section 5.5.

This series of sensitivity analyses is not only meaningful for testing the estimation performance of StraPCost+ as an improved cost model, but also for finding out the key parameters that have high impact on a wind turbine and the entire wind farm. The eight key cost model parameters show different impact on StraPCost+, among which wind and wave show clear sensitivity impact on all cost model results, followed by failure rate. What is noticeable, StraPCost+ cost related estimations have high positive sensitivity to the CM *detectability*, which reveals the positive impact of CM systems on the offshore wind turbine. These three parameters have shown their importance for the offshore wind turbine system, and need to be considered with emphasis while at

the wind farm installation planning stage and making the operation and maintenance plan.

More specifically, the wind and wave parameters show the highest impact on the first four selected cost model results, and CM *detectability* shows the highest impact on the revenue loss. CM *falsepos* and distance to shore show generally less sensitivity to all cost model results. Wind turbine availability and capacity factor show the most dramatic decreases along with the increase of the weather window threshold for heavy maintenance (*A* and *B*) for the adjustment below -30%. What is noticeable, although all other sensitivity items show constant positive or negative impact on all five selected cost model results, the weather window threshold for light maintenance (*C, D* and *E*) shows negative impact on the first four cost model results and positive impact on the revenue loss, which might be investigated in the future work. The future work might also be undertaken on the investigation of the lack of sensitivity of the annual maintenance cost, total O&M cost and revenue loss to the failure rate.

Chapter 6 Cost model applications: cost effectiveness of condition monitoring

Following on from the introduction, improvement and analyses of the cost model in this thesis, this section gives applications based on actual data for existing and planned offshore wind farms. For the two case studies considered here, the data and information are from the existing offshore wind farm W and the planned offshore wind farm N, as introduced in Chapter 3. The wind farm N was planned to be a multi-hundred-MW offshore wind farm located 14.3 km from the shore in the south of England. However, it has recently announced that the wind farm has been refused planning approval.

Even so, it does not affect the wind and wave data collected from the planned area, and this application of the cost model is still meaningful. It demonstrates that as well as assessing the operation and performance of an existing wind farm, the cost model can also be used in wind farm planning. Compared to the virtual data applied in the previous section, this thesis studies examine how the cost model can be used to support decision making in the real world.

With the analyses on the different measure points in wind farm T, it also, to some extent, shows the effect to the cost model on the distance to shore, which is also a special concern for wind farm study in general.

The results for wind farms T and wind farm N in this chapter are compared with the results from previous chapter and ECUME, the commercial cost model, respectively.

6.1 Cost model application on offshore wind farm T

This section presents the case study on wind farm T and compares with the FINO virtual wind farm studied in Section 5.4. As introduced in Section 3.1, the offshore wind farm T is located 1.5 km north from the coast in the north-east of England with site area of 10 km^2. The wind farm uses 27 Siemens SWT-2.3-93 in 3 rows with total installed capacity of 62MW. The wind turbine hub height is 80m with total turbine height of 126.5m, and rotor diameter is 93m. The turbine capacity is 2.3MW, with a cut in wind speed of 4 m/s, rated wind speed of 12 m/s, and cut out wind speed of 25 m/s.

6.1.1 Cost model inputs and middle stage parameter calculations

6.1.1.1 Cost model inputs

Apart from the basic information stated above, based on consultation with a number of experts, a series of financial assumptions as used in Chapter 5 Section 4, are used to overcome the lack of real data. The personnel hourly rate is assumed to be £25/h. The electricity sale price and ROC price are assumed to be £40/MWh and £45/MWh. The year length is 8760 hours and the shift length of technicians is 12 hours. The number of technicians is assumed to be 20. The delay charge for unscheduled and scheduled vessel usage is assumed to be 47% and 0% of their original rental price, separately.

The subsystem level failure rate breakdown follows the improved cost model with onshore/offshore translation, as introduced in Section 5.3.1, and the default overall turbine annual failure rate stays at 11.895, as introduced in Section 5.4.

According to the wind farm operator, there are two main types of vessels in use at wind farm T: the heavy-lift vessel for heavy maintenance and a windcat for personnel transfer and other lighter maintenance tasks. The light task vessel windcat B1 data is summarised in Table 56. Due to lack of real information, the initially assumed heavy-lift vessel usage here follows the virtual vessel HLV1 introduced in Table 37 in Section 5.4 as a generic type input for the cost model. However, the results shown in Appendix-B from Table 6b to Table 9 suggest this heavy-lift vessel assumption is unrealistically too expensive, which gives the final annual maintenance cost estimation in the range from £2033.5k to £4551.8k per turbine. Compared to the £165k-226k annual maintenance cost of the virtual wind farm in the previous section, and also considering that the size of the virtual wind farm is much larger, this cost estimation range is unrealistically high. The reason of this is somehow understandable: in the virtual wind farm operational settings in Section 5.4, there are three levels of vessel application, and the HLV1 is only applied in major replacement (repair type A), and the field support vessel FSV1 for major repair (repair type B) is 15 times cheaper; while in this section, for wind farm T, there are only two types of vessel in use, and for both major replacement (repair type A) and major repair (repair type B) the application of HLV1 shows uneconomically overused. Therefore, after consulting with the operator of wind farm N analysed in Section 6.2, the final heavy-lift vessel assumed here is the same jack up barge JUB1 originally planned for use in wind farm N. The vessel usage assumption is shown below.

Table 56. Vessels statistics input in the cost model StraPCost+ for wind farm T

Vessel	Code	Max wave height (m)	Max wind speed (m/s)	Speed (knots)	Positioning time (hrs)	Day rate (£)
Windcat	B1	1.5	15	6	1	1,500
Jack up barge	JUB1	1.83	30	12.9	3	33,300

Table 57. Maintenance category settings for study of wind farm T

	reactive maintenance					
	Major Replacement	Major Repair	Medium Repair	Minor Repair	Manual Reset	Annual service
	Au	Bu	Cu	Du	Eu	F
weight limit	500	500	10	10	10	10
repair time	168	120	48	8	3	60
lead time	168	168	48	1	1	1
people reqd	7	7	4	2	2	4
vessel	JUB1	JUB1	B1	B1	B1	B1
Generator Assembly	6.00%	4.00%	12.00%	14.00%	55.59%	8.41%
Gearbox Assembly	6.00%	4.00%	12.00%	14.00%	55.59%	8.41%
Blades	3.00%	2.00%	6.00%	7.00%	73.59%	8.41%
Pitch System	0.00%	0.00%	20.00%	12.00%	59.59%	8.41%
Yaw System	0.50%	0.00%	17.50%	10.00%	63.59%	8.41%
Frequency Converter	2.00%	2.00%	10.00%	8.00%	69.59%	8.41%
L.V. Switchgear	0.00%	0.00%	10.00%	10.00%	71.59%	8.41%
M.V. Switchgear	2.00%	1.00%	10.00%	7.00%	71.59%	8.41%
Transformer	2.00%	2.00%	10.00%	6.00%	71.59%	8.41%
Power Module Other	0.00%	0.00%	10.00%	10.00%	71.59%	8.41%
Hub	2.00%	1.00%	18.00%	12.00%	58.59%	8.41%
Sliprings	3.00%	2.00%	8.00%	7.00%	71.59%	8.41%
Blade Bearings	15.00%	8.00%	16.00%	11.00%	41.59%	8.41%
Rotor Other	2.00%	0.00%	10.00%	8.00%	71.59%	8.41%
Safety Chain	0.00%	0.00%	12.00%	8.00%	71.59%	8.41%
Sensors	2.00%	1.00%	10.00%	7.00%	71.59%	8.41%
Communications	2.00%	0.00%	10.00%	8.00%	71.59%	8.41%
Controller H/W	0.00%	0.00%	12.00%	8.00%	71.59%	8.41%
Controller S/W	0.00%	0.00%	0.00%	0.00%	91.59%	8.41%
Control & Comms Other	3.00%	2.00%	8.00%	7.00%	71.59%	8.41%
Mechanical Brake	1.00%	0.00%	12.00%	8.00%	70.59%	8.41%
High Speed Shaft transmission	2.00%	0.00%	20.00%	18.00%	51.59%	8.41%
Main Shaft	15.00%	10.00%	8.00%	7.00%	51.59%	8.41%
Generator Silent Blocks	16.00%	9.00%	7.00%	8.00%	51.59%	8.41%
Hydraulic System	2.00%	1.00%	15.00%	14.00%	59.59%	8.41%
Cooling System	0.00%	0.00%	12.00%	8.00%	71.59%	8.41%
Meteorological Station	0.00%	0.00%	11.00%	9.00%	71.59%	8.41%
Auxiliary Equipment Other	0.00%	0.00%	12.00%	8.00%	71.59%	8.41%
Tower	0.50%	0.00%	10.00%	9.50%	71.59%	8.41%
Foundation	0.50%	0.00%	11.00%	8.50%	71.59%	8.41%
Wind Farm System	0.00%	0.00%	12.00%	8.00%	71.59%	8.41%
Condition Monitoring System	1.00%	1.00%	10.00%	8.00%	71.59%	8.41%

The maintenance category follows the settings shown in Table 57. The assumption of the maintenance failure rate for each category no longer follows the one value setting used for all turbine components in Section 5.4 where uniform failure rate values are set for the comparison of other cost models without breakdown categorized failure rate shown. In this section, the maintenance categorized failure rates are assumed based on the empirical settings and the only publication which includes the major/minor split subsystem level failure rate [166]. As introduced in Section 5.3.2, the raw input

categorized failure rate values under the reactive maintenance categories shown in Table 57 are not the final values. The final estimated failure rate values are processed by the calculation listed in the formulae at the end of Section 5.3.2.

In wind farm T, there are 6 met ocean points spread in the area of the wind farm measuring the wave height and current velocity, and the data from 4 of them are accessible for this thesis. Since the significant weather variables, wind speed and direction are recorded by the SCADA systems of each wind turbine, for matching of the location of both the measured wind and wave data, this thesis selects the closest wind turbine to match each met ocean point, and processes the wind data from these selected wind turbines in order to get the wind Weibull parameters required as inputs of the cost model. From the wind farm plan introduced in Section 3.2.1, the matched wind turbines are shown in Table 58.

Table 58. Matched wind turbines and the wave metocean points for wind farm T

Wave metocean point	Wind turbine	Distance to shore (km)
Point01	WTG04	3.3
Point02	WTG09	2.7
Point05	WTG22	1.5
Point06	WTG27	1.5

This table also shows the distance to shore of each matched point. Since there is only information of the distance to shore of the entire wind farm in the public domain, the distance to shore value of the wind turbine at the nearest row of the wind farm is considered to be the distance of the nearest row to shore (Point05 and Point06), and other points (Point01 and Point02) are calculated by adding the distance between rows to this value.

6.1.1.2 Wind parameters

By using the wind Weibull parameter calculator introduced in Section 5.3.3, the wind shape parameter k and the wind scale parameter C from the selected wind turbine 6-month long 10-min interval SCADA data are listed in Table 59, and the wind Weibull location parameter is fixed at 0. Because of the fact that the wind turbines are located closely together, in order to highlight any differences in the final results, the calculated parameters are given to 2 decimal places. Some of these differences are likely to be due to wake effects.

Table 59. Wind Weibull parameters for selected wind turbines for wind farm T

Parameter	WTG04	WTG09	WTG22	WTG27
Shape parameter k	2.19	2.39	2.38	2.34
Scale parameter C	10.00	10.47	10.05	10.13

6.1.1.3 Wave parameters

By using the wave parameter calculator introduced in Section 5.1.2, the wave parameters calculated from the 20-year long 3-hourly interval wave and current records of the four selected metocean points are listed below. For the best comparison, the decimal places of each parameter are kept until there are no repeated values among all four points unless the values are really the same.

Table 60. Wave parameters for the selected metocean points for wind farm T

	Point01	Point02	Point05	Point06
Wave location parameter (m)	0.01	0.01	0.01	0.01
Wave shape parameter	0.925	0.924	0.915	0.912
Wave scale parameter (m)	0.63	0.62	0.60	0.59
Characteristic wave duration (hrs)	41.72	41.62	41.93	41.71
Wave duration exponent	0.6886	0.6878	0.6826	0.6883
Duration parameter scaling	0.8921	0.8923	0.8868	0.8972
Wave exponent	0.056	0.047	0.062	0.097

6.1.2 Results

Table 61 to Table 64 show the results from the StraPCost+ model. For easier reading and comparison, the cost per unit in this chapter is multiplied by the annual energy generated and shows the wind turbine level annual value. From the listed tables, even though all distances to shore are quite close due to the size of the wind farm, it still can be seen that inputs from different measure points vary the results slightly, which also shows the sensitivity of the cost model.

Table 61. Cost model results for wind farm T Point01

	Reactive Maintenance	Condition-based Maintenance	Change due to CM	Change/ Baseline
downtime	17.7 days	15.3 days	-2.4 days	-13.71%
availability	95.1 %	95.8 %	0.7 %	0.70%
capacity factor	42.8 %	43.3 %	0.4 %	1.04%
energy lost	553.4 MWh	464.1 MWh	-89.3 MWh	-16.14%
mean power generated over year	0.99 MW	1.00 MW	0.01 MW	1.04%
total annual energy generated	8631.5 MWh	8720.8 MWh	89.3 MWh	1.04%
annual revenue	733.7 £k	741.3 £k	7.6 £k	1.04%
annual maintenance cost	167.9 £k	151.4 £k	-16.6 £k	-9.86%
entire wind farm annual maintenance cost	22.5 £m	18.3 £m	-2.0 £m	-8.90%
vessel cost	79.96 £k	72.80 £k	-7.16£k	-8.96%
wage cost	31.63 £k	28.55 £k	-3.08£k	-9.72%
component cost	56.35 £k	50.02 £k	-6.33£k	-11.23%
Total O&M cost (w/o revenue loss)	167.94 £k	151.37 £k	-16.57£k	-9.86%
revenue lost	47.04 £k	39.45 £k	-7.59£k	-16.14%
Total O&M cost (with revenue loss)	214.98 £k	190.82 £k	-24.16£k	-11.24%
Entire wind farm revenue loss	5,692.01 £k	4,773.17 £k	-918.84£k	-16.14%

Table 62. Cost model results for wind farm T Point02

	Reactive Maintenance	Condition-based Maintenance	Change due to CM	Change/ Baseline
downtime	17.6 days	15.2 days	-2.4 days	-13.67%
availability	95.2 %	95.8 %	0.7 %	0.69%
capacity factor	46.7 %	47.2 %	0.5 %	0.97%
energy lost	580.3 MWh	488.6 MWh	-91.7 MWh	-15.80%
mean power generated over year	1.07 MW	1.08 MW	0.01 MW	0.97%
total annual energy generated	9412.1 MWh	9503.8 MWh	91.7 MWh	0.97%
annual revenue	800.0 £k	807.8 £k	7.8 £k	0.97%
annual maintenance cost	167.4 £k	150.9 £k	-16.4 £k	-9.83%
entire wind farm annual maintenance cost	22.4 £m	18.3 £m	-2.0 £m	-8.87%
vessel cost	79.63 £k	72.54 £k	-7.09£k	-8.90%
wage cost	31.38 £k	28.35 £k	-3.03£k	-9.67%
component cost	56.35 £k	50.02 £k	-6.33£k	-11.23%
Total O&M cost (w/o revenue loss)	167.36 £k	150.91 £k	-16.45£k	-9.83%
revenue lost	49.33 £k	41.53 £k	-7.79£k	-15.80%
Total O&M cost (with revenue loss)	216.69 £k	192.44 £k	-24.24£k	-11.19%
Entire wind farm revenue loss	5,968.72 £k	5,025.55 £k	-943.17£k	-15.80%

Table 63. Cost model results for wind farm T Point05

	Reactive Maintenance	Condition-based Maintenance	Change due to CM	Change/ Baseline
downtime	17.3 days	14.9 days	-2.3 days	-13.52%
availability	95.3 %	95.9 %	0.6 %	0.67%
capacity factor	43.8 %	44.3 %	0.4 %	0.97%
energy lost	540.2 MWh	454.7 MWh	-85.5 MWh	-15.82%
mean power generated over year	1.01 MW	1.02 MW	0.01 MW	0.97%
total annual energy generated	8834.0 MWh	8919.5 MWh	85.5 MWh	0.97%
annual revenue	750.9 £k	758.2 £k	7.3 £k	0.97%
annual maintenance cost	165.2 £k	149.3 £k	-15.9 £k	-9.64%
entire wind farm annual maintenance cost	22.2 £m	18.1 £m	-1.9 £m	-8.69%
vessel cost	78.31 £k	71.57 £k	-6.74 £k	-8.60%
wage cost	30.55 £k	27.69 £k	-2.86 £k	-9.36%
component cost	56.35 £k	50.02 £k	-6.33 £k	-11.23%
Total O&M cost (w/o revenue loss)	165.20 £k	149.28 £k	-15.92 £k	-9.64%
revenue lost	45.92 £k	38.65 £k	-7.27 £k	-15.82%
Total O&M cost (with revenue loss)	211.12 £k	187.94 £k	-23.19 £k	-10.98%
Entire wind farm revenue loss	5,556.17 £k	4,677.09 £k	-879.08 £k	-15.82%

Table 64.Cost model results for wind farm T Point06

	Reactive Maintenance	Condition-based Maintenance	Change due to CM	Change/ Baseline
downtime	17.1 days	14.8 days	-2.3 days	-13.49%
availability	95.3 %	95.9 %	0.6 %	0.66%
capacity factor	44.4 %	44.8 %	0.4 %	0.95%
energy lost	537.0 MWh	452.5 MWh	-84.5 MWh	-15.74%
mean power generated over year	1.02 MW	1.03 MW	0.01 MW	0.95%
total annual energy generated	8935.8 MWh	9020.3 MWh	84.5 MWh	0.95%
annual revenue	759.5 £k	766.7 £k	7.2 £k	0.95%
annual maintenance cost	164.7 £k	148.9 £k	-15.8 £k	-9.59%
entire wind farm annual maintenance cost	22.1 £m	18.0 £m	-1.9 £m	-8.64%
vessel cost	78.04 £k	71.38 £k	-6.66 £k	-8.54%
wage cost	30.32 £k	27.51 £k	-2.81 £k	-9.27%
component cost	56.35 £k	50.02 £k	-6.33 £k	-11.23%
Total O&M cost (w/o revenue loss)	164.71 £k	148.91 £k	-15.80 £k	-9.59%
revenue lost	45.65 £k	38.47 £k	-7.18 £k	-15.74%
Total O&M cost (with revenue loss)	210.36 £k	187.38 £k	-22.98 £k	-10.92%
Entire wind farm revenue loss	5,523.41 £k	4,654.29 £k	-869.12 £k	-15.74%

6.1.3 Discussion

The discussion is addressed to three aspects: comparing the reactive maintenance with the FINO virtual wind farm in Section 5.4, subsystem contribution to the reactive maintenance cost, and effect of the condition-based maintenance.

According to actual experience with wind farm T, the total O&M cost (without revenue loss) is in the range from £150k to £250k. The fact that all four points (from Table 61 to Table 64) present around £210k for the reactive maintenance and £190k for condition-based maintenance shows that StraPCost+ gives a relatively reliable estimate.

6.1.3.1 Comparison of wind farm T with FINO virtual wind farm

The same wind farm operational assumptions with regard to costs, technicians, default overall failure rate setting and the turbine subsystem breakdown failure rates allows the rough comparison in reactive maintenance baseline with the values obtained in Section 5.4 (shown in Table 45 in Section 5.4.2.1). Here for easier comparison, the cost results are all transferred from per unit values into the wind turbine level, as shown in Table 65. Despite this, the two wind farms have significant differences, such as the turbine size, number of turbines, distance to shore, wind and wave conditions, and importantly, the vessel usage. Take heavy-lift vessel usage as an example, the HLV1 used in Section 5.4 (with day rate of £150,000) is 450% of the JUB1 used in this section (with day rate of £33,300). These differences show their impact in many results, especially the cost related results.

Table 65. Mirrored table of comparison of StraPCost+ reactive maintenance outputs with different failure rate inputs for FINO virtual wind farm in Section 5.4.2

WITH DOWNTIME based on	Overall one value	Original Onshore	Exp-translated
downtime	26.8 days	26.7 days	23.6 days
time-based availability	92.6 %	92.7 %	93.5 %
capacity factor	45.1 %	45.2 %	45.8 %
energy lost	1389.4 MWh	1382.2 MWh	1221.8 MWh
mean power generated over year	1.35 MW	1.35 MW	1.37 MW
total annual energy generated	11860.8 MWh	11868.1 MWh	12028.5 MWh
annual revenue	1067.5 £k	1068.1 £k	1082.6 £k
annual maintenance cost	226.1 £k	187.7 £k	165.7 £k
entire wind farm annual maintenance cost	19.7 £m	16.6 £m	14.9 £m
vessel cost	142.33 £k	142.42 £k	120.29 £k
wage cost	24.91 £k	24.92 £k	21.65 £k
component cost	61.68 £k	23.74 £k	20.45 £k
Total O&M cost (w/o revenue loss)	226.54 £k	187.52 £k	165.99 £k
revenue lost	124.54 £k	124.62 £k	109.46 £k
Total O&M cost (with revenue loss)	351.08 £k	312.13 £k	275.45 £k

Reactive maintenance is taken as the baseline. Take downtime as the first example, from Table 61 to Table 64, Point01, with distance to shore of 3.3 km, shows 17.7 days for reactive maintenance, 15.3 days for condition-based maintenance, and the change due to condition monitoring system is -13.71%; Point02, with distance to shore of 2.7 km, shows 17.6 days for reactive maintenance, 15.2 days for condition-based maintenance, and the change due to condition monitoring system is -13.67%; Point05, with distance to shore of 1.5 km, shows 17.3 days for reactive maintenance, 14.9 days for condition-based maintenance, and the change is -13.52%; and Point06, also with distance to shore of 1.5 km, shows 17.1 days for reactive maintenance, 14.8 days for condition-based maintenance, and the change is -13.49%.

From the distance to shore aspect, the results of the reactive maintenance show the downtime difference between Point01 and Point05 is 0.4 days with 1.8 km difference of the distance to shore; whereas Point05 and Point06 which are in the same row in the wind farm and considered to have the same distance to shore show only 0.2 days' difference. Similarly, the results of the condition-based maintenance show the downtime difference between Point01 and Point05 is 0.4 days; whereas Point05 and

Point06 show only 0.1 days' difference. The average downtime of 17.4 days calculated from all four points in this section is 32.2% lower than what is shown in the FINO virtual wind farm analysis, where the average downtime from StraPCost+ of all three methods is 25.7 days.

When it comes to availability, all measure points show values around 95%. It shows the availability obtained from StraPCost+ in this section (an average of 95.2%) is 2.3% higher than the ones obtained from the same cost model in Section 5.4 (an average of 92.9%), and 14.5% higher than other cost models (an average of 83.2%).

However, as stated at the beginning, the significant differences between the two wind farms show their impact on many other results.

Firstly, even though downtime is lower and availability is higher, the baseline capacity factor in this section is not higher than that in the Section 5.4. The range of 42.8% - 46.7% in this section is a bit wider than those around 45% in Section 5.4, and the average value of 44.4% in this section is even 2.1% lower than that of 45.4% in Section 5.4. Even though this difference is quite small and can be ignored when compared with the rest estimation items, this phenomenon can be explained by the different wind and wave conditions at the two wind farms, especially when the virtual wind farm in Section 5.4 is much further to shore. The wind and wave conditions are normally steadier with the increase of the distance to shore and the capacity factor can thereby be higher. However, when the distance to shore is further, the required maintenance weather window is longer, and this can cause the longer downtime for the wind turbine waiting for the vessel bringing maintenances and therefore results in lower availability.

Similarly, the average value of mean power generated over the year, total annual energy generated, and energy lost are 24.6%, 24.9% and 58.5% lower than the ones in Section 5.4. This suggests that even though the power and energy generated at wind farm T is lower than the virtual wind farm in Section 5.4, the energy lost is much lower than the one in Section 5.4. Apart from the stated reason, this phenomenon can also be affected by the lower turbine rated power (2.3MW) than in Section 5.4 (3MW).

On the other hand, the cost related results show various differences between the two wind farms, basically in three groups. In the first group, annual maintenance cost, whose value is considered roughly the same as the total O&M cost without revenue loss here, has a relatively small difference among the three groups, with 13.9% lower than the average counterpart in Section 5.4. In the second group, the mean difference is around 30%. Annual revenue, entire wind farm annual maintenance cost, wage cost and total O&M cost with revenue loss are 29.1% lower, 30.7% higher, 30% higher, and 31.8% lower than the ones in Section 5.4, separately. The third group shows a relatively high difference. Vessel cost, component cost and revenue lost are 41.5% lower, 59.7% higher and 60.7% lower than the ones in Section 5.4. As stated earlier, this section applies a much cheaper heavy lift vessel for heavy maintenance, and this assumption makes it reasonable that the vessel cost is much lower than the ones in Section 5.4. Apart from the main reason of the different wind and wave conditions and distance to shore, this might also due to the properly assumed detailed maintenance categorized failure rate on each subsystem in this section, as discussed next.

6.1.3.2 Subsystem contribution to maintenance cost

Figure 77 shows the typical subsystem contribution to the reactive maintenance cost with measure point01. The distribution does not change very much from point to point. The subtle difference only starts to display on the second decimal place. This can be understood as wind farm T is a small-sized wind farm with relatively similar distance to shore for each turbine.

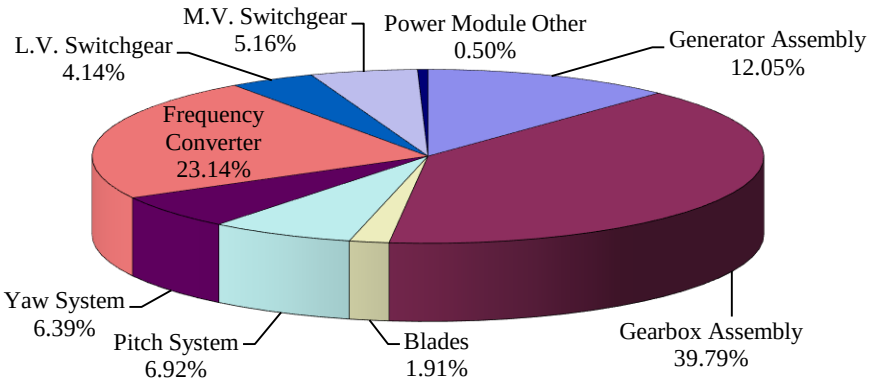

Figure 77. Baseline major contributions to maintenance cost by subsystem for wind farm T (from top to bottom: Point01)

Since with each subsystem, each point has no more than 0.04% deviation with the average value, here it discusses with the average values. From the pie chart, it can be seen that gearbox assembly takes the largest share from the entire maintenance cost which is considered as the O&M cost without revenue loss in this cost model. The contribution is 39.98% in average. The frequency converter makes the second largest contribution, with 23.10% in average. The third largest contribution is taken by generator assembly, with 12.07% in average. Apart from these three subsystems, all other subsystems take up no more than 7% of entire annual maintenance cost. Table 66 lists the detailed contribution in the sequence of the subsystem with from the largest to the smallest share.

This subsystem contribution of the total annual maintenance cost investigation provides a certain level of evidence to rank of consequences (S for severity in the RPN [S,O,D] criteria) for the maintenance of each subsystem, which is another RPN calculation concern other than failure occurrence in the FMEA analyses introduced in Chapter 4 Section 2 (all three elements in RPN [S,O,D] criteria are severity, occurrence and detection). It highlights the subsystems where improvement effort should be directed to make most impact on maintenance cost. In this way it gives support to the condition monitoring subsystem analysis, and can be applied to FMEA study in future work.

Table 66. Annual maintenance cost contribution, average value and deviations in StraPCost+ for reactive maintenance of wind farm T in the sequence of from the largest to the smallest share; total cost given at the first row and highlighted

	Contribution				Average	Deviation			
	Point01	Point02	Point05	Point06		Point01	Point02	Point05	Point06
total cost	167.9	167.4	165.2	164.7					
gearbox	39.79%	39.83%	39.94%	39.98%	39.89%	-0.10%	-0.05%	0.05%	0.10%
frequency converter	23.14%	23.13%	23.07%	23.06%	23.10%	0.04%	0.03%	-0.03%	0.01%
generator	12.05%	12.06%	12.07%	12.08%	12.07%	-0.02%	-0.01%	0.00%	0.00%
pitch system	6.92%	6.90%	6.88%	6.87%	6.89%	0.03%	0.01%	-0.01%	-0.01%
yaw system	6.39%	6.37%	6.34%	6.33%	6.36%	0.03%	0.01%	-0.02%	0.01%
M.V.Switchgear	5.16%	5.16%	5.15%	5.15%	5.16%	0.01%	0.01%	-0.01%	-0.04%
L. V. Switchgear	4.14%	4.14%	4.15%	4.15%	4.15%	-0.01%	-0.01%	0.01%	-0.03%
blades	1.91%	1.91%	1.90%	1.90%	1.91%	0.00%	0.00%	-0.01%	-0.02%
power module	0.50%	0.50%	0.49%	0.49%	0.50%	0.01%	0.01%	0.00%	-0.01%

6.1.3.3 Effect of Condition-based maintenance

Figure 78 shows the typical comparison of reactive maintenance (unscheduled) and condition-based (scheduled) maintenance impact on the total O&M cost with and without revenue loss, together with the selected main breakdown costs from StraPCost+. This figure shows the absolute annual cost values at the wind turbine level. The “total cost” is the summation of the total O&M cost without revenue loss (“total

cost (w/o rev)") at the turbine level and revenue loss. This figure illustrates the benefits of condition-based maintenance.

All four measure points have close distribution on the vessel cost, wage cost, component cost and revenue loss mostly due to their close location in the relatively small-sized wind farm, therefore Figure 78 only shows the results from measure point01.

The total cost comparison shows clearly and aggregate benefit from condition-based maintenance amounting to roughly £210k - £190k = £20k per annum. If considering the annually £1.8-4k CM device and service cost with 2.3MW turbines as introduced in Chapter 2, (since the CM is charged annually, it is treated as OPEX rather than CAPEX), the net cost reduction is in the order of £16-18k per annum per turbine.

Among all cost items, the reduction of wage cost seems to have the smallest impact on the total costs due to the condition monitoring system.

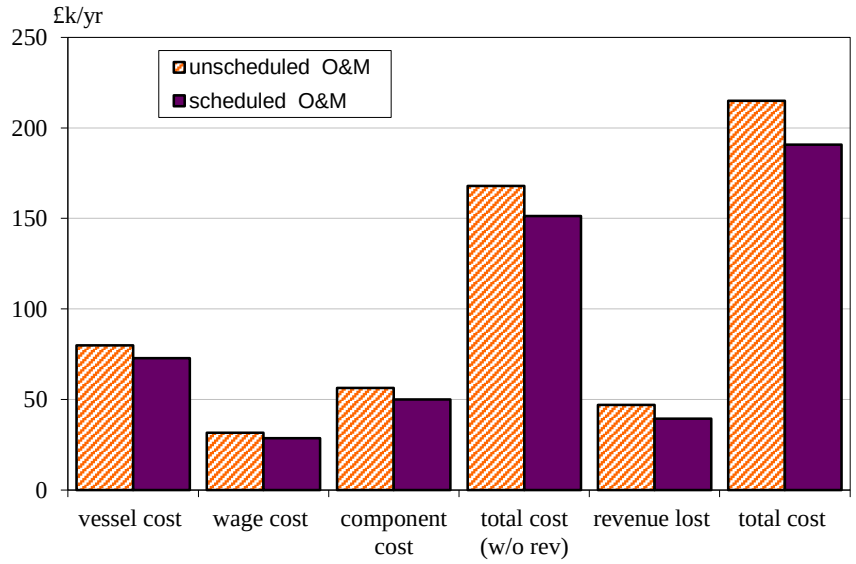

Figure 78. Expected annual contributions to O&M cost in unscheduled and scheduled maintenance (from top to bottom: Point01) for wind farm T

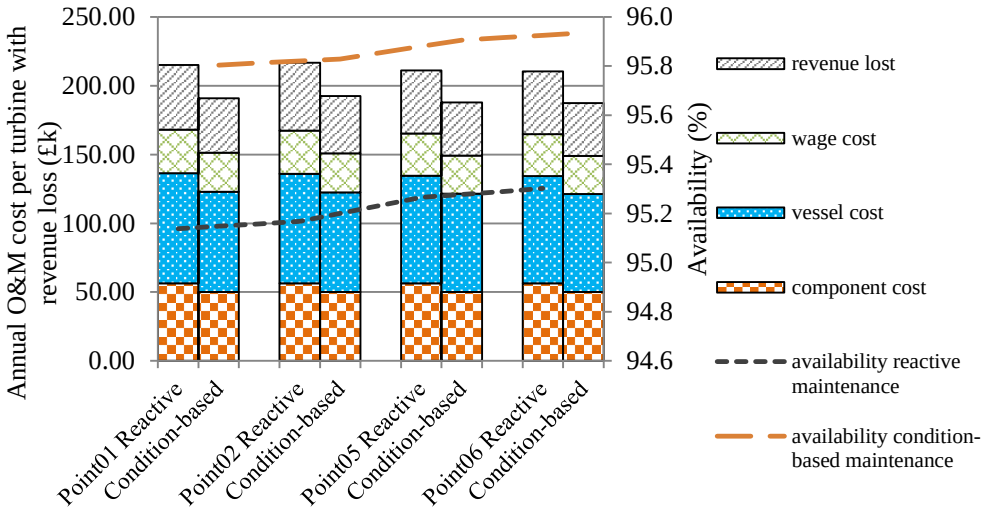

Figure 79. StraPCost+ break down annual O&M cost per turbine with revenue loss and availability for wind farm T with reactive maintenance (left columns) and condition-based maintenance (right columns)

Figure 79 composes all breakdown costs and revenue lost in stacked columns in order to compare the cost effectiveness of condition monitoring system with all four measure points in one chart. It can be seen that with the shortening of the distance to shore (from Point01 to Point 06 from left to right), the annual O&M cost per turbine with revenue loss reduces in a reasonably small amount.

This figure also compares the availability respectively from the reactive maintenance and the condition-based maintenance. It can be seen a clear around 0.6% improvement of availability of condition-based maintenance (orange long dashed curve) from the reactive maintenance (black short dashed curve).

This result supports the discussion earlier. From the distance to shore aspect, it can be seen that both reactive and condition-base maintenance show increase of availability from Point01 to Point06, which suggests with closer distance to shore, the wind turbine shows higher availability. As discussed, longer distance to shore can cause longer

travel and weather waiting time for the wind turbine and therefore cause longer downtime and lower availability.

Table 67 lists the percentage changes due to condition-based maintenance from Table 61 to Table 64, and calculates the average values. All points show similar reduction in downtime, energy lost and costs and increases in availability, capacity factor, and power and energy generated.

Table 67. Percentage changes due to condition-based maintenance in StraPCost+ for wind farm T

	Point01	Point02	Point05	Point06	Average
downtime	-13.71%	-13.67%	-13.52%	-13.49%	-13.60%
availability	0.70%	0.69%	0.67%	0.66%	0.68%
capacity factor	1.04%	0.97%	0.97%	0.95%	0.98%
energy lost	-16.14%	-15.80%	-15.82%	-15.74%	-15.88%
mean power generated over year	1.04%	0.97%	0.97%	0.95%	0.98%
total annual energy generated	1.04%	0.97%	0.97%	0.95%	0.98%
annual revenue	1.04%	0.97%	0.97%	0.95%	0.98%
annual maintenance cost	-9.86%	-9.83%	-9.64%	-9.59%	-9.73%
entire wind farm annual maintenance cost	-8.90%	-8.87%	-8.69%	-8.64%	-8.78%
vessel cost	-8.96%	-8.90%	-8.60%	-8.54%	-8.75%
wage cost	-9.72%	-9.67%	-9.36%	-9.27%	-9.51%
component cost	-11.23%	-11.23%	-11.23%	-11.23%	-11.23%
total O&M cost (w/o revenue loss)	-9.86%	-9.83%	-9.64%	-9.59%	-9.73%
revenue lost	-16.14%	-15.80%	-15.82%	-15.74%	-15.88%
total O&M cost (with revenue loss)	-11.24%	-11.19%	-10.98%	-10.92%	-11.08%
entire wind farm revenue loss	-16.14%	-15.80%	-15.82%	-15.74%	-15.88%

It shows that the degree of reduction for the appropriate factors is mostly over 10%, with the highest reduction of 15.88% in average. The absolute values of deviations between the average value and values for each measure point are no more than 0.26% confirming the similarity that follows from the almost identical distances to shore. The wind turbine operational results and revenue loss show modest increases below 1%. Capacity factor, mean power generated over year, total annual energy generated and annual revenue show the same average increased percentage of 0.98% with the maximum deviation of 0.06% from measure point01. The availability has a relatively smaller increase of 0.68% with absolute values of deviations no more than 0.02%.

Interestingly, some factors show the same percentage changes for all four measure points. It can be seen that the items with the same percentage changes have certain relations, but it is hard to say whether this is because of the inner algorithm of the cost model, or just coincidence since the absolute values are different. The high degree of uniformity exhibited can be used in future to explore the cost model with a view to improvement.

From this table, it can be observed that Point01 has the highest degree of change due to the condition-based maintenance, and this degree of change decrease from Point 01 to Point06, where the measure points are closer to shore. This phenomenon shows that with the increase of distance to shore, the benefit of condition monitoring system and condition-based maintenance are more obvious.

6.1.4 Conclusion

In this section, estimations using StraPCost+ at four different measure points in offshore wind farm T have been undertaken. The results for reactive and condition-based maintenance are compared for the different subsystems and for the four measure points. They are also compared externally with the reactive maintenance results obtained in Section 5.4. This section examined the breakdown of values at subsystem level instead of assuming the same value for all wind turbine subsystems as used in the previous section. This is considered to provide more realistic estimates.

This section also provides a more detailed investigation of the subsystem contributions to the annual maintenance cost. It shows that among all wind turbine subsystems, gearbox assembly makes the largest contribution with almost 40% of the total annual maintenance cost, and power module accounts for only 0.5% of the cost, as the least.

The subsystem contribution to total annual maintenance cost provides a useful ranking of the consequence, an initial RPN calculation element, which can be used in future to refine the application of FMEA on offshore wind farms.

The effect of the application of condition-based maintenance is another analysis concern. This section shows the points that closely located positions give rise to similar results for both condition-based and reactive maintenance, in summary at least £20k reduction in annual O&M cost (with revenue loss) due to the application of the condition-based maintenance and in the order of £16-18k deducting the CM device and service costs. There is also a clear availability improvement due to the application of the condition-based maintenance. It can be seen that with the shortening of the distance to shore, the availability increases. This phenomenon supports the earlier discussion on the effect of distance to shore to the downtime and availability.

Apart from the lower vessel costs with condition-based maintenance, the noticeable cost reduction is also benefit from the increase of the turbine operational results. It can be seen that the degree of change due to the condition-based maintenance decrease with the shortening of the distance to shore. This phenomenon suggests the benefit of condition monitoring system is more obvious with the increase of the distance to shore, as with the planned UK round 3 wind farms.

6.2 Cost model application to planned offshore wind farm N

This section presents the case study on wind farm N and the results are compared with those from ECUME. Since wind farm N was in its planning stage, there wasn't a clear decision on most of detailed technical information excluding the size of the turbine and the site location. The turbine was awarded to MHI Vestas with V164-8MW model, with hub height of 112m and rotor diameter of 164m. The total planned area of the wind farm is 153km^2. The detailed plan for the wind farm kept changing. The latest plans were to install 121 of the Vestas turbines generating in total up to 968MW.

6.2.1 Cost model inputs and middle stage parameter calculations

6.2.1.1 Cost model inputs

The stated wind turbine has a rated power of 8MW, rated wind speed of 11m/s, cut-in wind speed of 4m/s and cut-out wind speed of 25m/s. As stated, the number of turbines input to the cost model is 121.

Since wind farm N was planned to be operated by the same company as wind farm T, for a close set-up, the number of technicians and the personnel hourly rate remain the same. This has ignored the difference in size of the two wind farms. The electricity sale price per unit in this section is higher to make it consistent with the ECUME setting at £140/MWh.

The default overall turbine annual failure rate is set the same value as for ECUME (7.83), and the subsystem level maintenance categorized failure rates are set the same as for wind farm T in Section 6.1.

The maintenance category settings are generally the same as with wind farm T. It applies the jack-up barge as the heavy-lift vessel for maintenance categories A and B, but for light maintenance, it uses a series of non-heavy-lift transport to replace the windcat in categories C, D and E. There are three strategies for the non-heavy-lift vessels, and the methods involved are crew boats, a helicopter and a mother ship. Since it involves helicopters, the term "transportation" is used from now on in place of "vessel". Table 68 lists the detailed transportation information.

For better comparison with the results from ECUME, the non-heavy-lift transportation covers the same three scenarios assumed in ECUME: with strategy 1 there are crew boats only, strategy 2 there are crew boats and helicopters, and strategy 3 there is the mother ship only.

As shown in Table 68, from strategy 1 to 3 the transportation hire rates increase. The equivalent hire day rate for a helicopter is about 7 times that for a crew boat. The mother ship equivalent day rate is about 30 times that of a crew boat and 4 times that for a helicopter. Since strategy 2 is a combination of crew boat and helicopter, the hire rate for this strategy is between 1 and 7 times costlier than strategy 1, and strategy 3 is between 4 and 30 times that of strategy 2. The exact transportation costs can differ significantly and will affect the modelling results.

Table 68. Transportation (vessel) data input to StraPCost+ for wind farm N

Vessel	Code	Max wave height (m)	Max wind speed(m/s)	Speed (knots)	Positioning time (hrs)	Day rate (£)
Jack up barge	JUB1	1.83	30	12.9	3	33,333.3
Crew boat	CB1	1.5	20	20	0.083	1,111.1
Helicopter	H1	50	27	137	0.083	8,219.2
Mother ship	MS1	6	30	12	0.25	20,000

6.2.1.2 Wind and wave parameters

Wind and wave data at a single measurement point has been made available for the planned wind farm N. The distance to shore is 14.3km but to the onshore service base is 59km. Since StraPCost+ only considers the distance for the vessel transit, the input distance is 59km. The wind and wave parameters, as presented in Table 69 and Table 70, are calculated from 12 months of hourly wind and wave records.

Table 69. Wind Weibull parameters for wind farm N

Parameter	WTG04
Shape parameter k	2.26
Scale parameter C	8.07

Table 70. Wave parameters for the wind farm N

Wave location parameter (m)	0.13
Wave shape parameter	1.03
Wave scale parameter (m)	0.74
Characteristic wave duration (hrs)	20.24
Wave duration exponent	0.62
Duration parameter scaling	0.56
Wave exponent	0.29

6.2.2 ECUME results

Table 71 shows the results from the ECUME cost model for wind farm N with the stated three transportation options. The model assessment period is 20 years. As introduced in Section 5.2, ECUME is a mature commercial cost model that considers optimal multiple turbine visits for a single transportation operation. This algorithm is more realistic and to some extent reduces the estimation of vessel waiting time and thus the cost. In the table, all cost related results are the cost for a single turbine per year, except the “Annual O&M costs” which is the average annual cost for all 121 turbines during the 20 years’ operational period. The “Total Annual Cost” in this table

refers to the total annual maintenance cost. Even though the itemed costs considered are slightly different from those for StraPCost+, the corresponding items will be compared. What should be noticed here is that the terminology "loss of production" in Table 71 is in unit of £, so in fact this term has the same meaning of "loss of revenue" in StraPCost+. Apart from this, different terminologies apply: "Technicians" in ECUME reflects "Wage cost" in StraPCost+; "logistics" in ECUME represents "Vessel cost" in StraPCost+; and "wind turbine spare parts" means "component cost" in StraPCost+.

Table 71. ECUME estimation for wind farm N with 121 wind turbines for 20 years running (supplied by EDF)

Number of Turbines:	121		
	Crew Boats Only	Crew Boats and Helicopters	Mother Ship
Wind Turbine Spare Parts (£/turbine/year)	18,767	19,253	19,577
Logistics (£/turbine/year)	90,696	116,327	149,350
Technicians (£/turbine/year)	11,020	13,013	12,779
Onshore and Overheads (£/turbine/year)	36,776	36,776	36,775
Total per turbine per year (£/turbine/year)	157,259	185,369	218,481
Annual O&M Costs (£)	19,028,365	22,429,650	26,436,225
Availability (%)	89.1	92.4	94.5
Total Loss of Production (£/turbine/year)	493,165	356,399	262,680
Total Annual Cost (£/turbine/year)	157,827	185,369	218,481

Figure 80 shows the annual O&M cost per turbine breakdown costs (without loss of production) and how this relates to turbine availability. It can be seen that from strategy 1 (crew boats only) to strategy 2 (crew boats and helicopters) to strategy 3 (mother ship only), the total annual O&M cost increases steadily, whereas onshore costs and overheads, wind turbine spare parts and technician costs do not change significantly. The key factor which changes is logistics (vessel costs), and this is also the dominant contribution to overall operational costs.

Figure 81 shows the annual O&M cost per turbine breakdown, this time also including loss of production together with turbine availability. Since onshore costs and overheads are not related to transportation strategies, they have been omitted in this figure. It can be observed that loss of production accounts for the bulk of the entire annual O&M costs. With reference to Table 71, for strategy 1 with crew boats only, the loss of production value is about 5 times the logistics cost. The significant decrease in lost production with the costlier O&M options results in an overall annual O&M cost decrease from strategy 1 to 3.

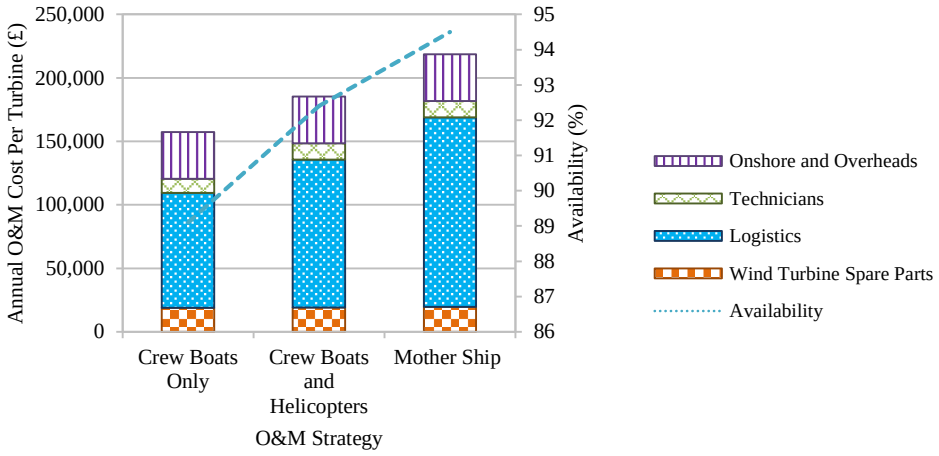

Figure 80. ECUME break down of annual O&M cost per turbine without loss of production and availability for wind farm N

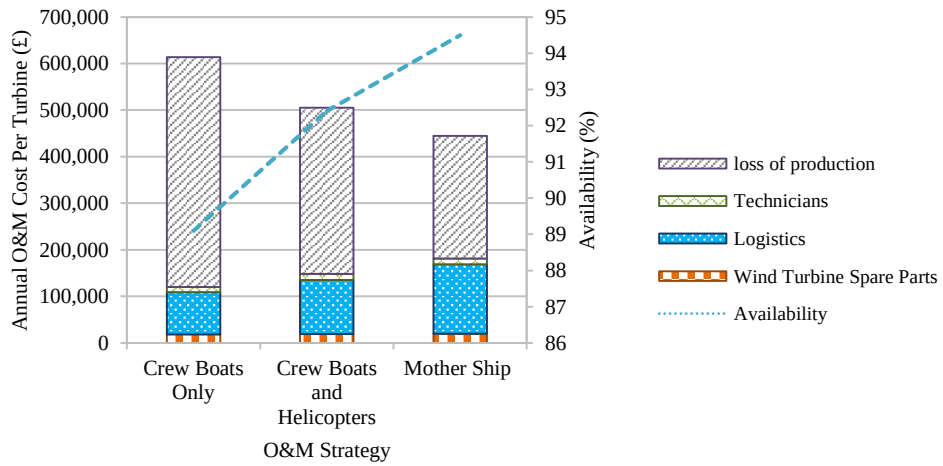

Figure 81. ECUME break down of annual O&M cost per turbine with loss of production and availability included for wind farm N

6.2.3 StraPCost+ Results

Table 72 to Table 74 show the results from StraPCost+ with the stated input settings for the three transportation strategies. As in Section 6.1, the costs are shown at wind turbine level for better comparison with ECUME.

Table 72. StraPCost+ results for wind farm N for transportation strategy 1: crew boats only

	Reactive Maintenance	Condition-based Maintenance	Change due to CM	Change/ Baseline
downtime	13.6 days	11.5 days	-2.1 days	-15.40%
availability	96.3 %	96.9 %	0.6 %	0.60%
capacity factor	34.5 %	34.9 %	0.4 %	1.12%
energy lost	1421.2 MWh	1149.2 MWh	-272.0 MWh	-19.14%
mean power generated over year	2.76 MW	2.79 MW	0.03 MW	1.12%
total annual energy generated	24184.6 MWh	24456.6 MWh	272.0 MWh	1.12%
annual revenue	4474.2 £k	4524.5 £k	50.3 £k	1.12%
revenue lost	262.9 £k	212.6 £k	-50.3 £k	-19.14%
annual maintenance cost	288.7 £k	253.2 £k	-35.5 £k	-12.30%
entire wind farm annual maintenance cost	37.1 £m	30.6 £m	-4.3 £m	-11.58%
vessel cost	111.637 £k	98.438 £k	-13.199 £k	-11.82%
wage cost	26.1733 £k	22.9444 £k	-3.2289 £k	-12.34%
component cost	150.8695 £k	131.7845 £k	-19.0850 £k	-12.65%
Total O&M cost (w/o revenue loss)	288.680 £k	253.167 £k	-35.513 £k	-12.30%
revenue lost	262.920 £k	212.596 £k	-50.323 £k	-19.14%
Total O&M cost (with revenue loss)	551.60 £k	465.76 £k	-85.837 £k	-15.56%
Entire wind farm revenue loss	31,813.28 £k	25,724.16 £k	-6,089.13 £k	-19.14%
Entire wind farm total O&M cost (w/o revenue loss)	34,930.25 £k	30,633.16 £k	-4,297.09 £k	-12.30%

Table 73. StraPCost+ results for wind farm N for transportation strategy 2: crew boat and helicopter

	Reactive Maintenance	Condition-based Maintenance	Change due to CM	Change/ Baseline
downtime	11.6 days	9.7 days	-1.8 days	-15.84%
availability	96.8 %	97.3 %	0.5 %	0.52%
capacity factor	34.9 %	35.3 %	0.3 %	0.93%
energy lost	1119.7 MWh	892.8 MWh	-226.9 MWh	-20.26%
mean power generated over year	2.80 MW	2.82 MW	0.03 MW	0.93%
total annual energy generated	24486.1 MWh	24713.0 MWh	226.9 MWh	0.93%
annual revenue	4529.9 £k	4571.9 £k	42.0 £k	0.93%
revenue lost	207.1 £k	165.2 £k	-42.0 £k	-20.26%
annual maintenance cost	309.0 £k	274.3 £k	-34.8 £k	-11.25%
entire wind farm annual maintenance cost	39.6 £m	33.2 £m	-4.2 £m	-10.63%
vessel cost	134.891£k	122.191 £k	-13.199 £k	-9.42%
wage cost	23.2886£k	20.3049 £k	-3.2289 £k	-12.81%
component cost	150.8695£k	131.7845 £k	-19.0850 £k	-12.65%
Total O&M cost (w/o revenue loss)	309.049£k	274.280 £k	-35.513 £k	-11.25%
revenue lost	207.143£k	165.170 £k	-50.323 £k	-20.26%
Total O&M cost (with revenue loss)	516.19£k	439.45 £k	-85.837 £k	-14.87%
Entire wind farm revenue loss	25,064.32£k	19,985.56 £k	-6,089.13 £k	-20.26%
Entire wind farm total O&M cost (w/o revenue loss)	37,394.92£k	33,187.87 £k	-4,297.09 £k	-11.25%

Table 74. StraPCost+ results for wind farm N for transportation strategy 3: mother ship only

	Reactive Maintenance	Condition-based Maintenance	Change due to CM	Change/ Baseline
downtime	10.2 days	8.8 days	-1.4 days	-14.01%
availability	97.2 %	97.6 %	0.4 %	0.40%
capacity factor	35.3 %	35.5 %	0.2 %	0.58%
energy lost	840.6 MWh	696.4 MWh	-144.2 MWh	-17.16%
mean power generated over year	2.83 MW	2.84 MW	0.02 MW	0.58%
total annual energy generated	24765.2 MWh	24909.4 MWh	144.2 MWh	0.58%
annual revenue	4581.6 £k	4608.2 £k	26.7 £k	0.58%
revenue lost	155.5 £k	128.8 £k	-26.7 £k	-17.16%
annual maintenance cost	456.2 £k	421.6 £k	-34.5 £k	-7.57%
entire wind farm annual maintenance cost	57.4 £m	51.0 £m	-4.2 £m	-7.28%
vessel cost	284.51£k	270.97 £k	-13.54 £k	-4.76%
wage cost	20.80£k	18.90 £k	-1.90 £k	-9.15%
component cost	150.87£k	131.78 £k	-19.09 £k	-12.65%
Total O&M cost (w/o revenue loss)	456.18£k	421.65 £k	-34.53 £k	-7.57%
revenue lost	155.52£k	128.83 £k	-26.68 £k	-17.16%
Total O&M cost (with revenue loss)	611.70£k	550.48 £k	-61.21 £k	-10.01%
Entire wind farm revenue loss	18,817.56£k	15,588.91 £k	-3,228.65 £k	-17.16%
Entire wind farm total O&M cost (w/o revenue loss)	55,197.73£k	51,316.74 £k	-4,178.12 £k	-7.57%

6.2.4 Discussion

The discussion focus on the results from the three transportation strategies, the subsystem contribution to the reactive maintenance costs, the comparison of reactive maintenance costs calculated by ECUME, and effect of the condition-based maintenance.

6.2.4.1 Comparison among the transportation strategies within StraPCost+

The comparison of the transportation strategies covers two main aspects: the wind turbine operation and the costs. From the wind turbine operational perspective, Table 72 to Table 74 show that a higher cost transportation strategy results in reduced downtime for both reactive and condition-based maintenance. There is also a small increase in availability, capacity factor, mean power generated and total annual energy generated. Energy lost, on the other hand, shows a dramatic decrease with more expensive transportation strategies. With more expensive transportation strategies,

annual revenue, annual maintenance cost and thus the entire wind farm annual maintenance cost increases.

Table 75 shows the percentage change between different transportation strategies. The changes are small for most of the cost model results; the exceptions are the annual maintenance cost (per turbine) and the entire wind farm annual maintenance cost. Take reactive maintenance as an example, the annual maintenance cost percentage increase from strategy 1 (£288.7k) to strategy 2 ((£309.0k) is 7%; while the percentage increase from strategy 2 to strategy 3 (£456.2) is 47%. Similarly, for condition-based maintenance, the annual maintenance cost at both turbine level and entire wind farm level sees around an 8% increase from strategy 1 to 2, and 53% increase from strategy 2 to 3. These trends also apply to the total O&M cost per turbine without revenue loss.

Most costs items change by similar amounts, except vessel cost which shows a 20.8% increase from strategy 1 to strategy 2 and a 110.9% increase from strategy 2 to strategy 3 for reactive maintenance, and 24.1% and 121.8% respectively for condition-based maintenance. Wage cost shows for both cases an 11% decrease with reactive maintenance with 11.5% and 6.9% for condition-based maintenance. Component costs are unaffected by operational maintenance strategy. Revenue lost shows a 21.2% decrease from transportation strategy 1 to strategy 2 and a 24.9% increase from strategy 2 to strategy 3 for reactive maintenance, and both around 22% for condition-based maintenance.

From the comparison of transportation strategies, it can be seen that the benefits and costs steadily increase with application of more expensive transportation strategies. The vessel costs are the only drawback for upgrading to strategy 3, where vessel cost

increases by over 110% for both reactive and condition-based maintenance and results in a 50% increase in O&M costs. In this circumstance, upgrade to strategy 2 seems to be a more economic choice with a 7% to 8% increase in total O&M costs. Further discussion that supports of reactive maintenance can be found in Figure 83 and Figure 84 in Section 6.2.4.3.

Table 75. Cost changes for transportation strategies relative to the lower-cost strategy for wind farm N

	Reactive maintenance		Maintenance-based maintenance	
	Strategy 1 to Strategy 2	Strategy 2 to Strategy 3	Strategy 1 to Strategy 2	Strategy 2 to Strategy 3
downtime	-14.8%	-11.5%	-15.7%	-9.3%
availability	0.6%	0.4%	0.4%	0.3%
capacity factor with downtime	1.2%	1.1%	1.1%	0.6%
energy lost	-21.2%	-24.9%	-22.3%	-22.0%
mean power generated over year with downtime	1.2%	1.1%	1.1%	0.7%
total annual energy generated with downtime	1.2%	1.1%	1.0%	0.8%
annual revenue with downtime	1.2%	1.1%	1.0%	0.8%
revenue lost	-21.2%	-24.9%	-22.3%	-22.0%
annual maintenance cost	7.1%	47.6%	8.3%	53.7%
entire wind farm annual maintenance cost	6.6%	45.0%	8.5%	53.6%
vessel cost	20.8%	110.9%	24.1%	121.8%
wage cost	-11.0%	-10.7%	-11.5%	-6.9%
component cost	0.0%	0.0%	0.0%	0.0%
Total O&M cost (w/o revenue loss)	7.1%	47.6%	8.3%	53.7%
revenue lost	-21.2%	-24.9%	-22.3%	-22.0%
Total O&M cost (with revenue loss)	-6.4%	18.5%	-5.6%	25.3%
Entire wind farm revenue loss	-21.2%	-24.9%	-22.3%	-22.0%
Entire wind farm total O&M cost (w/o revenue loss)	7.1%	47.6%	8.3%	54.6%

6.2.4.2 Subsystem contribution to maintenance cost

Figure 82 shows the contributions to maintenance cost by subsystem for the three transportation strategies. To assist the analysis, Table 76 lists the contribution in order from the largest to smallest in reactive maintenance. It shows absolute costs depending on the percentage contribution and the absolute total annual maintenance cost of each strategy.

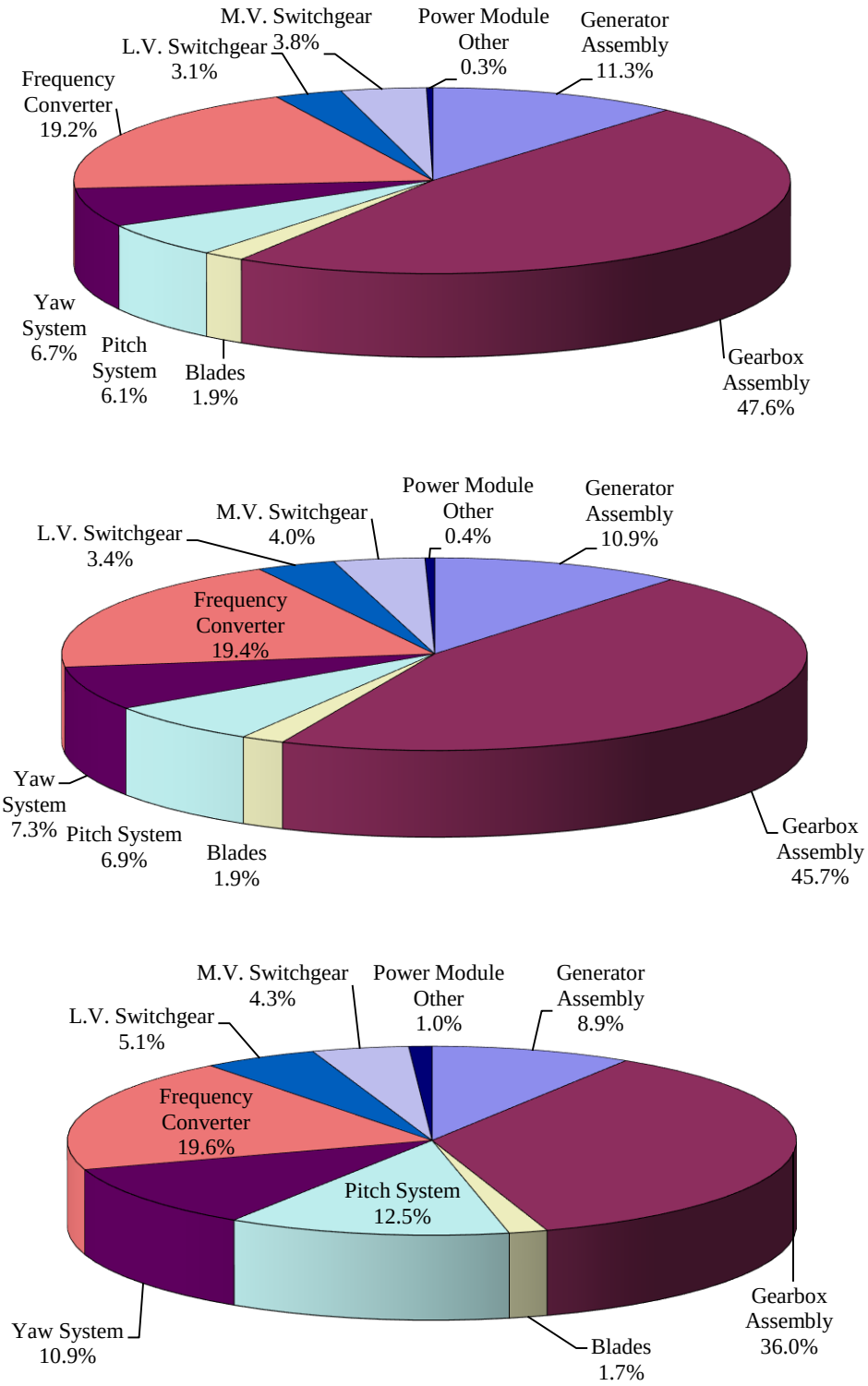

Figure 82. StraPCost+ baseline contributions to maintenance cost by subsystem for wind farm N with transportation strategy 1(upper), 2(middle) and 3(lower)

According to the results in Table 72 to Table 74, the annual maintenance costs at wind turbine level are £288.7k, £309.0k and £456.2k for the three transportation options. By combining the absolute wind turbine level cost with the percentage contribution, a quantitative view of the cost contribution based on subsystems for the baseline reactive maintenance is provided.

Interestingly, the ranking of the subsystem maintenance cost contribution remains the same but the contributions vary with different transportation strategies. As shown in Figure 82, for all transportation strategies, the gearbox assembly has the highest proportion of the entire turbine level maintenance cost. With more expensive transportation strategies, this portion becomes smaller. The gearbox assembly with the cheapest strategy 1 takes almost half (47.6%) of the total cost. This proportion reduces to 45.7% for strategy 2 and 36% for the most expensive strategy 3. However, even though the percentage proportion reduces, the absolute cost values increase with more expensive transportation strategies: £137.4k, £141.2k and £164.2k, as shown in Table 76. This also applies to generator assembly with 11.3%, 10.9% and 8.9% for the three strategies, with the corresponding absolute values being £32.6k, £33.7k and £40.6k.

Table 76. Annual maintenance cost contribution by subsystem in StraPCost+ for reactive maintenance of wind farm N ordered by share of total cost; total cost highlighted in the top row

	Contribution			Absolute costs (£k)		
	strategy1	strategy2	strategy3	strategy1	strategy2	strategy3
total cost				288.7	309	456.2
Gearbox assembly	47.60%	45.70%	36.00%	137.42	141.21	164.23
frequency converter	19.20%	19.40%	19.60%	55.43	59.95	89.42
generator	11.30%	10.90%	8.90%	32.62	33.68	40.6
yaw system	6.70%	7.30%	10.90%	19.34	22.56	49.73
pitch system	6.10%	6.90%	12.50%	17.61	21.32	57.03
M. V. Switchgear	3.80%	4.00%	4.30%	10.97	12.36	19.62
L. V. Switchgear	3.10%	3.40%	5.10%	8.95	10.51	23.27
blades	1.90%	1.90%	1.70%	5.49	5.87	7.76
power module	0.30%	0.40%	1.00%	0.87	1.24	4.56

On the other hand, it can be observed that the contribution of frequency converter does not change much with transportation strategies. This is because, although this electronic subsystem fails frequently, maintenance can be undertaken relatively easily, using the cheapest transportation such as crew boat for strategy 1 and 2. However, when it comes to strategy 3, the cheapest option is the mother ship which is much more expensive than a crew boat, so the cost contribution is slightly higher. This effect can be seen more clearly with other electronic subsystems such as M.V. Switchgear, L.V. Switchgear and the power module.

This jump change with strategy 3 can be also observed clearly in mechanical subsystems. Pitch system shows the most dramatic increase with the upgrade of the transportation strategies. It doubles the proportions in strategy 1 (6.1%) and 2 (6.9%), and takes 12.5% with strategy 3. For yaw system, the jump can also be seen clearly as 6.7%, 7.3% and 10.9%.

Another reason for this step change is the different vessel weather tolerance. The waiting time for the turbine subsystems is also different. The effect of waiting time is more obvious with unscheduled vessel usage as in reactive maintenance. For heavy subsystems, weather waiting time is markedly longer for vessels that have low weather tolerance, and where the vessel schedule time requirement is longer. Moreover, longer waiting time can also cause consequential subsystem failure. With the current settings, more expensive transportation has higher weather tolerance, and the maintenance waiting time is shorter. There is therefore a trade-off between vessel cost and the economic benefit resulting from higher weather tolerance.

One more interesting point to be noticed is that compared with wind farm T in Section 6.1, the order of the contribution for each subsystem is almost the same. The only difference is the sequence of pitch system and yaw system. Since the wind farms in the two case studies are quite different, it seems that the cost ranking of subsystem maintenance reflects their respective failure rates, even where the weather statistics of the sites are different.

6.2.4.3 Baseline comparison with ECUME for the three transportation strategies

Table 77 compares selected significant turbine level results at wind farm level from ECUME and StraPCost+.

StraPCost+ presents higher availability than ECUME, but this difference decreases with the application of more expensive transportation strategies. At the same time, StraPCost+ shows around 60% lower energy lost than ECUME, and the difference decreases with the application of more expensive transportation, and this is reflected in revenue loss, for example £230.1k (47%) less with crew boats strategy, and £148.9k (41%) with the mother ship.

For annual O&M cost, StraPCost+ estimates £130.9k (83%) more with crew boats only, £123.6k (67%) more with boats and helicopters and £237.7k (109%) more with mother ship only strategy than ECUME. For the entire wind farm annual maintenance cost, StraPCost+ presents £18.1m (95%) more for crew boats only, £17.2m (77%) for crew boats with helicopter and £31.0m (117%) for mother ship only.

There is no simple relationship between results from StraPCost+ for wind turbine level annual O&M cost and the entire wind farm maintenance cost and those from ECUME. This is most likely due to different approaches to whole wind farm cost calculation.

Table 77. Comparison of results from ECUME and StraPCost+

	Crew boats only			Crew boats with helicopter			Mother ship only		
	StraPCost+	ECUME	Diff	StraPCost+	ECUME	Diff	StraPCost+	ECUME	Diff
Availability (%)	96.3	89.1	7.2	96.8	92.4	4.4	97.2	94.5	2.7
Energy lost (MWh)	1421.2	3586.7	-2165.5	1119.7	2592.0	-1472.3	840.6	1910.4	-1069.8
Revenue lost (£k)	262.9	493	-230.1	207.1	356	-148.9	155.5	263	-107.5
Annual O&M cost (£k)	288.7	157.8	130.9	309.0	185.4	123.6	456.2	218.5	237.7
Entire wind farm annual maintenance cost (£m)	37.1	19.0	18.1	39.6	22.4	17.2	57.4	26.4	31.0

The comparison of annual O&M cost with reactive maintenance can usefully be split into two groups: one with onshore costs and overheads alone (i.e. without revenue loss), as in Figure 80 and Figure 83; the other with revenue loss only, as shown in Figure 81 and Figure 84. Since onshore costs and overheads are not calculated in StraPCost+, here for comparison integrity it uses the same assumption from ECUME for each transportation strategy in Figure 83.

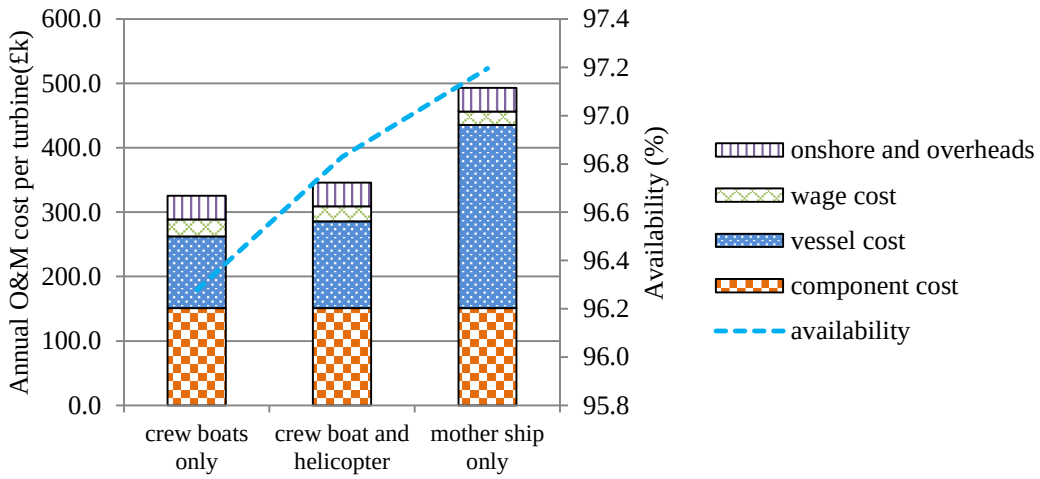

Figure 83. StraPCost+ break down of annual O&M cost per turbine without revenue loss and availability in wind farm N

Compared to Figure 80, supported by results in Table 71 and Table 72 to Table 74, the overall annual O&M costs per turbine in StraPCost+ as in Figure 83 are generally much higher than those from ECUME for all transportation strategies. The overall annual O&M costs per turbine in ECUME are in the range from £150k to £250k for all three strategies, while in StraPCost+, this range is £300k to £500k.

Actual experience from wind farm T indicates the annual O&M cost per turbine to be in the range of £150k to £250k. Since wind farm T is located much closer to its vessel base (1.5km) than wind farm N (59km) considerably higher O&M costs would be expected for wind farm N, suggesting that ECUME projections are too low and those from StraPCost+ is more reasonable.

As already explored choice of transportation option can significantly affect the costs. The overall annual O&M costs without loss of production from ECUME in Figure 80 show a steady increase from the cheapest to the most expensive transportation strategy, whereas the corresponding values from StraPCost+ in Figure 83 are more sensitive to the mother ship option than the other two strategies. Since the cost items onshore and overheads, wage cost and component cost do not change much with the three transportation strategies; the overall annual O&M costs without loss of production are generally in proportion to the vessel costs.

When considering the O&M cost with revenue loss, the result from ECUME in Figure 81 shows rigid decrease with the upgrade of the transportation strategy, and the breakdown of the cost shows loss of production (revenue loss) and logistics (vessel cost) take the majority of the cost where loss of production can be almost 5/6 of the total cost and as almost 5 times high as logistics, which can hardly be the real case;

while StraPCost+ shows a more reliable result. With more realistic breakdown of the sub-costs, Figure 84 shows that although strategy 1 shows the lowest O&M cost without revenue loss, strategy 2 shows the lowest with revenue loss.

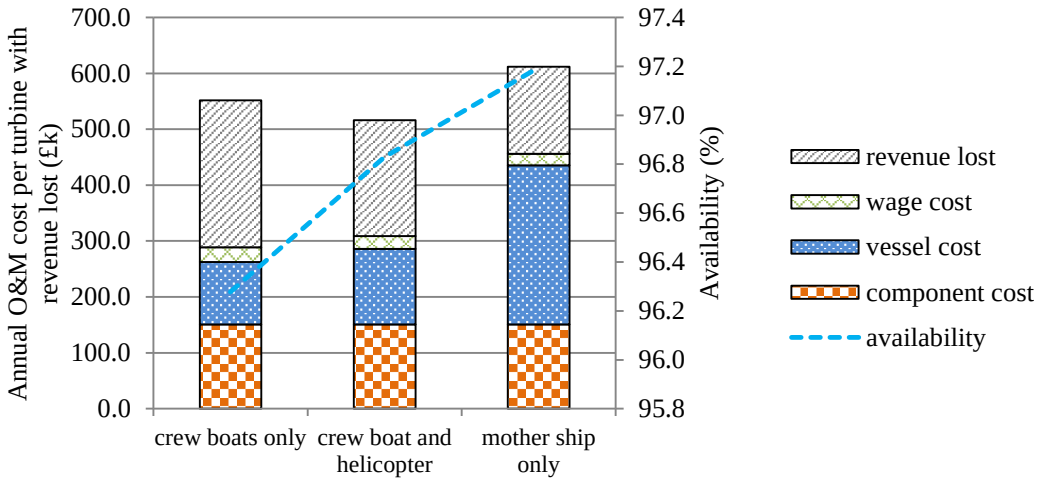

Figure 84. StraPCost+ break down of annual O&M cost per turbine with revenue loss and availability for wind farm N

More specifically, logistics (vessel cost) make a greater contribution to the annual O&M cost without revenue loss but with onshore and overheads with ECUME than those with StraPCost+. As shown in Table 78 and Table 79, the vessel cost accounts for 34.3%, 39.0% and 57.7% of O&M cost for the three transportation strategies with StraPCost+ but 57.5%, 62.8% and 68.4% with ECUME. The vessel costs from StraPCost+ are 10%-24% less than in ECUME. Component cost, in contrast, accounts for a larger proportion in StraPCost+ than in ECUME.

When it comes to annual O&M cost with revenue loss without onshore and overheads, the two cost models show distinct differences. Even though both cost models show that revenue loss accounts for an important part of overall O&M cost, the impact is very different. StraPCost+ shows the proportions are 47.7%, 40.1% and 25.4% of total costs, whilst ECUME estimates are almost double these, at 80.4%, 70.6% and 59.1%,

respectively. On the other hand, StraPCost+ sees dramatically more proportion in component cost than ECUME. ECUME only sees 3.1%, 3.8% and 4.4% out of total cost, while StraPCost+ shows 27.4%, 29.2% and 24.7%, separately.

In contrast to the reduction of annual O&M cost and revenue loss resulting from the upgrade of the transportation strategy as calculated by ECUME, StraPCost+ indicates that strategy 2 with crew boat and helicopter presents the lowest annual O&M cost (with revenue loss). The most expensive strategy 3 (mother ship only) presents the highest corresponding annual O&M cost. The reason of this is the high sensitivity to the mother ship only strategy to vessel cost and the overall O&M cost in StraPCost+, whilst the decrease of revenue loss with the three strategies is not as dramatic.

From this comparison, it can be seen that StraPCost+ suggests that strategy 2 is the most cost effective way when considering the revenue loss, while ECUME suggests that strategy 3 is best.

Table 78. Breakdown of overall annual O&M cost with StraPCost+ for wind farm N

StraPCost+	proportion to O&M cost w/o revenue loss			proportion to O&M cost with revenue loss without onshore and overheads		
	Crew Boats Only	Crew Boats and Helicopters	Mother Ship	Crew Boats Only	Crew Boats and Helicopters	Mother Ship
vessel cost	34.3%	39.0%	57.7%	20.2%	26.1%	46.5%
wage cost	8.0%	6.7%	4.2%	4.7%	4.5%	3.4%
component cost	46.4%	43.6%	30.6%	27.4%	29.2%	24.7%
revenue lost	-	-	-	47.7%	40.1%	25.4%
onshore and overheads	11.3%	10.6%	7.5%	-	-	-

Table 79. Breakdown of overall annual O&M cost with ECUME for wind farm N

ECUME	proportion to O&M cost w/o revenue loss			proportion to O&M cost with revenue loss without onshore and overheads		
	Crew Boats Only	Crew Boats and Helicopters	Mother Ship	Crew Boats Only	Crew Boats and Helicopters	Mother Ship
vessel cost	57.5%	62.8%	68.4%	14.8%	23.0%	33.6%
wage cost	7.0%	7.0%	5.8%	1.8%	2.6%	2.9%
component cost	11.9%	10.4%	9.0%	3.1%	3.8%	4.4%
revenue lost	-	-	-	80.4%	70.6%	59.1%
onshore and overheads	23.3%	19.8%	16.8%	-	-	-

6.2.4.4 Effect of condition-based maintenance

Figure 85 shows the comparison of reactive maintenance and condition-based maintenance results from StraPCost+. As in Section 6.1, the "total cost" is the total O&M cost per turbine. Table 80 lists the percentage changes that result from condition-based maintenance.

From all three graphs in Figure 85, it can be seen that condition monitoring reduces costs and revenue losses irrespective of the transportation strategy used. The graphs and table shows that the cheaper the transportation strategy, more costs are reduced due to the condition monitoring in comparison with reactive maintenance. It also seems that the reduction in total component cost is not affected by the choice of transportation strategy.

More expensive transportation strategies reduce the impact of condition based maintenance. This is because the cheaper transportation strategy requires a longer waiting time for the unscheduled vessel usage due to its relatively low weather tolerance. In this situation, scheduled maintenance underpinned by condition monitoring can improve the timing of maintenance and thereby reduce the waiting time. More expensive transportation strategies, on the other hand, have higher weather tolerance and thus reduce the cost difference. Even here condition monitoring is clearly beneficial.

It suggests that the condition monitoring system can reduce the overall O&M cost from 10% to 15.6%, with exact reduction values from £34,500 to £35,500 for this wind farm per turbine per year. Considering the cost for CM and SCADA device of generally

£6,300-12,700 with 8MW turbines as introduced in Chapter 2, the CM system has shown the net reduced cost of £21,800-29,200 per annum per turbine.

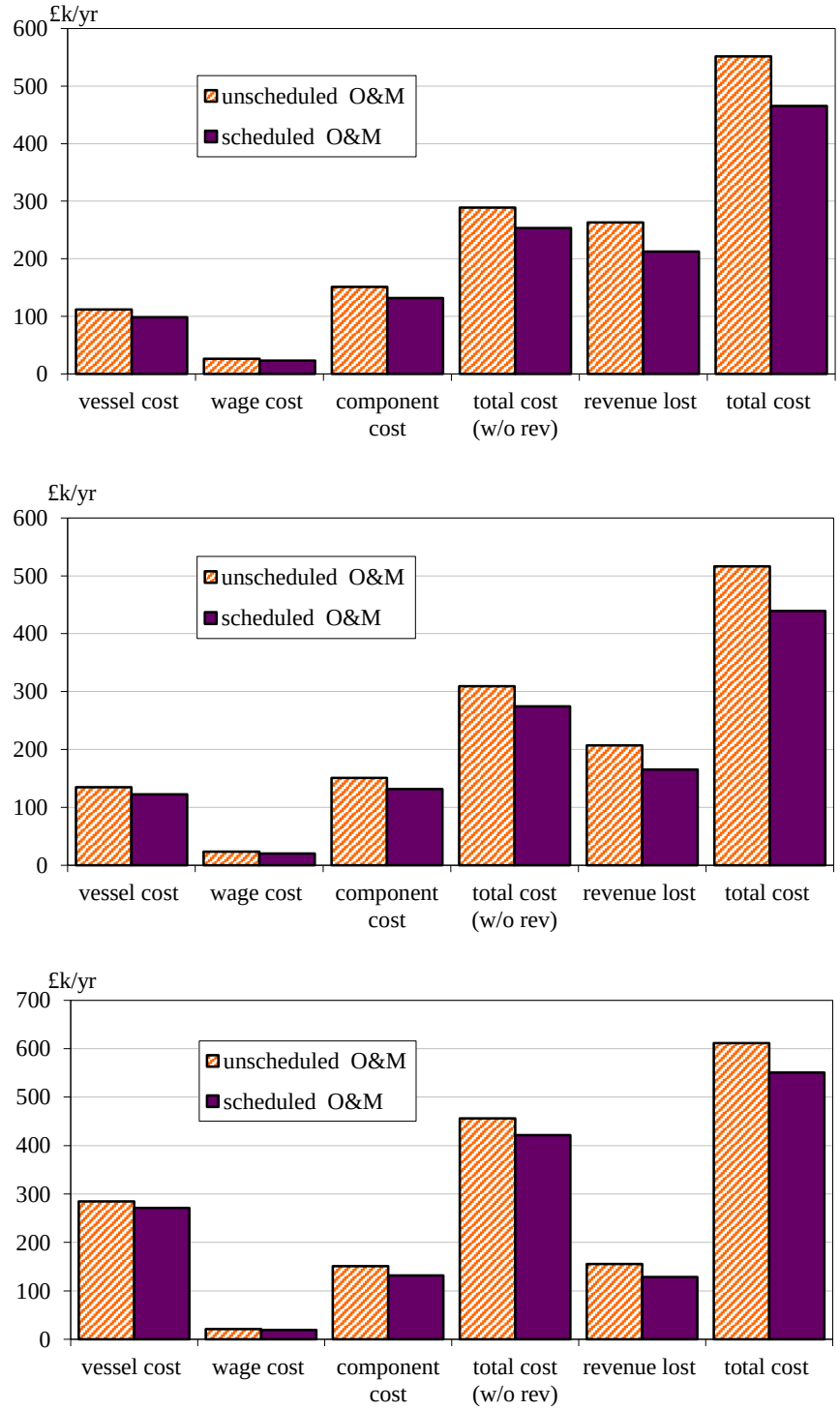

Figure 85. StraPCost+ expected annual contributions to O&M cost in unscheduled and scheduled maintenance for transportation strategy 1(upper), 2(middle) and 3(lower) for wind farm N

Table 80. The percentage changes due to condition monitoring as calculated with StraPCost+ for wind farm N

	Strategy1	Strategy2	Strategy3
vessel cost	-11.8%	-9.4%	-4.8%
wage cost	-12.3%	-12.8%	-9.2%
component cost	-12.7%	-12.7%	-12.7%
Total O&M cost (w/o revenue loss)	-12.3%	-11.3%	-7.6%
revenue lost	-19.1%	-20.3%	-17.2%
Total O&M cost (with revenue loss)	-15.6%	-14.9%	-10.0%

6.2.5 Conclusion

This section has examined operational costs for a large planned wind farm. Different transportation strategies have been assessed and the results from StraPCost+ and the commercial model ECUME are compared and discussed. This impact of condition monitoring has been analysed using both models and for a range of transportation strategies.

Both cost models agree that turbine availability increases with the cost of the transportation strategy, whilst energy loss decreases. Comparison with the results for wind farm T together with actual operational experience suggests that StraPCost+ is more reliable than ECUME for wind farm N.

Overall, StraPCost+ suggests the application of crew boats and helicopters is the most economic transportation strategy for both reactive and condition-based maintenance, whilst the most expensive strategy with mother ship is the least attractive. ECUME, on the other hand, shows proportionate decrease of the overall O&M cost with revenue loss, and it suggests that the most expensive strategy with mother ship is the most cost effective strategy, whilst the cheapest strategy results in the highest overall operational costs.

The models differ in other regards. With StraPCost+ component costs contribute significantly to the overall O&M cost, whilst for ECUME revenue loss is much more important. ECUME also shows higher proportion of vessel cost in the total O&M cost than StraPCost+.

With its innovative capability to investigate condition-based maintenance, StraPCost+ suggests that the condition monitoring system can reduce the overall O&M cost from 10% to 16%, with exact reduction values from £21,800-29,200 after deducting the annual cost of CM device and service for this wind farm per turbine per year.

StraPCost+ also calculates the component and subsystem contributions to maintenance cost for wind farm N to rank in a similar way of wind farm T, although the actual values are of course different. Both wind farms see gearbox assembly, frequency converter and generator account for highest costs.

Chapter 7 Conclusion and Future work

This thesis has developed a series of methods that together provide a methodical approach to assessing the capability of wind turbine condition monitoring to reduce the cost of offshore windfarm operations and maintenance. Specifically, it has created a methodology to investigate the reliability of offshore wind turbines based on a failure rate translator from onshore to offshore, improved a cost model with real case comparison to other cost models, and finally applied this improved cost model to provide a cost effectiveness analysis for a number of offshore wind farms. One of the highlights in the cost effectiveness analysis is the attention given to condition-based maintenance.

Chapter 2 presented the relevant literature reviews. It firstly reviewed wind energy development, compared onshore and offshore wind farms, and discussed offshore wind energy development in Europe and the UK.

This chapter then introduced the supplication of condition monitoring to wind energy generation, and discussed the benefits, performance and costs of such systems. It shows a general trend that the cost of condition monitoring system is gradually decreasing. The chapter has thoroughly listed the condition monitoring techniques from both data acquisition and data processing algorithm perspectives. It was concluded that there was a lack of data demonstrating the performance of these condition monitoring approaches.

This chapter also reviewed wind turbine component failure rate data and contrasted onshore and offshore operation. It was noted that the failure rate data are rarely

accessible, especially for the offshore ones, and this motivates the creation of an approach to compensate for this using onshore data.

Chapter 3 introduced specific onshore and offshore wind farms for which data was available. An investigation including a wind resource assessment (wind rose and wind speed distribution), turbine availability, capacity factor, array efficiency and operational characteristics was undertaken. It has showed that the array efficiency of the investigated wind farm is higher or equal to other large existing offshore wind farms in Europe.

This chapter also developed a methodology of yaw and turbine nacelle direction sensor error identification using SCADA data, and applied it to two offshore wind farms. For wind farm T, with the results from the time-based animation of the yaw direction, time series of yaw angle, time series of power output, and the power curve-cosine-cubed law analysis, it has suggested that a number of turbines are having turbine nacelle direction sensor error rather than actual yaw problems. For wind farm L, additional mathematical techniques have been applied, in terms of a direction-based animations, wake loss alignment test and correlation analyses. It highlighted potential turbine nacelle direction sensor problems, and also gave the bias angles for specific time ranges.

In future work, met mast data of wind farm T and yaw error measured by nacelle wind vanes which were not available for analysis are expected to be provided and analysed. Data of higher sampling frequency is also expected to be helpful for accurate analysis and diagnosis, and would be beneficial for further wake losses studies.

Chapter 4 investigated offshore wind turbine component reliability. In this chapter, an innovative failure rate translator from onshore to offshore has been created to overcome the lack of offshore failure rate data. The translator calculates the environmental factors from onshore to offshore by using a cumulative probability density (CPD) function method aiming to provide a reasonably generic onshore failure rate trend for key turbine components and subsystems. This chapter has compared different fitting functions to the staircase-shaped CPD, and finally selected a variation of exponential as the fitting function. This translation method, as a train of thought, has a wide potential and has been applied in the later research. However, at this stage, the only accessible failure data used for the translation procedure have limited the accuracy of the results. Some of the results seem counter-intuitive and should be checked when more extensive data becomes available.

An offshore Failure Modes Effect Analysis (FMEA) translation process is presented, based on the developed reliability data translation method. Even though FMEA has been applied to many traditional industries, it has not been used for offshore wind energy. This chapter calculated the Risk Priority Number (RPN) of each offshore turbine component or subsystem by translating the accessible onshore RPN in the public domain. It is the first time that a quantification of the risk ranking for offshore wind has been listed. From the results obtained in this chapter, control system becomes the highest risk element for an offshore wind turbine, followed by the rotor and blades (which is the highest risk subsystem onshore), and the main gearbox. The lowest risk subsystems are the mechanical brake and the main shaft assembly for both onshore and offshore wind. The risk ranking has an indicative meaning for offshore wind farm O&M strategy development.

In the future, the translator could consider more factors that influence failure rate in addition to wind speed and temperature, e.g. wind and wave turbulence. The database should be expanded to cover more wind farms and different turbine types. When available, longer averaging periods of environmental factor data should be investigated and used in addition to the daily mean values. In addition to the translation algorithm improvement stated above, from the FMEA and RPN perspective, future work should consider upgrading the simple multiplication calculation of the individual environmental factor translation ratios to provide a more sophisticated algorithm. The first step could be the application of weights to the ratios. With the results from Chapter 6, the RPN calculation which currently only considers the failure occurrence can be expanded into the failure severity. The condition monitoring detection effectiveness analyses in Chapter 5 also has an indicative meaning to the RPN calculation expansion into the failure *detectability*. This requires more accessible condition monitoring data from different devices for each component in the future.

Chapter 5 has introduced a probabilistic O&M cost model which innovatively contains the comparison of the effect of condition-based maintenance with the reactive maintenance. The chapter presents the methodology used by the cost model and its interfaces. The cost model provides a number of estimates covering wind turbine performance and wind farm O&M cost.

This chapter thoroughly reviewed other O&M cost models from the research and commercial domains, and compared these with the cost model developed in this thesis from the methodology perspective. This review and comparison has given an

important hint to improving the existing cost model. The improved model that has resulted is called StraPCost+.

The two most important improvements to StraPCost+ are the application of the failure rate translator developed in Chapter 4 and the expansion of the maintenance categories for both reactive and condition-based maintenance. With these improvements, StraPCost+ is expected to provide more credible and realistic estimates.

In order to test and verify the improved model, this chapter has also undertaken a case study comparison with other accessible cost models for a baseline case and also sensitivity to key parameters. It is concluded that shown that StraPCost+ provides reasonable and believable estimates.

Further verification analyses and applications have been undertaken with StraPCost+, with focus on the condition monitoring (CM) system detection effectiveness. This section has undertaken CM sensitivity analysis on how the condition monitoring system *detectability*, *pre-empt* (advance warning of failure) and *falsepos* (false positive) statuses affect the cost model results. It has shown that the cost models results are the most sensitive to *detectability* and least sensitive to the false positive rates. From the cost model result perspective, the availability and capacity factors have a positive correlation, while the remainder of the three cost model results have negative correlation to CM detection characteristics. This CM detection analysis has shown an indicative way of complete the RPN calculation in FMEA discussed in Chapter 4 by verification one of the three parameters: *detectability*. Of course, more accessible data on individual CM device are expected for the actual application in the future.

Wider sensitivity analyses have been undertaken with StraPCost+ including wind and wave parameters, weather window threshold for heavy (*A* and *B*) and light maintenance (*C*, *D* and *E*), overall turbine annual failure rate and distance to shore, together with the CM detection parameters analysed in the previous section. Among the five selected cost model results with eight sensitivity parameters, wind turbine availability and capacity factor show the most dramatic decreases along with the increase of the weather window threshold for heavy maintenance (*A* and *B*) for the adjustment below -30%. The wind and wave parameters show the highest impact on the first four selected cost model results, and CM *detectability* shows the highest impact on the revenue loss. Distance to shore and CM *falsepos* show low impact on all the five cost model results.

In the future, the cost model condition monitoring system detection rates from different CM devices can be improved from the simple addition calculation into a more sophisticated and realistic relationship. The false positive effectiveness can be improved with an advanced algorithm for more realistic condition-based maintenance estimation. The CM detection effectiveness analysis can be extended to subsystem level with different types of CM system. From the entire cost model perspective, the cost model can also consider the estimation on a wind farm level rather than a simple multiplication of the individual wind turbine estimations, and allow the vessel usage with multiple tasks at individual maintenance visit. Effects due to different seasons can also be considered by showing results on a seasonal basis.

The case studies in this chapter suggested that the time-based availability estimation of StraPCost+ is too optimistic and this needs to be investigated in the future work.

The current calculation related to the number of technicians in StraPCost+ is too simple which results in no interconnection with some of the cost model results, e.g. the time-based availability, and this can be improved in future. Some of the cost model results are currently having the same sensitivity with the CM detection, and some do not show any sensitivity to the default overall failure rate. The weather window threshold for light maintenance (*C*, *D* and *E*) shows inconsistent cost model results while other parameters show constant positive or negative impacts on all selected cost model results. These issues need to be investigated in the future work. In the future, more sensitivity parameters such as repair time and on land lead time etc. can be investigated. In addition, this model considers the percentage change of annual maintenance cost is equal to the O&M cost without revenue loss. This algorithm assumption works for rough estimation, but needs to be refined.

Chapter 6 presented case studies of StraPCost+ applications for an existing offshore wind farm, and also a wind farm in its planning phase. In the first wind farm case, data measured from different distances to shore are investigated and compared with the reactive maintenance results obtained in Chapter 5. This section has also provided a detailed investigation of the subsystem contribution to annual maintenance cost. It has shown that among all wind turbine subsystems, the gearbox assembly makes the largest contribution and power module makes the least. This subsystem contribution to total annual maintenance cost provides a useful ranking of the *consequence* of faults, another initial RPN calculation element as discussed in Chapter 4. The effect of the condition-based maintenance is another emphasis in this chapter section. It has shown a remarkable reduction in O&M cost and availability improvement due to the application of the condition-based maintenance. Deducting the annual CM device and

service costs, the reduction of O&M cost is in the order of £16,000-18,000 per annum per turbine.

The other case study in this chapter applied StraPCost+ to a planned large offshore wind farm. It proved the reliability of using StraPCost+ for helping decision making, in this case, for transportation strategy. With comparison of the commercial trusted O&M cost model, ECUME, it has suggested that StraPCost+ has provided more credible estimates. This chapter section confirmed the significant reduction of O&M cost due to condition monitoring system. With the same calculation of the component and subsystem contribution to maintenance cost as the previous case study, it has shown that even though the actual contribution values are different, both wind farms show gearbox assembly, frequency converter and generator account for highest costs. It has shown the O&M cost reduction due to the CM system is in the order of £20,000 per turbine per year deducting the annual cost of CM device and service (equivalent to 6.5% of the annual reactive maintenance cost per turbine per year).

In future work, as mentioned in Chapter 4, the results which support the subsystem failure *severity* can be added in the FMEA RPN calculation. It also needs to be investigated the phenomenon that the percentage change due to the application of condition based maintenance for wind farm T are the same for some of the cost model results in the sensitivity analyses, even though the absolute values are different. In the future, when more cost information of CM devices is available, the cost effectiveness of condition monitoring can be assessed in a more accurate manner. It is also worth investigating the impact and effectiveness of different types of condition monitoring systems.

Reference

[1] Operation and maintenance costs of wind generated power, *wind stats* vol.19, No.3, 2006.

[2] The crown estate, A guide to an offshore wind farm, [online] http://www.thecrownestate.co.uk/media/5408/ei-a-guide-to-an-offshore-wind-farm.pdf last access: 17th Feb 2016.

[3] The crown estate, A guide to UK offshore wind operations and maintenance, [online] http://www.thecrownestate.co.uk/media/5419/ei-km-in-om-om-062013-guide-to-uk-offshore-wind-operations-and-maintenance.pdf last access: 17th Feb 2016.

[4] Broehl J. et al, Executive Summary: World Wind Energy Market Update 2015—International Wind Energy Development: 2015-2019, A BTM Navigant wind report, *navigantresearch.com* [online] http://www.provedor.nuca.ie.ufrj.br/estudos/navigant1.pdf last access: 15th May 2016.

[5] Xinhua News Agency, Jiuquan Wind Power Base Completes First Stage, *China Daily*, 4th November, 2010. [online] http://www.chinadaily.com.cn/bizchina/2010-11/04/content_11502951.htm last access: 7th July 2015.

[6] Watts J., Winds of change blow through China as spending on renewable energy soars, *the Guardian*, 19th March 2012, [online] http://www.theguardian.com/world/2012/mar/19/china-windfarms-renewable-energy last access: 7th July 2015.

[7] Dong Energy, Burbo Offshore Wind Farm, [online] http://www.dongenergy.co.uk/uk-business-activities/wind-power/offshore-wind-farms-in-the-uk/burbo-bank-offshore-wind-farm, last access: 18th May 2016.

[8] Muppandal (India), *The Wind Power*, [online] http://www.thewindpower.net/windfarm_en_449_muppandal.php last access: 7th July 2015.

[9] EWEA, *The European offshore wind industry - key trends and statistics 2015*, February 2016.

[10] London Array, *4C offshore*, [online] http://www.4coffshore.com/windfarms/london-array-phase-1-united-kingdom-uk14.html, last access: 7th July 2015.

[11] Denholm-Hall R., World's second largest offshore wind farm opens off coast of Wales, *Wales online*, 18th June 2015.

[12] Top 10 biggest offshore wind farms, *power-technology.com*, 30th September 2013, [online] http://www.power-technology.com/features/feature-top-10-biggest-offshore-wind-farms-uk/ last access: 7th July 2015.

[13] Anholt, 4C Offshore, [online] http://www.4coffshore.com/windfarms/anholt-denmark-dk13.html last access: 7th July, 2015.

[14] West of Duddon Sands, *4C Offshore*, [online] http://www.4coffshore.com/windfarms/west-of-duddon-sands-united-kingdom-uk33.html last access: 7th July 2015.

[15] Walney 1 Offshore Wind Farm, *LORC knowledge*, [online] http://www.lorc.dk/offshore-wind-farms-map/walney-1 last access: 7th July 2015.

[16] Thornton Bank phase II, *4C Offshore*, [online] http://www.4coffshore.com/windfarms/thornton-bank-phase-ii-belgium-be09.html last access:7th July 2015.

[17] Thornton Bank phase III, *4C Offshore*, [online] http://www.4coffshore.com/windfarms/thornton-bank-phase-iii-belgium-be10.html last access: 7th July 2015.

[18] Sheringham Shoal, [online] http://www.scira.co.uk/ last access: 7th July 2015.

[19] Thanet, 4C Offshore, [online] http://www.4coffshore.com/windfarms/thanet-united-kingdom-uk29.html last access: 7th July, 2015.

[20] Moliona M. G. and Alvarez J. M. G., Technical and Regulatory Exigencies for Grid Connection of Wind Generation, Suvire G. O. (Ed.), *Wind Farm - Technical Regulations, Potential Estimation and Siting Assessment*, [Online]

http://www.intechopen.com/books/wind-farm-technical-regulations-potential-estimation-and-siting-assessment/technical-and-regulatory-exigencies-for-grid-connection-of-wind-generation last access: 11 Jan 2016.

[21] Enercon, [online] http://www.wwindea.org/technology/ch01/en/1_2_3_2.html, viewed March, 2013.

[22] Report on wind turbine gearbox and direct-drive systems out now, http://www.offshorewind.biz/2014/09/19/report-on-wind-turbine-gearbox-and-direct-drive-systems-out-now/ last access: 18 June 2016.

[23] McMillan D. and Ault G. W., Techno-Economic Comparison of Operational Aspects for Direct Drive and Gearbox-driven Wind Turbines, IEEE Trans. On Energy Conversion, vol. 25 (1), March 2010.

[24] Gamesa 5.0 MW Innovating for reliability, [online] http://www.gamesacorp.com/recursos/doc/productos-servicios/aerogeneradores/catalogo-g10x-45mw-eng.pdf last access: 11 Jan 2016.

[25] Castell D., Haliade 150-6MW Direct drive from concept to operation, battle of the drive trains, *EWEA conference*, Vienna 2013.

[26] Markard, J. and Petersen, R., The offshore trend: Structural changes in the wind power sector, *Energy Policy*, Vol. 37(9), Pages: 3545-3556, September 2009.

[27] EWEA, Operation and maintenance costs of wind generated power, *Wind Energy—the Facts*,[online] http://www.wind-energy-the-facts.org/operation-and-maintenance-costs-of-wind-generated-power.html last access: 7th July 2015.

[28] EWEA, *Wind in power—2015 European statistics*, February 2016.

[29] EWEA, *The European offshore wind industry - key trends and statistics 2014*, January 2015.

[30] Faulstich, S., Component reliability ranking with respect to WT concept and external environmental conditions, Deliverable WP7.3.3, WP7 Condition monitoring, *Project Upwind*, 2010.

[31] Neale M., *Guide to the condition monitoring of machinery*, Department of Trade and Industry, Dec 1979.

[32] Crabtree, C.J., Feng, Y. and Tavner, P.J., Detecting Incipient Wind Turbine Gearbox Failure: A Signal Analysis Method for Online Condition Monitoring, *Scientific Track Proceedings, European Wind Energy Conference 2010*, Warsaw, Poland, 2010.

[33] McMillan D. and Ault G., Quantification of Condition Monitoring Benefit for offshore Wind Turbines, *Wind Engineering*, Vol. 31, No.4, pp 267-285, 2007.

[34] Vibrotech reliability services, What are the benefits of condition monitoring, Offshore Europe 2011, [online] http://www.vibrotech.co.uk/benefits-condition-monitoring, last access: 8th July 2015.

[35] LeBlanc m. and Graves A., Condition Monitoring Systems: Trends and Cost Benefits, Garrad Hassan presentation, [online] http://www.nrel.gov/wind/pdfs/day1_sessioni_04_garradhassan_leblanc.pdf last access: 8th July 2015.

[36] PTC-Relex Durham University, Summary of Deliverable D 2.0.4—Whole System Reliability Model, *ReliaWind Project report*, 2011.

[37] Wilkinson M. and Darnell B. et al, Comparison of Methods for Wind Turbine Condition Monitoring with SCADA Data, *EWEA 2013*, 2013.

[38] Verbruggen T. W., Wind turbine operation & maintenance based on condition monitoring, *Wind Turbine Operation and Maintenance based on Condition Monitoring Final report*, ECN-C-03-047, April 2003.

[39] Hyers, R. W. and Mcgowan J. G. et al., Condition monitoring and prognosis of utility scale wind turbines, *Energy Materials: Materials Science and Engineering for Energy Systems*, Vol. 1 (3), pp: 187-203, 2006.

[40] Hameed, Z. and Hong Y. S. et al, Condition monitoring and fault detection of wind turbines and related algorithms: A review, *Renewable and Sustainable Energy Reviews*, Vol. 13 (1), pp: 1-39, January 2009.

[41] Apt J., The spectrum of power from wind turbines, *Journal of Power Sources* Vol. 169, pp: 369-374, March 2007.

[42] Murtagh P. J., Basu B. and Broderick B. M., Along-wind response of a wind turbine tower with blade coupling subjected to rotationally sampled wind loading, *Engineering Structures*, Vol. 27 (8), pp: 1209-1219, July 2005.

[43] Röbel, A, and Rodet X., Efficient spectral envelope estimation and its application to pitch shifting and envelope preservation, *Proc. of the 8th Int. Conference on Digital Audio Effects (DAFx'05)*, Madrid, Spain, September 20-22, 2005.

[44] Salem A. A., Abu-Siada A., and Islam S., Condition monitoring techniques of the wind turbines gearbox and rotor, *International Journal of Electrical Energy*, Vol. 2 (1), March 2014.

[45] Peng Z. K., Chu F. L. and Tse P. W., Singularity analysis of the vibration signals by means of wavelet Modulus Maximal method, *Mechanical Systems and Signal Processing*, Vol. 21 (2), pp:780-794, 2007.

[46] Baydar N. and Ball A., Detection of gear failures via vibration and acoustic signals using wavelet transform, *Mechanical Systems and Signal Processing*, Vol. 17 (4), pp:787-804, 2003.

[47] Guo, P., Wind turbine generator bearing Condition Monitoring with NEST method *Control and Decision Conference (CCDC), 2012 24th Chinese*, pp: 235–239, 23-25 May 2012.

[48] Wang, Y. and Infield D. G., SCADA Data Based Nonlinear State Estimation Technique for Wind Turbine Gearbox Condition Monitoring, *EWEA conference 2012*, Copenhagen, 2012.

[49] Leaney V. C., Sharpe D. J. and Infield D. G., The applicability of spatial analysis techniques to monitoring wind farms, *Proceedings of the European Wind Energy Conference*, Nice, France, pp: 216-219, 1-5 March 1999.

[50] Haykin S. O., *Neural Networks: A Comprehensive Foundation*, Prentice Hall, 1 December 1997.

[51] Baraldi P. and Compare, M. et al., Fatigue Crack Growth Prognostics by Particle Filtering and Ensemble Neural Networks. *First European conference of the prognostics and health management society 2012*, pp: 1-8, 2012.

[52] Mohandes M. A. and Halawani T. O. et al., Support vector machines for wind speed prediction, *Renewable Energy*, Vol. 29 (6), pp: 939-947, May 2004.

[53] Zeng J. W. and Qiao W., Support vector machine-based short-term wind power forecasting, *Power Systems Conference and Exposition (PSCE), 2011 IEEE/PES*, pp: 1-8, March 2011.

[54] Byon E. and Ntaimo L. et al, Wind energy facility reliability and maintenance, *Handbook of wind power systems*, part III, pp 639-672, Springer Berlin Heidelberg, 2013.

[55] Kusiak A. and Li W. Y., Short-term prediction of wind power with a clustering approach, *Renewable Energy*, Vol. 35 (10), pp: 2362-2369, October 2010.

[56] Ocak H and Loparo K. A. A new bearing fault detection and diagnosis Scheme based on Hidden Markov modeling of vibration signals. *Proceeding of IEEE ICASSP 2001*, Vol. 5, pp: 3141-3144, May 2001.

[57] Jafarzadeh, S. et al, Hour-ahead wind power prediction for power systems using Hidden Markov Models and Viterbi Algorithm, *Power and Energy Society General Meeting, 2010 IEEE*, pp:1-6, 25-29 July 2010.

[58] Ward K., et al, Modelling residual wind farm variability using HMMs, *18th World IMACS/MODSIM Congress*, Cairns, Australia, 13-17 July 2009.

[59] Márquez, F. P. G., et al., Condition monitoring of wind turbines: Techniques and methods, *Renewable Energy*, Vol. 46, pp: 169–178, October 2012.

[60] Caselitz P. and Giebhardt J., Fault prediction techniques for offshore wind farm maintenance and repair strategies, *Proceedings of the EWEC2003*, 2003.

[61] Caselitz P. and Giebhardt J., Rotor condition monitoring for improved operational safety of offshore wind energy converters, Transactions of the ASME, *Journal of Solar Energy Engineering*, Vol. 127(2), pp: 253-261, 2005.

[62] de Novaes Pires Leite G., Feitosa E.A., and Kraj A.G., Remote conditioning monitoring system for a hybrid wind diesel system-application at Fernando de Naronha Island, Brasil. [online] http://www.globalislands.net last access:5 Jan 2016.

[63] Giebel G. and Oliver G, et al, Common Access to wind turbines data for condition monitoring, *Proceedings of the 27th Risø International Symposiumon Material Science*, pp.157-164, Denmark, 2006.

[64] Ghoshal A. and Sundaresan M. J. et al, Structural health monitoring techniques for wind turbines blades, *Journal of Wind Engineering and Industrial Aerodynamics* Vol. 85, pp: 309-324, 2000.

[65] Hong J-C. and Kim Y. Y. et al, Damage detection using the Lipschitz exponent estimated by the wavelet transform: application to vibration modes of a Beam. *International Journal of Solids and Structures* Vol. 39 (7): 1803-1816, 2002.

[66] Tandon N, Nakra BC. Defect detection in rolling element bearings by acoustic emission method. *Journal of Acoustic Emission,* Vol. 9(1), pp: 25-28, 1990.

[67] Beattie A. G. Acoustic emission monitoring of a wind turbines blade during a fatigue test. *Proceeding AIAA Aerospace Sciences Meeting*, Nevada, Jan 6-9, 1997.

[68] Lu, B. et al, A review of recent advances in wind turbine condition monitoring and fault diagnosis, *IEEE Power Electronics and Machines in Wind Applications (PEMEA 2009)*, pp:1-7, 24-26 June 2009.

[69] Nienhaus, K. et al., Statistical and time domain signal analysis of the thermal behaviour of wind turbine drive train components under dynamic operation conditions, *Journal of Physics: Conference Series*, Vol. 364, 2012.

[70] Hamilton, A., Detailed State of the Art Review for the Different Online/Inline Oil Analysis Techniques in Context of Wind Turbine Gearboxes, *Journal of Tribology*, Vol.133 (4), 2011.

[71] Dempsey P. J., Certo J. M. and Morales W., Current status of hybrid bearing damage detection, *NASA/TM—2004-212882 and ARL–TR–3119*, 2004.

[72] Rossi, P. and Young, K. A., HIAC's Low Cost Online Contamination/Condition Monitor, *Machinery Lubrication*, [Online]

http://www.machinerylubrication.com/Read/2/online-contamination-monitor Last access: 6 Jan 2016.

[73] Wieland, G., and Fischer, K., *Water Determination by Karl-Fischer Titration: Theory and Practice*, GIT, Darmstadt, 1987.

[74] Stachowiak, G. W., and Batchelor, A. W., *Engineering Tribology*, Elsevier, Oxford, 2005.

[75] Viswanath, D. S. et al, *Viscosity of Liquids: Theory, Estimation, Experiment and Data*, Springer, Dordrecht, Netherlands, 2007.

[76] Lakowicz, J. R., *Topics in Fluorescence Spectroscopy*, Vol. 2, Plenum, Principle, New York, 1991.

[77] Mahon J. and Lynn T., Diagnostic Test for Water in Oil, DEXSIL DTR-22-01, [Online] http://www.dexsil.com/uploads/docs/dtr_22_01.pdf last assess: 7 Jan 2016.

[78] Foster, N. S. and Amonette, J. E. et al, Detection of Trace Levels of Water in Oil by Photoacoustic Spectroscopy, *Sensors and Actuators B: Chemical*, Vol. 77 (3), pp. 620–624, 2001.

[79] MICEPAS: Miniaturised-Cell-Enhanced PhotoAcoustic Spectroscopy, [online] http://www.micepas.basnet.by last access: 7 Jan 2016.

[80] Kerem D., Solid-state Viscometer for Oil Condition Monitoring, *Practicing Oil Analysis*, November Edition, 2004.

[81] Jansen E. B. M., Knipscheer J. H., and Nagtegaal, M., Rapid and Accurate Element Determination in Lubricating Oils Using Inductively Coupled Plasma Optical Emission Spectrometry, *Journal of Analytical Atomic Spectrometry*, Vol. 7(2), pp. 127–130, 1992.

[82] Wu, T. H., and Mao, J. H. et al, A New On-Line Visual Ferrograph, *Tribology Transactions*, Vol. 52(5), pp. 623–631, 2009.

[83] Myshkin, N. K. and Markova, L. V. et al, Wear Monitoring Based on the Analysis of Lubricant, 2003 Contamination by Optical Ferroanalyzer, *Wear*, Vol. 255(7), pp. 1270–1275, 2003.

[84] Miller R. L., Fraser L. M., and Winefordner, J. D., A Combination Flame Atomic Fluorescence-Atomic Emission dc Spectrometer for Analysis of Trace Wear Metals in Jet Engine Oils, *Applied Spectroscopy*, Vol. 25 (4), pp. 477–482, 1971.

[85] Iwai, Y. and Honda, T. et al, Quantitative Estimation of Wear Amounts by Real Time Measurement of Wear Debris in Lubricating Oil, *Tribology International*, Vol. 43(1–2), pp. 388–394, 2010.

[86] Sandler, M. P., Coleman, R. E., and Patton, J. A., *Diagnostic Nuclear Medicine*, Lippincott Williams & Wilkins, Philadelphia, 2003.

[87] Goldstein, J. and Newbury, D. et al, *Scanning Electron Microscopy and X-ray Microanalysis*, 3rd ed., Plenum, New York, 2003.

[88] Lord, C. J., Determination of Trace Metals in Crude Oil by Inductively Coupled Plasma Mass Spectrometry with Micro-emulsion Sample Introduction, *Analytical Chemistry*, Vol. 63 (15), pp. 1594–1599, 1991.

[89] Escobar, M. P., Smith, B. W., and Winefordner, J. D., Determination of Metallo-organic Species in Lubricating Oil by Electrothermal Vaporization Inductively Coupled Plasma Mass Spectrometry, *Analytica Chimica Acta*, Vol. 320 (1), pp: 11–17, 1996.

[90] Goncalves I. M., Murillo M., and Gonzalez A. M., Determination of Metals in Used Lubricating Oils by AAS using Emulsified Samples, *Talanta*, Vol. 47 (7), pp: 1033–1042, 1998.

[91] Yaroshchyk, P. and Morrison, R. J. S., et al, Quantitative Determination of Wear Metals in Engine Oils Using LIBS: the Use of Paper Substrates and a Comparison between Single- and Double-pulse LIBS, *Spectrochimica Acta Part B: Atomic Spectroscopy*, Vol. 60 (11), pp: 1482–1485, 2005.

[92] Butler D. E., The shock pulse method for the detection of damaged rolling bearings, *Non-Destructive Testing*, Vol. 6(2), pp: 92-95, 1973.

[93] Zhen L. and Zhengjia H. et al, Bearing condition monitoring based on shock pulse method and improved redundant lifting scheme, *Mathematics and Computers in Simulation*, Vol. 79(3), pp:318-338, 2008.

[94] Smith B. M., Condition monitoring by thermography, *NDT International*, Vol. 11(3), pp: 121-1222, 1978.

[95] Ciang, C. C., Lee J.-R. and Bang H.-J., Structural health monitoring for a wind turbine system: a review of damage detection methods, *Measurement Science and Technology*, Vol. 19(12), pp: 20, 2008.

[96] Castaings M. and Cawley P. et al, Single Sided Inspection of Composite Materials Using Air Coupled Ultrasound, *Journal of Non-destructive Evaluation,* Vol. 17(1), pp:37-45, 1998.

[97] Yang, S. Y. and Xiang D. W. et al, Condition Monitoring for Device Reliability in Power Electronic Converters: A Review, *IEEE transactions on Power Electronics*, Vol. 25 (11), pp: 2734-2752, Nov 2010.

[98] Raghavan A. and Cesnik C. E. S., Review of guided-wave structural health monitoring, *The Shock and Vibration Digest*, Vol. 39 (2), pp:91-114, 2007.

[99] Igarashi T. and Kato J. Studies on Vibration and Sound of Defective Rolling Bearings: Third Report, Vibration of Ball Bearing with Multiple Defects, *Bulletin of JSME*, Vol. 28 (237), pp: 492-499, 1985.

[100] Jasiunien E and Raiutis R et al, NDT of wind turbine blades using adapted ultrasonic and radiographic techniques, *Insight Non-Destructive Testing and Condition Monitoring*, Vol. 51(9), pp:477-483, 2009.

[101] Fantidis J. G., Potolias C. and Bandekas D. V., Wind Turbine Blade Nondestructive Testing with a Transportable Radiography System, *Science and Technology of Nuclear Installations*, Vol. 2011, 2011.

[102] Tchakoua P. and Wamkeue R. et al, Wind Turbine Condition Monitoring: State-of-the-Art Review, New Trends, and Future Challenges, *Energies*, Vol. 7 (4), 2014.

[103] Collis W. B., White P. R. and Hammond J.K., Higher-order Spectra: the Bispectrum and Trispectrum, *Mechanical Systems and Signal Processing*, Vol. 12 (3), pp: 375–394, May 1998.

[104] Jones R. M., Enveloping for bearing analysis, *Sound and Vibration*, pp: 10-16, Feb 1996, [Online] http://www.engr.colostate.edu/~dga/mech307/handouts/bearing_signature_analysis.pdf, last access: 7 Jan 2016.

[105] Drakos N. and Schwarz D., LPC Spectral Envelope, *Spectral Envelopes in Sound Analysis and Synthesis*, 1998, [Online] http://recherche.ircam.fr/anasyn/schwarz/da/specenv/4_2LPC_Spectral_Envelope.html last access: 7 Jan 2016.

[106] Drakos N. and Schwarz D., Cepstrum Spectral Envelope, *Spectral Envelopes in Sound Analysis and Synthesis*, 1998, [Online] http://recherche.ircam.fr/anasyn/schwarz/da/specenv/4_3Cepstrum_Spectral_Envelo.html last access: 8 Jan 2016.

[107] Röbel A., and Rodet X., Efficient spectral envelope estimation and ITS application to pitch shifting and envelope preservation, *Proc. of the 8th Int. Conference on Digital Audio Effects (DAFx'05)*, Madrid, Spain, September 20-22, 2005.

[108] Lee D. T. L and Yamamoto A., Wavelet analysis: theory and applications, *Hewlett Packard Journal*, pp: 44-52, Dec 1994.

[109] Kroese D. P., Taimre T. and Botev Z. I., *Handbook of Monte Carlo Meth*ods, John Wiley & Sons, Hoboken, New Jersey, 2011.

[110] Sanabria L. A. Cechet R. P., Severe Wind Hazard Assessment using Monte Carlo Simulation, *Environ Model Assess*, Vol. 15, pp:147–154, 2010.

[111] Gamerman D. and Lopes H. F., *Markov Chain Monte Carlo: Stochastic Simulation for Bayesian Inference, Second Edition*, Chapman and Hall/CRC, May 2006.

[112] Rasmussen C. E. and Williams C. K. I., *Gaussian Processes for Machine Learning*, University Press Group Limited, 2006.

[113] Chen N. Y. and Qian Z. et al, Wind Power Forecasts Using Gaussian Processes and Numerical Weather Prediction, *IEEE Transactions on Power Systems*, Vol. 29 (2), Mar 2014.

[114] Catalão J. P. S., Pousinho H. M. I. and Mendes V. M. F., An artificial neural network approach for short-term wind power forecasting in Portugal, *Engineering Intelligent Systems*, Vol. 7(1), pp: 5-11, Mar 2009.

[115] Bilgili M., Sahin B. and Yasar A., Application of artificial neural networks for the wind speed prediction of target station using reference stations data, *Renewable Energy*, Vol. 32(14), pp: 2350-2360, Nov 2007.

[116] Liu Z. and Gao W. et al, Wind Power Plant Prediction by Using Neural Networks, *IEEE Energy Conversion Conference and Exposition*, Sep 2012.

[117] Li L. L. and Wang M. H. et al, Wind Power Forecasting Based on Time Series and Neural Network, *Proceedings of the Second Symposium International Computer Science and Computational Technology(ISCSCT '09)*, pp: 293-297, Dec 2009.

[118] SangitaB P. and Deshmukh S. R., Use of support vector machine for wind speed prediction, *2011 International Conference on Power and Energy Systems (ICPS)*, pp: 1-8, Dec 2011.

[119] Ji G. R., Han P. and Zhai Y. J., Wind Speed Forecasting Based on Support Vector Machine with Forecasting Error Estimation, *Proceedings of the Sixth International Conference on Machine Learning and Cybernetics*, pp: 2735-2739, Aug 2007.

[120] Wang J. Z. and Zhou Q. P. et al, Short-Term Wind Speed Forecasting Using Support Vector Regression Optimized by Cuckoo Optimization Algorithm, *Mathematical Problems in Engineering*, Vol. 2015, pp:1-14, 2015.

[121] Yang L. and He M. et al, Support-Vector-Machine-Enhanced Markov Model for Short-Term Wind Power Forecast, *IEEE Transactions on Sustainable Energy*, Vol. 6 (3), July 2015.

[122] Futter D.N. et al, ETI-INFLOW-M9.2 Final Report on an Holistic Approach to Wind Turbine Monitoring, *E.ON New Build & Technology*, July 2013.

[123] Wilkinson M. and Hendriks B., Deliverable D.1.3, Report on wind turbine reliability profiles, *ReliaWind Project*, 2011.

[124] Feuchtwang, J. B. and Infield, D. G. Offshore wind turbine maintenance access: a closed form probabilistic method for calculating delays caused by sea-state, *Wind Energy*, pp: 1049-1066, 2013.

[125] Dahlberg J. A. and Thor S. E., Assessment of the Lillgrund Windfarm: Power performance, wake effects, *Lillgrund Pilot Project*, Sep 2009.

[126] Lillgrund wind farm, *LORC Knowledge*, [Online] http://www.lorc.dk/offshore-wind-farms-map/lillgrund, last access: 23rd July 2015.

[127] Horns Rev 2, *4C Offshore*, [online] http://www.4coffshore.com/windfarms/horns-rev-2-denmark-dk10.html, last access: 23rd July 2015.

[128] Nygaard N. G., Systematic quantification of wake model uncertainty, EWEA Offshore 2015, [online] http://www.eera-dtoc.eu/wp-content/uploads/files/Nygaard_Systematic_quantification_of_wake_model_uncertainty_offshore2015presentation.pdf last access: 23rd May 2016.

[129] Sørensen T. et al, Recalibrating Wind Turbine Wake Model Parameters - Validating the Wake Model Performance for Large Offshore Wind Farms, 2006, [Online] http://docs.wind-watch.org/wake-0693_Ewec2006fullpaper.pdf last access: 15 Jan 2016.

[130] Hebenicht G., Offshore Wake Modelling, *Renewable UK Offshore Wind 2011*, 29th June 2011.

[131] X. Yu et al., Wind direction error in the Lillgrund offshore wind farm, *Renewable Power Generation Conference (RPG 2013), 2nd IET*, 9-11th September. 2013.

[132] Siemens, *Outstanding Efficiency—Siemens Wind Turbine SWT-2.3-93*, 2009.

[133] Burton T. et al, *Wind Energy Handbook*, John Wiley & Sons Ltd, England, 2001.

[134] Croxton, F. E. et al, *Applied general statistics*, Prentice-Hall, 1967.

[135] Barthelmie R.J. et al, Flow and wakes in large wind farms: Final report for UpWind WP8, *UpWind Project*, Feb 2011.

[136] Wilson G. and McMillan D., Modeling the relationship between wind turbine failure modes and the environment, *Safety, Reliability and Risk Analysis: Beyond the Horizon – Steenbergen et al. (Eds)*, Taylor & Francis Group, London, 2014

[137] Faulstich S., Hahn B., Lyding P., and Tavner P., Reliability of offshore turbines – identifying risks by onshore experience, *European Wind Energy Association Proceedings*, 2009.

[138] Tavner P. J. and Greenwood D. M. et al, Study of weather and location effects on wind turbine, *Wind Energy*, pp: 175–187, May 2012.

[139] Dong W., Moan T., and Gao Z., Fatigue reliability analysis of the jacket support structure for offshore wind turbine considering the effect of corrosion and inspection, *Reliab. Eng. Syst. Saf.*, vol. 106, pp. 11–27, Oct. 2012.

[140] Marino E., Borri C., and Peil U., A fully nonlinear wave model to account for breaking wave impact loads on offshore wind turbines, *J. Wind Eng. Ind. Aerodyn.*, vol. 99, no. 4, pp. 483–490, Apr 2011.

[141] Thomsen K. and Sørensen P., Fatigue loads for wind turbines operating in wakes, *J. Wind Eng. Ind. Aerodyn.*, vol. 80, no. 1–2, pp. 121–136, Mar. 1999.

[142] Lee S., and Churchfield M. et al, Atmospheric and Wake Turbulence Impacts on Wind Turbine Fatigue Loadings, *50th American Institute of Aeronautics and Astronautics Aerospace Sciences Meeting*, Nashville, Tennessee, 2012.

[143] Laplace, P., *Théorie analytique des probabilities*. Paris: Ve. Courcier, 1814.

[144] Epanechnikov, V., Non-Parametric Estimation of a Multivariate Probability Density. *Theory Probab. Appl.*, vol. 14(1), pp: 153-158, 1969.

[145] Burton T., Jenkins N., Sharpe D., Bossanyi E., and Jenkins N., *Wind Energy Handbook Second Edition*, Wiley, 2011.

[146] Arabian-Hoseynabadi H., Oraee H., and Tavner P. J., Failure Modes and Effects Analysis (FMEA) for Wind Turbines, *Int. J. Electr. Power Energy Syst.*, vol. 32, no. 7, pp. 817–824, Sep. 2010.

[147] Das M., Panja S., Chowdhury S., Chowdhury S. & Elombo A., Expert-based FMEA of wind turbine system. Industrial Engineering and Engineering Management (IEEM), *2011 IEEE International Conference*, pp. 1582–1585, 2011.

[148] PRC-Relex, *Reliawind Summary of Deliverable D2.0.4, Whole System Reliability Model*, 2009.

[149] Kahrobaee, S. & Asgarpoor, S., Risk-based Failure Mode and Effect Analysis for wind turbines (RB-FMEA), *North American Power Symposium (NAPS) 2011*, pp. 1–7, 2011.

[150] Zhu, P., Liu, Y., Robert, R. & Hao, X., Offshore wind converter reliability evaluation. Power Electronics and ECCE Asia (ICPE \& ECCE), *2011 IEEE 8th International Conference*, pp. 966–971, 2011.

[151] Department of Defense of United States of America, *MIL-STD-1629A, Military standard, Procedures for Performing a Failure Mode, Effects and Criticality Analysis*, 24th Nov 1980.

[152] Wilkinson F., Spianto M., and Knowles M., Towards the Zero Maintenance Wind Turbine, *University of Newcastle Power Engineering Conference*, no. 12, 2006.

[153] Wiggelinkhuizen E. J. and Rademakers L.W.M.M. et al, Condition Monitoring for Offshore Wind Farms, *CONMOW report, ECN*, 2007.

[154] Van Bussel G.J.W. and Zaaijer M.B., Reliability, availability and maintenance aspects of large-scale offshore wind farms, a concepts study, *MAREC* 2001.

[155] Moné C. and Stehly T. et al, 2014 Cost of Wind Energy Review, NREL, Oct 2015.

[156] Feuchtwang, J. B. and Infield, D. G., Estimating the cost of offshore maintenance and the benefit from condition monitoring, *European Offshore Wind Conference*, Amsterdam, 2011.

[157] van Bussel G.J.W and Schöntag C., Operation and maintenance aspects of large offshore wind farms, *European Wind Energy Conference (EWEC)*, Dublin, pp: 272–275, 1997.

[158] Douard F. et al., A probabilistic approach to introduce risk measurement indicators to an offshore wind project evaluation– Improvement to an existing tool ECUME, *Energy Procedia*, June 2012.

[159] Dinwoodie I. and McMillan D. et al, Development of a Combined Operational and Strategic Decision Support Model for Offshore Wind, *Energy Procedia*, Vol. 35, pp 157-166, 2013.

[160] Hofmann M. and Sperstad I.B., NOWIcob – A Tool for Reducing the Maintenance Costs of Offshore Wind Farms, *Energy Procedia*, Vol. 35, pp:177-186, 2013.

[161] NASA Jet Propulsion Laboratory, [Online] https://sealevel.jpl.nasa.gov/education/classactivities/onlinetutorial/tutorial1/windwaves/ last access: 25th May 2016.

[162] Dahl P. H. and Zhang R. H. et al, An Overview of the ASIAEX East China Sea Program, *IEEE J. Oceanic. Eng. (Special Issue)*, 2004.

[163] GEOS F., Wind and wave frequency distributions for sites around the British Isles, *HSE Books*, Her Majesty's Stationery Office, 2001.

[164] Spinato F., Tavner P.J., et al, Reliability of wind turbine subassemblies, *IET Renew Power Gen.*,Vol.3(4), pp: 387–401, 2009.

[165] Wilkinson M, Hendriks B, Spinato F, et al, Methodology and Results of the Reliawind Reliability Field Study, *EWEC2010,* No.58, 2010.

[166] Faulstich S., Hahn B., and Tavner P.J. , Wind turbine downtime and its importance for offshore deployment, *Wind Energy 2011*, Issue 14, pp: 327–337, 2011.

[167] Rademakers L.W.M.M and Braam H., O&M ASPECTS OF THE 500 MW OFFSHORE WIND FARM AT NL7 - (80 × 6 MW Turbines) - Baseline Configuration, *DOWEC Report Nr.10080 rev 2*, ECN & TUDelft, NL, 2002.

[168] Malcolm D.J. and Hansen A.C., WindPACT Turbine Rotor Design Study, *NREL subcontract report NREL-SR-500-32495 rev*, April 2006.

[169] Rademakers L., Braam H. and Wessels H.R.A. et al, Lightning Damage of OWECS, Part 1 - Parameters Relevant for Cost Modelling, *ECN report ECN-C—02-05*, 2002.

[170] Van de Pieterman R. P. and Braam H. et al, Optimisation of maintenance strategies for offshore wind farms, *The offshore 2011 conference,* Amsterdam, the Netherlands, 2011.

[171] Braam H. and Obdam T.S. et al, Properties of the O&M Cost Estimator (OMCE), *the ECN report*, July 2011.

[172] Mackay D.J.C. Introduction to Monte Carlo Methods, *Proceedings of the NATO Advanced Study Institute on Learning in graphical models*, pp: 175-204, 1998.

[173] Yeomans, J., Statistical mechanics of phase transitions, *Clarendon Press*, Oxford, 1992.

[174] Rabiner L.R. and Juang B.H., An Introduction to Hidden Markov Models, *IEEE ASSP Magazine*, pp: 4-16, January 1986.

[175] Ben-Gal I., Bayesian Networks, *Encyclopaedia of Statistics in Quality & Reliability*, Wiley & Sons, 2007.

[176] Zell A., Mathematical Models, [online] http://www.ra.cs.uni-tuebingen.de/software/JCell/tutorial/ch03s03.html last access: 25th May 2016.

[177] Dagum P. and Galper A., Forecasting Sleep Apnea with Dynamic Network Models, *Proceedings of the Ninth Conference on Uncertainty in Artificial Intelligence*, pp: 64-71, AUAI Press, 1993.

[178] May A. and Thöns S., Integrating Structural Health and Condition Monitoring: A Cost Benefit Analysis for Offshore Wind Energy, *Proceeding of the ASME 2015 34th International Conference on Ocean, Offshore and Arctic Engineering OMAE*, Canada, 2015.

[179] Endrerud O.-E.V., Liyanage J.P. and Keseric N., Marine logistics decision support for operation and maintenance of offshore wind park with a multi simulation model, *2014 Winter Simulation conference*, pp: 1712-1722, Dec 2014.

[180] Ofgem, [online] https://www.ofgem.gov.uk/environmental-programmes/renewables-obligation-ro, last access: 15th May 2016.

[181] Department of Energy & Climate Change, Gov. UK, Electricity Market Reform: Contracts for Difference, [online] https://www.gov.uk/government/collections/electricity-market-reform-contracts-for-difference, last access: 15th May 2016.

[182] Box G.E.P. and Cox D.R., An analysis of transformations, *Journal of the Royal Statistical Society Series B*, Vol. 26 (2), pp: 211-252, 1964.

[183] Neumaier A. and Schneider T., Estimation of parameters and eigenmodes of multivariate autoregressive models, *ACM Trans. Math. Softw.*, Vol. 27, pp: 27-57, 2001.

[184] Farrar C.R. and Worden K., An introduction to structural health monitoring, *Phil. Trans. R. Soc. A,* Issue 365, pp: 303–315, 2007.

[185] Thöns, S., and Faber, M. H., Assessing the value of structural health monitoring, *Safety, Reliability, Risk and Life-Cycle Performance of Structures and Infrastructures*, pp: 2543–2550, Taylor & Francis, 2013.

[186] Thöns, S., and McMillan, D., Condition monitoring benefit for offshore wind turbines, *12th International Conference on Probabilistic Methods Applied to Power Systems*, Istanbul, Turkey, 2012.

[187] BMU, PTJ, FINO 1 Meteorological Dataset 2004 – 2012, [online] http://fino.bsh.de, last accessed 1st Mar 2015.

[188] Dinwoodie I. and Endrerud O-E. V., at al, Reference cases for verification of operation and maintenance simulation models for offshore wind farms, *Wind Engineering*, Volume 39, No.1, pp1-14, 2015.

APPENDIX-A

Table 1a. High frequent value (>10 times) of Yaw direction (stoppage) and percentage of each turbine in Descending order

WTG1		
direction	stoppage (stamps)	percentage
213.3	9473	27.9324
109.6	4175	12.3106
213.4	1628	4.80038
272.7	1398	4.12219
183.4	1164	3.43221
268	1085	3.19927
183.3	873	2.57416
245.4	171	0.50422
129.3	144	0.4246
243.5	121	0.35679

WTG2		
direction	stoppage (stamps)	percentage
103.9	3030	8.93357
186.9	2725	8.03432
103.8	1037	3.05746
108.8	269	0.79311
143.5	160	0.47174
186.8	141	0.41572
148	16	0.04717
234.1	14	0.04128
222.8	13	0.03833

WTG3		
direction	stoppage (stamps)	percentage
146.7	1887	5.56342
143.9	146	0.43045
67.7	144	0.42455
167.4	38	0.11204
180.5	16	0.04717
328.3	16	0.04717

WTG4		
direction	stoppage (stamps)	percentage
199.7	2875	8.47608
151.5	1929	5.68708
219.4	1387	4.08915
189.9	851	2.50892
199.5	841	2.47944
23.2	535	1.57729
320.2	440	1.29721
0	409	1.20581
121.5	272	0.80191
336	144	0.42454
219.8	37	0.10908
24.2	23	0.06781
31.7	15	0.04422
241.9	13	0.03833

WTG5		
direction	stoppage (stamps)	percentage
228.4	3530	10.4075
194.3	1457	4.29565
226	550	1.62156
0	529	1.55964
85	269	0.79309
45.7	143	0.42161
155.4	15	0.04422
164.3	11	0.03243

WTG6		
direction	stoppage (stamps)	percentage
271.4	3530	10.4072
186.5	2599	7.66237
88.1	704	2.07553
269.7	554	1.6333
0	525	1.54781
111.8	144	0.42454
181.1	138	0.40685
155.4	48	0.14151
67	41	0.12088
231	21	0.06191
175.9	17	0.05012
204	16	0.04717
195.3	13	0.03833
236.8	13	0.03833

WTG7		
direction	stoppage (stamps)	percentage
273.9	3530	10.4075
167.8	1721	5.074
227.7	753	2.22006
227.5	691	2.03727
0	528	1.5567
265.1	430	1.26776
118.6	269	0.79309
61.1	144	0.42455
356.4	19	0.05602

WTG9		
direction	stoppage (stamps)	percentage
243.5	1048	3.0899
95.7	270	0.79606
70.1	146	0.43046
172.7	21	0.06192
231.5	11	0.03243

WTG11		
direction	stoppage (stamps)	percentage
224.9	4606	13.5798
232.2	733	2.16109
216.9	144	0.42455

WTG13		
direction	stoppage (stamps)	percentage
167.7	854	2.51776
167.6	285	0.84024
163.6	265	0.78127
161.4	155	0.45697
218.3	12	0.03538

WTG15		
direction	stoppage (stamps)	percentage
156	1512	4.45794
129.2	1018	3.00145
139.4	806	2.37639
155.9	286	0.84324
103.3	270	0.79606
139.6	165	0.48648
138.2	144	0.42457
201.5	107	0.31548
191.2	30	0.08845

WTG17		
direction	stoppage (stamps)	percentage
222.8	6968	20.5449
257.3	5248	15.4735
162.8	1853	5.4635
170.1	1507	4.44333
174.5	588	1.7337
257.4	564	1.66293
170.2	210	0.61918

WTG8		
direction	stoppage (stamps)	percentage
0	16539	48.7646
225	4330	12.7668
80.5	3237	9.54417
253.2	1787	5.2689
191.7	1096	3.23151
147.2	604	1.78087
1.7	481	1.41821
191.4	378	1.11452
64.2	321	0.94646
191.8	285	0.84031

WTG10		
direction	stoppage (stamps)	percentage
230.1	3463	10.2111
228.5	3228	9.51819
230.2	2573	7.58684
234	2060	6.07419
228.6	1526	4.49962
234.3	1230	3.62682
254.9	426	1.25612
143.8	322	0.94946
223.9	30	0.08846

WTG12		
direction	stoppage (stamps)	percentage
23.7	3403	10.0336
25.7	1580	4.65857
21.5	445	1.31207
21.6	275	0.81083
103.1	119	0.35087
74.2	94	0.27716
333	94	0.27716
54.9	20	0.05897

WTG14		
direction	stoppage (stamps)	percentage
199.1	2728	8.04293
198.9	2614	7.70682
80	1154	3.40232
243.1	603	1.77782
214.6	433	1.27661
199	426	1.25597
92.5	260	0.76656
223.1	147	0.4334
249.7	41	0.12088
5.6	26	0.07666
262.2	12	0.03538

WTG19		
direction	stoppage (stamps)	percentage
190	7899	23.2892
40.9	5943	17.5222
201.3	3457	10.1925
199.3	1015	2.9926
190.1	319	0.94053

WTG21		
direction	stoppage (stamps)	percentage
168.1	4439	13.0875
168	1890	5.57226
182.4	1322	3.89764
332.1	402	1.18521
167.9	144	0.42455
332	141	0.41571

WTG23		
direction	stoppage (stamps)	percentage
143.5	853	2.51482
199.3	707	2.08438
199.4	590	1.73944
204.5	570	1.68047
204.4	429	1.26478
52.1	382	1.12621
187.3	153	0.45108
52.2	141	0.4157
185.1	141	0.4157
175.3	29	0.0855
342.9	19	0.05602
176.6	16	0.04717
150.4	12	0.03538

WTG25		
direction	stoppage (stamps)	percentage
194.3	3023	8.91267
108.4	1615	4.76148
257.3	1209	3.56448
108.5	1150	3.39053
226.8	12	0.03538
136.4	11	0.03243

WTG16		
direction	stoppage (stamps)	percentage
190.2	1742	5.13592
178.5	576	1.69821
174	414	1.22059
112.9	269	0.79309
242.2	22	0.06486
86.3	11	0.03243

WTG18		
direction	stoppage (stamps)	percentage
180.5	6454	19.0288
80.3	2023	5.96456
180.4	999	2.94543
187.7	877	2.58572
237	877	2.58572
245.6	354	1.04372
85.3	307	0.90515
94	270	0.79606
187.5	263	0.77542
196.2	157	0.4629
229.6	142	0.41867
85.4	31	0.0914
187.6	21	0.06192
244.3	20	0.05897

WTG20		
direction	stoppage (stamps)	percentage
319.7	4679	13.7946
250.6	2753	8.1164
319	1419	4.1835
305.7	1188	3.50246
331.3	895	2.63864
283	858	2.52956
26.8	737	2.17282
218.5	429	1.26478
305.8	426	1.25593
306.8	285	0.84024
305.9	282	0.83139
307.4	282	0.83139
318.8	282	0.83139
186.4	17	0.05012
95.7	15	0.04422

WTG27		
direction	stoppage (stamps)	percentage
286.9	2516	7.41789
220.5	2363	6.9668
220.7	855	2.52079
51.3	846	2.49425
231.9	693	2.04316
25.3	682	2.01073
300.7	426	1.25597
45.1	419	1.23533
87.2	269	0.79309
219.9	158	0.46583
220	143	0.42161
265.1	141	0.41571
0	20	0.05897
203.5	12	0.03538

WTG22		
direction	stoppage (stamps)	percentage
173.1	3744	11.0387
226.3	3610	10.6436
181.6	3002	8.85102
99.9	1765	5.20388
226.1	852	2.51202
202.3	753	2.22013
181.8	300	0.88451
173.9	204	0.60147
313.2	22	0.06486

WTG24		
direction	stoppage (stamps)	percentage
285.7	5593	16.4898
181.1	1845	5.43959
109.6	1126	3.31977
85	1063	3.13403
81.6	843	2.48541
269	391	1.15278
254.3	345	1.01716
244.1	342	1.00831
281.3	30	0.08845
108.5	21	0.06191
261.8	17	0.05012
236	11	0.03243

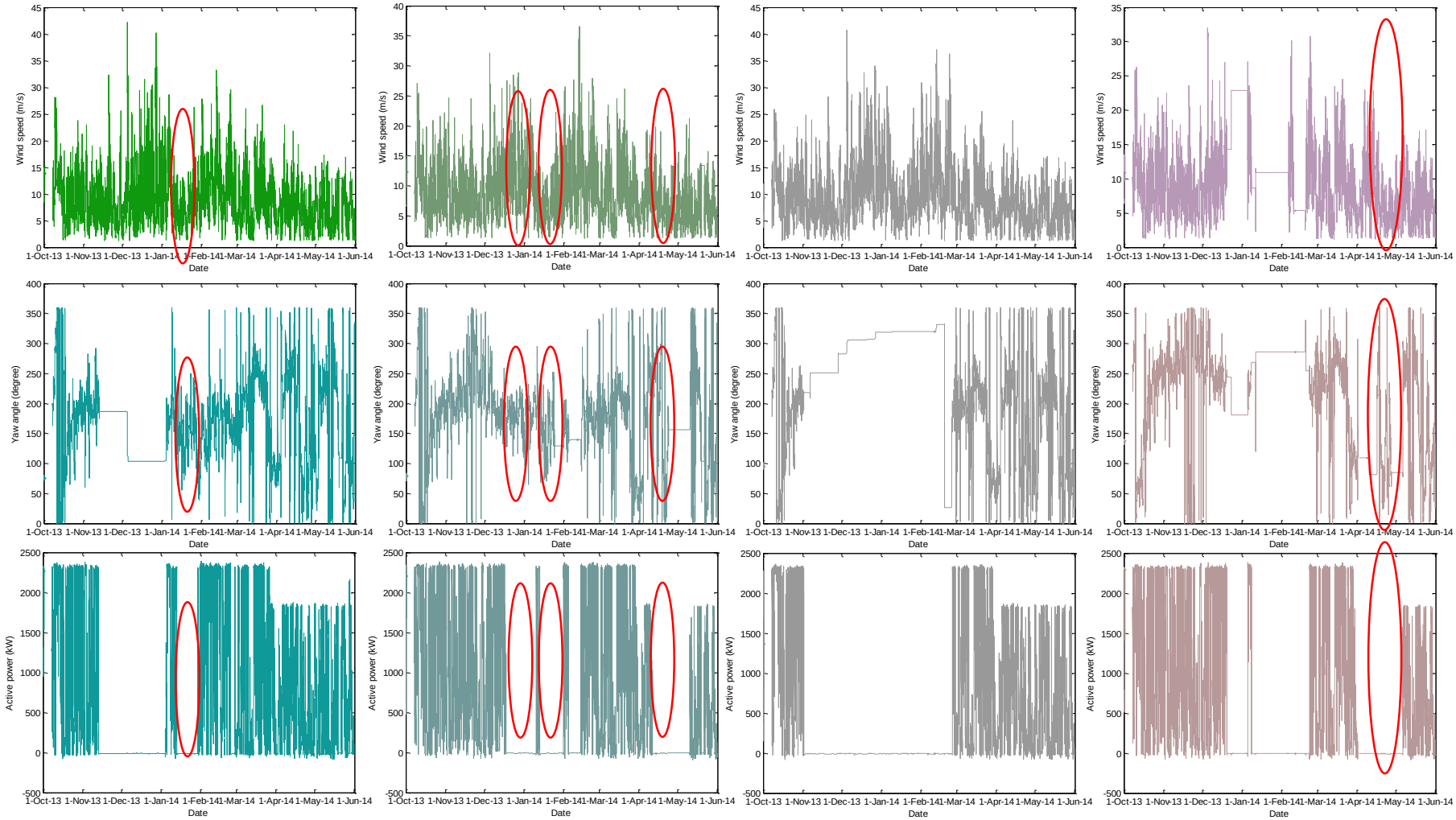

Figure 1a. time series of local wind speed (top), yaw angle (middle) and active power (bottom) of WTG 2, 15, 20 and 24 (Left to right)

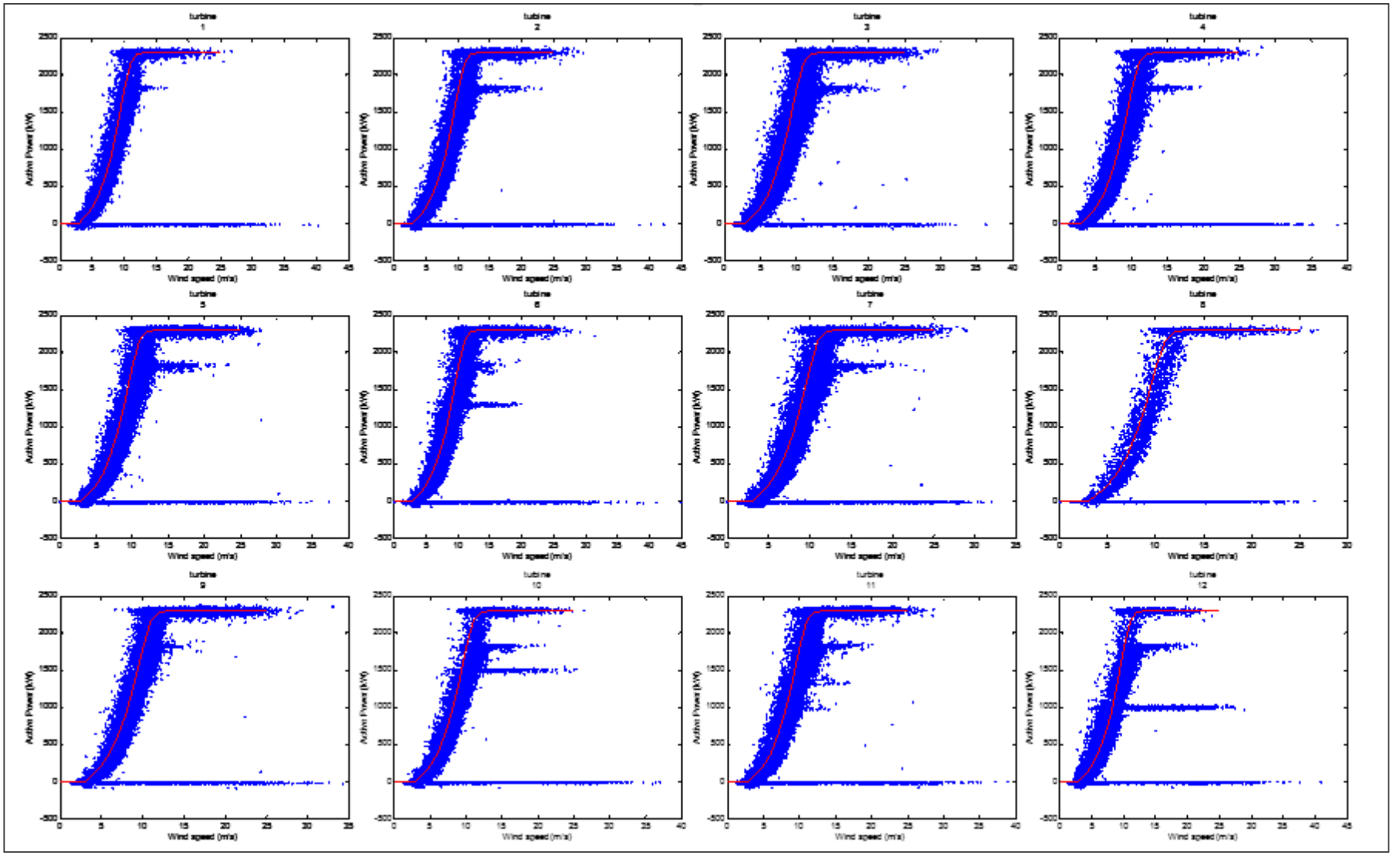
turbine 1
turbine 2
turbine 3
turbine 4
turbine 5
turbine 6
turbine 7
turbine 8
turbine 9
turbine 10
turbine 11
turbine 12
Active Power (kW)
Wind speed (m/s)

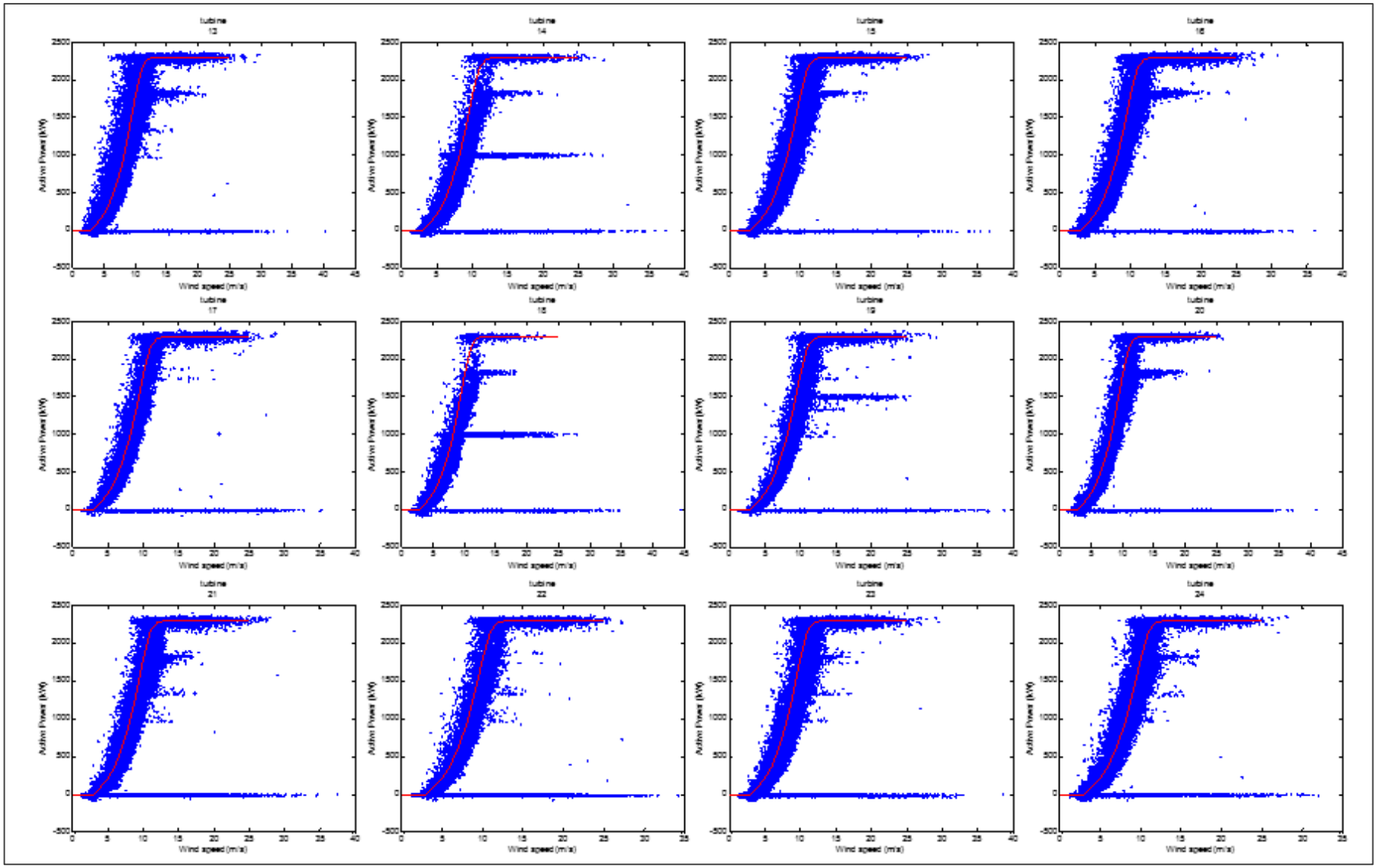
turbine
13
turbine
14
turbine
15
turbine
16
turbine
17
turbine
18
turbine
19
turbine
20
turbine
21
turbine
22
turbine
23
turbine
24
Active Power (kW)
Wind speed (m/s)

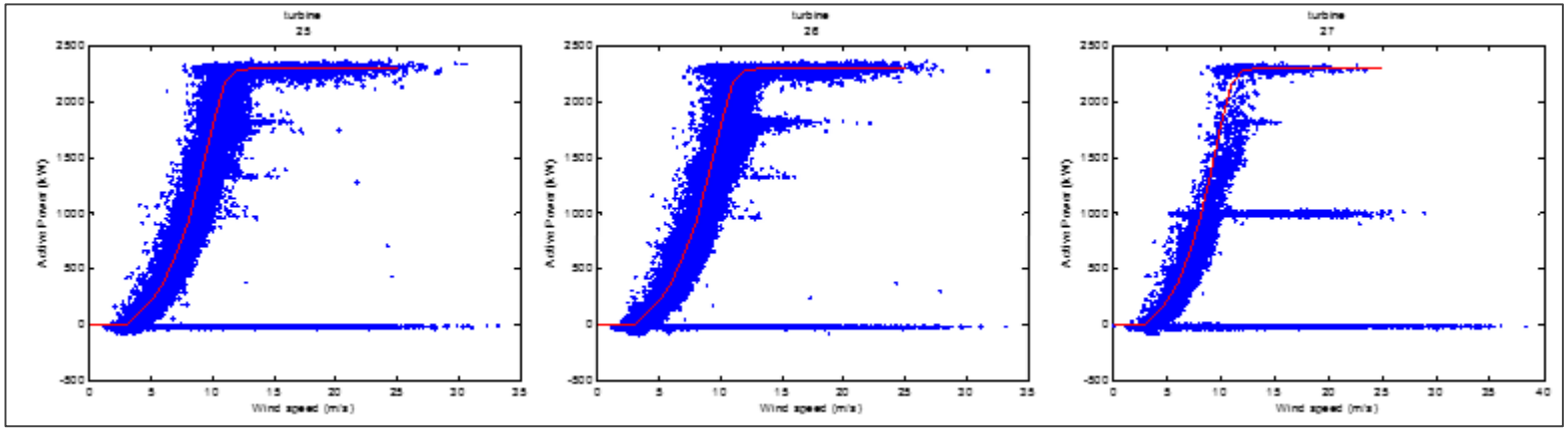

Figure 2a. Power curves of each turbine from 6-month SCADA in wind farm T with nominal power curve from the manufacturer (WTG1-4 from left to right on the first row, the same to the rest)

APPENDIX-B

Equation 1b and 2b: Maintenance category formulae D_{s1} and E_{s1} in condition monitoring system detection effectiveness sensitivity analyses with regime1 transferring falsepos from maintenance category Au to Eu into Es in scheduled maintenance.

$$D_{S1} = D_U \cdot detectability \cdot (1 + edet) + C_U \cdot preempt \cdot (1 + epre) \quad (96a)$$

$$E_{S1} = E_U \cdot detectability \cdot (1 + edet) + D_U \cdot preempt \cdot (1 + epre) + (A_U + B_U + C_U + D_U + E_U) \cdot falsepos \cdot (1 + efalse) \quad (97a)$$

Table 2b. Condition monitoring system detection effectiveness sensitivity analyses with regime transferring falsepos from maintenance category A to E into E in scheduled maintenance; baseline values given in the top row

Detectability	Pre-empt	Falsepos	Availability	Capacity factor with downtime	Annual maintenance cost per turbine(£k)	Total o&m cost (without revenue loss) per kwh per turbine(£)	Revenue loss per kwh per turbine(£)
0%	0%	0%	94.4%	46.5%	144.9	0.0120	0.0077
-50%	0%	0%	94.1%	46.2%	152.2	0.0127	0.0083
-40%	0%	0%	94.1%	46.3%	150.7	0.0125	0.0082
-30%	0%	0%	94.2%	46.3%	149.3	0.0124	0.0081
-20%	0%	0%	94.3%	46.4%	147.8	0.0123	0.0079
-10%	0%	0%	94.4%	46.4%	146.4	0.0122	0.0078
0%	0%	0%	94.4%	46.5%	144.9	0.0120	0.0077
10%	0%	0%	94.5%	46.6%	143.4	0.0119	0.0076
20%	0%	0%	94.6%	46.6%	142.0	0.0118	0.0075
30%	0%	0%	94.7%	46.7%	140.5	0.0117	0.0073
40%	0%	0%	94.7%	46.8%	139.1	0.0116	0.0072
50%	0%	0%	94.8%	46.8%	137.6	0.0114	0.0071
0%	-50%	0%	94.4%	46.4%	148.4	0.0123	0.0078
0%	-40%	0%	94.4%	46.5%	147.7	0.0123	0.0078
0%	-30%	0%	94.4%	46.5%	147.0	0.0122	0.0078
0%	-20%	0%	94.4%	46.5%	146.3	0.0122	0.0077
0%	-10%	0%	94.4%	46.5%	145.6	0.0121	0.0077
0%	0%	0%	94.4%	46.5%	144.9	0.0120	0.0077
0%	10%	0%	94.4%	46.5%	144.2	0.0120	0.0077
0%	20%	0%	94.5%	46.5%	143.5	0.0119	0.0077
0%	30%	0%	94.5%	46.5%	142.8	0.0119	0.0076
0%	40%	0%	94.5%	46.6%	142.1	0.0118	0.0076
0%	50%	0%	94.5%	46.6%	141.4	0.0118	0.0076
0%	0%	-50%	94.4%	46.5%	144.5	0.0120	0.0077
0%	0%	-40%	94.4%	46.5%	144.6	0.0120	0.0077
0%	0%	-30%	94.4%	46.5%	144.7	0.0120	0.0077
0%	0%	-20%	94.4%	46.5%	144.8	0.0120	0.0077
0%	0%	-10%	94.4%	46.5%	144.8	0.0120	0.0077
0%	0%	0%	94.4%	46.5%	144.9	0.0120	0.0077
0%	0%	10%	94.4%	46.5%	145.0	0.0121	0.0077
0%	0%	20%	94.4%	46.5%	145.0	0.0121	0.0077
0%	0%	30%	94.4%	46.5%	145.1	0.0121	0.0077
0%	0%	40%	94.4%	46.5%	145.2	0.0121	0.0077
0%	0%	50%	94.4%	46.5%	145.3	0.0121	0.0077

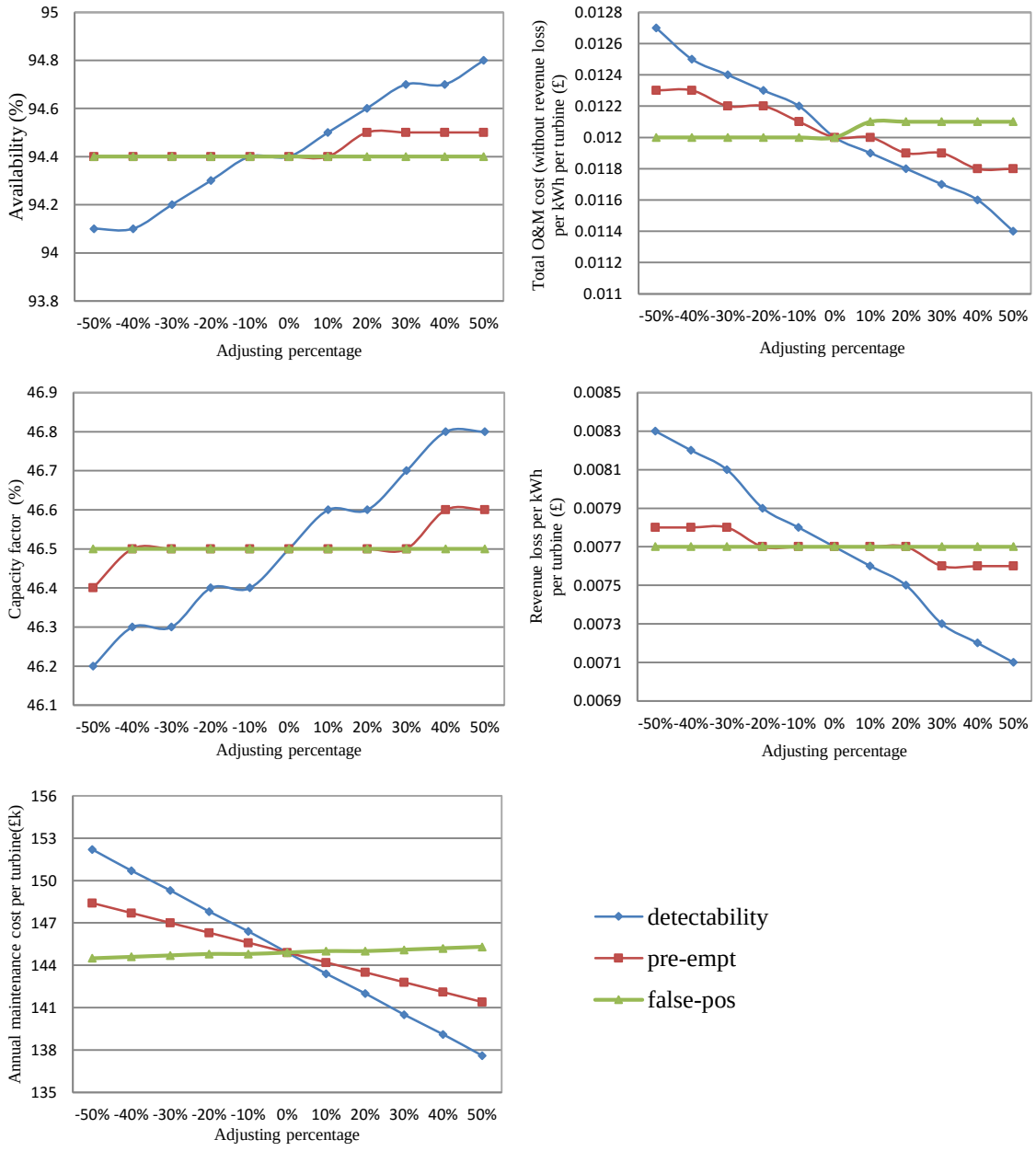

Figure 3b. Condition monitoring detection effectiveness sensitivity analysis with regime transferring falsepos from maintenance category A to E into only E in scheduled maintenance

Table 3b. Exact values in comparison of 0 adjustment of CM detection effectiveness sensitivity analysis with regime transferring falsepos from maintenance category A to E into D and E in scheduled (condition-based) maintenance; baseline values given in top row

Detectability	Pre-empt	Falsepos	Availability (%)	Capacity factor with downtime (%)	Annual maintenance cost per turbine(£k)	Total o&m cost (without revenue loss) per kwh per turbine(p)	Revenue loss per kwh per turbine (p)
0%	0%	0%	94.43	46.51	144.899	1.205	0.7697
-50%	0%	0%	94.06	46.19	152.168	1.265	0.8308
-40%	0%	0%	94.13	46.26	150.714	1.253	0.8186
-30%	0%	0%	94.21	46.32	149.26	1.241	0.8064
-20%	0%	0%	94.28	46.38	147.806	1.229	0.7941
-10%	0%	0%	94.36	46.44	146.353	1.217	0.7819
0%	0%	0%	94.43	46.51	144.899	1.205	0.7697
10%	0%	0%	94.51	46.57	143.445	1.193	0.7575
20%	0%	0%	94.58	46.63	141.992	1.180	0.7452
30%	0%	0%	94.66	46.69	140.538	1.168	0.7330
40%	0%	0%	94.73	46.75	139.084	1.156	0.7208
50%	0%	0%	94.81	46.82	137.63	1.144	0.7085
0%	-50%	0%	94.35	46.45	148.423	1.234	0.7811
0%	-40%	0%	94.37	46.46	147.718	1.228	0.7788
0%	-30%	0%	94.38	46.47	147.013	1.222	0.7765
0%	-20%	0%	94.40	46.48	146.309	1.216	0.7743
0%	-10%	0%	94.42	46.49	145.604	1.211	0.7720
0%	0%	0%	94.43	46.51	144.899	1.205	0.7697
0%	10%	0%	94.45	46.52	144.194	1.199	0.7674
0%	20%	0%	94.47	46.53	143.489	1.193	0.7651
0%	30%	0%	94.48	46.54	142.785	1.187	0.7628
0%	40%	0%	94.50	46.55	142.08	1.181	0.7605
0%	50%	0%	94.52	46.56	141.375	1.175	0.7583
0%	0%	-50%	94.44	46.51	144.534	1.2016	0.76940
0%	0%	-40%	94.44	46.51	144.607	1.2022	0.76945
0%	0%	-30%	94.44	46.51	144.68	1.2028	0.76951
0%	0%	-20%	94.44	46.51	144.753	1.2034	0.76957
0%	0%	-10%	94.43	46.51	144.826	1.2040	0.76963
0%	0%	0%	94.43	46.51	144.899	1.2046	0.76968
0%	0%	10%	94.43	46.50	144.972	1.2053	0.76974
0%	0%	20%	94.43	46.50	145.045	1.2059	0.76980
0%	0%	30%	94.43	46.50	145.118	1.2065	0.76986
0%	0%	40%	94.43	46.50	145.191	1.2071	0.76991
0%	0%	50%	94.43	46.50	145.264	1.2077	0.76997

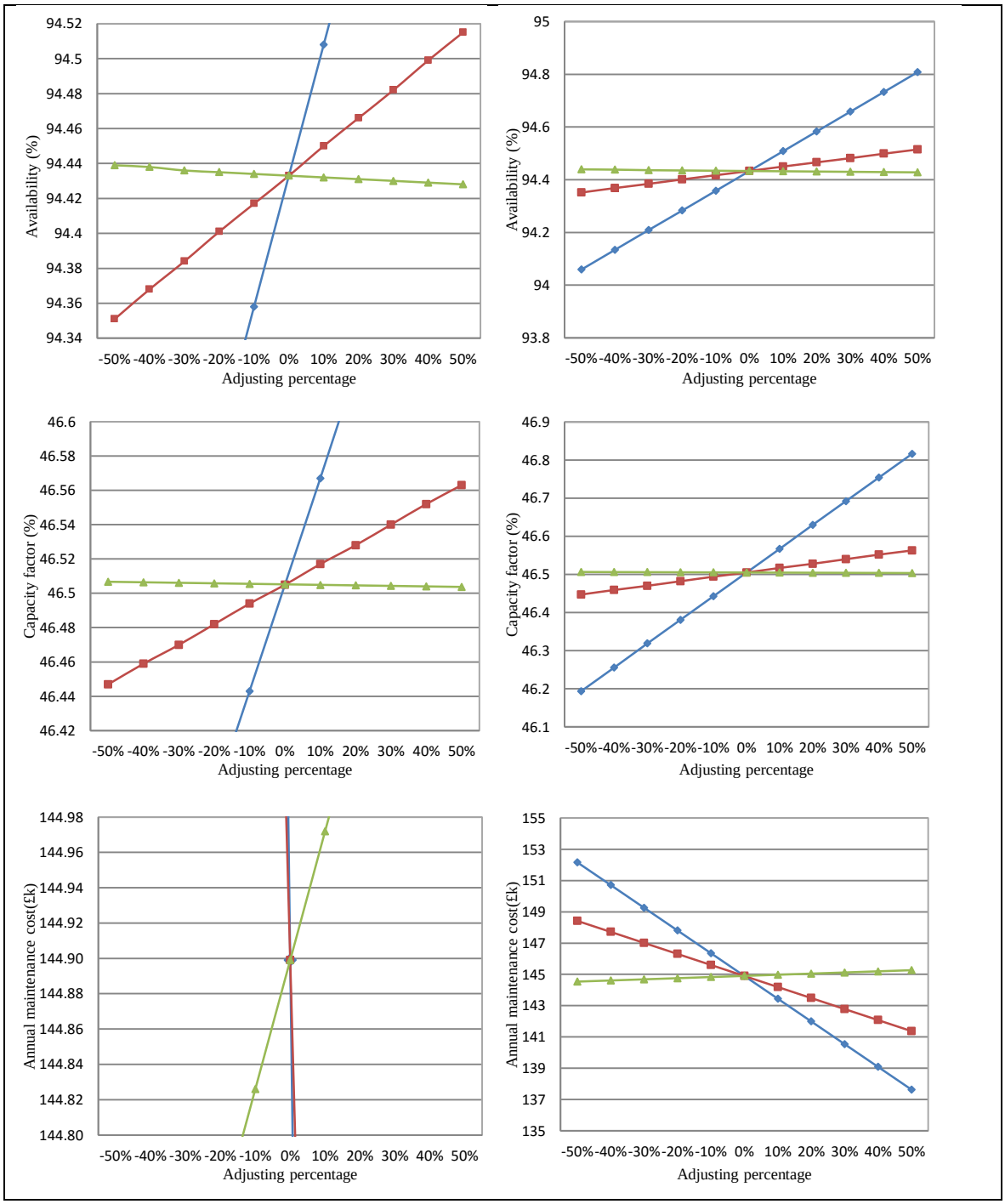
94.52
94.5
94.48
94.46
94.44
94.42
94.4
94.38
94.36
94.34
Availability (%)
-50% -40% -30% -20% -10% 0% 10% 20% 30% 40% 50%
Adjusting percentage
95
94.8
94.6
94.4
94.2
94
93.8
Availability (%)
-50% -40% -30% -20% -10% 0% 10% 20% 30% 40% 50%
Adjusting percentage
46.6
46.58
46.56
46.54
46.52
46.5
46.48
46.46
46.44
46.42
Capacity factor (%)
-50% -40% -30% -20% -10% 0% 10% 20% 30% 40% 50%
Adjusting percentage
46.9
46.8
46.7
46.6
46.5
46.4
46.3
46.2
46.1
Capacity factor (%)
-50% -40% -30% -20% -10% 0% 10% 20% 30% 40% 50%
Adjusting percentage
144.98
144.96
144.94
144.92
144.90
144.88
144.86
144.84
144.82
144.80
Annual maintenance cost(£k)
-50% -40% -30% -20% -10% 0% 10% 20% 30% 40% 50%
Adjusting percentage
155
153
151
149
147
145
143
141
139
137
135
Annual maintenance cost(£k)
-50% -40% -30% -20% -10% 0% 10% 20% 30% 40% 50%
Adjusting percentage

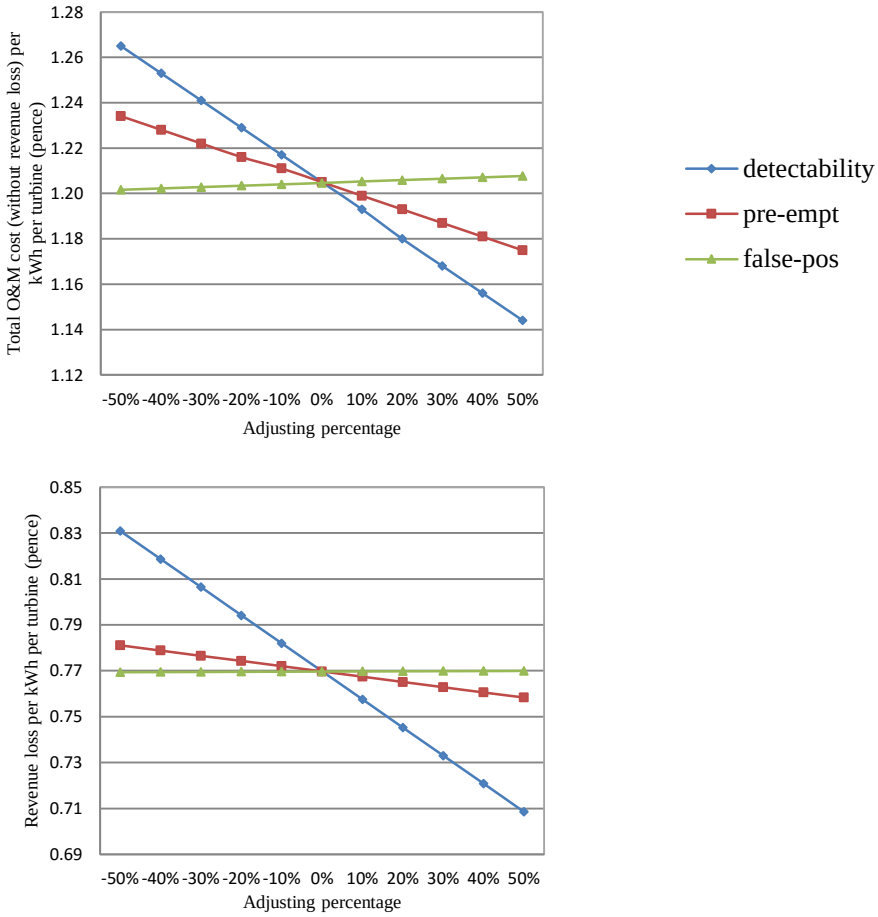

*Figure 4b. CM detection effectiveness sensitivity in **exact value** with regime transferring falsepos from maintenance category A to E into D and E in scheduled maintenance with zoom-in figures in step of 0.02 (left) and full scale (right)*

Table 4b. Curve gradients of exact value against detectability, pre-empt and falsepos in figures from Figure 4a.

Adjustment	Availability	Capacity factor with downtime	Annual maintenance cost per turbine	Total O&M cost (without revenue loss) per kWh per turbine	Revenue loss per kWh per turbine
Detectability	0.75	0.62	-14.5	-0.12	-0.12
Pre-empt	0.16	0.12	-7.05	-0.059	-0.023
Falsepos	-0.011	-0.003	0.73	0.006	0.00057

Table 5b. Value change in percentage due to condition-based maintenance in StraPCost+ sensitivity analysis: (condition based maintenance – reactive maintenance)/ reactive maintenance; baseline figures given in the top row.

Adjustment		Availability (%)	Capacity factor with downtime (%)	Annual maintenance cost per turbine (%)	Total O&M cost (without revenue loss) per kWh per turbine (%)	Revenue loss per kWh per turbine (%)
Baseline value	0%	0.96	1.61	-12.58	-12.58	-15.81
Wind and wave parameters	-50%	0.35	0.56	-3.55	-3.55	-13.51
	-40%	0.41	0.76	-4.98	-4.98	-14.56
	-30%	0.51	0.96	-6.89	-6.89	-15.16
	-20%	0.63	1.17	-8.92	-8.92	-15.49
	-10%	0.78	1.38	-10.85	-10.85	-15.69
	0%	**0.96**	**1.61**	**-12.58**	**-12.58**	**-15.81**
	10%	1.18	1.85	-14.09	-14.09	-15.91
	20%	1.43	2.12	-15.37	-15.37	-15.99
	30%	1.73	2.43	-16.42	-16.42	-16.08
	40%	2.1	2.8	-17.27	-17.27	-16.19
	50%	2.56	3.28	-17.93	-17.93	-16.33
Weather window threshold for heavy maintenance (*A* and *B*)	-50%	7.6	10.64	-19.46	-19.46	-18.74
	-40%	2.53	3.79	-18.8	-18.8	-17.74
	-30%	1.61	2.56	-17.57	-17.57	-17.04
	-20%	1.26	2.07	-15.96	-15.96	-16.54
	-10%	1.08	1.79	-14.23	-14.23	-16.15
	0%	**0.96**	**1.61**	**-12.58**	**-12.58**	**-15.81**
	10%	0.89	1.47	-11.11	-11.11	-15.51
	20%	0.84	1.36	-9.85	-9.85	-15.23
	30%	0.8	1.28	-8.79	-8.79	-15.01
	40%	0.77	1.22	-7.92	-7.92	-14.82
	50%	0.74	1.18	-7.22	-7.22	-14.67
Weather window threshold for light maintenance (*C*, *D* and *E*)	-50%	2.64	3.98	-13.17	-13.17	-15.37
	-40%	1.94	3.07	-12.98	-12.98	-15.48
	-30%	1.53	2.5	-12.84	-12.84	-15.58
	-20%	1.27	2.12	-12.73	-12.73	-15.67
	-10%	1.09	1.83	-12.65	-12.65	-15.75
	0%	**0.96**	**1.61**	**-12.58**	**-12.58**	**-15.81**
	10%	0.87	1.43	-12.53	-12.53	-15.86
	20%	0.81	1.29	-12.49	-12.49	-15.9
	30%	0.75	1.18	-12.46	-12.46	-15.93
	40%	0.72	1.1	-12.44	-12.44	-15.96
	50%	0.69	1.04	-12.42	-12.42	-15.98
Default overall failure rate	-50%	0.47	0.76	-12.58	-12.58	-15.81
	-40%	0.56	0.93	-12.58	-12.58	-15.81
	-30%	0.66	1.09	-12.58	-12.58	-15.81
	-20%	0.76	1.26	-12.58	-12.58	-15.81
	-10%	0.86	1.43	-12.58	-12.58	-15.81
	0%	**0.96**	**1.61**	**-12.58**	**-12.58**	**-15.81**
	10%	1.07	1.78	-12.58	-12.58	-15.81
	20%	1.17	1.97	-12.58	-12.58	-15.81
	30%	1.28	2.15	-12.58	-12.58	-15.81
	40%	1.39	2.34	-12.58	-12.58	-15.81
	50%	1.5	2.54	-12.58	-12.58	-15.81

CM Detectability	-50%	0.56	0.93	-8.20	-8.20	-9.13
	-40%	0.64	1.06	-9.07	-9.07	-10.46
	-30%	0.72	1.20	-9.95	-9.94	-11.80
	-20%	0.80	1.33	-10.83	-10.81	-13.14
	-10%	0.88	1.47	-11.70	-11.69	-14.48
	0%	**0.96**	**1.61**	**-12.58**	**-12.59**	**-15.81**
	10%	1.04	1.74	-13.46	-13.43	-17.14
	20%	1.12	1.88	-14.34	-14.37	-18.49
	30%	1.20	2.01	-15.21	-15.24	-19.82
	40%	1.29	2.15	-16.09	-16.11	-21.16
	50%	1.37	2.29	-16.97	-16.98	-22.50
CM Pre-empt	-50%	0.88	1.48	-10.46	-10.45	-14.56
	-40%	0.89	1.51	-10.88	-10.89	-14.81
	-30%	0.91	1.53	-11.31	-11.32	-15.07
	-20%	0.93	1.56	-11.73	-11.76	-15.31
	-10%	0.95	1.58	-12.16	-12.12	-15.56
	0%	**0.96**	**1.61**	**-12.58**	**-12.59**	**-15.81**
	10%	0.98	1.63	-13.01	-12.99	-16.06
	20%	1.00	1.66	-13.43	-13.43	-16.31
	30%	1.02	1.68	-13.86	-13.86	-16.56
	40%	1.03	1.71	-14.28	-14.30	-16.82
	50%	1.05	1.73	-14.71	-14.73	-17.06
CM Falsepos	-50%	0.971	1.610	-12.802	-12.803	-15.843
	-40%	0.970	1.609	-12.758	-12.760	-15.837
	-30%	0.968	1.608	-12.714	-12.716	-15.831
	-20%	0.967	1.608	-12.670	-12.672	-15.824
	-10%	0.965	1.607	-12.626	-12.629	-15.818
	0%	**0.964**	**1.606**	**-12.582**	**-12.585**	**-15.812**
	10%	0.963	1.606	-12.538	-12.535	-15.805
	20%	0.962	1.605	-12.494	-12.491	-15.799
	30%	0.961	1.604	-12.450	-12.447	-15.792
	40%	0.960	1.604	-12.406	-12.404	-15.787
	50%	0.959	1.603	-12.362	-12.360	-15.780
Distance to Shore	-80%	0.874	1.453	-12.375	-12.375	-15.749
	-60%	0.896	1.491	-12.426	-12.426	-15.765
	-40%	0.919	1.529	-12.478	-12.478	-15.781
	-20%	0.941	1.567	-12.530	-12.530	-15.797
	0%	**0.964**	**1.606**	**-12.582**	**-12.582**	**-15.812**
	20%	0.988	1.646	-12.635	-12.635	-15.827
	40%	1.011	1.686	-12.688	-12.688	-15.841
	60%	1.035	1.727	-12.742	-12.742	-15.855
	80%	1.059	1.769	-12.796	-12.796	-15.869
	100%	1.083	1.811	-12.851	-12.851	-15.883
	120%	1.108	1.854	-12.905	-12.905	-15.896
	140%	1.133	1.898	-12.960	-12.960	-15.909
	160%	1.158	1.942	-13.015	-13.015	-15.922
	180%	1.184	1.987	-13.071	-13.071	-15.935
	200%	1.210	2.033	-13.126	-13.126	-15.947

Table 6b. Cost model results for Point01 using HLV1 for repair type A and B for wind farm T

	Reactive Maintenance	Condition-based Maintenance	Change due to Condition monitoring	Change/ Baseline (%)
downtime	41.8 days	31.6 days	-10.3 days	-24.53%
availability	88.5 %	91.4 %	2.8 %	3.17%
capacity factor	36.9 %	39.3 %	2.4 %	6.43%
energy lost	1741.8 MWh	1262.9 MWh	-478.8 MWh	-27.49%
mean power generated over year	0.85 MW	0.90 MW	0.05 MW	6.43%
total annual energy generated	7443.1 MWh	7921.9 MWh	478.8 MWh	6.43%
annual revenue	632.7 £k	673.4 £k	40.7 £k	6.43%
revenue lost	148.0 £k	107.3 £k	-40.7 £k	-27.49%
annual maintenance cost	2033.5 £k	1459.2 £k	-574.3 £k	-28.24%
entire wind farm annual maintenance cost	57.1 £m	39.40 £m	-15.5 £m	-27.16%
vessel cost per unit	£0.25 /kWh	£0.18 /kWh	-£0.07 /kWh	-28.85%
wage cost per unit	£0.0178 /kWh	£0.0130 /kWh	-£0.005 /kWh	-27.08%
component cost per unit	£0.0076 /kWh	£0.0067 /kWh	-£0.0008 /kWh	-11.23%
Total O&M cost (w/o revenue loss) per unit	£0.27 /kWh	0.20 /kWh	-£0.08 /kWh	-28.24%
revenue lost per unit	£0.02 /kWh	0.01 /kWh	-£0.01 /kWh	-27.49%
Total O&M cost (with revenue loss) per unit	£0.29 /kWh	£0.21 /kWh	-£0.08 /kWh	-28.19%
Entire wind farm revenue loss per unit	£0.54 /kWh	£0.39 /kWh	-£0.15 /kWh	-27.49%
Entire wind farm total O&M cost (w/o revenue loss) per unit	£7.38 /kWh	£5.29 /kWh	-£2.08 /kWh	-28.24%

Table 7b. Cost model results for Point02 using HLV1 for repair type A and B for wind farm T

	Reactive Maintenance	Condition-based Maintenance	Change due to Condition monitoring	Change/ Baseline (%)
downtime	78.6 days	56.5 days	-22.1 days	-28.13%
availability	78.5 %	84.5 %	6.1 %	7.73%
capacity factor	31.6 %	37.0 %	5.4 %	16.93%
energy lost	3622.7 MWh	2544.0 MWh	-1078.7 MWh	-29.78%
mean power generated over year	0.73 MW	0.85 MW	0.12 MW	16.93%
total annual energy generated	6369.7 MWh	7448.4 MWh	1078.7 MWh	16.93%
annual revenue	541.4 £k	633.1 £k	91.7 £k	16.93%
revenue lost	307.9 £k	216.2 £k	-91.7 £k	-29.78%
annual maintenance cost	4551.8 £k	3166.9 £k	-1384.9 £k	-30.43%
entire wind farm annual maintenance cost	125.1 £m	85.51 £m	-37.4 £m	-29.89%
vessel cost per unit	£0.66 /kWh	£0.46 /kWh	-£0.20 /kWh	-30.72%
wage cost per unit	£0.0451 /kWh	£0.0317 /kWh	-£0.013 /kWh	-29.84%
component cost per unit	£0.0088 /kWh	£0.0079 /kWh	-£0.0010 /kWh	-11.23%
Total O&M cost (w/o revenue loss) per unit	£0.71 /kWh	0.50 /kWh	-£0.22 /kWh	-30.43%
revenue lost per unit	£0.05 /kWh	0.03 /kWh	-£0.01 /kWh	-29.78%
Total O&M cost (with revenue loss) per unit	£0.76 /kWh	£0.53 /kWh	-£0.23 /kWh	-30.38%
Entire wind farm revenue loss per unit	£1.31 /kWh	£0.92 /kWh	-£0.39 /kWh	-29.78%
Entire wind farm total O&M cost (w/o revenue loss) per unit	£19.29 /kWh	£13.42 /kWh	-£5.87 /kWh	-30.43%

Table 8b. Cost model results for Point05 using HLV1 for repair type A and B for wind farm T

	Reactive Maintenance	Condition-based Maintenance	Change due to Condition monitoring	Change / Baseline (%)
downtime	59.0 days	43.1 days	-15.8 days	-26.85%
availability	83.8 %	88.2 %	4.3 %	5.17%
capacity factor	33.6 %	37.4 %	3.7 %	11.14%
energy lost	2598.6 MWh	1843.6 MWh	-755.0 MWh	-29.06%
mean power generated over year	0.77 MW	0.86 MW	0.09 MW	11.14%
total annual energy generated	6775.6 MWh	7530.6 MWh	755.0 MWh	11.14%
annual revenue	575.9 £k	640.1 £k	64.2 £k	11.14%
revenue lost	220.9 £k	156.7 £k	-64.2 £k	-29.06%
annual maintenance cost	3228.2 £k	2269.1 £k	-959.1 £k	-29.71%
entire wind farm annual maintenance cost	89.4 £m	61.26 £m	-25.9 £m	-28.98%
vessel cost per unit	£0.44 /kWh	£0.31 /kWh	-£0.13 /kWh	-30.11%
wage cost per unit	£0.0303 /kWh	£0.0216 /kWh	-£0.009 /kWh	-28.96%
component cost per unit	£0.0083 /kWh	£0.0074 /kWh	-£0.0009 /kWh	-11.23%
Total O&M cost (w/o revenue loss) per unit	£0.48 /kWh	0.33 /kWh	-£0.14 /kWh	-29.71%
revenue lost per unit	£0.03 /kWh	0.02 /kWh	-£0.01 /kWh	-29.06%
Total O&M cost (with revenue loss) per unit	£0.51 /kWh	£0.36 /kWh	-£0.15 /kWh	-29.67%
Entire wind farm revenue loss per unit	£0.88 /kWh	£0.62 /kWh	-£0.26 /kWh	-29.06%
Entire wind farm total O&M cost (w/o revenue loss) per unit	£12.86 /kWh	£9.04 /kWh	-£3.82 /kWh	-29.71%

Table 9b. Cost model results for Point06 using HLV1 for repair type A and B for wind farm T

	Reactive Maintenance	Condition-based Maintenance	Change due to Condition monitoring	Change / Baseline (%)
downtime	57.3 days	42.0 days	-15.3 days	-26.72%
availability	84.3 %	88.5 %	4.2 %	4.97%
capacity factor	34.5 %	38.1 %	3.6 %	10.51%
energy lost	2522.4 MWh	1791.6 MWh	-730.7 MWh	-28.97%
mean power generated over year	0.79 MW	0.88 MW	0.08 MW	10.51%
total annual energy generated	6950.5 MWh	7681.2 MWh	730.7 MWh	10.51%
annual revenue	590.8 £k	652.9 £k	62.1 £k	10.51%
revenue lost	214.4 £k	152.3 £k	-62.1 £k	-28.97%
annual maintenance cost	3119.3 £k	2195.2 £k	-924.1 £k	-29.63%
entire wind farm annual maintenance cost	86.4 £m	59.27 £m	-25.0 £m	-28.87%
vessel cost per unit	£0.41 /kWh	£0.29 /kWh	-£0.12 /kWh	-30.04%
wage cost per unit	£0.029 /kWh	£0.020 /kWh	-£0.008 /kWh	-28.86%
component cost per unit	£0.0081 /kWh	£0.0072 /kWh	-£0.0009 /kWh	-11.23%
Total O&M cost (w/o revenue loss) per unit	£0.45 /kWh	0.32 /kWh	-£0.13 /kWh	-29.63%
revenue lost per unit	£0.03 /kWh	£0.02 /kWh	-£0.01 /kWh	-28.97%
Total O&M cost (with revenue loss) per unit	£0.48 /kWh	£0.34 /kWh	-£0.14 /kWh	-29.58%
Entire wind farm revenue loss per unit	£0.83 /kWh	£0.59 /kWh	-£0.24 /kWh	-28.97%
Entire wind farm total O&M cost (w/o revenue loss) per unit	£12.12 /kWh	£8.53 /kWh	-£3.59 /kWh	-29.63%